NAVAL POSTGRADUATE SCHOOL
MONTEREY, CALIFORNIA

THESIS

COMPUTATIONAL INVESTIGATION OF LOW SPEED FLOW OVER LOW ASPECT RATIO AIRCRAFT CONFIGURATIONS

by

Alain Carrier

December, 1995

Thesis Advisor: Max F. Platzer

Approved for public release; distribution is unlimited.

DISCLAIMER NOTICE

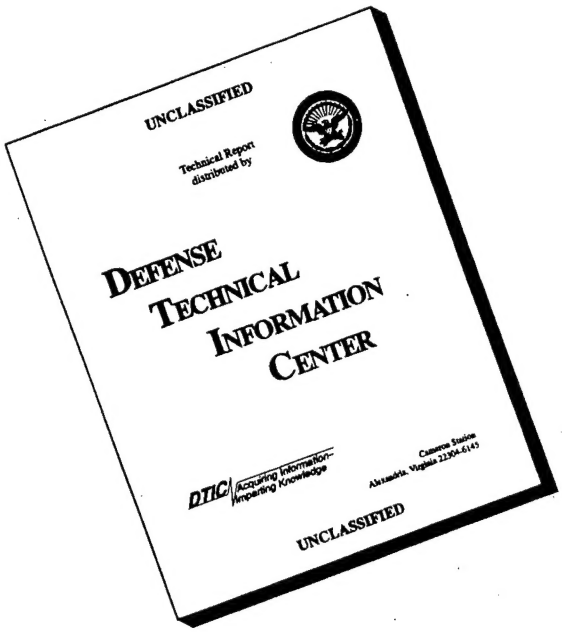

THIS DOCUMENT IS BEST QUALITY AVAILABLE. THE COPY FURNISHED TO DTIC CONTAINED A SIGNIFICANT NUMBER OF PAGES WHICH DO NOT REPRODUCE LEGIBLY.

REPORT DOCUMENTATION PAGE

Form Approved OMB No. 0704-0188

1. AGENCY USE ONLY *(Leave blank)*	2. REPORT DATE December 1995	3. REPORT TYPE AND DATES COVERED Master's Thesis

4. TITLE AND SUBTITLE COMPUTATIONAL INVESTIGATION OF LOW SPEED FLOW OVER LOW ASPECT RATIO AIRCRAFT CONFIGURATIONS	5. FUNDING NUMBERS
6. AUTHOR(S) Carrier, A	
7. PERFORMING ORGANIZATION NAME(S) AND ADDRESS(ES) Naval Postgraduate School Monterey CA 93943-5000	8. PERFORMING ORGANIZATION REPORT NUMBER
9. SPONSORING/MONITORING AGENCY NAME(S) AND ADDRESS(ES)	10. SPONSORING/MONITORING AGENCY REPORT NUMBER

11. SUPPLEMENTARY NOTES The views expressed in this thesis are those of the author and do not reflect the official policy or position of the Department of Defense or the U.S. Government.

12a. DISTRIBUTION/AVAILABILITY STATEMENT Approved for public release; distribution is unlimited.	12b. DISTRIBUTION CODE

13. ABSTRACT *(maximum 200 words)*

The objective of this thesis was to contribute to the development of a second-order approximation to the steady and oscillatory lifting flow past low aspect ratio wings by establishing the validity of a NASA-Ames developed incompressible three-dimensional flow panel code named PMARC, which would subsequently be used to test the range of validity of this second-order theory. The steady state configurations modelled in the validation process include swept back, delta and rectangular wings, an F5 wing and three equivalent bodies of revolution. Oscillatory cases were also run with one delta and the F5 wings and their respective equivalent bodies of revolution, as well as with one spindle. In steady state, comparison with experimental and theoretical data proved PMARC to be very accurate for lift and pressure calculations, but revealed a discrepancy in the velocity distribution calculation around delta wings. This finding was corroborated by applying the slender body/slender wing theory (Oswatitsch-Keune theory) to the delta wing. The unsteady state results are presented, but their validation is left for future work. As part of its primary objective, this thesis also presents a computer code that generates the F5 wing equivalent body of revolution from its chordwise section definition. In order to be used as base software to the second-order theory, PMARC will have to be corrected, or a new software will have to be validated.

14. SUBJECT TERMS PMARC, Area Rule, Low Aspect Ratio Configurations, Equivalent Body of Revolution, Three-Dimensional Flow Solution, Panel Code, Steady and Oscillatory Lifting Flow, Velocity Perturbation, Pressure Perturbation.	15. NUMBER OF PAGES 261
	16. PRICE CODE

17. SECURITY CLASSIFICATION OF REPORT	18. SECURITY CLASSIFICATION OF THIS PAGE	19. SECURITY CLASSIFICATION OF ABSTRACT	20. LIMITATION OF ABSTRACT
Unclassified	Unclassified	Unclassified	UL

NSN 7540-01-280-5500

Standard Form 298 (Rev. 2-89)
Prescribed by ANSI Std. 239-18 298-102

Approved for public release; distribution is unlimited.

COMPUTATIONAL INVESTIGATION OF LOW SPEED FLOW OVER LOW ASPECT RATIO AIRCRAFT CONFIGURATIONS

by

Alain Carrier
Captain, Canadian Armed Forces
B.S., Ecole Polytechnique, University of Montreal, 1988

Submitted in partial fulfillment
of the requirements for the degree of

MASTER OF SCIENCE IN AERONAUTICAL ENGINEERING

from the

NAVAL POSTGRADUATE SCHOOL
December 1995

Author: 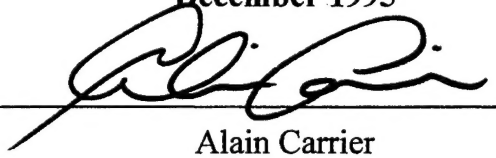
Alain Carrier

Approved by: 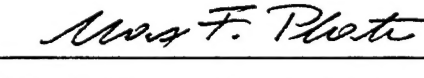
Max F. Platzer, Thesis Advisor


Ismail H. Tuncer, Second Reader

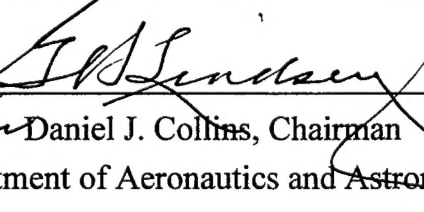
for Daniel J. Collins, Chairman
Department of Aeronautics and Astronautics

ABSTRACT

The objective of this thesis was to contribute to the development of a second-order approximation to the steady and oscillatory lifting flow past low aspect ratio wings by establishing the validity of a NASA-Ames developed incompressible three-dimensional flow panel code named PMARC, which would subsequently be used to test the range of validity of this second-order theory. The steady state configurations modelled in the validation process include swept back, delta and rectangular wings, an F5 wing and three equivalent bodies of revolution. Oscillatory cases were also run with one delta and the F5 wings and their respective equivalent bodies of revolution, as well as with one spindle. In steady state, comparison with experimental and theoretical data proved PMARC to be very accurate for lift and pressure calculations, but revealed a discrepancy in the velocity distribution calculation around delta wings. This finding was corroborated by applying the slender body/slender wing theory (Oswatitsch-Keune theory) to the delta wing. The unsteady state results are presented, but their validation is left for future work. As part of its primary objective, this thesis also presents a computer code that generates the F5 wing equivalent body of revolution from its chordwise section definition. In order to be used as base software to the second-order theory, PMARC will have to be corrected, or a new software will have to be validated.

TABLE OF CONTENTS

I. INTRODUCTION

Over the past quarter century, great advances have been made in the computation of the aerodynamic forces on aircraft and missiles. These advances were made possible by the development of high-speed computers which , in turn, made possible the numerical integration of the compressible flow equations. However, the numerical computation of the flow field around a typical military aircraft or missile configuration is still a very time consuming and expensive task because it requires the development of a complex three-dimensional computational grid and the solution of a system of nonlinear partial differential equations by means of a suitable numerical integration scheme. Furthermore, the design of aircraft or missiles requires not only the determination of the aerodynamic forces in steady flight but also of the transient and oscillatory forces in order to assure the flight vehicle's dynamic and aeroelastic stability and to predict the dynamic loads due to wind gusts. For these reasons there exists a continuing need to develop approaches which are sufficiently accurate, yet are computationally more efficient than full-fledged three-dimensional solutions of the inviscid compressible flow equations (Euler equations) or of the viscous compressible flow equations (Navier-Stokes equations).

It is the objective of this thesis to contribute to the development of a new approach to determine the steady and unsteady airloads on missiles and on low-aspect ratio aircraft configurations typically used for high-performance fighter aircraft. This approach is based on an extension of the well-known slender-body/slender-wing theory developed by Oswatitsch, Keune, R.T. Jones and others in the 1940's and 1950's (see e.g. the book by Ashley and Landahl, Ref. [8]). Oswatitsch and Keune showed that, in a first approximation, the non-lifting flow over bodies of revolution and low aspect ratio configurations can be obtained by the superposition of two flows, namely the flow in the planes normal to the freestream direction (the cross-flow) and the "spatial influence" which accounts for the contribution upstream and, in subsonic flow, also downstream of the cross-flow plane under consideration. The cross-flow can be treated as a purely incompressible flow (even though the missile or aircraft flies at transonic or supersonic speeds), whereas the spatial influence is Mach number dependent but has the remarkable feature that the spatial influence is the

same for all configurations which have the same cross-sectional area distribution in the streamwise direction. The lifting flow, on the other hand, can be obtained by merely considering the cross-flow, hence reducing the analysis to a purely incompressible flow analysis for high-speed flight vehicles of low aspect ratio.

M.F. Platzer has published a NASA technical memorandum (NASA TM X-53295, April, 1965) on his development of a second-order approximation to the steady and oscillatory lifting flow past low aspect ratio wings which exhibits the same fundamental division into an incompressible cross-flow and a Mach-number dependent spatial influence. To test the range of validity of this second-order theory it is necessary to compare it with an exact three-dimensional flow solution. Fortunately, such a solution has become available for low speed (incompressible) flow in recent years with the NASA-Ames developed PMARC code. Therefore, in this thesis, the following specific objectives were attempted, namely:

1. Demonstrate and document the PMARC code,

2. Compare the PMARC solutions with other available solutions in order to establish its validity,

3. Compute the incompressible flow over a delta wing at zero angle of attack using the Oswatitsch-Keune theory,

4. Obtain the equivalent area body of revolution of an F-5 wing,

5. Compare the Oswatitsch-Keune theory with the PMARC predictions, and

6. Generalize the non-lifting theory to incompressible flow past oscillating bodies of revolution and low-aspect ratio wings.

These tasks will be described in the subsequent chapters.

II. SOFTWARE OVERVIEW

A. THEORY BEHIND PMARC

PMARC stands for **Panel Method Ames Research Center**. It is a potential flow panel code developed at **NASA Ames Research Center** to numerically predict flow fields around complex three-dimensional geometries. The general idea behind this panel code is to cover the body under study with panels over which there is an unknown distribution of doublets and sources. (Recall that the doublet and source flows are two of several elementary flows used to model the flow field around arbitrary shapes.) These unknowns are solved through a set of simultaneous linear algebraic equations generated by calculating the induced velocity at each panel's control point and applying the flow tangency condition.

Two kinds of simplifications were made to allow this software to remain computationally cost effective. The first one has to do with the strength of the elementary flows (also called singularities). In PMARC, the strength of the singularities is constant over each panel allowing factorization of the doublet and source strengths in the thus greatly simplified analytical solution of the flow. The second kind of simplification is in the assumption of an inviscid, irrotational, and incompressible flow field, thus satisfying Laplace's equation:

$$\nabla^2\Phi=0 \tag{2.1}$$

With these simplifications, PMARC proceeds to solve for the potential at any point P by applying Green's Theorem, which results in the following integral equation:

$$\Phi_P=\frac{1}{4\pi}\iint_{S+W+S_\infty}[(\Phi-\Phi_i)\bar{n}\cdot\nabla(\frac{1}{r})]\ dS\ -\ \frac{1}{4\pi}\iint_{S+W+S_\infty}[(\frac{1}{r})\bar{n}\cdot(\nabla\Phi-\nabla\Phi_i)]\ dS \tag{2.2}$$

where r is the distance from the point P to the element dS on the surface and n is the unit vector normal to the surface pointing into the flow field of interest. In this equation the first integral represents the disturbance potential from a surface distribution of doublets with strength *'phi-phi$_i$'* per unit area and the second integral represents the contribution from a surface distribution of sources. As shown on Figure 2.1, *phi* corresponds to the external region (or flow field of interest), and *phi$_i$* is the internal region (or fictitious flow). This arrangement is required to model external flow problems such as a wing in a uniform stream.

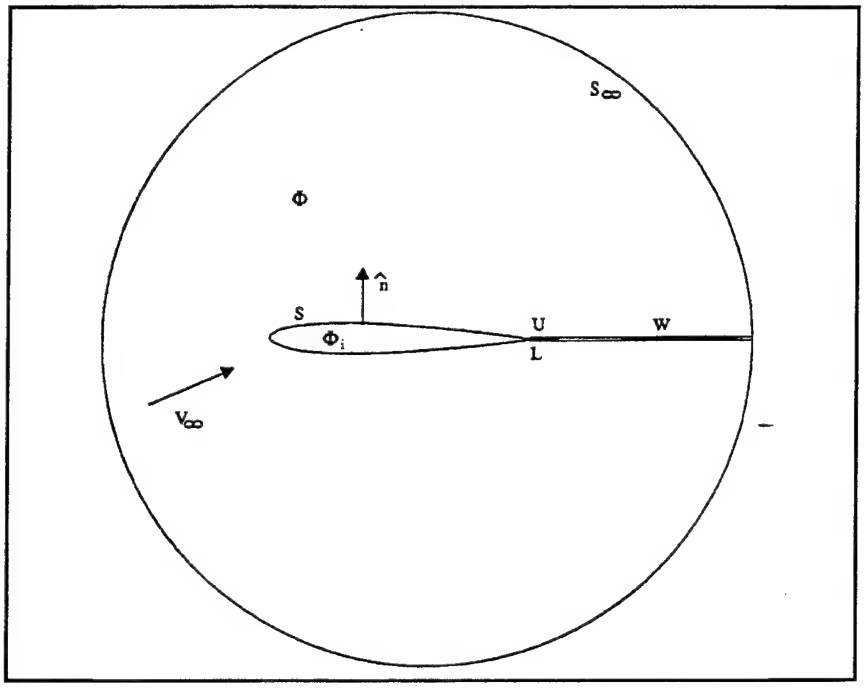

Figure 2.1. Potential Flow Model for PMARC.
(From Ref.[1])

PMARC actually solves a simpler form of Green's Theorem than the one presented above. The simplifications are made possible by noting that at the surface at infinity, the perturbation potential due to the configuration is essentially zero, leaving only the potential due to the uniform onset flow. Also, it is assumed that the wake is thin and there is no entrainment so the source term for the wake disappears and the jump in normal velocity across the wake is zero.

The theory described above makes for three major steps in the PMARC solution process. First, it solves for the doublet strengths leading to known values of the singularities on each of the panels. Second, it computes the velocity by differentiating the velocity potential expression in the appropriate direction for each tangential component of velocity. Using this information it calculates the resultant velocity at each panel control point. With this result it finally derives the pressure distribution using Equation (2.3). The forces and moments on the body are then obtained by performing a surface pressure integration.

$$C_{P_K} = 1 - \frac{V_K^2}{V_\infty^2} + \left(\frac{2*4\pi}{V_\infty^2}\right)\left(\frac{\mu(t)-\mu(t-1)}{\Delta t}\right) \qquad (2.3)$$

B. PMARC OPERATING MODE

Instead of giving all the details pertaining to the operation of the PMARC software within this section, only the generalities will be presented. For practicality and ease of understanding, the information and instructions for construction of a specific wing configuration will be presented in the software validation sections, each time a new configuration is introduced. For additional details, the reader should refer to Refs. [1], [2], and [3]. Installation instructions are also found in Ref. [1].

1. Generalities

There exists more than one way to construct a structure in PMARC. One is to make use of three levels of coordinates, as shown in Figure 2.2 , in order to join components built separately. Another way would be to build the whole structure at once referring all points to one coordinate system.

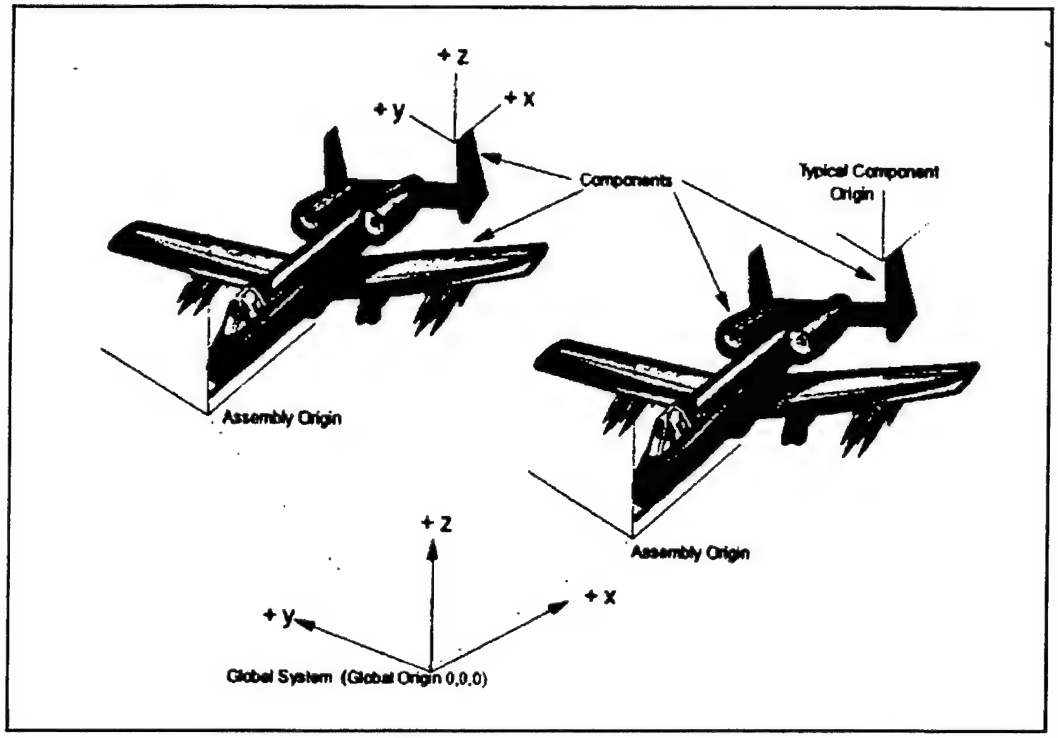

Figure 2.2. PMARC Hierarchy of Coordinate Systems.
(From Ref.[2])

But no matter which method is preferred, the physical representation of each component is made with sheets of panels called patches used to solve the required simultaneous flow equations for that particular group of panels . The panel density of these patches and the manner in which all the patches are joined together are defined within the input file as will be shown in later sections. The shape of theses patches is given by providing a point definition, or path, around or along which the patches will be laid down or wrapped. Figure 2.3 shows how a patch is rolled up on top of itself to make a surface in which two of the four sides are joined in a seam. There are a few rules about the numbering of each panel, and although most of them are transparent to the users upon construction of a model, others shall be known for output interpretation purposes. These rules will be explained later.

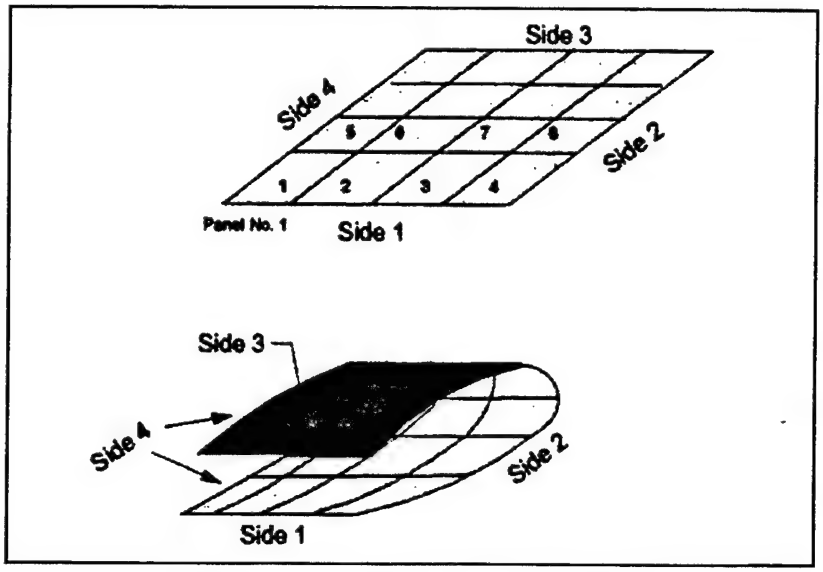

Figure 2.3. PMARC Patch of Panels.
(From Ref.[2])

The previous figure is a representation of how wings are modelled. Again, PMARC offers some flexibility as there are two ways to define a wing section. The first one is done by entering a series of points that define the wing cross-sectional shape. PMARC will then wrap the patch on top of that definition. The second method will automatically generate the point coordinates of a NACA Four Digit Series airfoil. All that is required are the airfoil's maximum thickness ratio, and the maximum camber and its location. A later section will show how to use these two options.

Once the shape of a section is defined, the third dimension of the component has to be modelled. Again, several options are available to this end. One is to position the leading edge origin of each end of the component, for instance the root and the tip cross-section of a wing, in some chosen coordinate system, and then to scale each of these ends to the desired size. Another method is to define the cross-section of each end of the component in relation to a coordinate system. This way, each cross-section is built originally to its desired size, instead of being scaled from the non-dimensionalized definition as with the previous method. Depending on the application, each of these methods, or a combination thereof, show significant advantages.

PMARC incorporates routines to automatically generate wing tips, whether they need to be flat or rounded. Also, by toggling the value of certain variables, complete components can be copied. A multitude of other features are available among which is found the wake generation and the streamline generation routine. The interested reader should refer to Refs. [1], [2], and [3].

2. PMARC Input File

Several decisions have to be made when building a geometry with PMARC. The number of panels spanwise and chordwise and their distribution are two important ones. More panels means better accuracy, but also means proportionately longer computational time. The optimal number of panels should be sought to make the results sufficiently accurate. The panels can be spaced following four types of distribution: full cosine, two types of half cosine, and equal spacing. These allow the user to concentrate more panels in areas of expected greater gradients. These decisions will be justified in the validation section each time a new configuration is tested.

Other information, geometry specifics, and test conditions are entered into PMARC via its input file. It is called DATA5 and is FORTRAN based. Over 200 fields or variables are required to be filled for PMARC to successfully read the file. Although not all the fields are pertinent to all cases, an uncompleted field will cause a software crash. The following paragraphs will laconically describe the DATA5 input file, identifying which fields should be filled with correct values to obtain correct output in the case where we are interested in the Cp, Vx, Vy, Vz, V, CL, and Cl but without wake or streamline generation. The reader should refer to Figure 2.4 before continuing. Also, each field of the DATA5 input file is represented by an acronym. The definition of these acronyms along with the valid entries are listed in Ref. [1] starting on page 33.

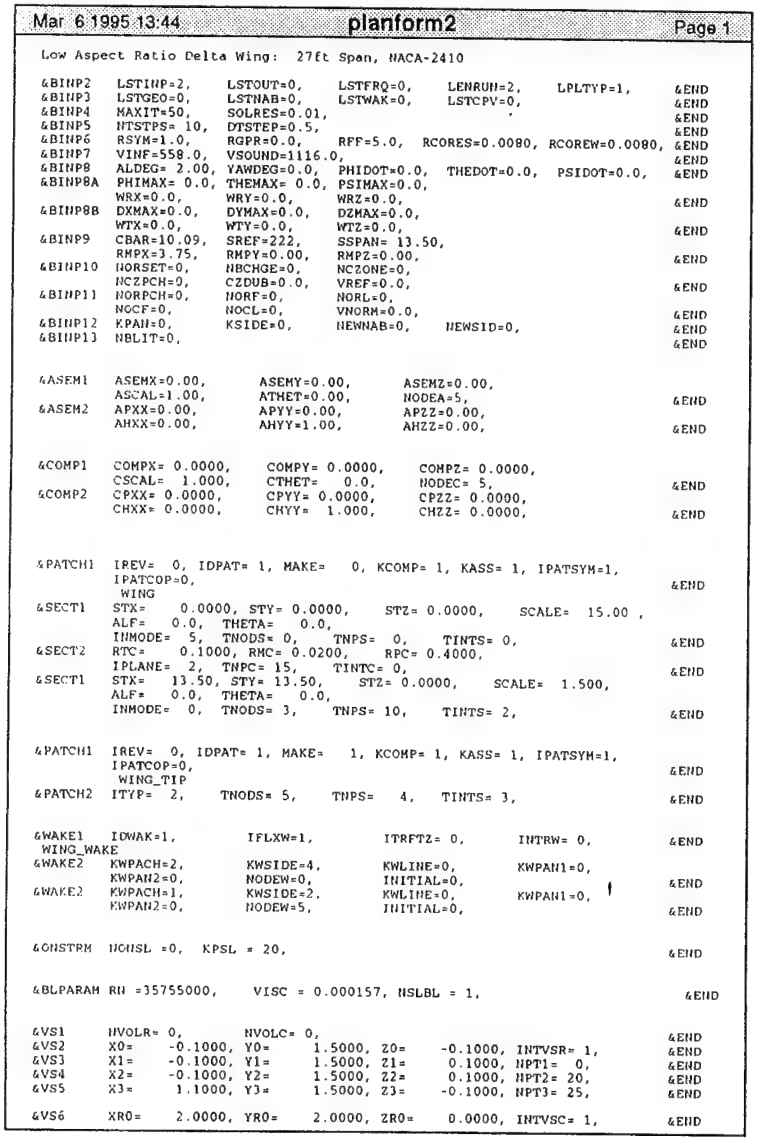

Mar 6 1995 13:44 planform2 Page 1

```
Low Aspect Ratio Delta Wing:  27ft Span, NACA-2410

&BINP2   LSTINP=2,     LSTOUT=0,     LSTFRQ=0,     LENRUN=2,     LPLTYP=1,     &END
&BINP3   LSTGEO=0,     LSTNAB=0,     LSTWAK=0,     LSTCPV=0,                   &END
&BINP4   MAXIT=50,     SOLRES=0.01,                                            &END
&BINP5   NTSTPS= 10,   DTSTEP=0.5,                                             &END
&BINP6   RSYM=1.0,     RGPR=0.0,     RFF=5.0,   RCORES=0.0080, RCOREW=0.0080, &END
&BINP7   VINF=558.0,   VSOUND=1116.0,                                          &END
&BINP8   ALDEG= 2.00, YAWDEG=0.0,  PHIDOT=0.0,  THEDOT=0.0,  PSIDOT=0.0,      &END
&BINP8A  PHIMAX= 0.0, THEMAX= 0.0, PSIMAX=0.0,
         WRX=0.0,      WRY=0.0,     WRZ=0.0,                                   &END
&BINP8B  DXMAX=0.0,    DYMAX=0.0,   DZMAX=0.0,
         WTX=0.0,      WTY=0.0,     WTZ=0.0,                                   &END
&BINP9   CBAR=10.09,   SREF=222,    SSPAN= 13.50,
         RMPX=3.75,    RMPY=0.00,   RMPZ=0.00,                                 &END
&BINP10  NORSET=0,     NBCHGE=0,    NCZONE=0,
         NCZPCH=0,     CZDUB=0.0,   VREF=0.0,                                  &END
&BINP11  NORPCH=0,     NORF=0,      NORL=0,
         NOCF=0,       NOCL=0,      VNORM=0.0,                                 &END
&BINP12  KPAN=0,       KSIDE=0,     NEWNAB=0,     NEWSID=0,                    &END
&BINP13  NBLIT=0,                                                              &END


&ASEM1   ASEMX=0.00,       ASEMY=0.00,       ASEMZ=0.00,
         ASCAL=1.00,       ATHET=0.00,       NODEA=5,                         &END
&ASEM2   APXX=0.00,        APYY=0.00,        APZZ=0.00,
         AHXX=0.00,        AHYY=1.00,        AHZZ=0.00,                       &END


&COMP1   COMPX= 0.0000,    COMPY= 0.0000,    COMPZ= 0.0000,
         CSCAL=  1.000,    CTHET=   0.0,     NODEC= 5,                        &END
&COMP2   CPXX= 0.0000,     CPYY= 0.0000,     CPZZ= 0.0000,
         CHXX= 0.0000,     CHYY=  1.000,     CHZZ= 0.0000,                    &END


&PATCH1  IREV=  0, IDPAT= 1, MAKE=   0, KCOMP= 1, KASS= 1, IPATSYM=1,
         IPATCOP=0,
          WING                                                                 &END
&SECT1   STX=    0.0000, STY= 0.0000,    STZ= 0.0000,    SCALE=  15.00 ,
         ALF=    0.0,  THETA=   0.0,
         INMODE=  5,  TNODS= 0,    TNPS=  0,    TINTS= 0,                     &END
&SECT2   RTC=    0.1000, RMC= 0.0200,    RPC= 0.4000,
         IPLANE=  2,  TNPC= 15,    TINTC= 0,                                  &END
&SECT1   STX=   13.50, STY= 13.50,    STZ= 0.0000,    SCALE=  1.500,
         ALF=    0.0,  THETA=   0.0,
         INMODE=  0,  TNODS= 3,    TNPS= 10,    TINTS= 2,                     &END


&PATCH1  IREV=  0, IDPAT= 1, MAKE=   1, KCOMP= 1, KASS= 1, IPATSYM=1,
         IPATCOP=0,
          WING_TIP                                                             &END
&PATCH2  ITYP=  2,    TNODS= 5,    TNPS=   4,   TINTS= 3,                    &END


&WAKE1   IDWAK=1,          IFLXW=1,          ITRFTZ= 0,       INTRW= 0,       &END
 WING_WAKE
&WAKE2   KWPACH=2,         KWSIDE=4,         KWLINE=0,        KWPAN1=0,
         KWPAN2=0,         NODEW=0,          INITIAL=0,                       &END
&WAKE2   KWPACH=1,         KWSIDE=2,         KWLINE=0,        KWPAN1=0,
         KWPAN2=0,         NODEW=5,          INITIAL=0,                       &END


&CONSTRM  NCHSL =0,  KPSL = 20,                                                &END


&BLPARAM RN =35755000,    VISC = 0.000157, NSLBL = 1,                          &END


&VS1     NVOLR= 0,        NVOLC= 0,                                           &END
&VS2     X0=    -0.1000, Y0=     1.5000, Z0=    -0.1000, INTVSR= 1,           &END
&VS3     X1=    -0.1000, Y1=     1.5000, Z1=     0.1000, NPT1=  0,            &END
&VS4     X2=    -0.1000, Y2=     1.5000, Z2=     0.1000, NPT2= 20,            &END
&VS5     X3=     1.1000, Y3=     1.5000, Z3=    -0.1000, NPT3= 25,            &END

&VS6     XR0=    2.0000, YR0=    2.0000, ZR0=    0.0000, INTVSC= 1,           &END
```

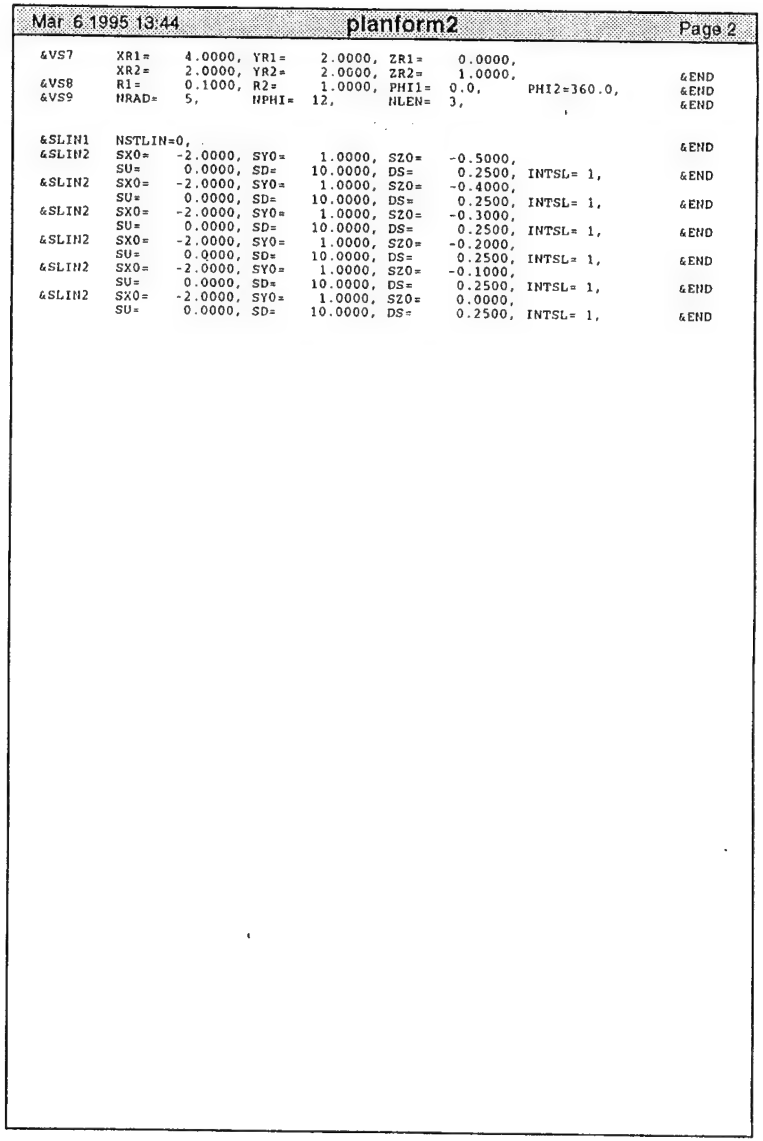

Mar 6 1995 13:44 planform2 Page 2

```
&VS7     XR1=    4.0000, YR1=    2.0000, ZR1=    0.0000,
         XR2=    2.0000, YR2=    2.0000, ZR2=    1.0000,                      &END
&VS8     R1=     0.1000, R2=     1.0000, PHI1=   0.0,      PHI2=360.0,        &END
&VS9     NRAD=   5,      NPHI=  12,      NLEN=   3,                           &END


&SLIN1   NSTLIN=0,                                                             &END
&SLIN2   SX0=   -2.0000, SY0=    1.0000, SZ0=   -0.5000,
         SU=     0.0000, SD=    10.0000, DS=     0.2500, INTSL= 1,            &END
&SLIN2   SX0=   -2.0000, SY0=    1.0000, SZ0=   -0.4000,
         SU=     0.0000, SD=    10.0000, DS=     0.2500, INTSL= 1,            &END
&SLIN2   SX0=   -2.0000, SY0=    1.0000, SZ0=   -0.3000,
         SU=     0.0000, SD=    10.0000, DS=     0.2500, INTSL= 1,            &END
&SLIN2   SX0=   -2.0000, SY0=    1.0000, SZ0=   -0.2000,
         SU=     0.0000, SD=    10.0000, DS=     0.2500, INTSL= 1,            &END
&SLIN2   SX0=   -2.0000, SY0=    1.0000, SZ0=   -0.1000,
         SU=     0.0000, SD=    10.0000, DS=     0.2500, INTSL= 1,            &END
&SLIN2   SX0=   -2.0000, SY0=    1.0000, SZ0=    0.0000,
         SU=     0.0000, SD=    10.0000, DS=     0.2500, INTSL= 1,            &END
```

Figure 2.4 PMARC Input File Sample.

a. Basic Input Section

This section allow the user to entitle the file, prescribe specific job requirements, control some solver and time-step parameters, define some of the testing conditions as far as the movement of the model and the freestream are concerned, and also to input reference dimensions. All the above make up for sixty fields. Not all of them require actual testing values in order to obtain valid output for the parameters listed in subsection **2** above. These fields can be filled with any number without altering the results. In the steady case, the critical fields are the type of run (LENRUN) that determines if a full flow calculation will be performed or just a geometry generation, the angle of attack (ALDEG), and the reference surface area (SREF), the latter being used in the local lift coefficient calculations. Other fields become critical when dealing with unsteady state cases. They will be discussed later in the oscillation chapter. Two of these fields (NTSTPS, DTSTEP) also require some attention in the steady state cases as will be seen.

One should always study the output carefully as some of the results might be the consequence of fields that were filled with arbitrary values instead of values corresponding to the test case. A prudent habit for the analysis of any kind of wing or wing-body combination fixed in space is to fill the following list of fields with the information corresponding to the object under study: LENRUN, VINF, VSOUND, ALDEG, CBAR, SREF, and SSPAN. The other fields can remain the same as the values used in example files presented in the PMARC manual (Ref. [1]).

b. Input Section for Surface Geometry

This portion of the input file includes the headings &ASEM1, &ASEM2, &COMP1, &COMP2, &PATCH1, &SECT1, and &BPNODE. For the example analysis described, the first four sets of fields don't change from what is shown on Figure 2.4. They will change if two or more independent components are studied. The last three sets (&PATCH1, &SECT1 and &BPNODE) are critical in the construction of components and the definition of its panel layout. Each individual field within these sets has to be entered with values specifically corresponding to the model being built and the conditions of the tests. As will be seen later, the sets of fields listed above are duplicated as often as required to define more complex components or assemblies. Also, &PATCH2, &PATCH3, &SECT2, and &SECT3 are other sets of field required in certain cases.

It becomes a complex matter to identify which cases require which ones of the sets of fields discussed above. The uninitiated should study the various test cases in the validation sections to acquire a broader view of the many possible applications.

c. Time-stepping Wakes and On-body Streamlines

Wake analysis with PMARC is a challenging undertaking. If wakes are to be modelled, each of the fields in the wake portion of the input file is important. These fields lose all significance when the wake routine is turned off (IDWAK = 0). The same comments are true for the on-body streamlines.

3. PMARC Output Files

Once the PMARC has successfully read the input file DATA5, it performs the flow calculations and generates two output files named DATA6 and DATA22. The latter is an unreadable file that contains all the information required for the visualization of the various parameter gradients along the body under study. This visualization is made possible via a satellite software named GVS. General information on GVS can be found in Ref. [3] and a detailed user guide is also available in Ref. [18].

DATA6 is the output file formatted for interpretation by the user. Its length could range from a few kilobytes for the simple geometry computation to several megabytes for full flow computation using several time-steps. DATA6 is a well formatted and structured output file. The following provides a succinct description of its structure.

a. Input list for Basic Data

The top of that file reiterate some of the important geometry and test conditions prescribed by the user within the input file, DATA5. It also lays out the position of the assembly and component coordinate systems. This portion of the file ends with the cross-sections definitions and a list of the basic patch data.

b. Time-step zero solution

For the first moment of the test, the following output will be produced:

(1) Basic wake information;

(2) Solution iteration history;

(3) Aerodynamic data for patch one which consists of a series of tables that lists for each of the panels in one chordwise row the x, y and z coordinate of the panel control point, as well as Cp, Vx, Vy, Vz, V, DUB, DPHI/DT, and MACH. This process is repeated for each row of panels of a patch.

(4) Section parameters for the series of rows of panels which aerodynamic data were just listed. The section parameters are CL, CD, CY, Cm, Cn, and Cl. These values can be regarded as the two-dimensional values for that strip of panels. They are given in two reference sets: wind, and body axes.

(5) Aerodynamic data and section parameters for all other patches. The same format as presented for the first patch is followed for all remaining patches.

(6) Wind axis force and moment coefficients. In this section, total CL, CD, CY, and Cm are given for each of the patches, each component, and finally for the whole assembly.

(7) Body axis force and moment coefficients. In this section, total CN, CA, CY, and Cm are given for each of the patches, each component, and finally for the whole assembly.

c. Time-step 1 and above

For the remaining time step except the last one, DATA6 will produce a condensed output in that it will not generate all the tables of aerodynamic data as for time step zero. Thus, all the steps listed above are executed except **(3)** and **(5)**.

d. The last time-step

For the last time-step, all of the seven steps listed in time-step zero are executed again. The results will be different than when the flow just started at time step zero.

C. CONCLUSION

The theoretical basis for PMARC, a low order potential-flow panel code for modelling complex three-dimensional geometries has been outlined. The input file was also detailed with the emphasis on the fact that although not all the fields apply to all cases, they all have to be filled with values for the software to run successfully. Finally, the output file was reviewed. Its format was studied along with the type of results that it holds.

III. SOFTWARE VALIDATION - CONVENTIONAL WINGS

A. INTRODUCTION

The objective of this chapter is to show that PMARC is a panel code that closely recreates **most** of the results from experimental testing, higher order panel codes, and theoretical analytical solutions. As it will be seen, there are restrictions to its capabilities in the area of velocity distribution over delta wings at zero angle of attack. This PMARC review will be done by modelling various types of wings for which analyses have been conducted and results are available.

Specifically, two types of swept back wings, four delta wings, various rectangular wings, an F5 wing and a parabolic arc delta wing will be studied. The lift-curve slopes, the pressure coefficient distribution in both chordwise and spanwise direction, the velocity distribution and the equivalence rule results will all be comparison factors for our validation process. The following chapter will conduct a similar study on three bodies of revolutions.

As mentioned in the previous chapter, PMARC operating instructions will also be presented here. Therefore the structure of the following sections, each corresponding to a wing configuration, will be as follows. A description of the wing studied will first be given. Then, an overview of the theory and results serving as the reference data will be presented, followed by the results obtained with PMARC, shown compared to the reference data, and complemented by explanatory comments and discussion. Also, the specific PMARC input steps for modelling the subject wing will be explained. Finally, the output data retrieval technique is presented.

B. SWEPT BACK WING I

A wing with relatively simple geometry was considered for the first comparison. The wing has an aspect ratio (AR) of 5, a taper ratio of unity, and an uncambered flat plate section. Since the taper ratio is unity, the leading edge, the quarter-chord line, the three-quarter-chord line, and the

trailing edge all have the same sweep, 45 degrees. All the dimensions and coordinates being in terms of the span b, an arbitrary value of b will be assumed at 10. The finite geometry of the wing is as shown in Figure 3.1.

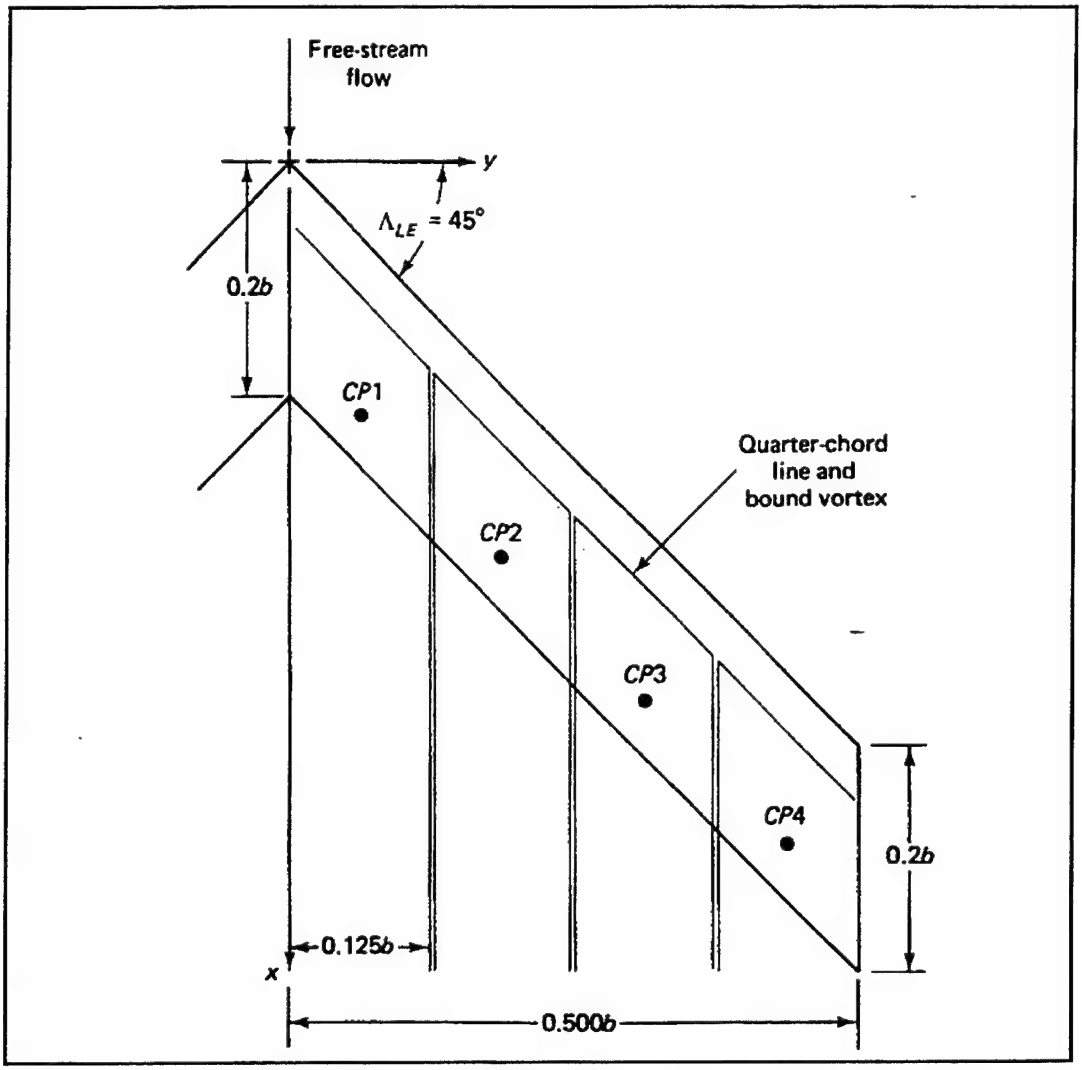

Figure 3.1 Four-Panel Representation of a Swept Planar Wing, Taper Ratio of Unity, AR=5, Sweep=45 Degrees. (From Ref.[4])

1. Theory, Background and Reference Data

Several lifting flow field computation methods have been developed. Probably one of the simplest is the Vortex Lattice Method (VLM). The VLM represents the wing as a planar surface on which a grid of vortex panels is superimposed. The velocities induced by each horseshoe vortex at a specified control point are calculated using the Bio-Savart law, Equation (3.1).

$$\vec{dV} = \frac{\Gamma_n(\vec{dl} \times \vec{r})}{4\pi r^3} \tag{3.1}$$

A summation is performed for all control points on the wing to produce a set of linear algebraic equations for the horseshoe vortex strengths that satisfy the boundary condition of no flow through the wing. The vortex strengths are related to the wing circulation and the pressure differential between the upper and lower wing surfaces. Bertin & Smith (Ref. [4]) present the derivation of the equations from the Bio-Savart law, and apply them to the case of the swept back flat plate shown above. The experimental results against which the PMARC and VLM results will be compared are reported in Ref. [5].

2. Results and Discussion

As shown on Figure 3.2, the coefficient results obtained by PMARC correspond very closely to the ones calculated with the Vortex Lattice Method. However, although good for the low angles of attack, both sets seem to gradually increase their spread with the experimental results. That does not discredit PMARC or VLM, as this behavior was to be expected. PMARC and VLM are both linear methods that do not account for boundary layer separation and stall. That is why the slope of the experimental results shown on Figure 3.2 start to decrease as the stall angle approaches, while the other two methods keep showing a steady increase of lift coefficient with increase in angle of attack.

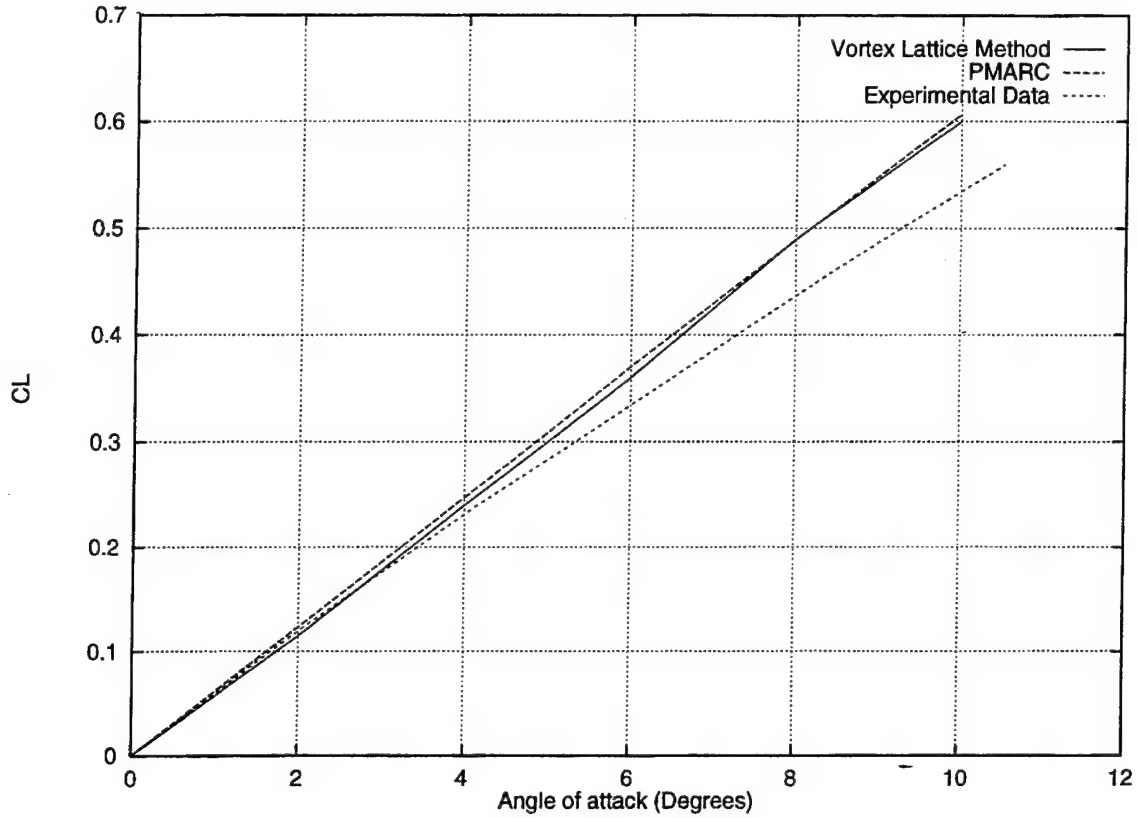

Figure 3.2 Comparison of The Lift Coefficient as a Function of Angle of Attack. Swept Planar Wing, Taper Ratio of Unity, AR=5, Sweep=45 Degrees.

3. PMARC Input Instructions

The following details complement Chapter **II** which presented the theory behind PMARC and its major operating instructions. This subsection will reiterate certain important details and introduce new factors that were intentionally left for this section for simplicity reasons. The following headings refer to the PMARC input file, DATA5, shown in Figure 3.3.

Jan 28 1995 11:59:41 **examp7_2.in** Page 1

```
 45 Degree Swept Back Flat Plate:  AR=5, Span=10, Ct/Cr=1

 &BINP2   LSTINP=2,    LSTOUT=0,    LSTFRQ=0,    LENRUN=0,    LPLTYP=1,     &END
 &BINP3   LSTGEO=0,    LSTNAB=0,    LSTWAK=0,    LSTCPV=0,                  &END
 &BINP4   MAXIT=50,    SOLRES=0.01,                                         &END
 &BINP5   NTSTPS= 10,  DTSTEP=0.5,                                          &END
 &BINP6   RSYM=1.0,    RGPR=0.0,    RFF=5.0,  RCORES=0.0080, RCOREW=0.0080, &END
 &BINP7   VINF=558.0,  VSOUND=1116.0,                                       &END
 &BINP8   ALDEG= 10.00, YAWDEG=0.0,  PHIDOT=0.0,  THEDOT=0.0,  PSIDOT=0.0,  &END
 &BINP8A  PHIMAX= 0.0, THEMAX= 0.0, PSIMAX=0.0,
          WRX=0.0,     WRY=0.0,     WRZ=0.0,                               &END
 &BINP8B  DXMAX=0.0,   DYMAX=0.0,   DZMAX=0.0,
          WTX=0.0,     WTY=0.0,     WTZ=0.0,                               &END
 &BINP9   CBAR=2.0,    SREF=20.0,   SSPAN= 5.0,
          RMPX=3.75,   RMPY=0.00,   RMPZ=0.00,                             &END
 &BINP10  NORSET=0,    NBCHGE=0,    NCZONE=0,
          NCZPCH=0,    CZDUB=0.0,   VREF=0.0,                              &END
 &BINP11  NORPCH=0,    NORF=0,      NORL=0,
          NOCF=0,      NOCL=0,      VNORM=0.0,                             &END
 &BINP12  KPAN=0,      KSIDE=0,     NEWNAB=0,    NEWSID=0,                 &END
 &BINP13  NBLIT=0,                                                          &END


 &ASEM1   ASEMX=0.00,       ASEMY=0.00,       ASEMZ=0.00,
          ASCAL=1.00,       ATHET=0.00,       NODEA=5,                     &END
 &ASEM2   APXX=0.00,        APYY=0.00,        APZZ=0.00,
          AHXX=0.00,        AHYY=1.00,        AHZZ=0.00,                   &END


 &COMP1   COMPX= 0.0000,    COMPY= 0.0000,    COMPZ= 0.0000,
          CSCAL=  1.000,    CTHET=   0.0,     NODEC= 5,                    &END
 &COMP2   CPXX= 0.0000,     CPYY= 0.0000,     CPZZ= 0.0000,
          CHXX= 0.0000,     CHYY=  1.000,     CHZZ= 0.0000,                &END


 &PATCH1  IREV=  0, IDPAT= 1, MAKE=   0, KCOMP= 1, KASS= 1, IPATSYM=1,
          IPATCOP=0,                                                      &END
           WING
 &SECT1   STX=    0.0000, STY= 0.0000,    STZ= 0.0000,    SCALE=  2.00 ,
          ALF=   0.0,  THETA=   0.0,
          INMODE=  5,  TNODS= 0,    TNPS=  0,    TINTS= 0,                &END
 &SECT2   RTC=    0.01, RMC= 0.00,    RPC= 1.00,
          IPLANE=  2,  TNPC= 15,    TINTC= 0,                             &END
 &SECT1   STX=   5.0, STY= 5.0,    STZ= 0.0000,    SCALE=  2.00,
          ALF=   0.0,  THETA=   0.0,
          INMODE=  0,  TNODS= 3,    TNPS= 10,    TINTS= 2,                &END


 &PATCH1  IREV=  0, IDPAT= 1, MAKE=   1, KCOMP= 1, KASS= 1, IPATSYM=1,
          IPATCOP=0,                                                      &END
           WING_TIP
 &PATCH2  ITYP=  2,    TNODS= 5,    TNPS=   4,   TINTS= 3,               &END


 &WAKE1   IDWAK=1,          IFLXW=1,          ITRFTZ= 0,        INTRW= 0,  &END
  WING_WAKE
 &WAKE2   KWPACH=2,         KWSIDE=4,         KWLINE=0,         KWPAN1=0,
          KWPAN2=0,         NODEW=0,          INITIAL=0,                   &END
 &WAKE2   KWPACH=1,         KWSIDE=2,         KWLINE=0,         KWPAN1=0,
          KWPAN2=0,         NODEW=5,          INITIAL=0,                   &END


 &ONSTRM  NONSL =0,  KPSL = 20,                                             &END


 &BLPARAM RN =35755000,    VISC = 0.000157, NSLBL = 1,                      &END


 &VS1     NVOLR= 0,        NVOLC= 0,                                       &END
 &VS2     X0=    -0.1000, Y0=     1.5000, Z0=    -0.1000, INTVSR= 1,       &END
 &VS3     X1=    -0.1000, Y1=     1.5000, Z1=     0.1000, NPT1=  0,        &END
 &VS4     X2=    -0.1000, Y2=     1.5000, Z2=     0.1000, NPT2= 20,        &END
```

Jan 28 1995 11:59:41 **examp7_2.in** Page 2

```
 &VS5     X3=     1.1000, Y3=     1.5000, Z3=    -0.1000, NPT3= 25,        &END

 &VS6     XR0=    2.0000, YR0=    2.0000, ZR0=    0.0000,'INTVSC= 1,       &END
 &VS7     XR1=    4.0000, YR1=    2.0000, ZR1=    0.0000,
          XR2=    2.0000, YR2=    2.0000, ZR2=    1.0000,                  &END
 &VS8     R1=     0.1000, R2=     1.0000, PHI1=  0.0,      PHI2=360.0,     &END
 &VS9     NRAD=   5,      NPHI=   12,     NLEN=   3,                       &END


 &SLIN1   NSTLIN=0,                                                         &END
 &SLIN2   SX0=   -2.0000, SY0=    1.0000, SZ0=   -0.5000,
          SU=     0.0000, SD=    10.0000, DS=    0.2500, INTSL= 1,         &END
 &SLIN2   SX0=   -2.0000, SY0=    1.0000, SZ0=   -0.4000,
          SU=     0.0000, SD=    10.0000, DS=    0.2500, INTSL= 1,         &END
 &SLIN2   SX0=   -2.0000, SY0=    1.0000, SZ0=   -0.3000,
          SU=     0.0000, SD=    10.0000, DS=    0.2500, INTSL= 1,         &END
 &SLIN2   SX0=   -2.0000, SY0=    1.0000, SZ0=   -0.2000,
          SU=     0.0000, SD=    10.0000, DS=    0.2500, INTSL= 1,         &END
 &SLIN2   SX0=   -2.0000, SY0=    1.0000, SZ0=   -0.1000,
          SU=     0.0000, SD=    10.0000, DS=    0.2500, INTSL= 1,         &END
 &SLIN2   SX0=   -2.0000, SY0=    1.0000, SZ0=    0.0000,
          SU=     0.0000, SD=    10.0000, DS=    0.2500, INTSL= 1,         &END
```

Figure 3.3 PMARC Input File for Swept Planar Wing, Taper Ratio of Unity, AR=5, Sweep=45 Degrees.

a. Basic Input Section

When referring to the PMARC manual (Ref. [1]) for the definition of each of the variables, it becomes rather straightforward which values are to be entered in each field of the Basic Input Section. As mentioned in Chapter **II**, for most of the cases, only the following fields require attention: LENRUN, NTSTPS, DTSTEP, ALDEG, and SREF, although we will also continually fill CBAR, and SSPAN. Some others like VINF and VSOUND can be entered with actual values to represent the freestream velocity and the altitude but these won't have any impact on the lift coefficients and pressure distribution results. It is to be noted that the lift, normal force, moment and drag coefficients are sensitive to the fields CBAR, SREF, and SSPAN, as the velocity components, the pressure coefficient, DUB, and dPHI/dT are not. The remaining fields should be filled with zeros or numbers taken from existing DATA5 files. Although they too don't have any impact on the above mentioned coefficients, numbers have to be entered for the software to operate.

One important point is the steady state status. Because of the time-stepping capability of PMARC, results are generated right from the first moment of the 'flight', while the circulation is initiated and the starting vortex generated. If the user is interested in the steady state results, which is when the starting vortex is far enough from the trailing edge (five or six chord length), a proper combination of number of time-steps (NTSTPS) and distance between each time-step (DTSTEP) will be required. Using the freestream velocity, this calculation is easy to perform. For instance, a wing with a chord of 11 units would require the starting vortex to be at a minimum of 55 units behind the trailing edge in order to assume steady state. If the freestream velocity is 11 units/sec, then 5 seconds of flight are needed (55 units divided by 11 units/sec). Then any combination of NTSTPS and DTSTEP whose product is at least 5 units will ensure steady state.

b. Assembly and Component Coordinate System Information

All the fields but two can be copied from those shown in Figure 3.3 for most of the cases we will be concerned with. The two fields that may require special attention are NODEA and NODEC. Their values indicate respectively if another assembly coordinate or component coordinate will be defined. Such additional coordinate systems could be required when modelling a wing-body combination, or two wings alone.

c. Patch and Section Coordinate System Information

All the fields in PATCH1 are straight forward when referring to the PMARC manual (Ref. [1]). The point to note here is the existence of more than one PATCH1 section within the input file. One introduces the patch that will be used to create the wing according to the geometric specifications given in the Section Coordinate section (SECT1 and SECT2), and the second one is for the wing tip which is further defined in PATCH2.

In SECT1, two fields are not relevant in steady state: ALF and THETA. All the others are crucial for a correct model definition. In this case, the origin of the root airfoil section definition is at coordinates (0, 0, 0). The root chord is two units. INMODE was set at 5 because in SECT2 we will generate a NACA 4 digit airfoil section for which PMARC has automatic section coordinate generation routines. All that is required are the thickness to chord ratio (RTC), the maximum camber to chord ratio (RMC), and the chordwise position of the airfoil's maximum camber (RPC). In this case, we are dealing with a flat plate. These three combinations all produce the same results:

RTC=0.01	RTC=0.01	RTC=0.01
RMC=0	RMC=0	RMC=0
RPC=0	RPC=1	RPC=0.5

In our case, the second approach was taken which corresponds to the NACA designation of 0001. It becomes obvious why the three combinations shown above work by noting that for a flat plate, there is no camber (RMC), therefore the position of maximum camber as described by the input field RPC has no impact, no matter what value is entered.

The second SECT1 section defines the location and section of the wing tip, or more specifically that flat surface where the wing tip would be attached. We see that in our case, the origin of that last patch's section is at the coordinates (5, 5, 0), and that its chord is also 2. As defined in Ref. [1], INMODE and TNODS seen in SECT1 and PATCH2 respectively are important fields. INMODE set to zero in the second SECT1 tells PMARC to copy the section definition of the previous SECT1. The TNODS fields indicate the status of the patch being defined: first, intermediate, last, etc.

Ten panels per side (TNPS=10) are requested spanwise for the specified patch. That means 20 panels spanwise for the complete wing on each surface. Fifteen panels are prescribed chordwise (TNPC=15) for the specified patch. That transpose into 15 panels on each surface of the wing. Note that TNPS can be specified only in the second SECT1 section. If both TNPS were set to zero, PMARC would use the points of the section definition it created to determine the number of panels.

As mentioned earlier, the second PATCH1 section along with PATCH2 are for the wing tip, and a circular arc tip patch was requested (ITYP=2).

Two fields were not discussed yet but become very important for the accuracy of the results. They are TINTS and TINTC. They are found in SECT1, SECT2, and PATCH2. They define the type of panel spacing on each patch (or wing and body surfaces). As it will be seen later for other configurations, the user might want to distribute more panels in areas where a sharper gradient of a parameter is known to exist. Figure 3.4 shows the available options of panel spacing for an arbitrary wing.

d. Wake and Streamlines

The streamlines are not required for our studies. However, the wake should be turned on (IDWAK=1) in all wing cases as it affects the flow field all around the wing. For the simple cases studied in this thesis, the type of wake selected (rigid or flexible) in the IFLXW field is not a crucial decision as this will not change the results.

4. PMARC Output - Data Retrieval

The results we are interested in are the lift coefficients (C_L) for various angles of attack. In order to do so, our input file has to be run repetitively, each time modifying the angle of attack. This will create a series of output files, DATA6, from which the C_L will be read. Several lift coefficients are presented in this output file: assembly, component, and total, in term of wind or body axes. For the present case, we need the total wing lift coefficient in terms of the wind axis which refers to the

freestream. This value is found towards the very end of the file under the heading *Wind Axes - Total coefficients*. The lift coefficient corresponding to our case is labelled CL. Note that when streamlines are requested, the related results are placed at the end of the file, following the coefficient results.

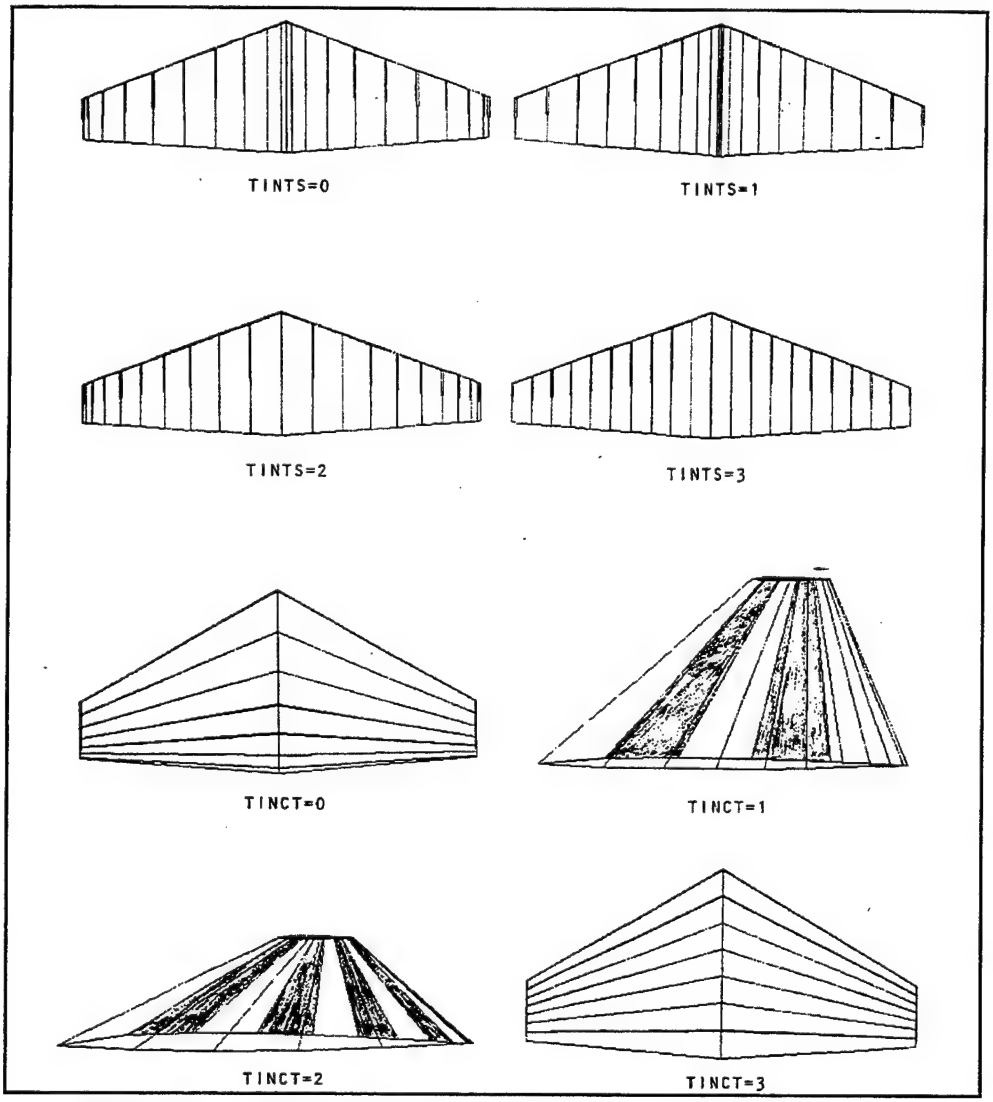

Figure 3.4 PMARC Options of Chordwise and Spanwise Panel Distributions.

C. SWEPT BACK WING II

Our second project was to model a cambered swept back wing. The wing considered had a NACA 64A010 section, an AR of 3, a tip to root chord ratio of 0.5 and a 45 degrees swept back of the quarter-chord line. A value of the root chord *Cr* was arbitrarily set at 10, allowing the finite coordinates as shown on Figure 3.5.

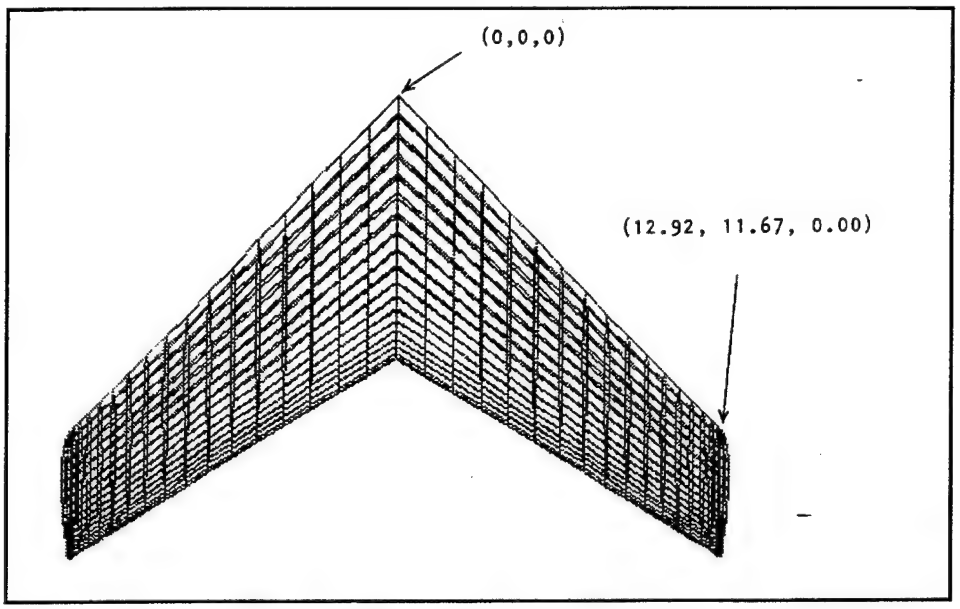

Figure 3.5 Swept Back Wing, NACA 64A010 Section, AR=3, Taper Ratio=0.5, Sweep=45 Degrees.

1. Theory, Background, and Reference Data

Margason et al. (Ref. [6]) compared computed aerodynamic coefficients using the Vortex Lattice Method, source panel method, low-order surface potential distributions, and high-order surface potential distributions to experimental data. This provided an ideal opportunity to see how PMARC would measure up.

2. Results and Discussion

The results are shown on Figure 3.6. It can be observed that all surface potential and source panel methods overpredict the experimental data. However, each of them show little difference between their lift coefficients, PMARC included. The results for the Vortex Lattice Method are not presented, but Margason reports that they predict the experimental data very well, due to the fact that VLM neglects both thickness and viscosity effects.

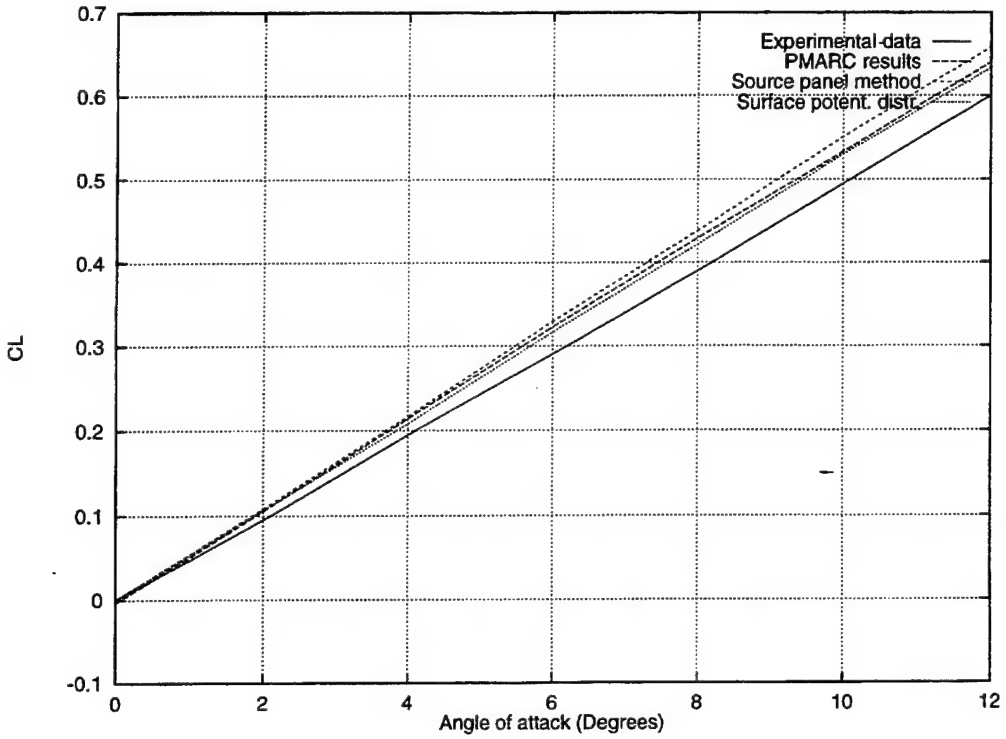

Figure 3.6 Comparison of The Lift Coefficient as a Function of Angle of Attack. Aft Swept Wing, NACA 64A010 Section, AR=3, Taper Ratio=0.5, Sweep=45 Degrees.

Although PMARC did not recreate exactly the experimental data for the NACA 64A010 swept back wing, its deviation from the latter is still acceptable. Furthermore, its results compare very well with other computer methods, even with panel codes of higher order.

3. PMARC Input Instructions

The following sub-subsections will not repeat information presented for the swept back flat plate that still hold for the cambered swept-back wing. Instead, we will concentrate on the differences, the particularities, and some lessons learned. The input file is shown in Figure 3.7.

a. Basic Input Section

All the fields in this section can remain the same as for the flat plate case, except for CBAR, SREF, and SSPAN. Of course, the angle of attack (ALDEG) has to be adjusted as required. Also, VINF and VSOUND could be changed, although there is no need to do so.

b. Assembly and Component Coordinate System Information

No changes are required in these two sections. As it can be seen in the definition section of Ref. [1], these terms become important when multiple components are involved, or when a component needs to be rotated or translated.

c. Patch and Section Coordinate System Information

The PATCH1 sections for both the flat plate and cambered cases are identical. The PATCH2 lines have for only difference the panel field (TNPS). It could have been the same as in each case it was an arbitrary decision. This field defines the number of chordwise (longitudinal) cuts on the wing tip, which along with the vertical cuts will define the number of panels on the tip (Figure 3.8). TNPS of PATCH2 can be kept low without altering the results. Fewer panels speeds up the computation and in this case alleviates a message in the output file warning the user that some panels have virtually no area. Although this warning did not seem to affect any of the results, caution should be exercised and more investigation should be pursued in this area. It is to be noted that Figure 3.8 shows a flat tip only for panels illustration purposes. All our wings have rounded tips (except in the case of the delta wings).

```
Aug 17 1995 14:19          swback1.in                Page 1

 Swept Back Wing: NACA-64A010  Sweep angle=45, AR=3, Ct/Cr=0.5

 &BINP2   LSTINP=2,     LSTOUT=0,     LSTFRQ=0,     LENRUN=0,     LPLTYP=1,     &END
 &BINP3   LSTGEO=0,     LSTNAB=0,     LSTMAK=0,     LSTCPV=0,                   &END
 &BINP4   MAXIT=50,     SOLRES=0.01,                                            &END
 &BINP5   NTSTPS= 10,   DTSTEP=0.5,                                             &END
 &BINP6   RSYM=1.0,     RGPR=0.0,     RFF=5.0,   RCORES=0.0080, RCOREW=0.0080, &END
 &BINP7   VINF=11.0,    VSOUND=1116.0,                                          &END
 &BINP8   ALDEG= 10.00, YAWDEG=0.0,   PHIDOT=0.0,  THEDOT=0.0,  PSIDOT=0.0,    &END
 &BINP8A  PHIMAX= 0.0,  THEMAX= 0.0,  PSIMAX=0.0,
          WRX=0.0,      WRY=0.0,      WRZ=0.0,                                  &END
 &BINP8B  DXMAX=0.0,    DYMAX=0.0,    DZMAX=0.0,
          WTX=0.0,      WTY=0.0,      WTZ=0.0,                                  &END
 &BINP9   CBAR=7.78,    SREF=181.48,     SSPAN= 11.67,
          RMPX=3.63,    RMPY=0.00,    RMPZ=0.00,                                &END
 &BINP10  NORSET=0,     NBCHGE=0,     NCZONE=0,
          NCZPCH=0,     CZDUB=0.0,    VREF=0.0,                                 &END
 &BINP11  NOCP=0,       NORP=0,       NORL=0,
          NOCP=0,       NOCL=0,       VNORM=0.0,                                &END
 &BINP12  KPAN=0,       KSIDE=0,      NEWNAB=0,     NEWSID=0,                   &END
 &BINP13  NBLIT=0,                                                              &END

 &ASEM1   ASEMX=0.00,   ASEMY=0.00,   ASEMZ=0.00,
          ASCALI=1.00,  ATHET=0.00,   NODEA=5,                                  &END
 &ASEM2   APXX=0.00,    APYY=0.00,    APZZ=0.00,
          AHXX=0.00,    AHYY=1.00,    AHZZ=0.00,                                &END

 &COMP1   COMPX= 0.0000,  COMPY= 0.0000,  COMPZ= 0.0000,
          CSCALI= 1.000,  CTHET=  0.0,    NODEC= 5,                            &END
 &COMP2   CPXX= 0.0000,   CPYY= 0.0000,   CPZZ= 0.0000,
          CHXX= 0.0000,   CHYY= 1.000   ,  CHZZ= 0.0000,                       &END

 &PATCH1  IREV=  0, IDPAT= 1, MAKE=   0, KCOMP= 1, KASS= 1, IPATSYM=1,
          IPATCOP=0,                                                          &END
          WING
 &SECT1   STX=    0.0000, STY= 0.0000,    STZ= 0.0000,    SCALE=  10,
          ALF=    0.0,    THETA=  0.0,
          INMODE=  4,     TNODS=  0,    TNPS=  18,    TINTS= 2,               &END
 1.00000  0.000  0.00021
 0.95000  0.000 -0.00541
 0.90000  0.000 -0.01062
 0.85000  0.000 -0.01582
 0.80000  0.000 -0.02103
 0.75000  0.000 -0.02623
 0.70000  0.000 -0.03127
 0.65000  0.000 -0.03597
 0.60000  0.000 -0.04021
 0.55000  0.000 -0.04388
 0.50000  0.000 -0.04684
 0.45000  0.000 -0.04894
 0.40000  0.000 -0.04995
 0.35000  0.000 -0.04968
 0.30000  0.000 -0.04837
 0.25000  0.000 -0.04606
 0.20000  0.000 -0.04272
 0.15000  0.000 -0.03813
 0.10000  0.000 -0.03199
 0.07500  0.000 -0.02905
 0.05000  0.000 -0.02327
 0.02500  0.000 -0.01688
 0.01250  0.000 -0.01225
 0.00750  0.000 -0.00969
 0.00500  0.000 -0.00804
 0.00000  0.000  0.00000
```

```
Aug 17 1995 14:19          swback1.in                Page 2

 0.20000  0.000  0.04272
 0.25000  0.000  0.04606
 0.30000  0.000  0.04837
 0.35000  0.000  0.04968
 0.40000  0.000  0.04995
 0.45000  0.000  0.04894
 0.50000  0.000  0.04684
 0.55000  0.000  0.04388
 0.60000  0.000  0.04021
 0.65000  0.000  0.03597
 0.70000  0.000  0.03127
 0.75000  0.000  0.02623
 0.80000  0.000  0.02103
 0.85000  0.000  0.01582
 0.90000  0.000  0.01062
 0.95000  0.000  0.00541
 1.00000  0.000  0.00021
 &BPNODE    TNODE=3      TNPC=40    TINTC=0     &END
 &SECT1     STX=  12.92, STY= 11.67,   STZ= 0.0000,   SCALE=  5 ,
            ALF=   0.0,  THETA=  0.0,
            INMODE=  4,  TNODS=  3,   TNPS=  18,   TINTS= 2,                &END
 1.00000  0.000  0.00021
 0.95000  0.000 -0.00541
 0.90000  0.000 -0.01062
 0.85000  0.000 -0.01582
 0.80000  0.000 -0.02103
 0.75000  0.000 -0.02623
 0.70000  0.000 -0.03127
 0.65000  0.000 -0.03597
 0.60000  0.000 -0.04021
 0.55000  0.000 -0.04388
 0.50000  0.000 -0.04684
 0.45000  0.000 -0.04894
 0.40000  0.000 -0.04995
 0.35000  0.000 -0.04968
 0.30000  0.000 -0.04837
 0.25000  0.000 -0.04606
 0.20000  0.000 -0.04272
 0.15000  0.000 -0.03813
 0.10000  0.000 -0.03199
 0.07500  0.000 -0.02905
 0.05000  0.000 -0.02327
 0.02500  0.000 -0.01688
 0.01250  0.000 -0.01225
 0.00750  0.000 -0.00969
 0.00500  0.000 -0.00804
 0.00000  0.000  0.00000
 0.00500  0.000  0.00804
 0.00750  0.000  0.00969
 0.01250  0.000  0.01225
 0.02500  0.000  0.01688
 0.05000  0.000  0.02327
 0.07500  0.000  0.02905
 0.10000  0.000  0.03199
 0.15000  0.000  0.03813
 0.20000  0.000  0.04272
 0.25000  0.000  0.04606
 0.30000  0.000  0.04837
 0.35000  0.000  0.04968
 0.40000  0.000  0.04995
 0.45000  0.000  0.04894
 0.50000  0.000  0.04684
 0.55000  0.000  0.04388
 0.60000  0.000  0.04021
 0.65000  0.000  0.03597
 0.70000  0.000  0.03127
 0.75000  0.000  0.02623
 0.80000  0.000  0.02103
 0.85000  0.000  0.01582
 0.90000  0.000  0.01062
 0.95000  0.000  0.00541
 1.00000  0.000  0.00021
 &DPNODE    TNODE=3      TNPC=40    TINTC=0     &END

 &PATCH1  IREV=  0, IDPAT= 1, MAKE=   1, KCOMP= 1, KASS= 1, IPATSYM=1,
```

Figure 3.7 PMARC Input File for an Aft Swept Wing, NACA 64A010 Section, AR=3, Taper Ratio=0.5, Sweep=45 Degrees

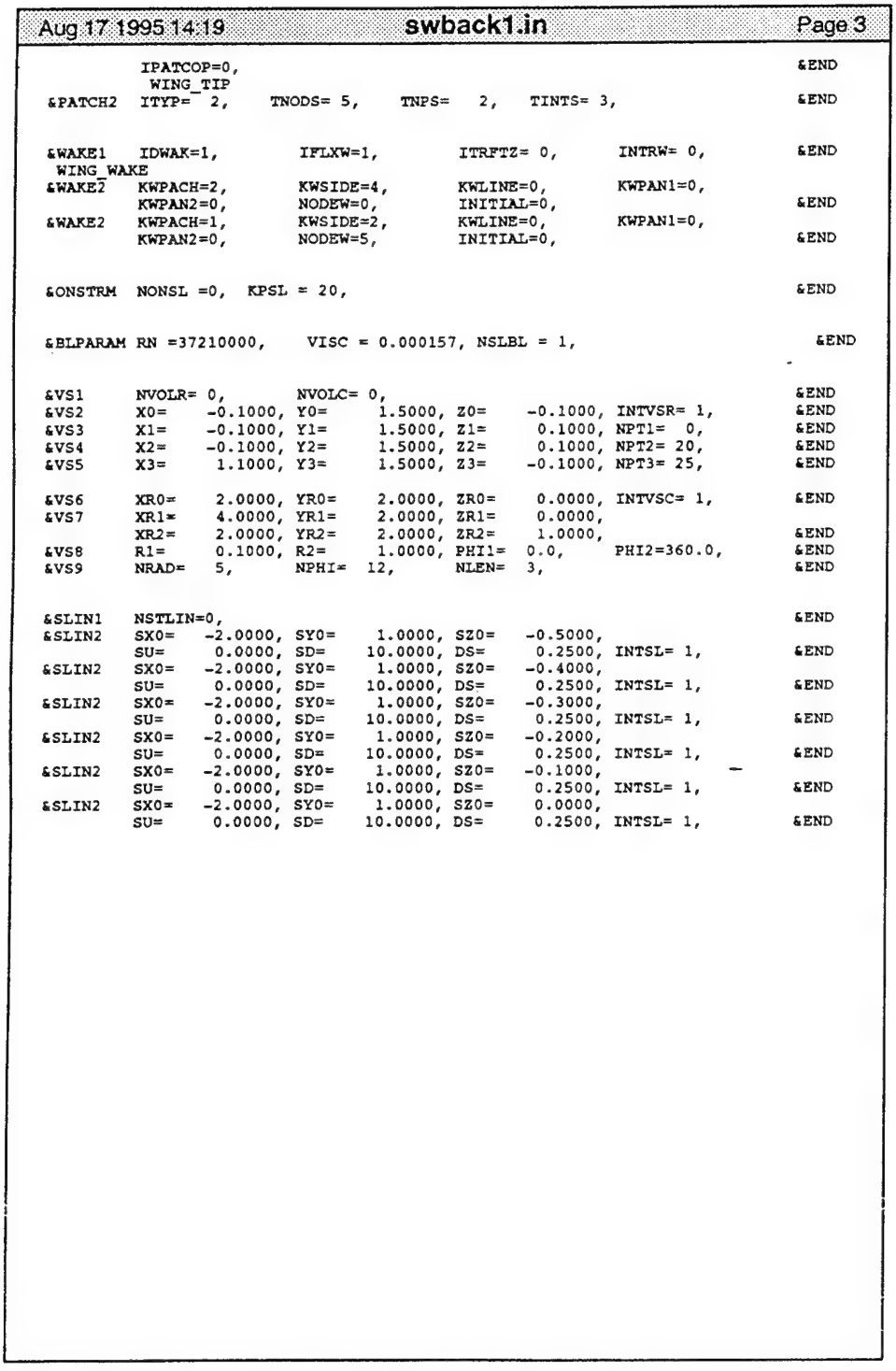

```
Aug 17 1995 14:19          swback1.in                    Page 3

          IPATCOP=0,                                                    &END
           WING_TIP
&PATCH2   ITYP=  2,    TNODS= 5,    TNPS=   2,   TINTS= 3,             &END


&WAKE1    IDWAK=1,        IFLXW=1,        ITRFTZ= 0,      INTRW= 0,     &END
 WING_WAKE
&WAKE2    KWPACH=2,       KWSIDE=4,       KWLINE=0,       KWPAN1=0,
          KWPAN2=0,       NODEW=0,        INITIAL=0,                    &END
&WAKE2    KWPACH=1,       KWSIDE=2,       KWLINE=0,       KWPAN1=0,
          KWPAN2=0,       NODEW=5,        INITIAL=0,                    &END


&ONSTRM   NONSL =0,  KPSL = 20,                                         &END


&BLPARAM RN =37210000,    VISC = 0.000157, NSLBL = 1,                     &END


&VS1      NVOLR= 0,       NVOLC= 0,                                     &END
&VS2      X0=    -0.1000, Y0=     1.5000, Z0=    -0.1000, INTVSR= 1,    &END
&VS3      X1=    -0.1000, Y1=     1.5000, Z1=     0.1000, NPT1=  0,     &END
&VS4      X2=    -0.1000, Y2=     1.5000, Z2=     0.1000, NPT2= 20,     &END
&VS5      X3=     1.1000, Y3=     1.5000, Z3=    -0.1000, NPT3= 25,     &END

&VS6      XR0=    2.0000, YR0=    2.0000, ZR0=    0.0000, INTVSC= 1,    &END
&VS7      XR1=    4.0000, YR1=    2.0000, ZR1=    0.0000,
          XR2=    2.0000, YR2=    2.0000, ZR2=    1.0000,               &END
&VS8      R1=     0.1000, R2=     1.0000, PHI1=  0.0,     PHI2=360.0,   &END
&VS9      NRAD=   5,      NPHI=  12,      NLEN=  3,                     &END


&SLIN1    NSTLIN=0,                                                     &END
&SLIN2    SX0=   -2.0000, SY0=    1.0000, SZ0=   -0.5000,
          SU=     0.0000, SD=    10.0000, DS=     0.2500, INTSL= 1,     &END
&SLIN2    SX0=   -2.0000, SY0=    1.0000, SZ0=   -0.4000,
          SU=     0.0000, SD=    10.0000, DS=     0.2500, INTSL= 1,     &END
&SLIN2    SX0=   -2.0000, SY0=    1.0000, SZ0=   -0.3000,
          SU=     0.0000, SD=    10.0000, DS=     0.2500, INTSL= 1,     &END
&SLIN2    SX0=   -2.0000, SY0=    1.0000, SZ0=   -0.2000,
          SU=     0.0000, SD=    10.0000, DS=     0.2500, INTSL= 1,     &END
&SLIN2    SX0=   -2.0000, SY0=    1.0000, SZ0=   -0.1000,
          SU=     0.0000, SD=    10.0000, DS=     0.2500, INTSL= 1,     &END
&SLIN2    SX0=   -2.0000, SY0=    1.0000, SZ0=    0.0000,
          SU=     0.0000, SD=    10.0000, DS=     0.2500, INTSL= 1,     &END
```

Figure 3.7 Cont'd PMARC Input File for an Aft Swept Wing, NACA 64A010 Section, AR=3, Taper Ratio=0.5, Sweep=45 Degrees

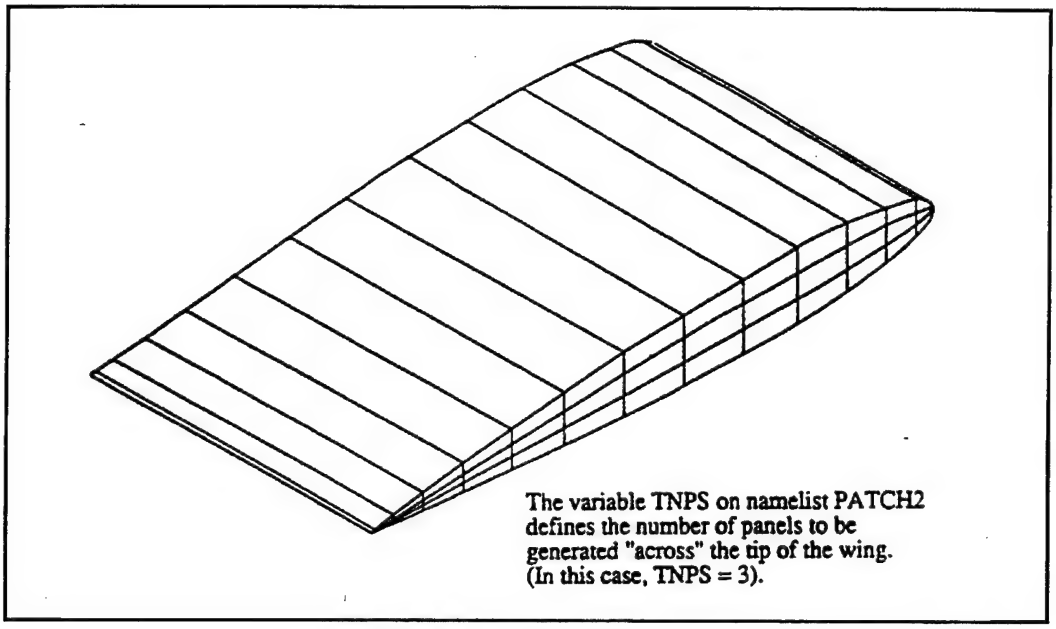

Figure 3.8 Wing Tip Panels.
(From Ref. [1])

The SECT1 and SECT2 combination is different for this case of cambered wing. Instead of a four digit NACA airfoil section, we now have a section definition for which PMARC has no automatic construction routine. We then have to enter the coordinates of the airfoil section definition. For this reason, SECT2 is not required anymore, as it is only used in the case where a four digit NACA airfoil is wanted.

We will still observe two SECT1 sections: one for each end of the patch (or wing). The differences between the two reside in the coordinates of the origins of each section starting and ending the patch. Also, the scaling is different, meaning that the outside edge of the patch (wing tip) has a different length than the inside edge (wing root). An important field here is INMODE. It is set at four in the first SECT1 of the cambered wing input file to indicate that the patch coordinates follow. In the flat plate input file, the first INMODE was set at five requesting that PMARC generate an NACA four digit airfoil section. The second INMODE is set at zero, instructing PMARC to copy the section definition of the previous section. The same thing could have been done with the cambered wing instead of redefining the section definition for the tip.

The manual entry of the section definition should be done carefully. Some entry will not cause a system error, but will produce bad results. For instance, if the patch coordinates are entered starting at the origin (0 0 0), PMARC will try to satisfy the Kutta condition at the leading edge instead of at the trailing edge. Therefore, an important lesson learned while exploring PMARC was to understand how the patches are defined and folded (Ref. [1]). For the case of any wing, the section definition always starts at the trailing edge, going under the wing, around the leading edge and up towards the trailing edge (Figure 3.9).

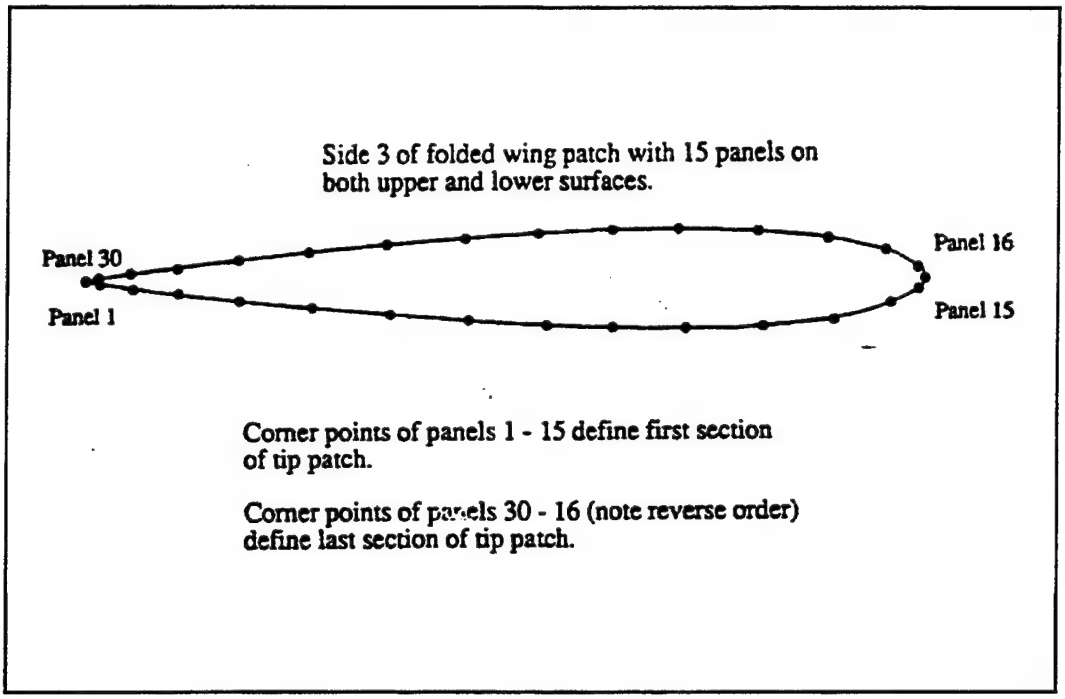

Figure 3.9 Wing Cross-Section Definition Sequence.
(From Ref. [1])

There is more than one way to use the coordinate system to define a section. That is controlled by the field INMODE in SECT1. Depending on its value, the three columns of data will have different meanings (refer to page 53 of Ref. [1]). In the present case, the three columns respectively represent the x, y, and z coordinates of each point defining the section. This section definition of the NACA 64A010 was taken in Ref. [7].

As well illustrated in Ref. [2], and in the test case of Ref. [1], more than one means are available to shape the required dimensions into our wing sections. In the present case, we elected to non-dimensionlize the section definition and then scale it to the chord and tip dimensions respectively. Another way would have been to enter the global coordinates of the root and tip sections.

d. Wake and Streamlines

As mentioned in the previous section, we need to leave the wake active (IDWAK=1) as we do not need the streamlines option.

4. PMARC Output - Data Retrieval

Once again, as for the swept back wing of the previous section, we are interested in are the lift coefficients (C_L) for various angles of attack. In order to do so, our input file has to be run repetitively, each time modifying the angle of attack. This will create a series of output files, DATA6, from which the C_L will be read. Several lift coefficients are presented in this output file: assembly, component, and total, in term of wind or body axes. For the present case, we need the total wing lift coefficient in terms of the wind axis which refers to the freestream. This value is found towards the very end of the file under the heading Wind Axes - Total coefficients. The lift coefficient corresponding to our case is labelled CL. Note that when streamlines are requested, the related results are placed at the end of the file, following the coefficient results.

D. DELTA WINGS

A good amount of experimental data is available for delta wings, allowing a wider spectrum of comparison. Four different delta wings were modeled, each having different aspect ratio (AR), but all with a NACA 0012 airfoil section designation. In order to obtain finite geometric parameters, the span was arbitrarily set at 10 in all cases. Figure 3.10 shows those configurations.

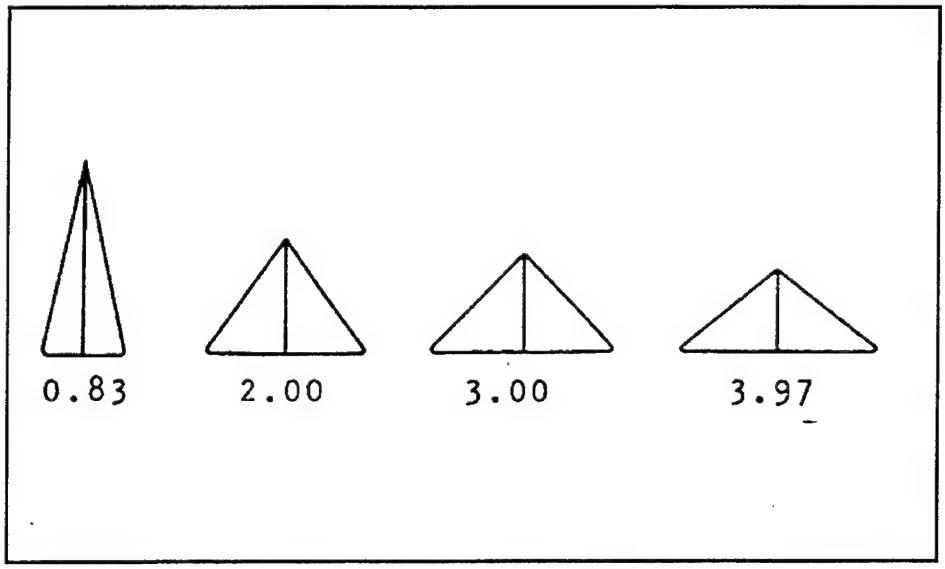

Figure 3.10 Delta Wings of Various Aspect Ratio.

1. Theory, Background and Reference Data

Prediction and control of flow separation is a major aerodynamic consideration in wing design. Effort to avoid undesirable compressibility effects leads to greater sweep angle and reduced section thickness. However, these efforts are offset by the increasing difficulty to prevent boundary-

layer separation. Schlichting and Truckenbrodt (Ref. [8]), and also Ashley and Landahl (Ref. [9]) studied the influence of the delta wing aspect ratio on the lift coefficients and the boundary layer separation. The purpose of our study is not to draw any conclusion with regard to flow separation and AR influence using our PMARC computation but rather to try to recreate some of the experimental results obtained by the above mentioned researchers.

Our comparative study will present five sets of data. We will first compare the lift coefficients of the delta wings of AR 0.83 and 3.97 obtained by PMARC with the available experimental data. Then a plot of the lift curve slope as a function of the AR will be built with the PMARC results of four different AR wings. Finally, the chordwise and spanwise pressure distributions for the delta wing of AR=3 will be established using PMARC and compared to the literature.

2. Results and Discussion

The first delta wing modeled had an aspect ratio of 0.83. The lift coefficient for various angles of attack as obtained with PMARC is shown compared to the experimental data on Figure 3.11. Very good agreement exists at low angles of attack but above 10 degrees, PMARC underpredicted the experimental data. This situation was encountered before in this paper and as it was mentioned then, this disparity at higher angles of attack does not invalidate PMARC. These results were expected as PMARC only models linear angle of attack effects and therefore does not account for nonlinear phenomena encountered at high angles of attack. Therefore, for the lower angles of attack, PMARC recreates the experimental data very well.

The same phenomena occur with the delta wing of aspect ratio 3.97 where the CL obtained by PMARC steadily and linearly increases with angle of attack (Figure 3.12). The difference here is that PMARC overpredicted the lift coefficient values. Again, for the linear portion of the experimental data, PMARC is in close agreement.

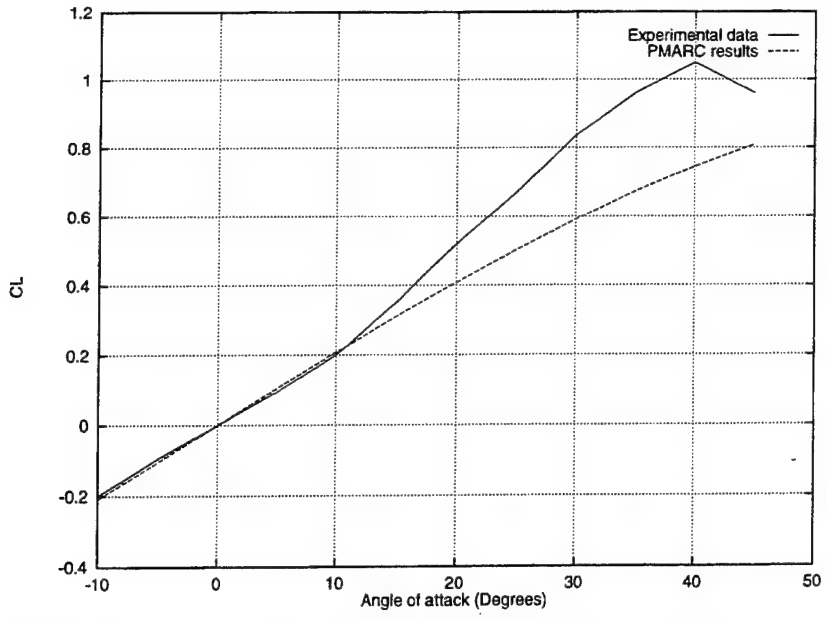

Figure 3.11 Comparison of The Lift Coefficient as a Function of Angle of Attack. Delta Wing, NACA 0012 Section, AR=0.83.

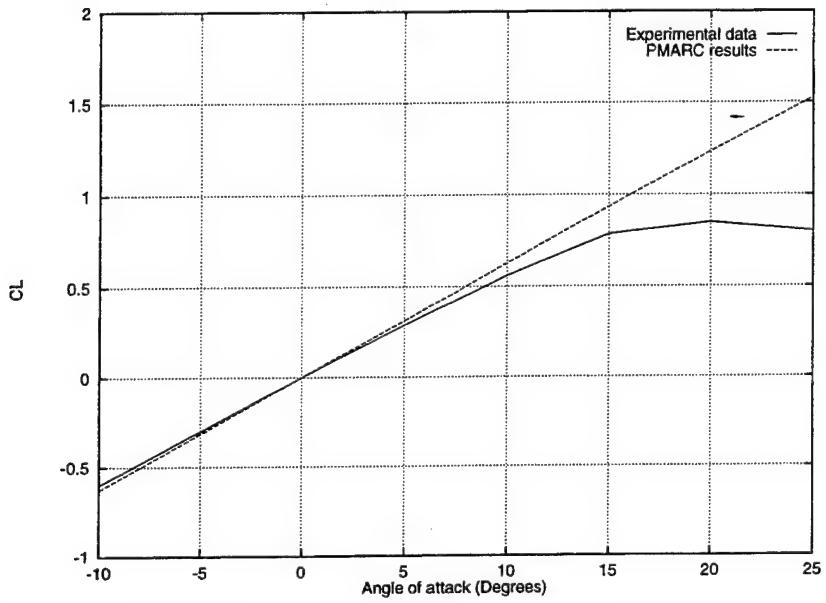

Figure 3.12 Comparison of The Lift Coefficient as a Function of Angle of Attack. Delta Wing, NACA 0012 Section, AR=3.97.

The next figure (Figure 3.13) shows the lift curve slope as a function of aspect ratio. Again, the PMARC results display good agreement with past work (Ref. [9]). It is shown there that the lifting-surface theory predicted very well two sets of experimental data produced at different time by different people. We superposed the PMARC output onto these combined results to show the very good agreement.

We have so far observed that PMARC seems to compute fairly accurately the lift coefficient. Another parameter should now be introduced in order to better assess this panel code. As such, the last two sets of results presented in this section will deal with the pressure distribution for a delta wing of aspect ratio equal to three and an angle of attack of 10 degrees.

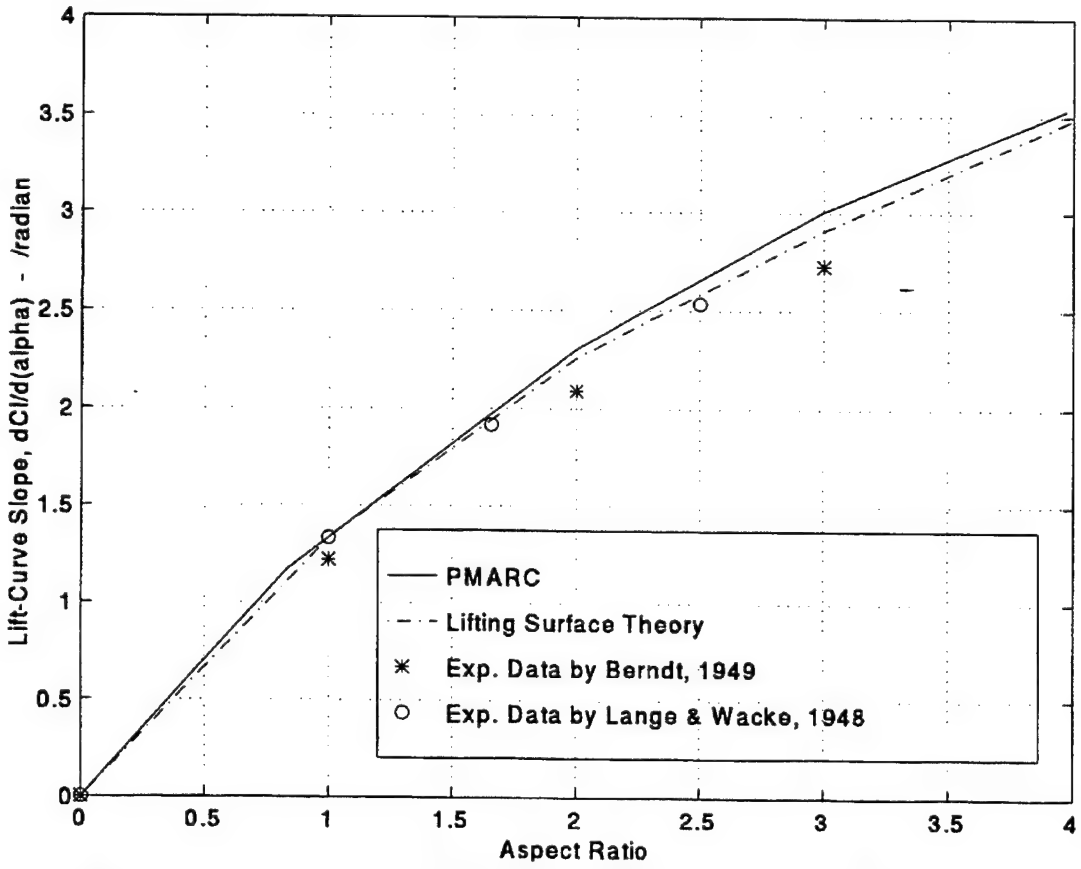

Figure 3.13 Comparison of Lift-Curve Slope as a Function of Aspect Ratio.

The chordwise and spanwise distributions are shown on Figures 3.14 and 3.15. Figures 3.16 and 3.17 taken from Ref. [17] show experimental spanwise pressure distributions. Some irregularities appear to be present in the PMARC output of the spanwise distribution towards the edges of the spanwise sections considered. The pressure do not seem to come back down as shown on Figure 3.17. Either we do not have enough points or the panel layout can not pick up the correct behavior of the flow in these regions of greater gradient. Note that the PMARC spanwise distribution plotted are in reality approximations to the real spanwise distribution. What is plotted is actually the pressure distribution along a slanted spanwise cross-section that corresponds to panel numbers easy to retrieve out of the output file. More detail on this topic will be given in subsection **4**. Also, the reader should keep in mind that Figures 3.16 and 3.17 represent visous flows.

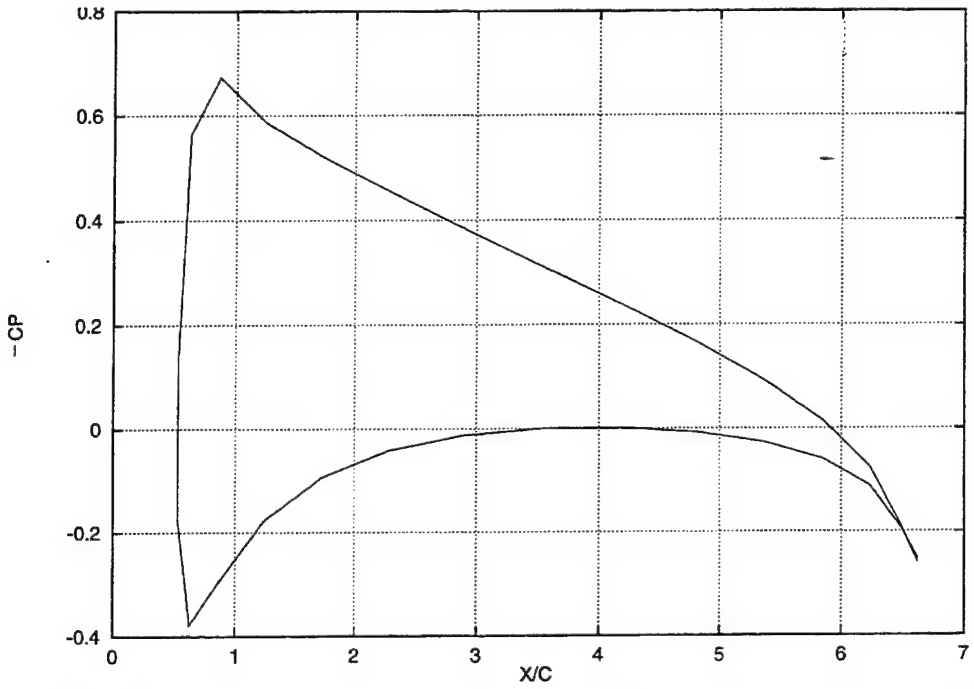

Figure 3.14 Chordwise Pressure Distribution at 10 Degrees Angle of Attack. Delta Wing, NACA 0012 Section, AR=3.

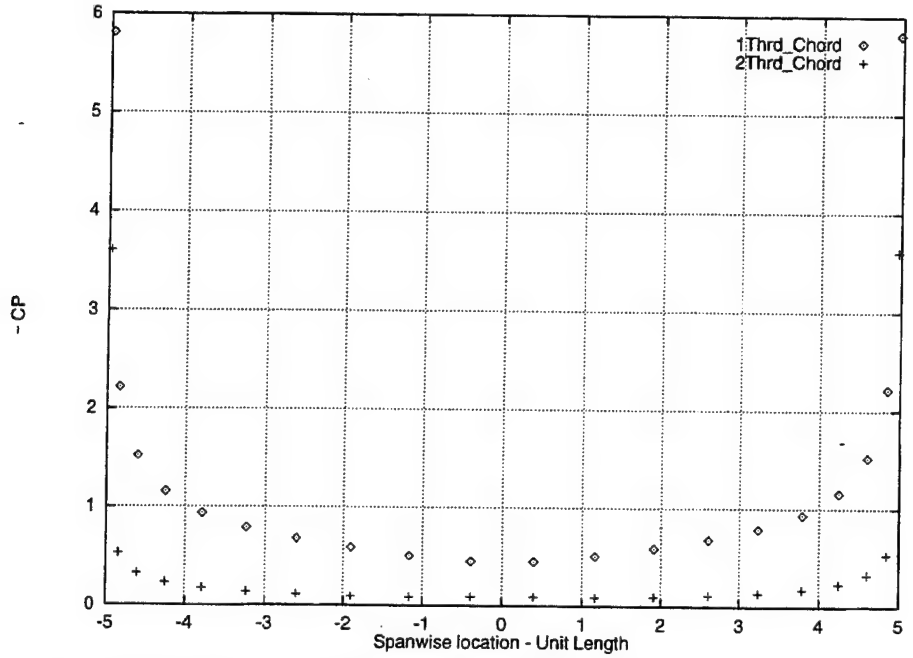

Figure 3.15 Approximate Top Spanwise Pressure Distribution at 10 Degrees Angle of Attack for 1/3 and 2/3 Chord Locations. Delta Wing, NACA 0012 Section, AR=3.

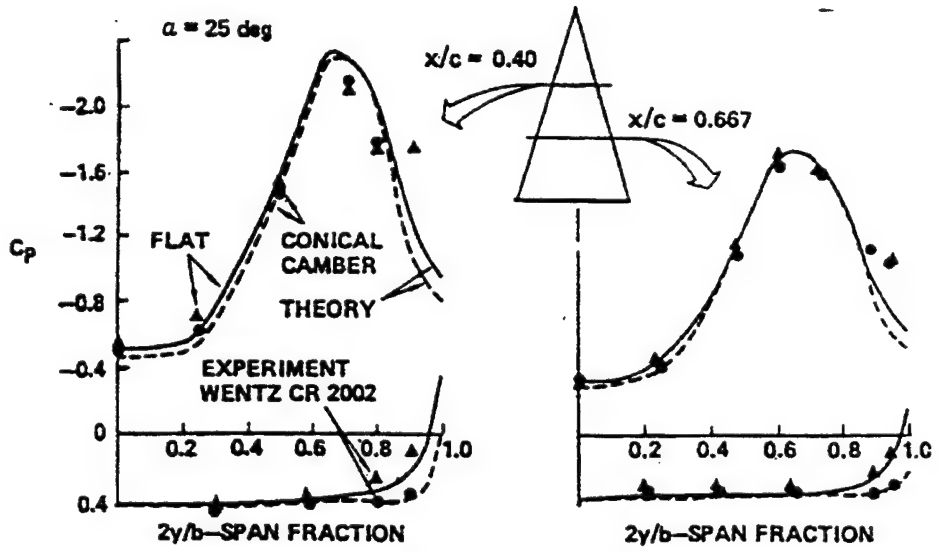

Figure 3.16 Spanwise Pressure Distribution Over a Flat and Cambered Delta Wing, AR=1.15, AOA=25 Degrees. (From Ref. [17])

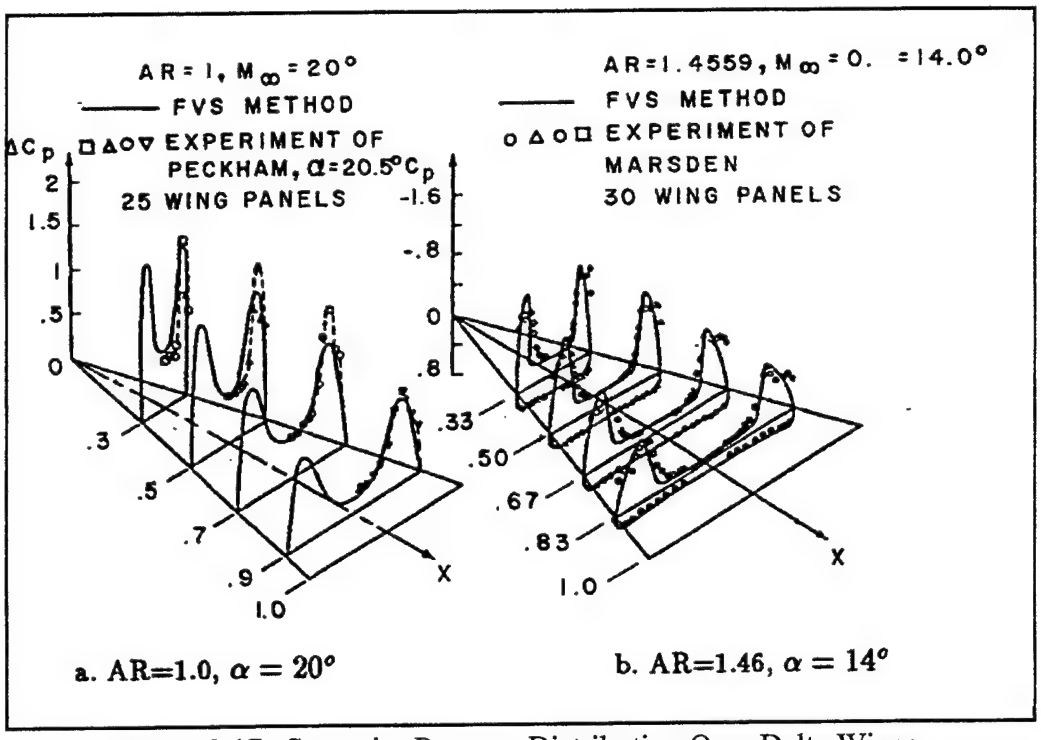

Figure 3.17 Spanwise Pressure Distribution Over Delta Wings. (From Ref. [17])

3. PMARC Input Instructions

Five input files were required to obtain all the results presented in this section. They were all identical except for the section sizing and coordinates (SECT1) and SREF. These sets of fields correspond to the specific wing geometry as well as to the root and tip section origins. One sample for the delta wing of aspect ratio 0.83 is shown in Figure 3.18. The fields mentioned above are also the only differences between the delta wing input files and the swept back flat plate input file of our first test case. Therefore, no time will be spent here to go over each section of the input file. Instead, we will discuss a particularity of the delta wing modelling in PMARC. Also a sensitivity test performed on some fields will be discussed.

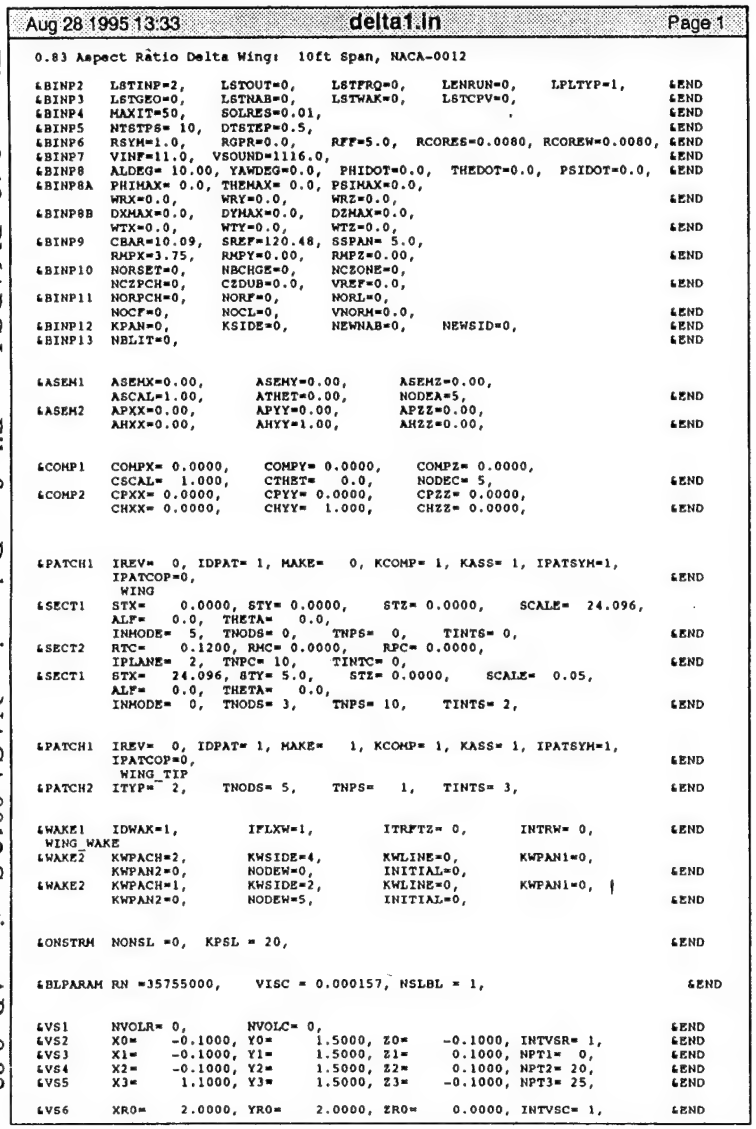

Aug 28 1995 13:33 **delta1.in** Page 1

```
0.83 Aspect Ratio Delta Wing:  10ft Span, NACA-0012

&BINP2   LSTINP=2,    LSTOUT=0,    LSTFRQ=0,    LENRUN=0,    LPLTYP=1,    &END
&BINP3   LSTGEO=0,    LSTNAB=0,    LSTWAK=0,    LSTCPV=0,                 &END
&BINP4   MAXIT=50,    SOLRES=0.01,                                        &END
&BINP5   NTSTPS= 10,  DTSTEP=0.5,                                         &END
&BINP6   RSYM=1.0,    RGPR=0.0,    RFF=5.0,  RCORES=0.0080, RCOREW=0.0080, &END
&BINP7   VINF=11.0,  VSOUND=1116.0,                                       &END
&BINP8   ALDEG= 10.00, YAWDEG=0.0,  PHIDOT=0.0,  THEDOT=0.0,  PSIDOT=0.0, &END
&BINP8A  PHIMAX= 0.0, THEMAX= 0.0, PSIMAX=0.0,
         WRX=0.0,     WRY=0.0,     WRZ=0.0,                              &END
&BINP8B  DXMAX=0.0,   DYMAX=0.0,   DZMAX=0.0,
         WTX=0.0,     WTY=0.0,     WTZ=0.0,                              &END
&BINP9   CBAR=10.09,  SREF=120.48, SSPAN= 5.0,
         RMPX=3.75,   RMPY=0.00,   RMPZ=0.00,                            &END
&BINP10  NORSET=0,    NBCHGE=0,    NCZONE=0,
         NCZPCH=0,    CZDUB=0.0,   VREF=0.0,                             &END
&BINP11  NORPCH=0,    NORF=0,      NORL=0,
         NOCF=0,      NOCL=0,      VNORM=0.0,                            &END
&BINP12  KPAN=0,      KSIDE=0,     NEWNAB=0,    NEWSID=0,                &END
&BINP13  NBLIT=0,                                                         &END


&ASEM1   ASEMX=0.00,       ASEMY=0.00,       ASEMZ=0.00,
         ASCAL=1.00,       ATHET=0.00,       NODEA=5,                    &END
&ASEM2   APXX=0.00,        APYY=0.00,        APZZ=0.00,
         AHXX=0.00,        AHYY=1.00,        AHZZ=0.00,                  &END


&COMP1   COMPX= 0.0000,    COMPY= 0.0000,    COMPZ= 0.0000,
         CSCAL=  1.000,    CTHET=   0.0,     NODEC= 5,                   &END
&COMP2   CPXX= 0.0000,     CPYY= 0.0000,     CPZZ= 0.0000,
         CHXX= 0.0000,     CHYY=  1.000,     CHZZ= 0.0000,               &END


&PATCH1  IREV=  0, IDPAT= 1, MAKE=   0, KCOMP= 1, KASS= 1, IPATSYM=1,
         IPATCOP=0,                                                      &END
          WING
&SECT1   STX=    0.0000, STY= 0.0000,    STZ= 0.0000,    SCALE=  24.096,
         ALF=   0.0,  THETA=   0.0,
         INMODE=  5,  TNODS= 0,    TNPS=  0,    TINTS= 0,                &END
&SECT2   RTC=    0.1200, RMC= 0.0000,    RPC= 0.0000,
         IPLANE=  2,   TNPC= 10,    TINTC= 0,                           &END
&SECT1   STX=   24.096, STY= 5.0,    STZ= 0.0000,    SCALE=  0.05,
         ALF=   0.0,  THETA=   0.0,
         INMODE=  0,  TNODS= 3,    TNPS= 10,    TINTS= 2,                &END


&PATCH1  IREV=  0, IDPAT= 1, MAKE=   1, KCOMP= 1, KASS= 1, IPATSYM=1,
         IPATCOP=0,                                                      &END
          WING_TIP
&PATCH2  ITYP=  2,    TNODS= 5,    TNPS=   1,    TINTS= 3,               &END


&WAKE1   IDWAK=1,         IFLXW=1,         ITRFTZ= 0,       INTRW= 0,    &END
 WING_WAKE
&WAKE2   KWPACH=2,        KWSIDE=4,        KWLINE=0,        KWPAN1=0,
         KWPAN2=0,        NODEW=0,         INITIAL=0,                    &END
&WAKE2   KWPACH=1,        KWSIDE=2,        KWLINE=0,        KWPAN1=0,
         KWPAN2=0,        NODEW=5,         INITIAL=0,                    &END


&ONSTRM  NONSL =0,  KPSL = 20,                                            &END


&BLPARAM RN =35755000,    VISC = 0.000157, NSLBL = 1,                      &END


&VS1     NVOLR= 0,        NVOLC= 0,                                       &END
&VS2     X0=    -0.1000, Y0=     1.5000, Z0=    -0.1000, INTVSR= 1,       &END
&VS3     X1=    -0.1000, Y1=     1.5000, Z1=     0.1000, NPT1=  0,        &END
&VS4     X2=    -0.1000, Y2=     1.5000, Z2=     0.1000, NPT2= 20,        &END
&VS5     X3=     1.1000, Y3=     1.5000, Z3=    -0.1000, NPT3= 25,        &END

&VS6     XR0=    2.0000, YR0=    2.0000, ZR0=    0.0000, INTVSC= 1,       &END
```

Aug 28 1995 13:33 **delta1.in** Page 2

```
&VS7     XR1=    4.0000, YR1=    2.0000, ZR1=    0.0000,
         XR2=    2.0000, YR2=    2.0000, ZR2=    1.0000,                 &END
&VS8     R1=     0.1000, R2=     1.0000, PHI1=  0.0,     PHI2=360.0,     &END
&VS9     NRAD=   5,      NPHI=   12,     NLEN=  3,                       &END


&SLIN1   NSTLIN=0,                                                        &END
&SLIN2   SX0=   -2.0000, SY0=    1.0000, SZ0=   -0.5000,
         SU=     0.0000, SD=    10.0000, DS=    0.2500, INTSL= 1,        &END
&SLIN2   SX0=   -2.0000, SY0=    1.0000, SZ0=   -0.4000,
         SU=     0.0000, SD=    10.0000, DS=    0.2500, INTSL= 1,        &END
&SLIN2   SX0=   -2.0000, SY0=    1.0000, SZ0=   -0.3000,
         SU=     0.0000, SD=    10.0000, DS=    0.2500, INTSL= 1,        &END
&SLIN2   SX0=   -2.0000, SY0=    1.0000, SZ0=   -0.2000,
         SU=     0.0000, SD=    10.0000, DS=    0.2500, INTSL= 1,        &END
&SLIN2   SX0=   -2.0000, SY0=    1.0000, SZ0=   -0.1000,
         SU=     0.0000, SD=    10.0000, DS=    0.2500, INTSL= 1,        &END
&SLIN2   SX0=   -2.0000, SY0=    1.0000, SZ0=    0.0000,
         SU=     0.0000, SD=    10.0000, DS=    0.2500, INTSL= 1,        &END
```

Figure 3.18 PMARC Input File for a Delta wing, NACA 0012 Section, AR=0.83

a. Shaping a delta wing tip

In order to bring our NACA 0012 airfoil section from its full chord length at the root to a point at the tip, an initial attempt was made by scaling it to zero (SCALE=0); but the system crashed. To alleviate this situation, it was found that a number other than zero had to be entered. So to keep the integrity of our geometry a very small number was selected, SCALE=0.05. In fact, that was the smallest value that would allow the system to run successfully. This number could vary as it will be seen in a later case where it was successfully set at 0.01. This variation is a function of the overall geometry of the wing, and may be related to the number of panels on the surface.

Although it has not been confirmed yet, the above situation may be related to the size of the panel in the region of the tip. Panels that are too small may cause problems. This area needs more investigation as we did run cases where the output warned the user about panels having virtually no area, but still produced valid lift coefficients and pressure distributions.

b. Testing Certain Fields

The software sensitivity to the number of panels on the tip was brought up before, but we want to warn potential PMARC users that it is even more true in the case of very small tips like for the delta wing. The wing tip section of the input file, the TNPS field of the PATCH2 line should be set at a very low value. The smaller the tip, the smaller the value. In the case of the delta wing, TNPS=1 seemed to be the most efficient value for a successful run.

4. PMARC Output - Data Retrieval

We already discussed where to find the lift coefficient in the output file DATA6. We need now to indicate how to obtain the data for the pressure distribution shown in the above plots. It will be different depending along which direction (spanwise or chordwise) we need the distribution. Either way, a clear picture of how the panels are labelled is crucial. Figure 3.19 details this important information for an arbitrary case where TNPS is 8 and TNPC is 12.

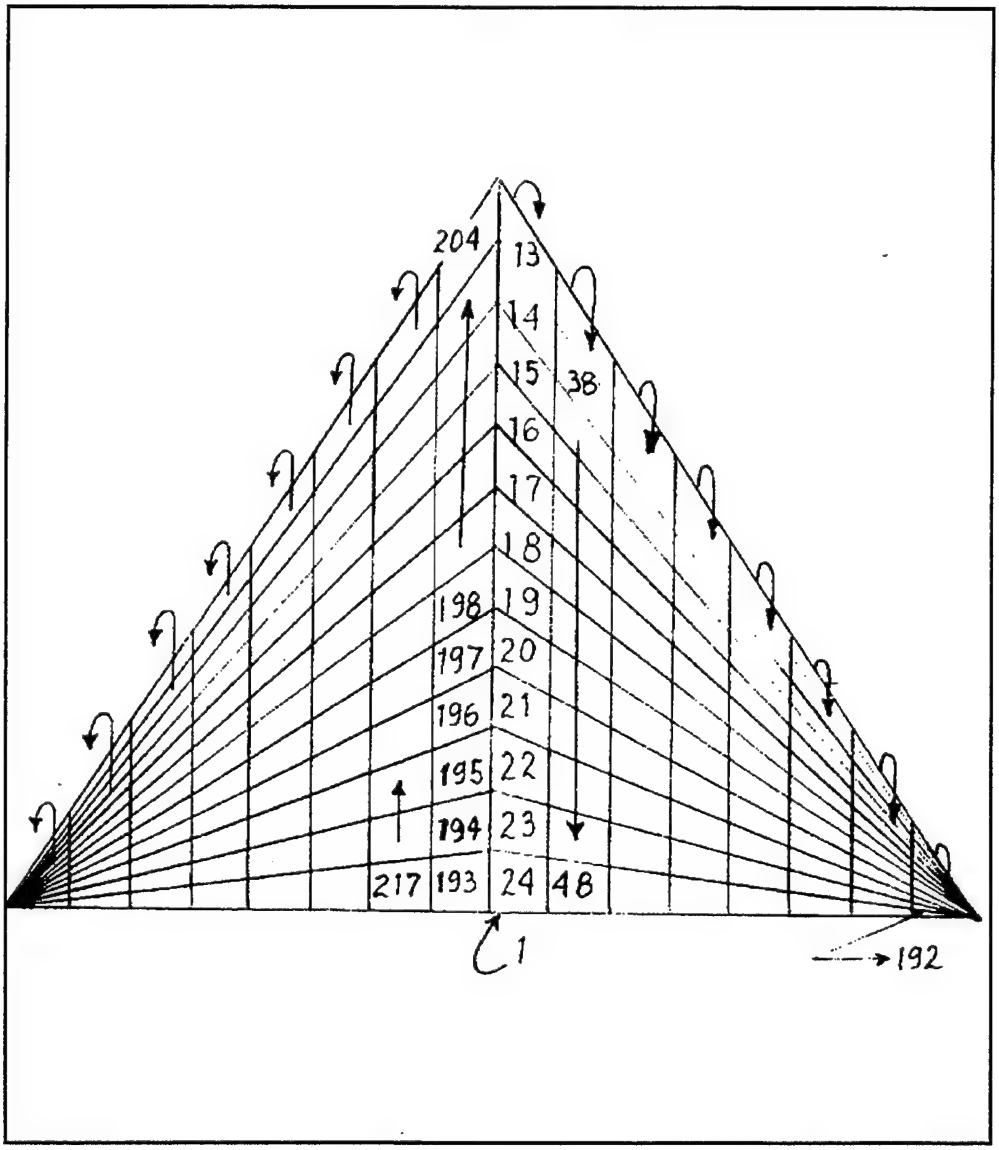

Figure 3.19 PMARC Panel Labelling Around a Delta Wing.

a. Chordwise Pressure Distribution

In order to plot the steady state chordwise pressure distribution , the user needs to scroll down the output file until the time-step corresponding to steady state is reached. If the time-step fields NTSTPS and DTSTEP are filled in accordance with the instructions provided in Chapter II, the data corresponding to the last time-step (towards the bottom of the file) are within the steady state regime. In the present case we wanted to plot the distribution at the root, and the output labels the root panels from one to thirty under column one.

As will be seen later, chordwise pressure distribution at spanwise locations other than the root can also be plotted using the PMARC output. The only additional step is to locate the column of data with a constant y value corresponding to the spanwise location desired.

b. Spanwise Pressure Distribution

In order to precisely retrieve the Cp value for each spanwise station along a spanwise cross-section, one has to select one panel per column whose coordinates are the closest to the cross-section and station under consideration. This could be a lengthy process, but some computer program can be written to do it automatically. What was done with the delta wing spanwise pressure distribution was an approximation believed to be good enough to analyze the trend.

The fifth to last panel from each of the ten columns was selected and the Cp value recorded for each. The process was repeated with the tenth from last panel of each column. As the panel selected in each column are closer to the trailing edge, the panels form a line more and more parallel with a normal spanwise distribution. As the panels get away from the trailing edge, this line moves more and more towards the leading edge, ultimately merging with it. Consequently, the results shown for the 2/3 chord location are more accurate than those of the 1/3 chord location, but the trend is reasonably the same.

E. RECTANGULAR WINGS

The rectangular wing is the simplest from the point of view of structural design and analysis. In this section we will put PMARC to the test with rectangular wings of aspect ratio 7, 4.5, and 2, respectively. All wings will have a NACA 0012 cross-section, except for a study shown at the end where the wing of AR=7 is gradually thinned out to observe the impact on the pressure distribution. Figure 3.20 shows the relative size of the three wings. For the PMARC input file, we arbitrarily selected all chord lengths to be 1, leading to a span of 7, 4.5, and 2 respectively.

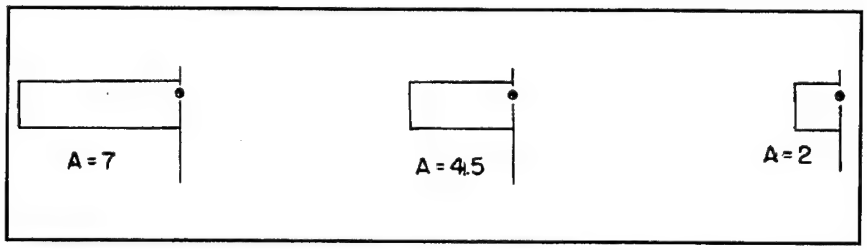

Figure 3.20 Rectangular Wings of Various Aspect Ratio.

1. Theory, Background and Reference Data

Two main references were consulted in order to compare the results obtained with PMARC. The first one is a Vortex-Lattice software output produced in 1971 by Margason and Lamar (Ref. [10]). The program represents the lifting planform with a vortex lattice and solves the system of equations in a manner summarized in section **III-B-1** and detailed in the above mentioned reference. The Vortex Lattice Method is not the most accurate method for estimating subsonic aerodynamic characteristics of lifting planforms. Consequently, the validation of the PMARC results should account for this fact.

The second reference is a two-dimensional computer panel code named *PANEL* developed by Dr. M. Platzer (Ref. [11]). For any airfoil coordinates and a selected number of panels, it computes the major aerodynamic coefficients. We will use *PANEL* pressure distribution results for a NACA 0012 to compare with the PMARC output of a large aspect ratio (20) NACA 0012 rectangular wing. Although PMARC is a three-dimensional code, the mid-span results for a high-aspect-ratio wing can be regarded as the same as the two-dimensional values as the wing tips have negligible effect at the root.

2. Results and Discussion

a. Comparing with the Vortex-Lattice Results

In addition to comparing the lift-curve slope of PMARC and Ref. [10], the following results will show the influence of the number of panels on the final output. Figure 3.21 presents the results obtained by Margason & Lamar superposed by those computed by PMARC. For all three

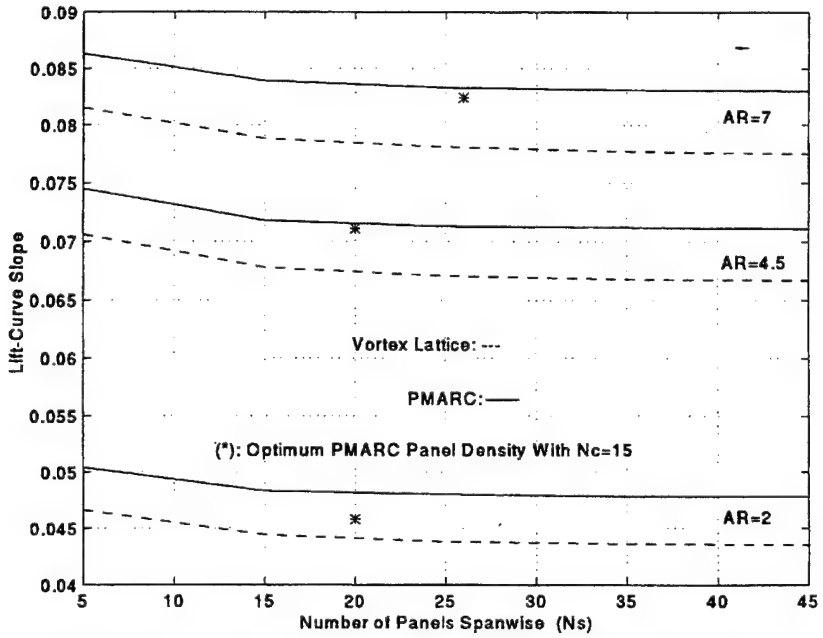

Figure 3.21 Effect of Panel Arrangement on Lift-Curve Slope for Rectangular Wings of Various Apsect Ratio.

wings, the lift-curve slopes as obtained by both methods asymptotically decrease as the panel density increases. In all cases PMARC overpredicted the Vortex-Lattice results by five to 10 percent, the largest disparities belonging to the smallest aspect ratio. Also shown on the figure is the result when the chordwise panel density is significantly higher than what is presented. It is suspected that the latter results are the most accurate simply because more panels allow for better wing definition. But again, these results do not differ from Margason and Lamar's highest panel density results by more than 7.7%.

b. Comparing Chordwise Cp Distribution with the 2-D Panel Code

In order to efficiently use PMARC to get exact two-dimensional results, a wing of infinite span should be constructed. As discussed earlier, a good approximation is a wing of sufficiently large aspect ratio. For the case of the rectangular wing, we elected to test a 20 unit wing span with an aspect ratio of 20. The object of the tests was to vary the thickness of the airfoil section from that of a NACA 0012 to a NACA 0001, and to compare the pressure distribution of each wing at an angle of attack of ten degrees, as computed by PMARC and PANEL.

As shown on Figures 3.22 to 3.28, very good agreement between the two codes exists for all airfoils. It is to be noted that the lack of smoothness in the PMARC Cp curves is due to the small number of panels used in the computation. That also explains why the peaks are sometimes cut-off. Additional panels would have meant more data points resulting in a better resolution of the curve.

Figure 3.29 is a composite Cp plot for all seven wings as computed by PMARC. This plot was included for general information to show on a relative scale how the pressure distribution changes as the wing gets thinner.

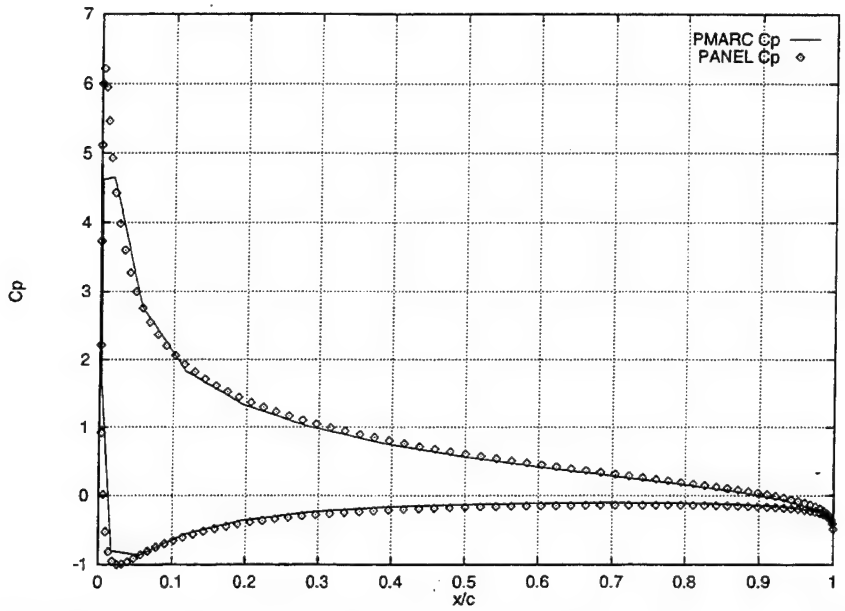

Figure 3.22 Comparison of The Pressure Coefficient as a Function of Chord Location. Rectangular Wing, AR=20, AOA=10 Degrees, NACA 0012 Section.

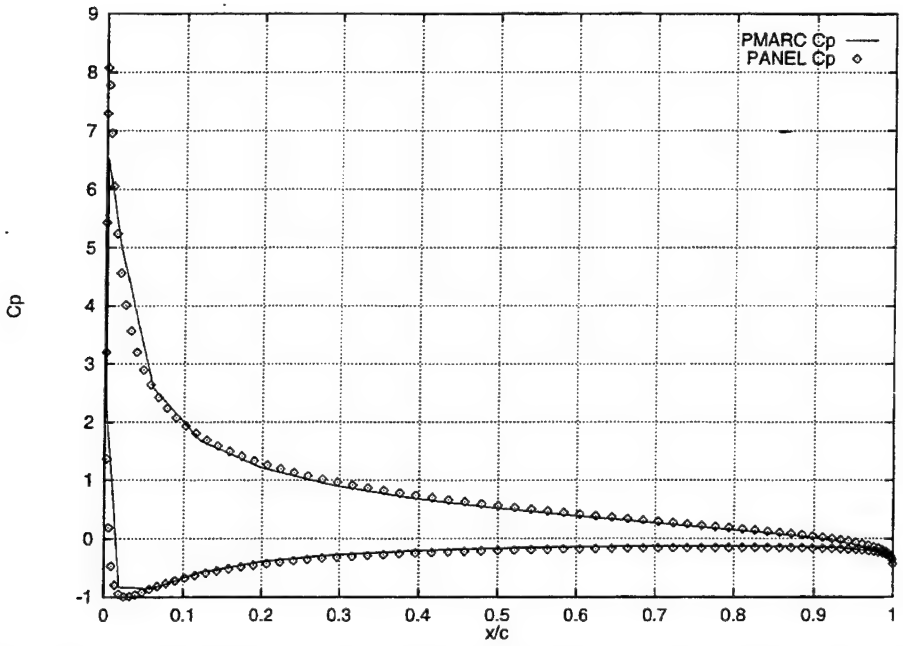

Figure 3.23 Comparison of The Pressure Coefficient as a Function of Chord Location. Rectangular Wing, AR=20, AOA=10 Degrees, NACA 0010 Section.

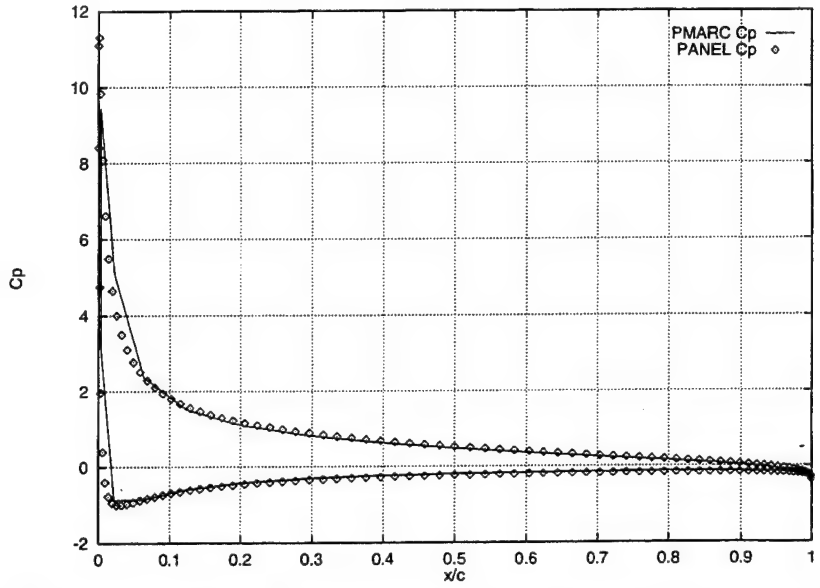

Figure 3.24 Comparison of The Pressure Coefficient as a Function of Chord Location. Rectangular Wing, AR=20, AOA=10 Degrees, NACA 0008 Section.

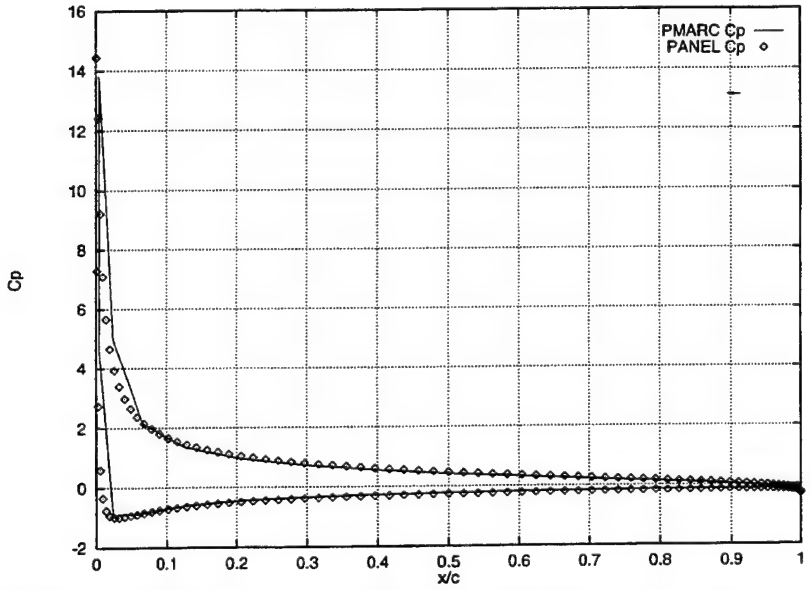

Figure 3.25 Comparison of The Pressure Coefficient as a Function of Chord Location. Rectangular Wing, AR=20, AOA=10 Degrees, NACA 0006 Section.

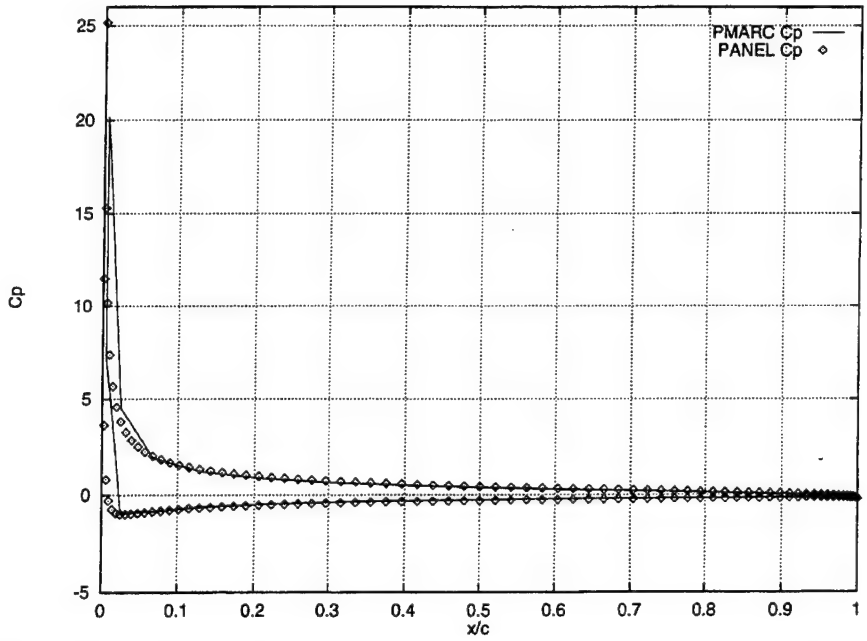

Figure 3.26 Comparison of The Pressure Coefficient as a Function of Chord Location. Rectangular Wing, AR=20, AOA=10 Degrees, NACA 0004 Section.

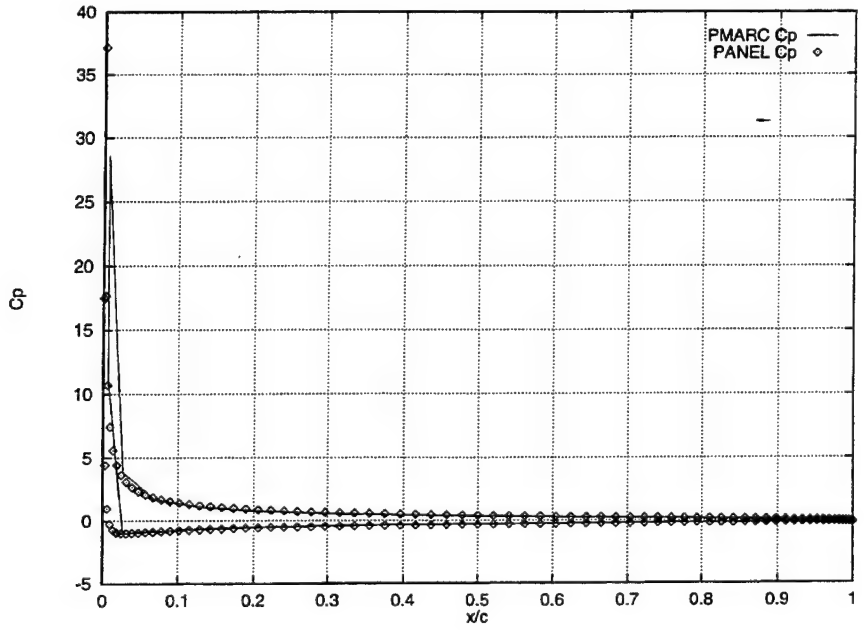

Figure 3.27 Comparison of The Pressure Coefficient as a Function of Chord Location. Rectangular Wing, AR=20, AOA=10 Degrees, NACA 0002 Section.

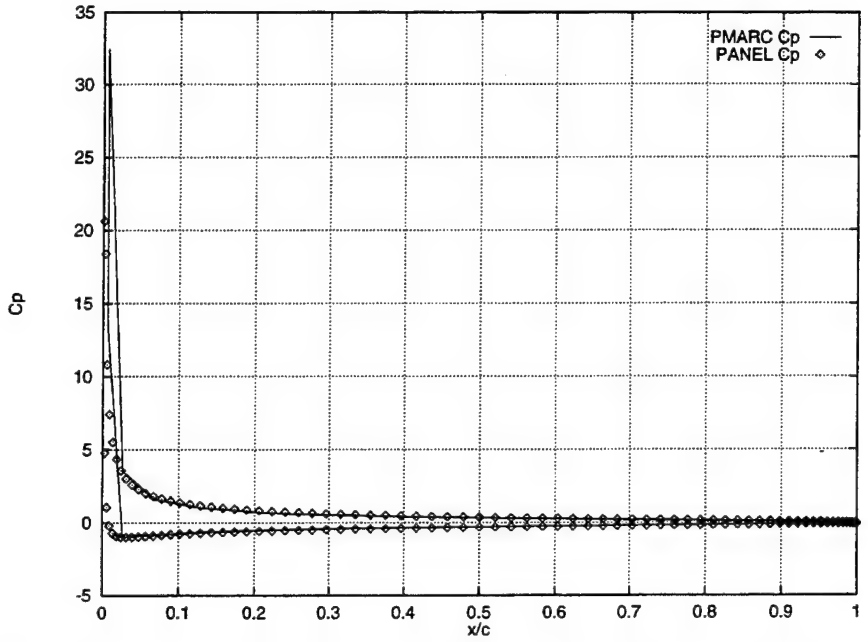

Figure 3.28 Comparison of The Pressure Coefficient as a Function of Chord Location. Rectangular Wing, AR=20, AOA=10 Degrees, NACA 0001 Section.

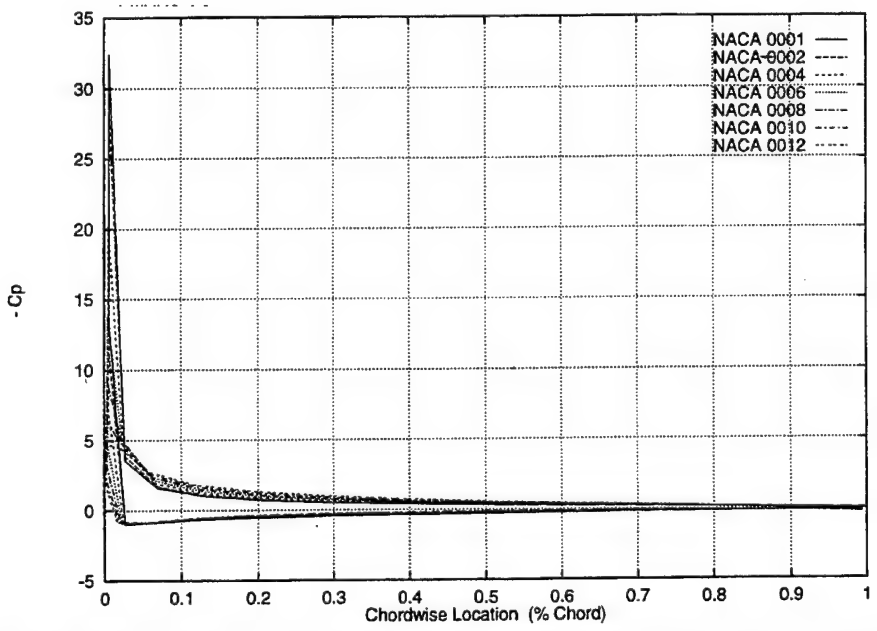

Figure 3.29 PMARC Chordwise Pressure Distribution for Various NACA Rectangular Wing Sections, AR=20, AOA=10 Degrees.

c. Spanwise Cp Distribution

Two wing thicknesses were tested in this section for the rectangular planform of aspect ratio 20. Figure 3.30 shows the comparative pressure distributions for the NACA 0001 and 0012, taken at one third of the chord length of each wing. Figures 3.31 and 3.32 show each wing spanwise Cp individually but taken at two different chordwise locations.

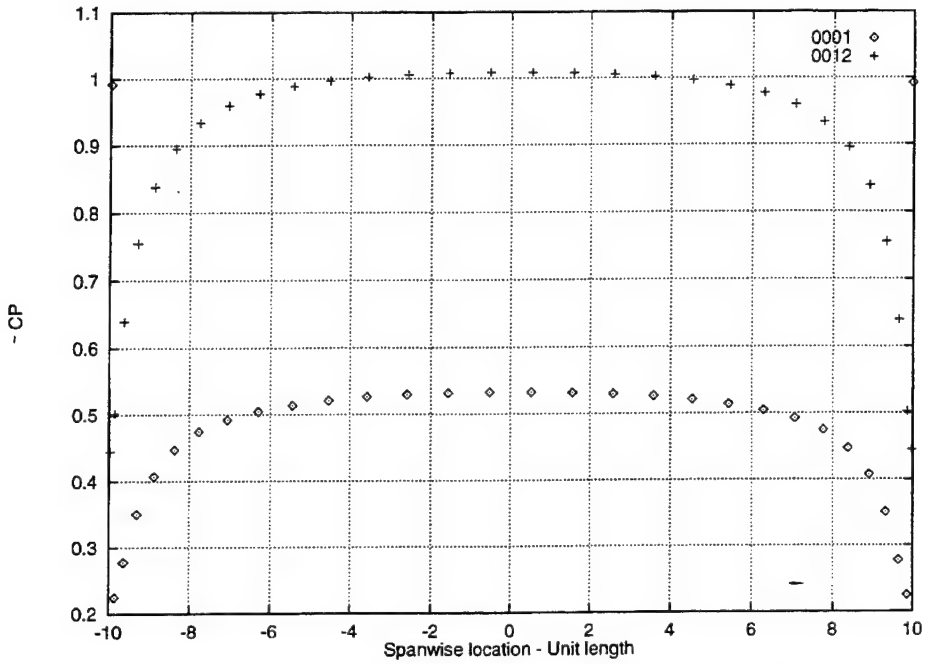

Figure 3.30 Spanwise Top Pressure Distribution at 1/3 Chord for Two NACA Sections. Rectangular Wing, AR=20, AOA=10 Degrees.

Although we do not present experimental data to corroborate the PMARC spanwise pressure distribution results, an intuitive analysis leads to a positively conclusive validation of the PMARC output. First, in all cases PMARC produced the expected elliptical distribution. Then, in Figure 3.30, the plots show higher Cp's for thicker wings, which was also to be expected. Figures 3.31 and 3.32 again present the expected behavior. However, one area of concern remains towards the tips where a sudden peak indicates that the panel layout may not pick up the correct behavior in these area of greater gradient.

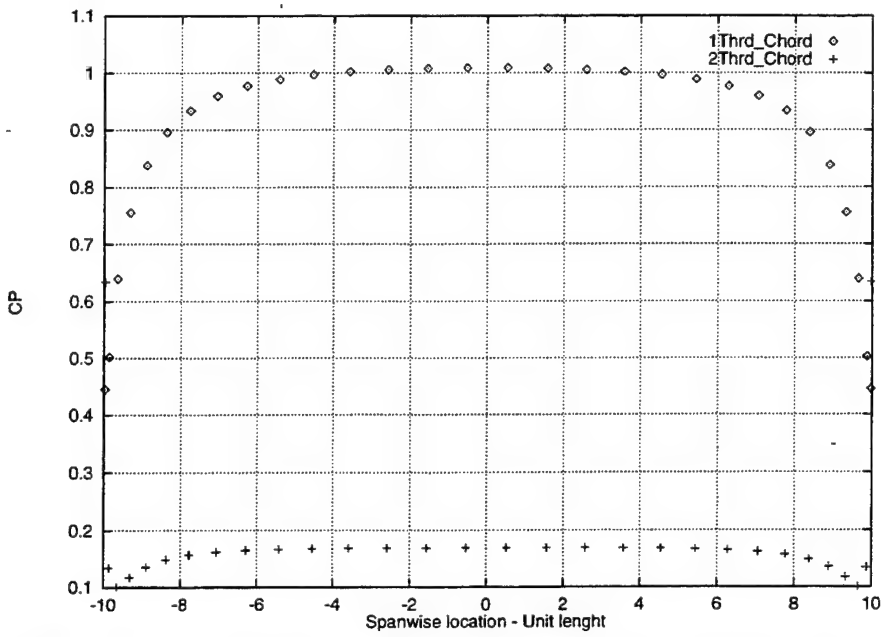

Figure 3.31 Spanwise Top Pressure Distribution at 1/3 and 2/3 Chord Locations. Rectangular Wing, AR=20, AOA=10 Degrees, NACA 0012 Section.

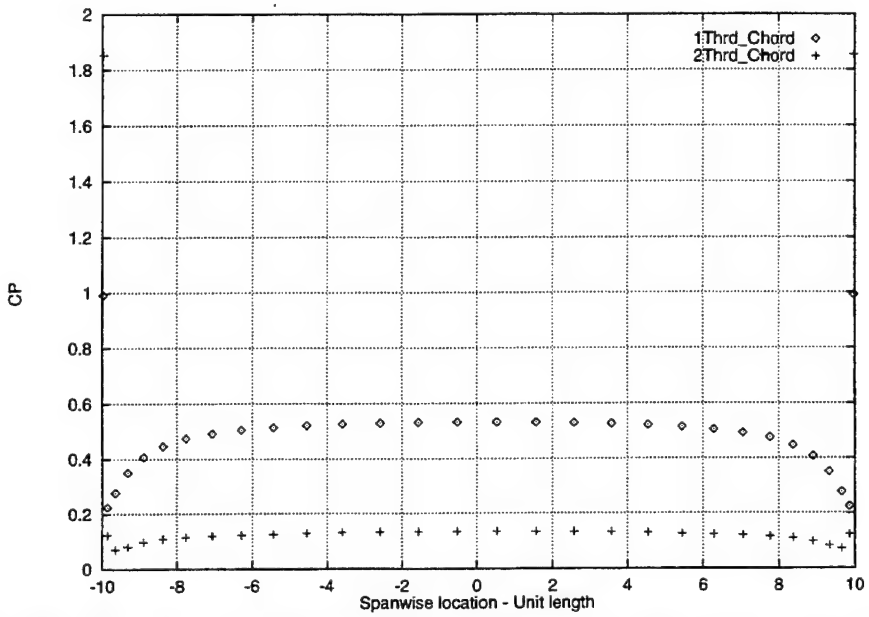

Figure 3.32 Spanwise Top Pressure Distribution at 1/3 and 2/3 Chord Locations. Rectangular Wing, AR=20, AOA=10 Degrees, NACA 0001 Section.

3. PMARC Input Instructions

Except for the fields specific to the wing geometry (CBAR, SREF, SSPAN, SCALE, STX, and STY), the test and panel prescription (ALDEG, TNPS, and TNPC) nothing is changed from the previous test case input file, the delta wing, to the rectangular wings of various aspect ratios. Figure 3.34 shows the input file for the rectangular wing of aspect ratio 7. Similarly, the input files of the other aspect ratios studied vary only by the above fields.

4. PMARC Output - Data Retrieval

As mentioned in the previous section, the data retrieval required in the PMARC output file when interested in plotting pressure distributions necessitates a complete understanding of the panel numbering method. Figure 3.33 illustrates this protocol for the case of the rectangular wing. The data retrieval for the lift coefficient, the chordwise and spanwise pressure distribution was discussed in the previous section.

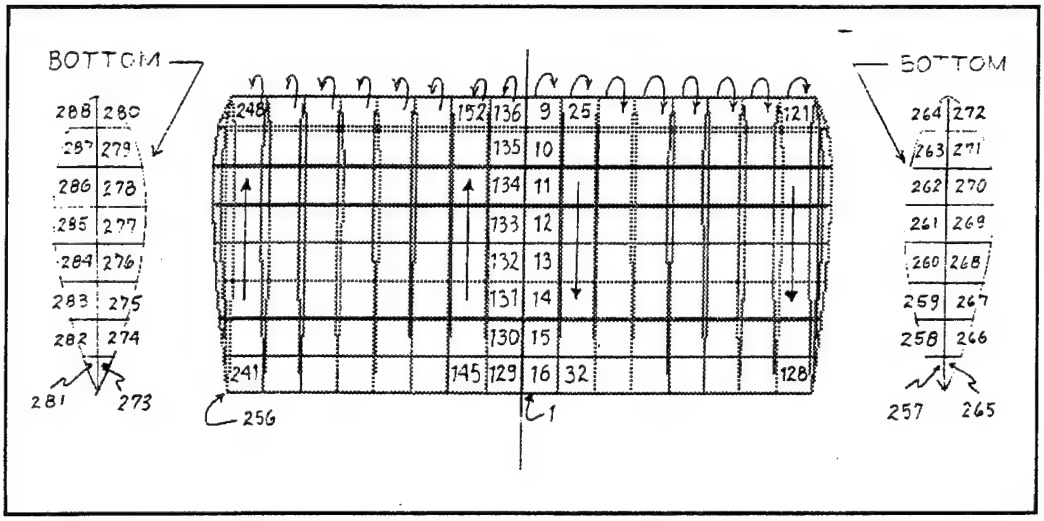

Figure 3.33 PMARC Panel Layout for a Rectangular Wing and Its Tips.

Figure 3.34 PMARC Input File for Rectangular Wing, NACA 0012 Section, AR=7

Sep 19 1995 09:59 **rectang1.in** Page 1

```
Rectangular Wing:  7ft Span, NACA-0012

 &BINP2   LSTINP=2,    LSTOUT=0,    LSTFRQ=0,    LENRUN=0,    LPLTYP=1,     &END
 &BINP3   LSTGEO=0,    LSTNAB=0,    LSTWAK=0,    LSTCPV=0,                  &END
 &BINP4   MAXIT=50,    SOLRES=0.01,                                         &END
 &BINP5   NTSTPS= 10,  DTSTEP=0.5,                                          &END
 &BINP6   RSYM=1.0,    RGPR=0.0,    RFF=5.0,  RCORES=0.0080, RCOREW=0.0080, &END
 &BINP7   VINF=11.0,   VSOUND=1116.0,                                       &END
 &BINP8   ALDEG= 0.00, YAWDEG=0.0,  PHIDOT=0.0,  THEDOT=0.0,  PSIDOT=0.0,   &END
 &BINP8A  PHIMAX= 0.0, THEMAX= 0.0, PSIMAX=0.0,
          WRX=0.0,     WRY=0.0,     WRZ=0.0,                                &END
 &BINP8B  DXMAX=0.0,   DYMAX=0.0,   DZMAX=0.0,
          WTX=0.0,     WTY=0.0,     WTZ=0.0,                                &END
 &BINP9   CBAR=1.0,    SREF=7.0,    SSPAN= 3.50,
          RMPX=3.75,   RMPY=0.00,   RMPZ=0.00,                              &END
 &BINP10  NORSET=0,    NBCHGE=0,    NCZONE=0,
          NCZPCH=0,    CZDUB=0.0,   VREF=0.0,                               &END
 &BINP11  NORPCH=0,    NORF=0,      NORL=0,
          NOCF=0,      NOCL=0,      VNORM=0.0,                              &END
 &BINP12  KPAN=0,      KSIDE=0,     NEWNAB=0,    NEWSID=0,                  &END
 &BINP13  NBLIT=0,                                                          &END


 &ASEM1   ASEMX=0.00,       ASEMY=0.00,       ASEMZ=0.00,
          ASCAL=1.00,       ATHET=0.00,       NODEA=5,                      &END
 &ASEM2   APXX=0.00,        APYY=0.00,        APZZ=0.00,
          AHXX=0.00,        AHYY=1.00,        AHZZ=0.00,                    &END


 &COMP1   COMPX= 0.0000,    COMPY= 0.0000,    COMPZ= 0.0000,
          CSCAL=  1.000,    CTHET=   0.0,     NODEC= 5,                     &END
 &COMP2   CPXX= 0.0000,     CPYY= 0.0000,     CPZZ= 0.0000,
          CHXX= 0.0000,     CHYY=  1.000,     CHZZ= 0.0000,                 &END


 &PATCH1  IREV=  0, IDPAT= 1, MAKE=   0, KCOMP= 1, KASS= 1, IPATSYM=1,
          IPATCOP=0,                                                        &END
           WING
 &SECT1   STX=    0.0000, STY= 0.0000,    STZ= 0.0000,    SCALE=  1.00 ,
          ALF=    0.0,  THETA=   0.0,
          INNODE=  5,  TNODS= 0,     TNPS=  26,    TINTS= 2,                 &END
 &SECT2   RTC=    0.12, RMC= 0.00,     RPC= 0.00,
          IPLANE=  2,   TNPC= 14,    TINTC= 0,                              &END
 &SECT1   STX=    0.0, STY= 3.5,    STZ= 0.0000,    SCALE=  1.00,
          ALF=    0.0,  THETA=   0.0,
          INMODE=  0,  TNODS= 3,     TNPS= 26,    TINTS= 2,                 &END


 &PATCH1  IREV=  0, IDPAT= 1, MAKE=   1, KCOMP= 1, KASS= 1, IPATSYM=1,
          IPATCOP=0,                                                        &END
           WING_TIP
 &PATCH2  ITYP=  2,    TNODS= 5,    TNPS=   3,   TINTS= 0,                 &END


 &WAKE1   IDWAK=1,          IFLXW=1,          ITRFTZ= 0,       INTRW= 0,     &END
  WING_WAKE
 &WAKE2   KWPACH=2,         KWSIDE=4,         KWLINE=0,        KWPAN1=0,
          KWPAN2=0,         NODEW=0,          INITIAL=0,                    &END
 &WAKE2   KWPACH=1,         KWSIDE=2,         KWLINE=0,        KWPAN1=0,
          KWPAN2=0,         NODEW=5,          INITIAL=0,                    &END


 &ONSTRM  NONSL =0,  KPSL = 20,                                             &END


 &BLPARAM RN =38378000,     VISC = 0.000157, NSLBL = 1,                     &END


 &VS1     NVOLR= 0,         NVOLC= 0,                                       &END
 &VS2     X0=    -0.1000, Y0=     1.5000, Z0=    -0.1000, INTVSR= 1,        &END
 &VS3     X1=    -0.1000, Y1=     1.5000, Z1=     0.1000, NPT1=  0,         &END
 &VS4     X2=    -0.1000, Y2=     1.5000, Z2=     0.1000, NPT2= 20,         &END
 &VS5     X3=     1.1000, Y3=     1.5000, Z3=    -0.1000, NPT3= 25,         &END

 &VS6     XR0=    2.0000, YR0=    2.0000, ZR0=    0.0000, INTVSC= 1,        &END
```

Sep 19 1995 09:59 **rectang1.in** Page 2

```
 &VS7     XR1=    4.0000, YR1=    2.0000, ZR1=    0.0000,
          XR2=    2.0000, YR2=    2.0000, ZR2=    1.0000,                   &END
 &V68     R1=     0.1000, R2=     1.0000, PHI1=  0.0,      PHI2=360.0,      &END
 &VS9     NRAD=   5,      NPHI=   12,     NLEN=  3,                        &END


 &SLIN1   NSTLIN=0,                                                         &END
 &SLIN2   SX0=   -2.0000, SY0=    1.0000, SZ0=   -0.5000,
          SU=     0.0000, SD=    10.0000, DS=    0.2500, INTSL= 1,          &END
 &SLIN2   SX0=   -2.0000, SY0=    1.0000, SZ0=   -0.4000,
          SU=     0.0000, SD=    10.0000, DS=    0.2500, INTSL= 1,          &END
 &SLIN2   SX0=   -2.0000, SY0=    1.0000, SZ0=   -0.3000,
          SU=     0.0000, SD=    10.0000, DS=    0.2500, INTSL= 1,          &END
 &SLIN2   SX0=   -2.0000, SY0=    1.0000, SZ0=   -0.2000,
          SU=     0.0000, SD=    10.0000, DS=    0.2500, INTSL= 1,          &END
 &SLIN2   SX0=   -2.0000, SY0=    1.0000, SZ0=   -0.1000,
          SU=     0.0000, SD=    10.0000, DS=    0.2500, INTSL= 1,          &END
 &SLIN2   SX0=   -2.0000, SY0=    1.0000, SZ0=    0.0000,
          SU=     0.0000, SD=    10.0000, DS=    0.2500, INTSL= 1,          &END
```

F. F5 WING

The F5 wing is the subject of an independent study. The results of the latter will be combined and analyzed with those of this paper in subsequent work. Also, some unsteady aerodynamic results will be introduced later in this paper. Here we merely present the PMARC predictions for steady flow. Figure 3.36 shows the half wing non-dimensionalized coordinates. From these coordinates, all the geometry was defined, an aspect ratio of 2.98 calculated, and a thickness ratio of 0.0480 derived. Figure 3.35 is the PMARC version of the F5 wing. The airfoil cross-section corresponds to a NACA 65004.8 whose coordinates were provided by Ref. [13]. The leading and trailing edge points were not presented in that reference and therefore had to be introduced using a curve fit of the available points. Figure 3.37 shows the given and the fitted points of the wing section.

The dimensionless chord coordinates exceed unity on Figure 3.37 to show the relative magnitude of the appended edges. However all data points were divided by the new chord length in the PMARC section definition in order to conserve a chord length of unity.

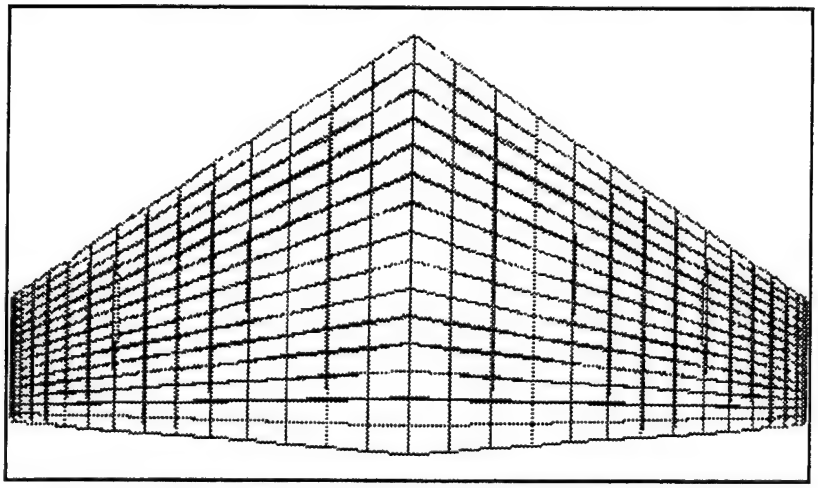

Figure 3.35 PMARC Representation of The F5 Wing.

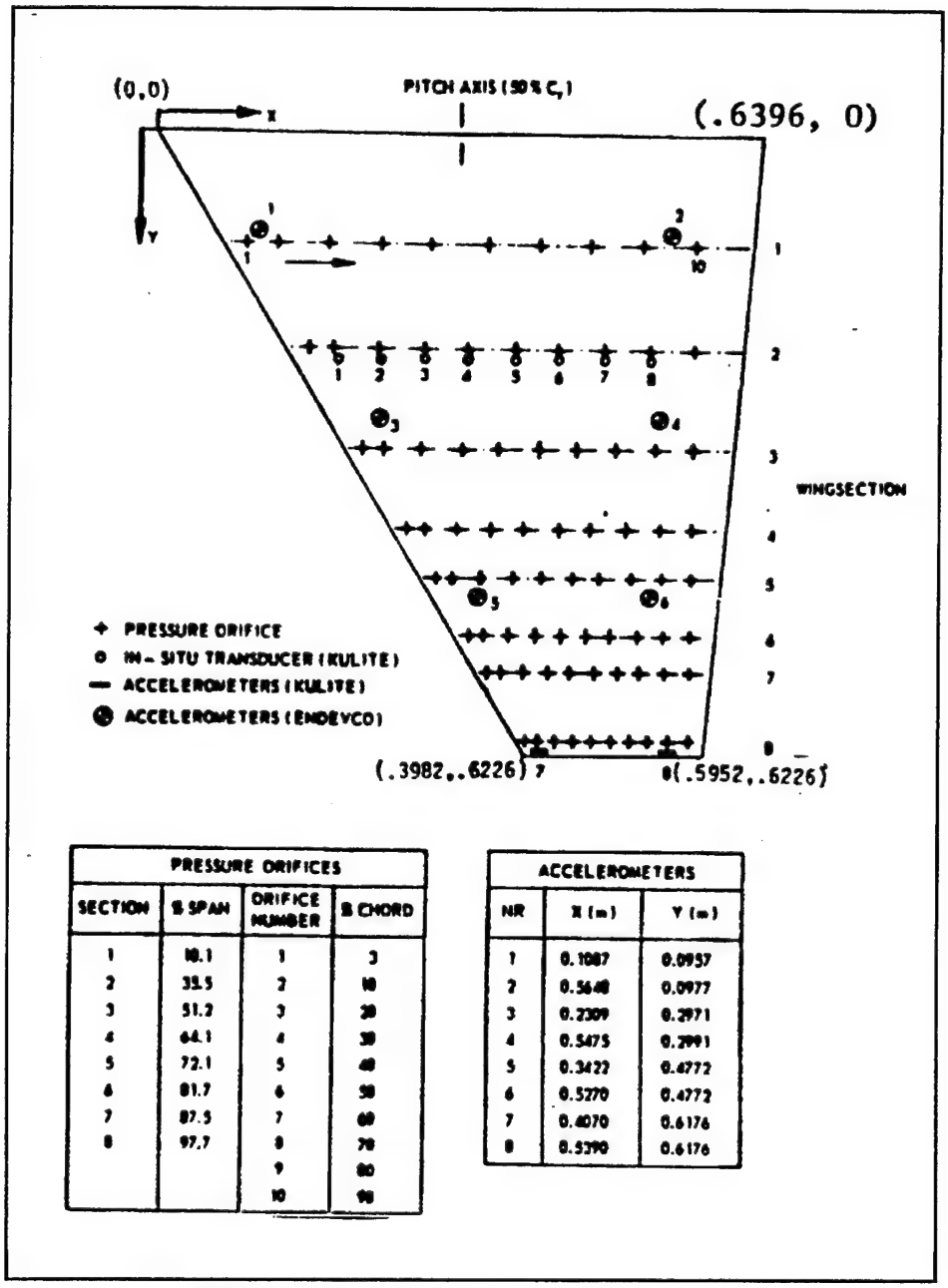

PRESSURE ORIFICES			
SECTION	% SPAN	ORIFICE NUMBER	% CHORD
1	10.1	1	3
2	35.5	2	10
3	51.2	3	20
4	64.1	4	30
5	72.1	5	40
6	81.7	6	50
7	87.5	7	60
8	97.7	8	70
		9	80
		10	90

ACCELEROMETERS		
NR	X (m)	Y (m)
1	0.1087	0.0957
2	0.5648	0.0977
3	0.2309	0.2971
4	0.5475	0.2991
5	0.3422	0.4772
6	0.5270	0.4772
7	0.4070	0.6176
8	0.5390	0.6176

Figure 3.36 Experimental F5 Wing Layout.

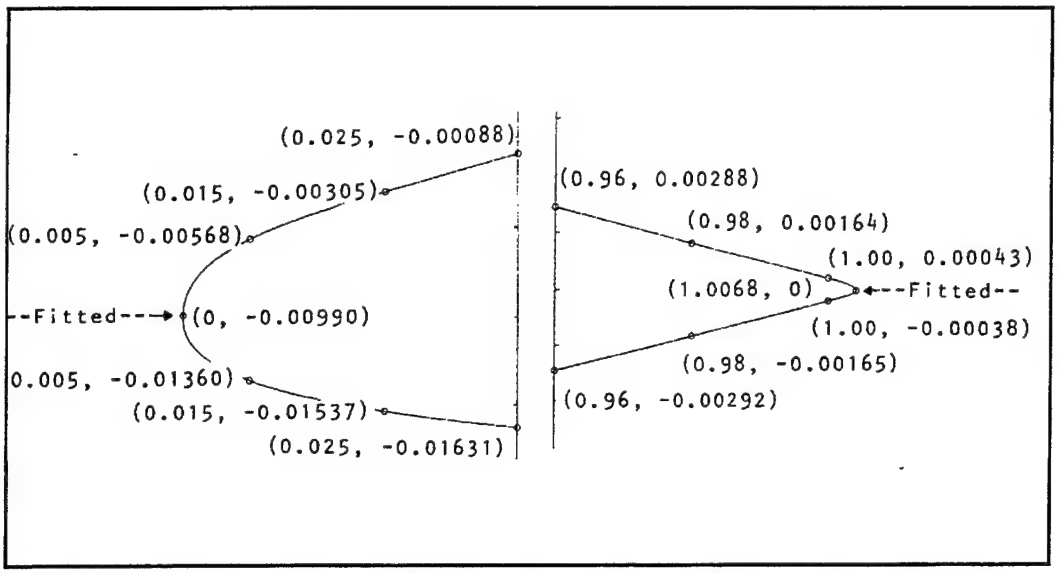

Figure 3.37 Leading and Trailing Edge Fitting. F5 Wing Cross-Section.

1. Theory, Background and Reference Data

a. Pressure Distribution - Experimental Results

The data used for comparison with the PMARC results are from experiments presented in Ref. [12]. Figure 3.36 displays the wing layout for the experiment with the pressure orifices, in-situ transducers, and accelerometers (Kulite and Endevco). One of the results presented in this study is the pressure distribution at different spanwise locations at zero degree geometric angle of attack. The experimental results considered were taken at a Mach speed of 0.6 and accounted for compressibility effects. As will be shown, the Prandlt-Glauert compressibility correction factor will be applied to the PMARC incompressible results in order to account for compressibility effects.

b. Velocity Distribution - Area Rule Analytical Results

In the early days of supersonic flights, aircraft designed to penetrate the sound barrier ran into difficulty as the thrust of their engines could not overcome the large peak drag near Mach 1. It is after the advent of the area rule that dramatic breakthrough in high-speed flight started to flourish. Richard T. Whitcomb, the father of the area rule, reasoned that the variation of cross-

sectional area for an airplane should be smooth, with no discontinuities. That is how the famous Convair F-102 finally broke the sound barrier; after its fuselage was modified to allow a reduction in its cross-sectional area in the region where the wings were located, in such a way as to smoothen the total cross-sectional area distribution.

The analytical derivations behind the area rule is presented later in Chapter **III**, section **G** where we verified the area rule by comparison with Ref. [15]. We will see there that the flow can be represented by a cross-sectional flow (or cross-flow) to which is added a spatial influence component. The velocity potential of the cross-sectional flow and the spatial influence are respectively expressed as follows:

$$\varphi = \frac{Q_x(x)}{2\pi}\ln\left[\, s(x)\sqrt{1-\left(\frac{z}{s(x)}\right)^2}\,\right] - \frac{1}{2\pi}\int_{-s(x)}^{+s(x)}\left[\frac{P_x(x,\zeta)}{\xi - z}\right] d\xi \qquad (3.2)$$

$$\Omega = -\frac{1}{4\pi}Q_x(x)[ln2x + ln2(x_o - x)] + \frac{1}{4\pi}\int_0^{x_o}\frac{Q_x(x)-Q_x(\xi)}{|x-\xi|}d\xi \qquad (3.3)$$

Chapter **III**, section **G** presents various forms of the velocity components (velocity fields, or partial derivatives) of the above equations.

In summary, the cross-sectional flow is produced in each y-z plane (Figure 3.38) by a distribution of two-dimensional sources along a spanwise axis. Each cross-flow is completely independent of conditions at any other y-z plane.

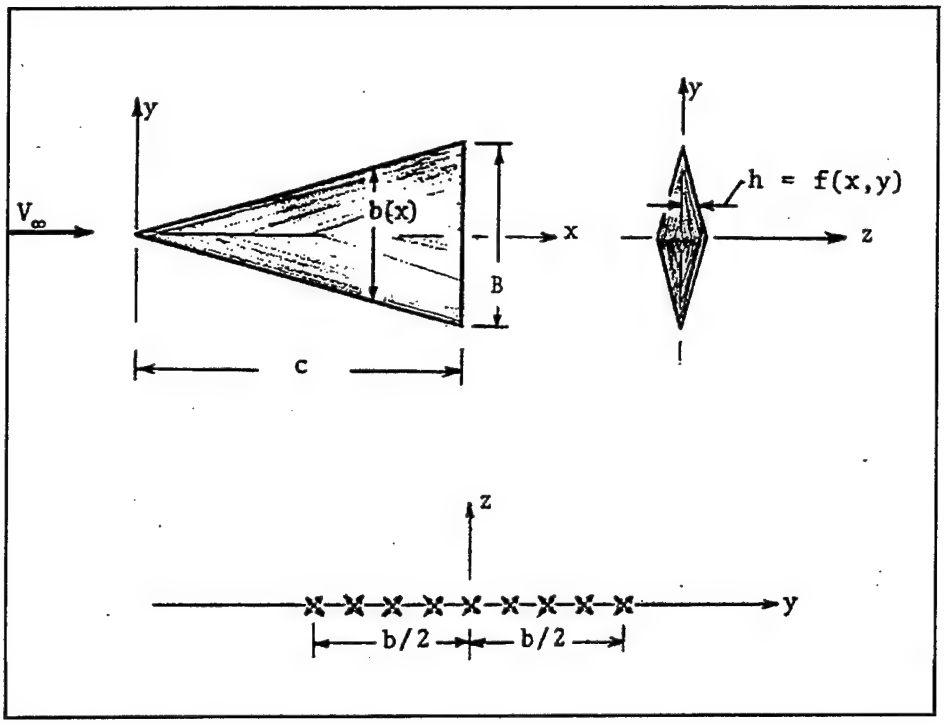

Figure 3.38 Low-Aspect-Ratio Wing and its Cross-Flow Potential. (From Ref. [14])

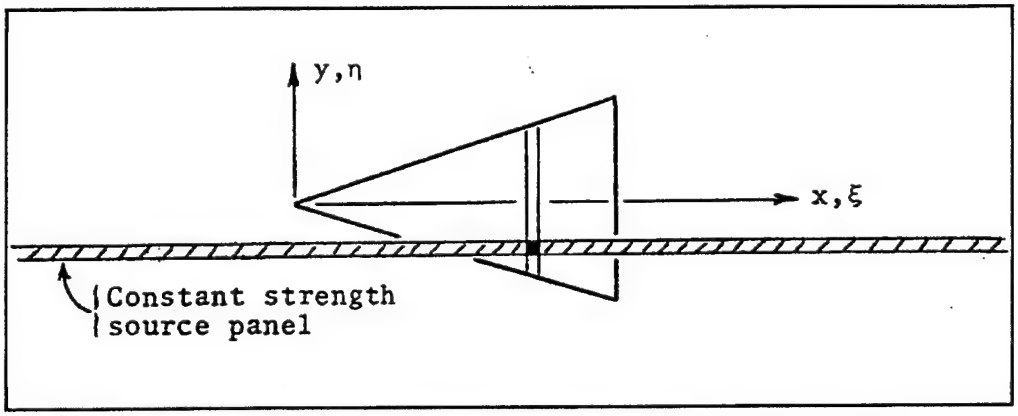

Figure 3.39 Substitution of Source Panels. (From Ref. [14])

The spatial influence expression accounts for those parts of the wing situated farther upstream (and downstream in subsonic flow) from the y-z plane under consideration (Figure 3.39). The essential aspect of this theory is that the spatial term is a function only of the total cross-sectional area distribution with x. The shape of the wing (or wing-body combination) is irrelevant, only the cross-section area is important. This will become a vital characteristic when complicated shapes are to be modeled by computer software. An equivalent area body of revolution could be modelled instead which is the easiest geometry to build. Of course, the cross-flow still has to be solved.

In the rest of this chapter, we will partially apply the concept of the two-component velocity potential on the F5 wing introduced earlier. We will discover that **PMARC does not recreate valid potential distributions**. For completeness, the results of the area rule using Equations (3.2) and (3.3) for the triangular wing will be presented in the next section. It will be shown that once more, PMARC can not reproduce an adequate velocity potential distribution.

2. Results and Discussion

a. Pressure Distribution

Figure 3.40 presents the chordwise pressure distribution on the F5 wing when at an angle of attack of zero degree. The spanwise location that produced this distribution is very close to the root. It corresponds to the control points of the first row of panels whose edges define the root. Although not shown, these results agree with the experimental results.

The next set of figures (Figures 3.41 to 3.44) better represents the agreement between PMARC and the experimental results. For four spanwise locations of the wing, the pressure distribution as calculated by PMARC is plotted against the experimental results. Also, since the latter account for compressibility and the former does not, the PMARC outputs were corrected with the Prandlt-Glauert factor and the results superposed on the respective figures.

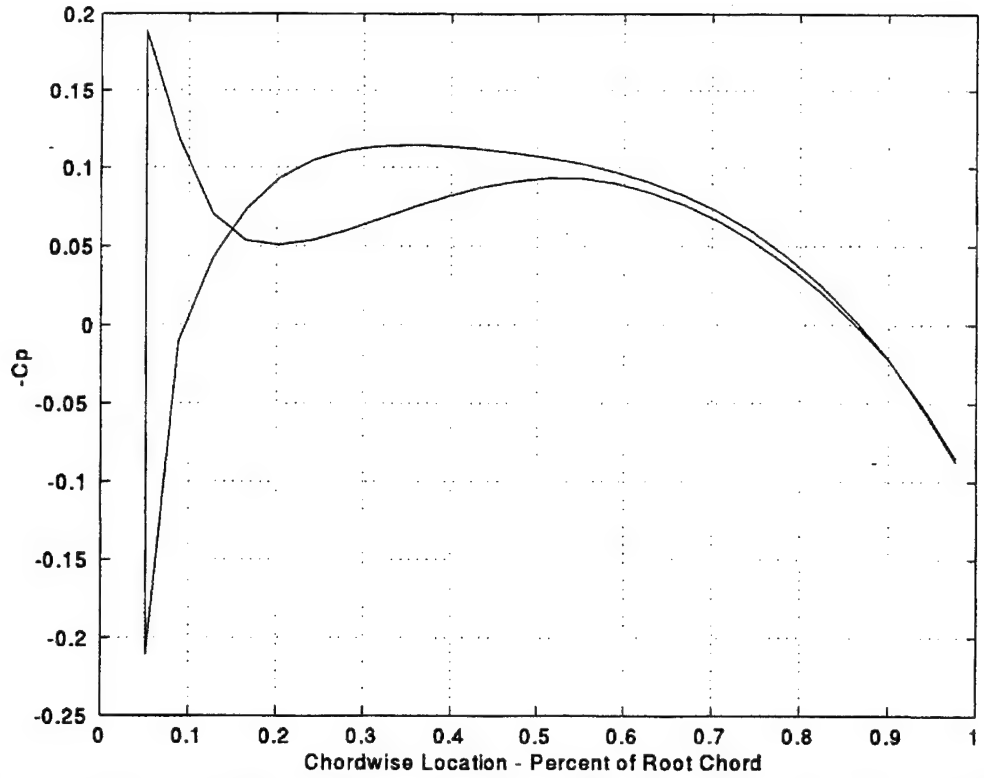

Figure 3.40 Pressure Distribution as a Function of The Root Chord Location. F5 Wing, NACA 65A004.8 Section, AR=2.98, AOA=0 Degree.

The PMARC output for the F5 wing did not allow for spanwise definition such as to have perfect correspondence with the spanwise locations selected for the experiment. However, the disparity is sufficiently small to be considered negligible in all but the first case where some care should be exercised as there is 11% difference between the PMARC and the experimental spanwise location.

With this observation in mind, the reader can still appreciate that all the results display correspondent behavior, and for the last three figures especially, the Prandlt-Glauert correction seems to bring the PMARC results progressively closer to the experimental results as we approach the wing tip.

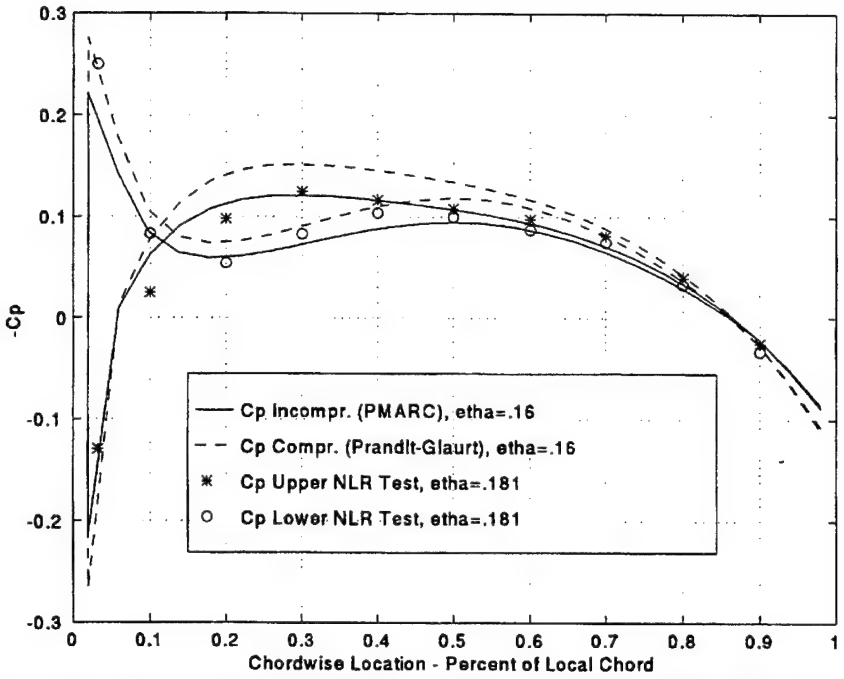

Figure 3.41 Comparison of The Chordwise Pressure Coefficient at a Spanwise Area. F5 Wing, NACA 65A004.8, AR=2.98, AOA=0 Degree.

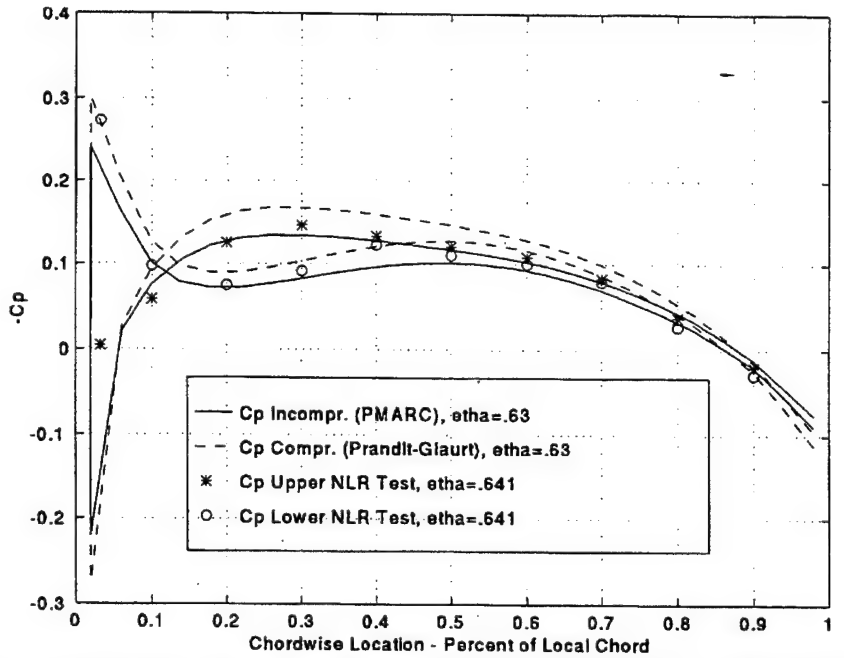

Figure 3.42 Comparison of The Chordwise Pressure Coefficient at a Spanwise Area. F5 Wing, NACA 65A004.8, AR=2.98, AOA=0 Degree.

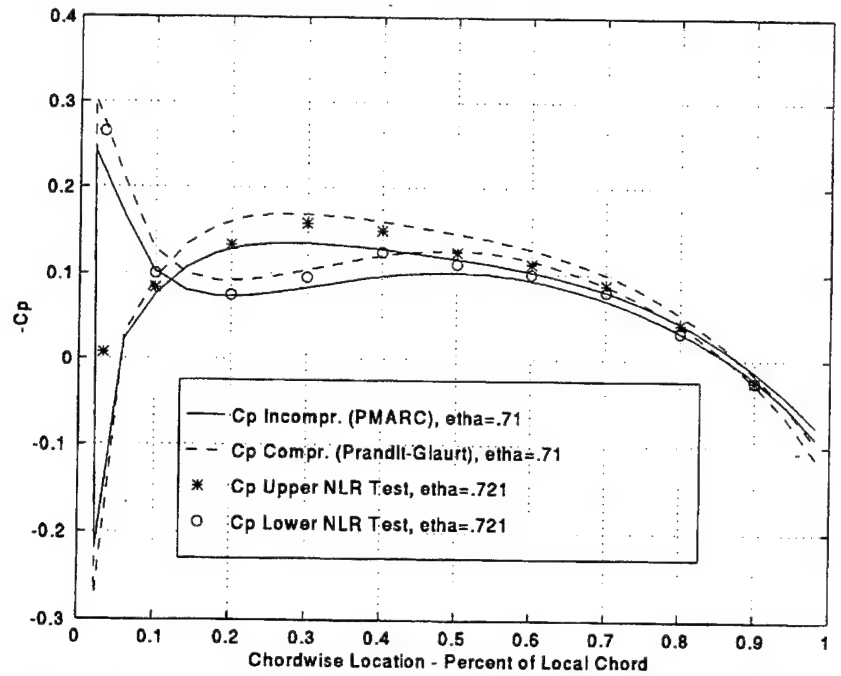

Figure 3.43 Comparison of The Chordwise Pressure Coefficient at a Spanwise Area. F5 Wing, NACA 65A004.8, AR=2.98, AOA=0 Degree.

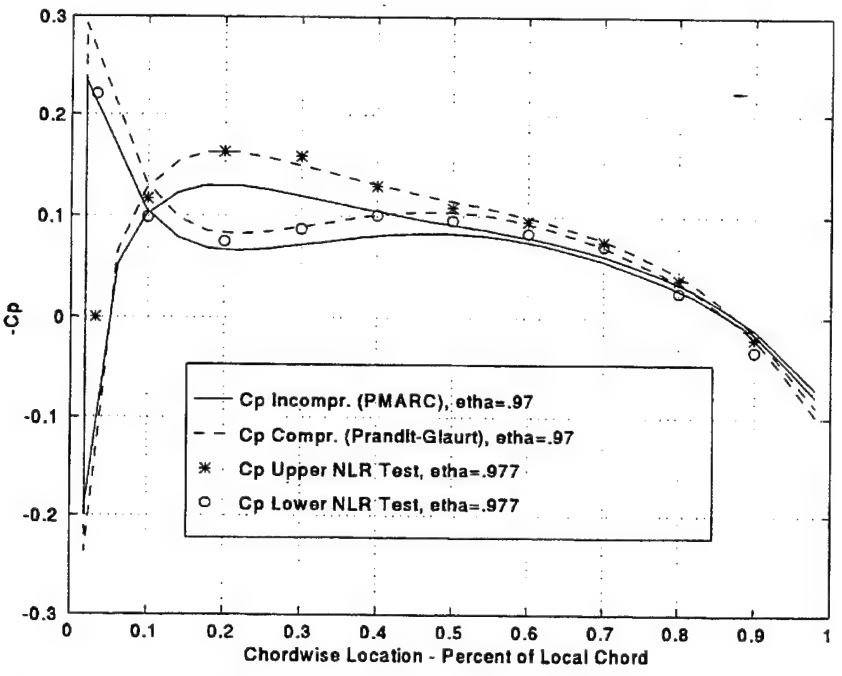

Figure 3.44 Comparison of The Chordwise Pressure Coefficient at a Spanwise Area. F5 Wing, NACA 65A004.8, AR=2.98, AOA=0 Degree.

Another result presented is the spanwise pressure distribution. Although we had no comparative data for these results, an intuitive analysis seems to validate them. Indeed, the general behavior combines those of the rectangular and delta wings. Spanwise cuts of the F5 wing in the region between the forward apex and the tip leading edge and similarly between the tip trailing edge and the aft apex correspond to cuts on a delta wing for which we see a bucket shape Cp distribution (Figure 3.45). Cuts in the region between the wing tips correspond to cuts on a rectangular wing for which we observe an elliptical Cp distribution (Figure 3.46). The PMARC spanwise pressure distribution on the F5 wing at zero degree angle of attack combines these behaviors and is shown on Figure 3.47.

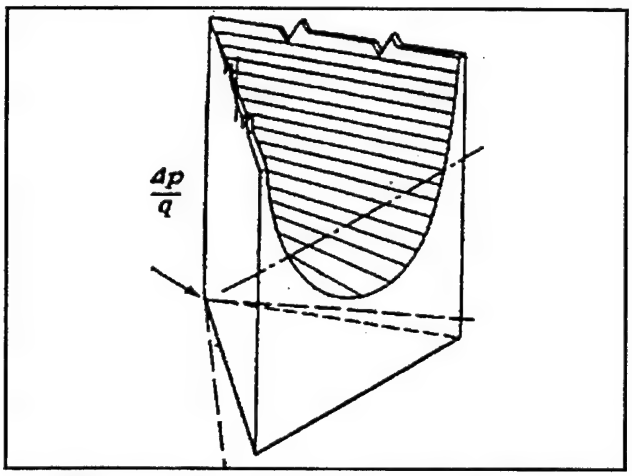

Figure 3.45 Typical Spanwise Pressure Distribution for a Delta Wing.

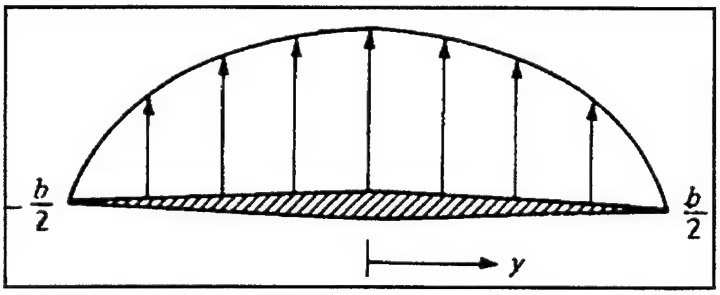

Figure 3.46 Typical Spanwise Pressure Distribution for a Rectangular Wing.

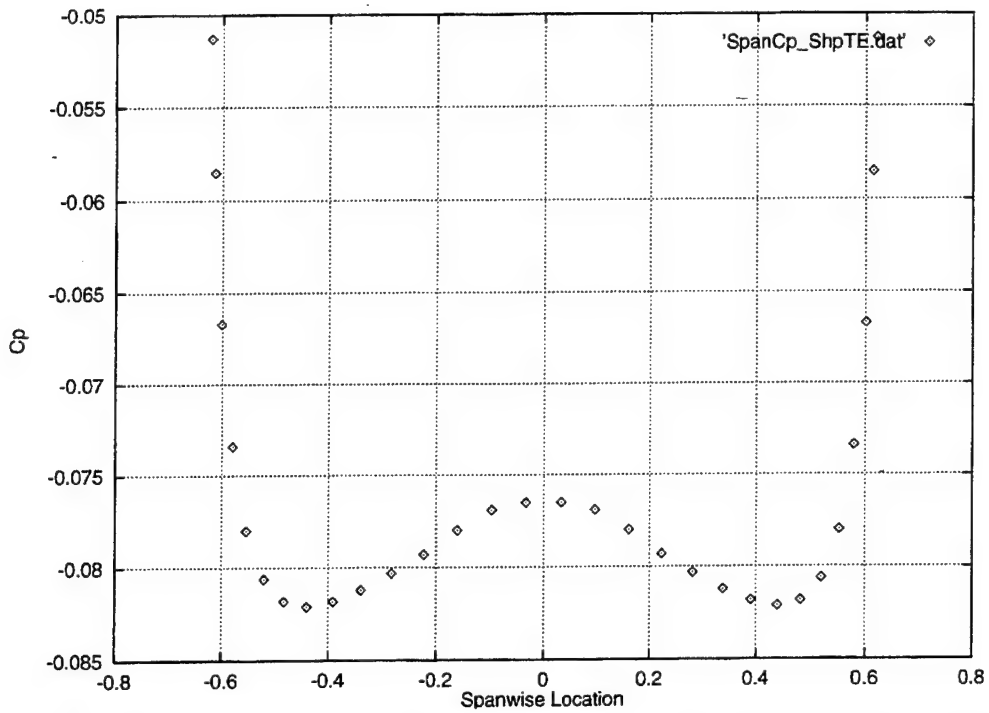

Figure 3.47 Approximate Pressure Distribution as a Function of Spanwise Location. F5 Wing, NACA 65A004.8, AR=2.98, AOA=0 Degree.

b. Velocity Potential Distribution

Comparison with the analytical results of Ref. [15] shows that the PMARC velocity potential output is erroneous. Figure 3.48 is the PMARC distribution of the x-component perturbation velocity u for various spanwise locations. It shows that the flow is faster as the spanwise location gets closer to the tip (that can be seen by noting that the peak velocities are higher as z increases). Here, z is the spanwise location. (This notation does not correspond to the PMARC one but rather matches the technical note from which the area rule was taken (Ref. [15])). The perturbation velocity u is computed as shown in Equation (3.4).

$$u = \frac{V_x - U_\infty}{U_\infty \delta} \tag{3.4}$$

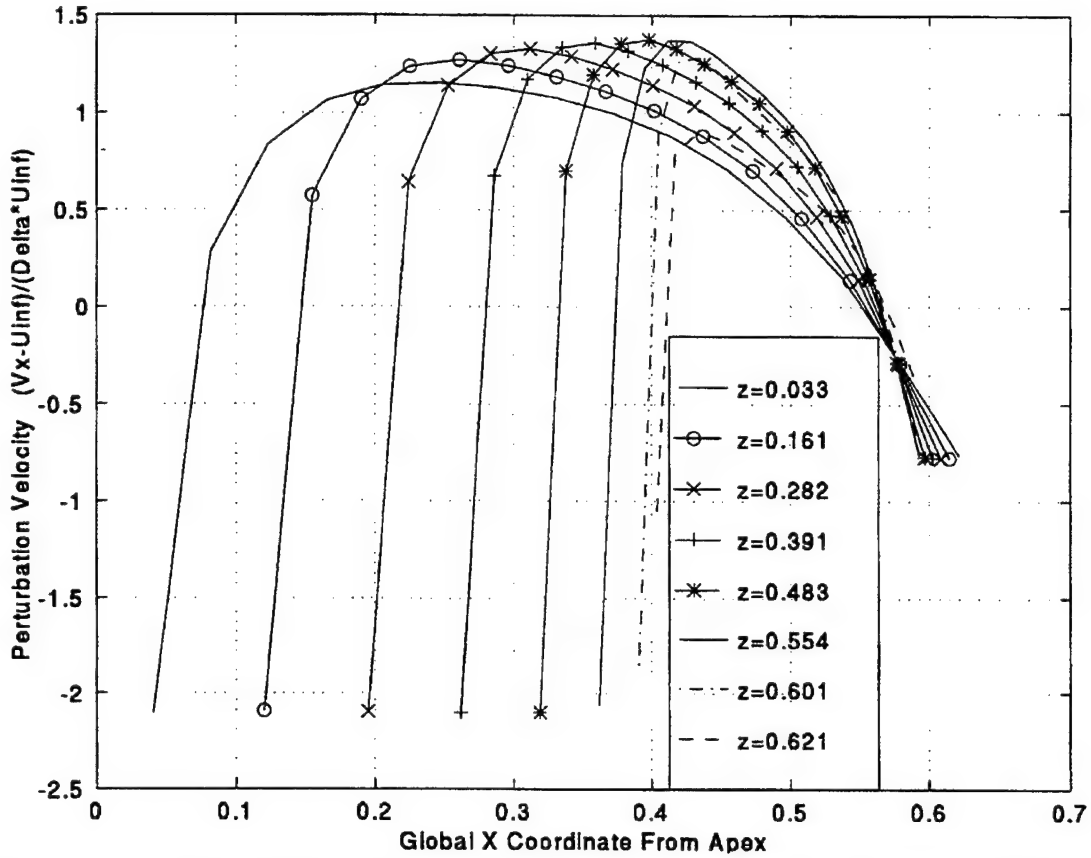

Figure 3.48 Perturbation Velocity on The Top Surface at Various Spanwise Locations. F5 Wing, NACA 65A004.8 Section, AR=2.98, AOA=0 Degree.

This behavior is obviously not realistic. As the wing thickness tapers down toward the tips, the velocity perturbation should decrease towards zero. Figure 3.49 shows the distribution of the same parameters but for the lower side of the wing. Once again, the velocity peaks are wrongfully increasing toward the tip.

Although we do not have any comparative data on the F5 wing spatial influence portion of the total flow, it was analytically solved using one form of Equation (3.3) shown later as Equation (3.23), and the results are plotted in Figure 3.50 for future consideration. The solved analytical steps can be found in Appendix **A**.

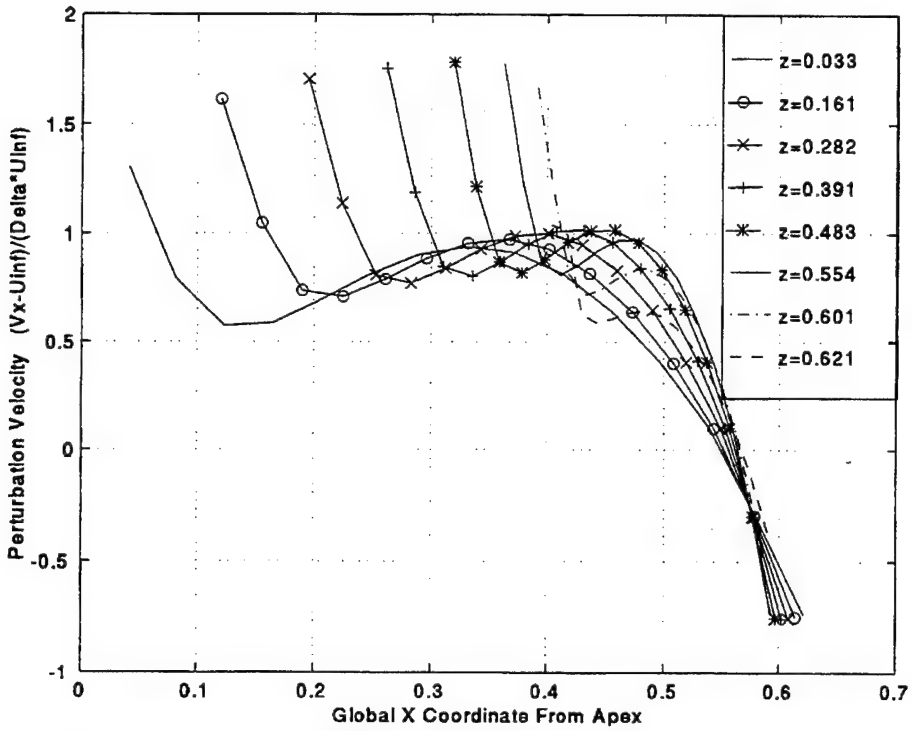

Figure 3.49 Perturbation Velocity on The Bottom Surface at Various Spanwise Locations. F5 Wing, NACA 65A004.8 Section, AR=2.98, AOA=0 Degree.

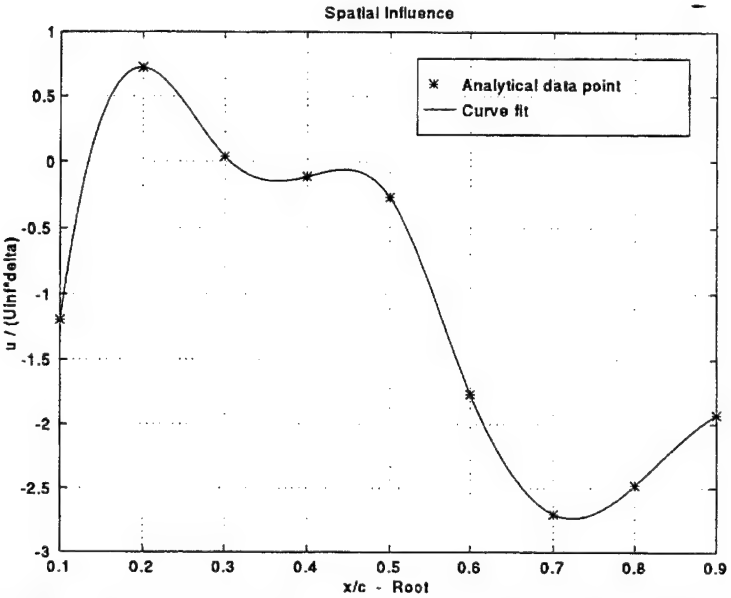

Figure 3.50 Spatial Influence u-Component of The Velocity Potential. F5 Wing, NACA 65A004.8 Section, AR=2.98, AOA=0 Degree.

The cross-sectional portion of the total flow (Equation (3.2)) could not be solved because one of its terms, the two-dimensional cross-sectional segment area P(x,z), could not be constructed. Only unidimensional expressions could be derived with the numerical data available.

3. PMARC Input Instructions

At this point, the reader should have acquired enough knowledge about PMARC input to adapt it to various configurations. The F5 wing does not show any differences from what we have seen before, except for the usual basic test condition and geometry fields (Figure 3.51).

One aspect of consideration which has already been mentioned is the importance of the order in which the airfoil section coordinates are defined. Figure 3.52 shows a pressure distribution calculated by PMARC for the same F5 wing, but with a section definition starting at the leading edge instead of the trailing edge (Figure 3.53) as required by the PMARC protocol for a wing. As it can be seen, although some of the results are relatively close from the valid distribution, major irregularities exist, as the Kutta condition is not met at the trailing edge. (Note that on Figure 3.52 the chord coordinates are not non-dimensionalized.)

4. PMARC Output - Data Retrieval

Again, all techniques for retrieval of the chordwise and spanwise pressure distribution data were introduced in a previous section. Section **E-4** of this chapter mentionned the importance of a complete understanding of the panel numbering method in order to refer to the correct data.

```
Oct 26 1995 15:15          F5wing_ShpTE.DATA5                    Page 1

 F5 Wing1 NACA-65A004.8  Sweep angle=32.6 def, AR=2.98, Ct/Cr=0.31

 &BINP2   LSTINP=2,      LSTOUT=0,     LSTFRQ=0,     LENRUN=0,     LPLTYP=1,     &END
 &BINP3   LSTGEO=0,      LSTNAB=0,     LSTWAK=0,     LSTCPV=0,                   &END
 &BINP4   HAXIS=50,      SOLRES=0.01,                                            &END
 &BINP5   NTSTPS= 5,     DTSTEP=0.2,                                             &END
 &BINP6   RSYM=1.0,      RGFR=0.0,     RFF=5.0,  RCOREB=0.0080, RCOREW=0.0080, &END
 &BINP7   VINF=11.0,     VSOUND=1116.0,                                          &END
 &BINP8   ALDEG= 0.00,   YAWDEG=0.0,   PHIDOT=0.0,  THEDOT=0.0,  PSIDOT=0.0,   &END
 &BINP8A  PHIMAX= 0.0,   THEMAX= 0.0,  PSIMAX=0.0,                               &END
          WRX=0.0,       WRY=0.0,      WRZ=0.0,                                  &END
 &BINP8B  DXMAX=0.0,     DYMAX=0.0,    DZMAX=0.0,                                &END
          WTX=0.0,       WTY=0.0,      WTZ=0.0,                                  &END
 &BINP9   CBAR=0.4577,   SREF=0.5209,  SSPAN= 0.6226,                            &END
          RMPX=0.00,     RMPY=0.00,    RMPZ=0.00,                                &END
 &BINP10  NORSET=0,      NBCHGE=0,     NCZONE=0,                                 &END
          NC2PCH=0,      C2DUB=0.0,    VREF=0.0,                                 &END
 &BINP11  NORPCH=0,      NORP=0,       NORL=0,                                   &END
          NOCP=0,        NOCL=0,       VNORM=0.0,                                &END
 &BINP12  KPAN=0,        KSIDE=0,      NEWNAB=0,     NEWSID=0,                   &END
 &BINP13  NBLIT=0,                                                               &END

 &ASEM1   ASEMX=0.00,    ASEMY=0.00,   ASEMZ=0.00,                               &END
          ASCAL=1.00,    ATHET=0.00,   NODEA=5,                                  &END
 &ASEM2   APXX=0.00,     APYY=0.00,    APZZ=0.00,                                &END
          AHXX=0.00,     AHYY=1.00,    AHZZ=0.00,

 &COMP1   COMPX= 0.0000, COMPY= 0.0000, COMPZ= 0.0000,                           &END
          CSCAL= 1.000,  CTHET= 0.0,    NODEC= 5,
 &COMP2   CPXX= 0.0000,  CPYY= 0.0000, , CPZZ= 0.0000,                           &END
          CHXX= 0.0000,  CHYY= 1.000    , CHZZ= 0.0000,

 &PATCH1  IREV= 0, IDPAT= 1, MAKE=   0, KCOMP= 1, KASS= 1, IPATSYM=1,            &END
          IPATCOP=0,
          WING
 &SECT1   STX=  0.0000, STY= 0.0000,   STZ= 0.0000,   SCALE= 0.6439,
          ALF=  0.0,    THETA= 0.0,
          INNODE= 4,    TNODS= 0,     TNPS= 15,     TINTS= 2,                   &END
     1.00000  0.000     0.00001
     0.99327  0.000    -0.00018
     0.97340  0.000    -0.00065
     0.95354  0.000    -0.00252
     0.92870  0.000    -0.00441
     0.90387  0.000    -0.00608
     0.87407  0.000    -0.00795
     0.84428  0.000    -0.00977
     0.81448  0.000    -0.01154
     0.78468  0.000    -0.01323
     0.75488  0.000    -0.01483
     0.72508  0.000    -0.01633
     0.69529  0.000    -0.01772
     0.66549  0.000    -0.01898
     0.63569  0.000    -0.02011
     0.60589  0.000    -0.02110
     0.57609  0.000    -0.02195
     0.54630  0.000    -0.02264
     0.51650  0.000    -0.02318
     0.48670  0.000    -0.02356
     0.45690  0.000    -0.02379
     0.42710  0.000    -0.02388
     0.39731  0.000    -0.02384
     0.36751  0.000    -0.02366
     0.33771  0.000    -0.02337
     0.30791  0.000    -0.02299
     0.27811  0.000    -0.02252
     0.24832  0.000    -0.02199
     0.21852  0.000    -0.02141
     0.18872  0.000    -0.02082
     0.15892  0.000    -0.02021
     0.12913  0.000    -0.01960
     0.09933  0.000    -0.01897
     0.07946  0.000    -0.01851
```



```
Oct 26 1995 15:15          F5wing_ShpTE.DATA5                    Page 2

     0.05960  0.000    -0.01796
     0.04470  0.000    -0.01742
     0.03476  0.000    -0.01695
     0.02483  0.000    -0.01631
     0.01490  0.000    -0.01537
     0.00497  0.000    -0.01360
     0.00000  0.000    -0.00990
     0.00497  0.000    -0.00568
     0.01490  0.000    -0.00305
     0.02483  0.000    -0.00088
     0.03476  0.000     0.00104
     0.04470  0.000     0.00279
     0.05960  0.000     0.00517
     0.07946  0.000     0.00796
     0.09933  0.000     0.01039
     0.12913  0.000     0.01349
     0.15892  0.000     0.01603
     0.18872  0.000     0.01810
     0.21852  0.000     0.01977
     0.24832  0.000     0.02111
     0.27811  0.000     0.02214
     0.30791  0.000     0.02292
     0.33771  0.000     0.02348
     0.36751  0.000     0.02384
     0.39731  0.000     0.02401
     0.42710  0.000     0.02402
     0.45690  0.000     0.02387
     0.48670  0.000     0.02358
     0.51650  0.000     0.02315
     0.54630  0.000     0.02258
     0.57609  0.000     0.02187
     0.60589  0.000     0.02103
     0.63569  0.000     0.02006
     0.66549  0.000     0.01895
     0.69529  0.000     0.01771
     0.72508  0.000     0.01635
     0.75488  0.000     0.01487
     0.78468  0.000     0.01327
     0.81448  0.000     0.01158
     0.84428  0.000     0.00980
     0.87407  0.000     0.00795
     0.90387  0.000     0.00605
     0.92870  0.000     0.00446
     0.95354  0.000     0.00288
     0.97340  0.000     0.00164
     0.99327  0.000     0.00043
     1.00000  0.000     0.00001
 &BPNODE      TNODE=3    TNPC=50    TINTC=3    &END
 &SECT1   STX= 0.3982, STY= 0.6226,   STZ= 0.0000,   SCALE= 0.1983 ,
          ALF=  0.0,    THETA=  0.0,
          INNODE=  0,   TNODS= 3,    TNPS= 15,     TINTS= 2,                   &END
 &BPNODE      TNODE=3    TNPC=50    TINTC=3    &END

 &PATCH1  IREV=  0, IDPAT= 1, MAKE=   1, KCOMP= 1, KASS= 1, IPATSYM=1,
          IPATCOP=0,
            WING_TIP
 &PATCH2  ITYP=  2,    TNODS= 5,    TNPS=  1,    TINTS= 3,                    &END

 &WAKE1   IDWAK=1,      IFLXW=1,      ITRFT2= 0,    INTRW= 0,                   &END
   WING_WAKE
 &WAKE2   KWPACH=2,     KWSIDE=4,     KWLINE=0,     KWPAN1=0,
          KWPAN2=0,     NODEW=0,      INITIAL=0,
 &WAKE2   KWPACH=1,     KWSIDE=-2,    KWLINE=0,     KWPAN1=0,                   &END
          KWPAN2=0,     NODEW=5,      INITIAL=0,                                &END


 &ONSTRM  NONSL =0,   KFSL =                                                     &END

 &BLPARAM RN =37210000,     VISC = 0.0001571, NSLBL = 1,                        &END

 &VS1     NVOLR= 0,     NVOLC= 0,                                               &END
 &VS2     XO=   -0.1000, YO=    1.5000, ZO=   -0.1000, INTVSR= 1,                &END
```

Figure 3.51 PMARC Input File for The F5 Wing, NACA 65A004.8 Section, AR=2.98. (Last Few Lines Not Presented).

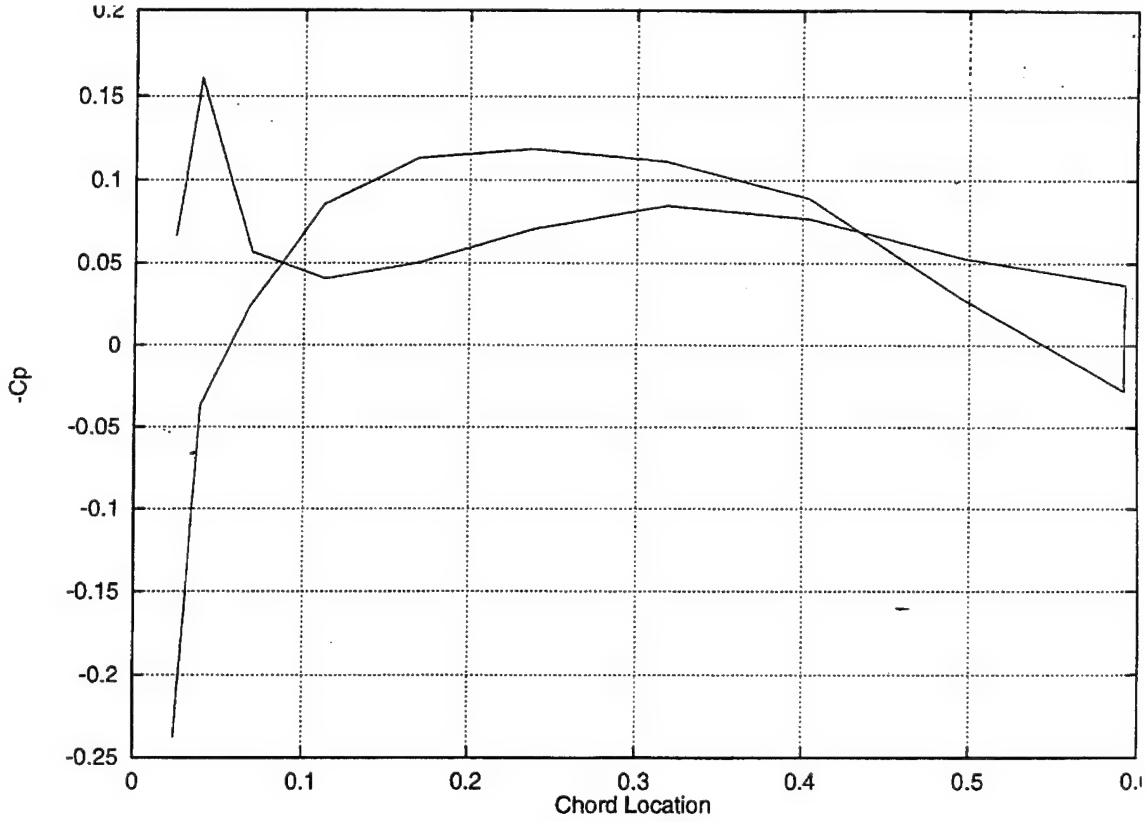

Figure 3.52 Chordwise Pressure Distribution From a Bad Input File With Reverse Section Definition. F5 Wing, NACA 65A004.8 Section, AR=2.98.

```
Apr 25 1995 11:31          SpTmxSp_DATA5          Page 1

F5 Wing: NACA-65A004.8  Sweep angle=32.6 def, AR=2.98, Ct/Cr=0.31

&BINP2    LSTINP=2,     LSTOUT=0,      LSTFRQ=0,     LENRUN=0,      LPLTYP=1,       &END
&BINP3    LSTGEO=0,     LSTNAB=0,      LSTWAK=0,     LSTCPV=0,                      &END
&BINP4    MAXIT=50,     SOLRES=0.01,                                                &END
&BINP5    NTSTPS= 3,    DTSTEP=0.5,                                                 &END
&BINP6    RSYM=1.0,     RGPR=0.0,      RFF=5.0,  RCORES=0.0080, RCOREW=0.0080,      &END
&BINP7    VINF=11.0,    VSOUND=1116.0,                                              &END
&BINP8    ALDEG= 0.00,  YAWDEG=0.0,    PHIDOT=0.0,   THEDOT=0.0,    PSIDOT=0.0,     &END
&BINP8A   PHIMAX= 0.0,  THEMAX= 0.0,   PSIMAX=0.0,
          WRX=0.0,      WRY=0.0,       WRZ=0.0,                                     &END
&BINP8B   DXMAX=0.0,    DYMAX=0.0,     DZMAX=0.0,
          WTX=0.0,      WTY=0.0,       WTZ=0.0,                                     &END
&BINP9    CBAR=0.4577,  SREF=0.5209,   SSPAN= 0.6226,
          RMPX=3.63,    RMPY=0.00,     RMPZ=0.00,                                   &END
&BINP10   NORSET=0,     NBCHGE=0,      NCZONE=0,
          NCZPCH=0,     CZDUB=0.0,     VREF=0.0,                                    &END
&BINP11   NORPCH=0,     NORF=0,        NORL=0,
          NOCF=0,       NOCL=0,        VNORM=0.0,                                   &END
&BINP12   KPAN=0,       KSIDE=0,       NEWNAB=0,     NEWSID=0,                      &END
&BINP13   NBLIT=0,                                                                  &END


&ASEM1    ASEMX=0.00,       ASEMY=0.00,       ASEMZ=0.00,
          ASCAL=1.00,       ATHET=0.00,       NODEA=5,                              &END
&ASEM2    APXX=0.00,        APYY=0.00,        APZZ=0.00,
          AHXX=0.00,        AHYY=1.00,        AHZZ=0.00,                            &END


&COMP1    COMPX= 0.0000,    COMPY= 0.0000,    COMPZ= 0.0000,
          CSCAL=  1.000,    CTHET=    0.0,    NODEC= 5,                             &END
&COMP2    CPXX= 0.0000,     CPYY= 0.0000,     CPZZ= 0.0000,
          CHXX= 0.0000,     CHYY=  1.000   ,  CHZZ= 0.0000,                         &END


&PATCH1   IREV=  0, IDPAT= 1, MAKE=   0, KCOMP= 1, KASS= 1, IPATSYM=1,
          IPATCOP=0,                                                                &END
           WING
&SECT1    STX=    0.0000, STY= 0.0000,    STZ= 0.0000,    SCALE= 0.6439,
          ALF=    0.0,  THETA=    0.0,
          INMODE=  4,  TNODS= 0,     TNPS=  48,     TINTS= 2,                       &END
0.00000  0.000  -0.00990
0.00497  0.000  -0.00568
0.01490  0.000  -0.00305
0.02483  0.000  -0.00088
0.03476  0.000   0.00104
0.04470  0.000   0.00279
0.05960  0.000   0.00517
0.07946  0.000   0.00796
0.09933  0.000   0.01039
0.12913  0.000   0.01349
0.15892  0.000   0.01603
0.18872  0.000   0.01810
0.21852  0.000   0.01977
0.24832  0.000   0.02111
0.27811  0.000   0.02214
0.30791  0.000   0.02292
0.33771  0.000   0.02348
0.36751  0.000   0.02384
0.39731  0.000   0.02401
0.42710  0.000   0.02402
0.45690  0.000   0.02387
0.48670  0.000   0.02358
0.51650  0.000   0.02315
0.54630  0.000   0.02258
0.57609  0.000   0.02187
0.60589  0.000   0.02103
0.63569  0.000   0.02006
0.66549  0.000   0.01895
0.69529  0.000   0.01771
0.72508  0.000   0.01635
0.75488  0.000   0.01487
0.78468  0.000   0.01327
0.81448  0.000   0.01158
0.84428  0.000   0.00980
```

```
Apr 25 1995 11:31          SpTmxSp_DATA5          Page 2

0.87407  0.000   0.00795
0.90387  0.000   0.00605
0.92870  0.000   0.00446
0.95354  0.000   0.00288
0.97340  0.000   0.00164
0.99327  0.000   0.00043
1.00000  0.000   0.00001
0.99327  0.000  -0.00038
0.97340  0.000  -0.00165
0.95354  0.000  -0.00292
0.92870  0.000  -0.00451
0.90387  0.000  -0.00608
0.87407  0.000  -0.00795
0.84428  0.000  -0.00977
0.81448  0.000  -0.01154
0.78468  0.000  -0.01323
0.75488  0.000  -0.01483
0.72508  0.000  -0.01633
0.69529  0.000  -0.01772
0.66549  0.000  -0.01898
0.63569  0.000  -0.02011
0.60589  0.000  -0.02110
0.57609  0.000  -0.02195
0.54630  0.000  -0.02264
0.51650  0.000  -0.02318
0.48670  0.000  -0.02356
0.45690  0.000  -0.02379
0.42710  0.000  -0.02388
0.39731  0.000  -0.02384
0.36751  0.000  -0.02366
0.33771  0.000  -0.02337
0.30791  0.000  -0.02299
0.27811  0.000  -0.02252
0.24832  0.000  -0.02199
0.21852  0.000  -0.02141
0.18872  0.000  -0.02082
0.15892  0.000  -0.02021
0.12913  0.000  -0.01960
0.09933  0.000  -0.01897
0.07946  0.000  -0.01851
0.05960  0.000  -0.01796
0.04470  0.000  -0.01742
0.03476  0.000  -0.01695
0.02483  0.000  -0.01631
0.01490  0.000  -0.01537
0.00497  0.000  -0.01360
0.00000  0.000  -0.00990
&BPNODE    TNODE=3     TNPC=18     TINTC=0     &END
&SECT1    STX= 0.3982, STY= 0.6226,     STZ= 0.0000,     SCALE= 0.1983 ,
          ALF=    0.0,  THETA=    0.0,
          INMODE=  0,  TNODS= 3,     TNPS= 48,     TINTS= 2,                        &END
&BPNODE    TNODE=3     TNPC=18     TINTC=0     &END


&PATCH1   IREV=  0, IDPAT= 1, MAKE=   1, KCOMP= 1, KASS= 1, IPATSYM=1,
          IPATCOP=0,                                                                &END
           WING_TIP
&PATCH2   ITYP=  2,     TNODS= 5,     TNPS=   2,    TINTS= 3,                       &END


&WAKE1    IDWAK=1,           IFLXW=1,          ITRFTZ= 0,        INTRW= 0,          &END
 WING_WAKE
&WAKE2    KWPACH=2,          KWSIDE=4,         KWLINE=0,         KWPAN1=0,
          KWPAN2=0,          NODEW=0,          INITIAL=0,                           &END
&WAKE2    KWPACH=1,          KWSIDE=2,         KWLINE=0,         KWPAN1=0,
          KWPAN2=0,          NODEW=5,          INITIAL=0,                           &END


&ONSTRM   NONSL =9,  KPSL = 12,30,48,1272,1290,1308,1686,1704,1722,                 &END


&BLPARAM RN =37210000,    VISC = 0.000157, NSLBL = 1,                               &END


&VS1      NVOLR= 0,         NVOLC= 0,                                               &END
&VS2      X0=     -0.1000, Y0=      1.5000, Z0=     -0.1000, INTVSR= 1,             &END
```

Figure 3.53 Bad PMARC Input File With Reverse Section Definition. F5 Wing, NACA 65A004.8 Section, AR=2.98. (Last Few Lines Not Shown).

G. TRIANGULAR WING

The following wing is also called delta wing. We changed the terminology to *triangular* to ensure distinction from the delta wings studied earlier and also to match the literature which was used as reference. The triangular wing modeled here has a thickness distribution represented by the Equation (3.5).

$$y = h(x,z) = 2\delta(x-\frac{|z|}{\sigma})(1-x) \tag{3.5}$$

which is a parabolic arc in all X,Y planes and which has linearly decreasing h in all Y,Z planes. (Note that the roll, pitch, and yaw axis correspond to the x, y, and z axis respectively in PMARC and to the x, z, and y axis respectively in our reference literature (Ref. [15]). Figure 3.54 illustrates the wing. Its aspect ratio is 2/3 and for the purposes of analytical and computer analysis, its root chord will be set at one. Using these data, it can be shown with basic relationships that the semi-span at the trailing edge is 1/6, and that it varies in the x-direction like x/6, where x is the non-dimensionalized root chord location.

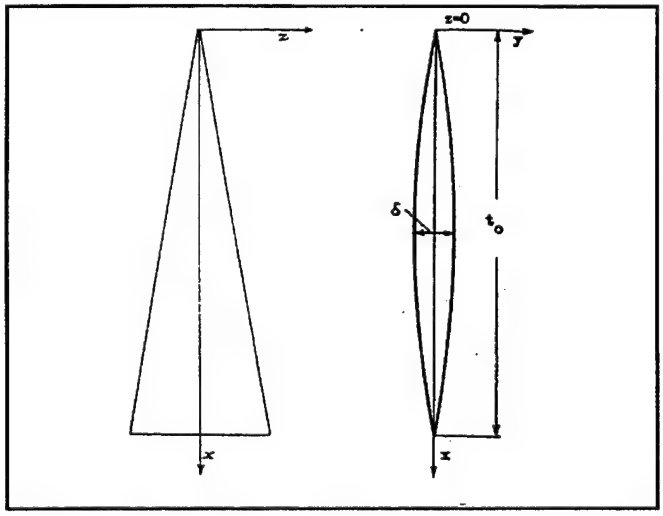

Figure 3.54 Triangular Wing, Parabolic Arc Section, AR=2/3.

Unlike the previous sections, the reference theory will be discussed in greater length before being compared to the PMARC results. The theory, introduced in the previous section, will first be presented in its general form, then we will analytically rework an example presented in the Reference in order to ascertain the validity and understanding of the theory. Once our results corroborate those of the author, we will finally proceed with the PMARC computation and comparison. As it will be seen, major disparities exist in the predicted velocity distributions.

1. Theory, Background and Reference Data

In the early fifties, Friedrich Keune (Ref. [15]) presented a theory on low aspect ratio wings with small thickness at zero lift in subsonic and supersonic flow. He showed that a first approximation of the flow around low aspect ratio wings can be obtained by dividing the flow into two components: the cross-sectional flow (*phi*) and the spatial influence (*omega*).

$$\Phi(x,y,z) = [\varphi(x,y,z)+\Omega(x,y,z)]U_{\infty} \tag{3.6}$$

a. Approximate Theory

The starting point of this approximate theory is the equation representing the exact velocity potential of a flow. With a thickness distribution over the wing plane represented by:

$$y = \pm h(x,z) \tag{3.7}$$

the source distribution in the wing area (Figure 3.55) is depicted by:

$$q(\xi,\zeta) = 2(\frac{dh(\xi,\zeta)}{d\xi})U\infty = 2h_x(\xi,\zeta)U\infty \tag{3.8}$$

Therefore the exact velocity potential is described with the following double integral:

$$\frac{\Phi}{U\infty} = -\frac{1}{2\pi}\int\int_{F(x,z)}\left[\frac{h_x(\xi,\zeta)}{\sqrt{((\xi-x)^2+y^2+(\zeta-z)^2)}}\right]d\xi d\zeta \qquad (3.9)$$

where F(x,z) is the wing area.

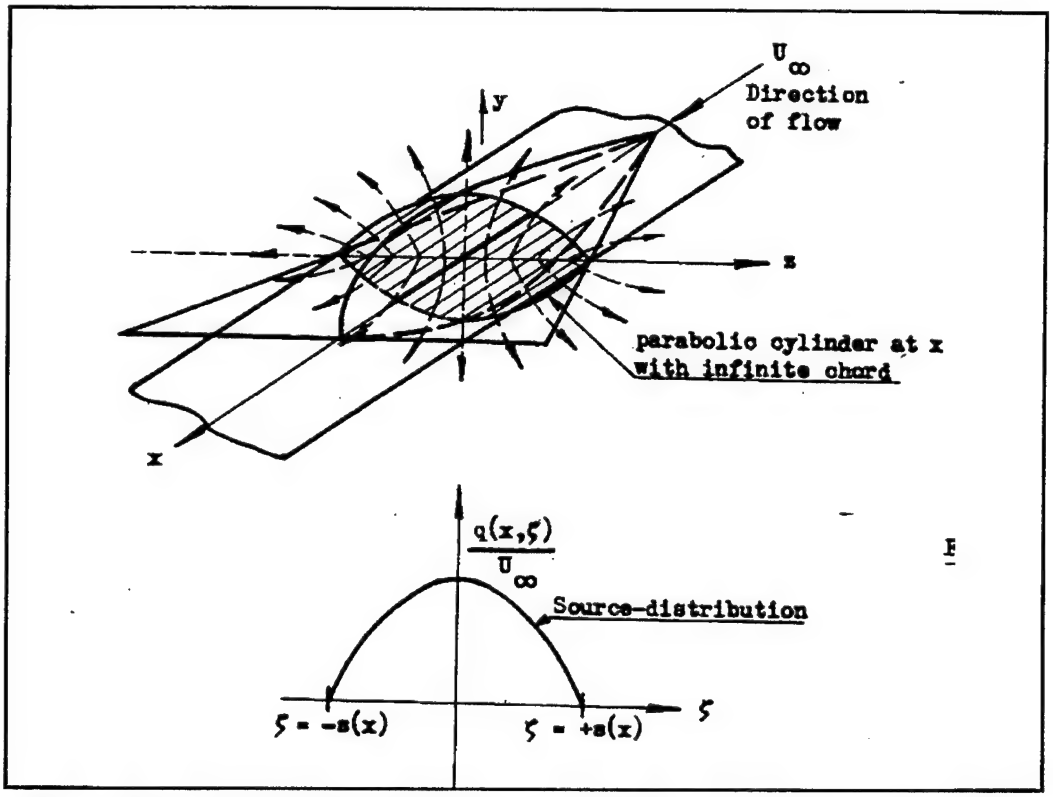

Figure 3.55 Two-Dimensional Flow Around a Low-Aspect-Ratio Wing with Thickness but Zero Lift. (From Ref. [15]).

When considering low aspect ratio wings, the ordinate *zeta* of the location of any source element may be considered small in comparison with the root chord of the wing, therefore allowing a Taylor series development of the exact equation for small *zeta*. Only the first order terms

are kept, the higher order terms being negligible. It is then possible to develop the expression into a two-dimensional (Equation (3.10)) and a rotational symmetric (Equation (3.11)) component of the potential flow . The derivation is detailed in Chapter **II** of Ref. [15].

$$\frac{\Delta\Phi}{U\infty} = \frac{1}{\pi}\int_{s_1(x)}^{s_2(x)}[h_x(x,\zeta)\ \ln\frac{\sqrt{(y^2+(\zeta-z)^2}}{\sqrt{(y^2+z^2)}}]d\zeta + 0(\sigma^3\ln\sigma) \tag{3.10}$$

$$\frac{\Phi}{U\infty} = -\frac{1}{4\pi}\int_0^{x_0} h(x,z)\ dz \tag{3.11}$$

The two-dimensional potential flow (Equation (3.10)) is caused by a two-dimensional source distribution $2*U_{inf}*(d/dx)[h(x,zeta)]$ on a line of constant chord location and at a thickness location of zero, between two outer spanwise limits (Figure 3.56). These sources inflate the flat plate to the thickness y(z)=+-h(x=const,z), or to the cross-sectional area defining the section.

The axisymmetric flow (Equation (3.11)) is induced by a source distribution along the x-axis within the wing (Figure 3.56). This flow is identical with that around a slender body of revolution.

Now the sum of the two terms shown above represents the first order term of the approximation of the velocity potential in the incompressible flow:

$$\frac{\Phi}{U_\infty} = \frac{1}{\pi}\int_{s_1(x)}^{s_2(x)}[h_x(x,\zeta)\ \ln\frac{\sqrt{(y^2+(\zeta-z)^2}}{\sqrt{(y^2+z^2)}}]d\zeta - \frac{1}{4\pi}\int_0^{x_0}\frac{Q_x(\xi)}{\sqrt{((\xi-x)^2+r^2)}}d\xi \tag{3.12}$$

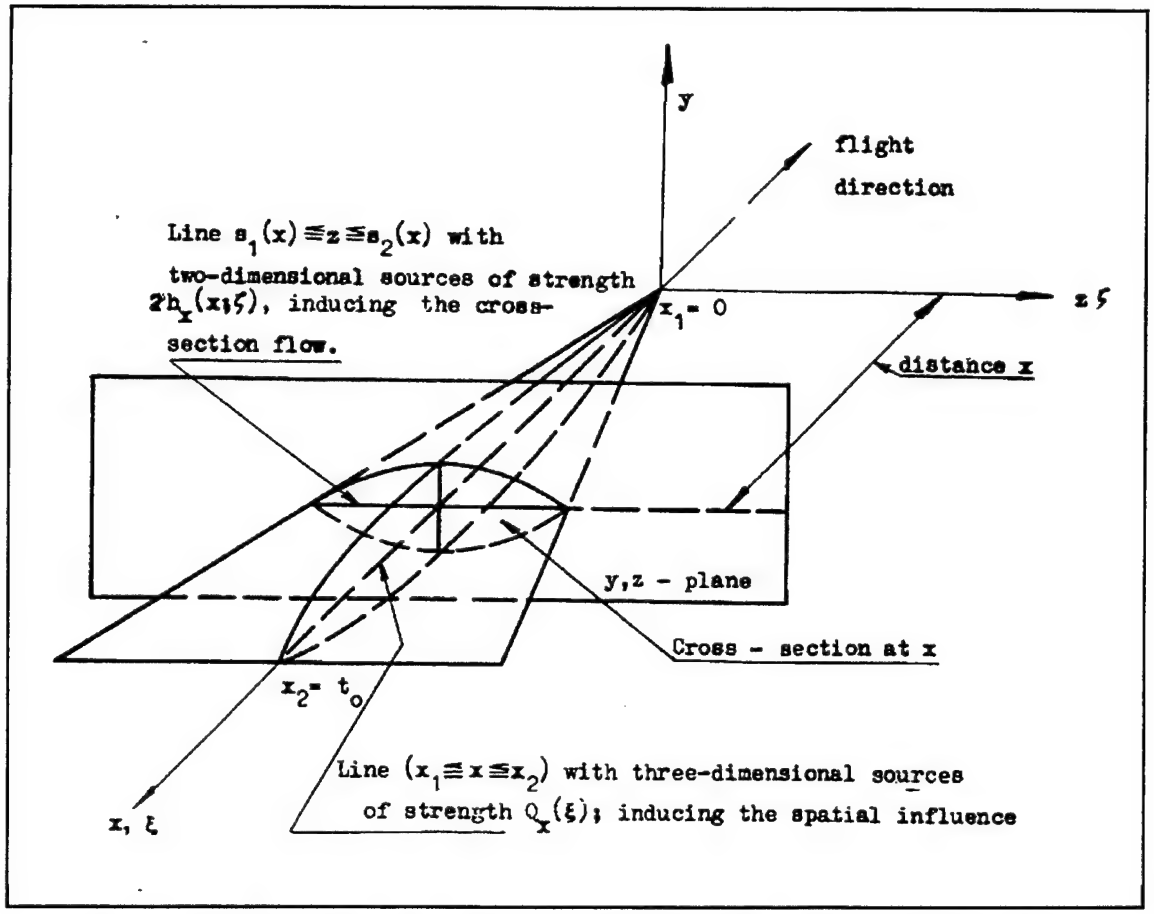

Figure 3.56 Cross-Sectional Flow and Spatial Influence. (From Ref. [15]).

The potential function for incompressible flow shown above is given for any distance from the wing. On the surface of the wing (y=0), the ordinate z has the same order of magnitude as the length *zeta*, so that z must consequently be neglected with *zeta* in this approximation. This leads to a transformation of the potential function as detailed in Chapter **IV** of Ref. [15]. The velocity field of the cross-sectional flow at y=0 is then given by:

$$\frac{\Phi}{U_\infty}: \qquad \varphi = \frac{Q_x(x)}{2\pi}\ln[s(x)\sqrt{(1-(\frac{z}{s(x)})^2)}] - \frac{1}{2\pi}\int_{-s(x)}^{+s(x)}\frac{P_x(x,\zeta)}{\zeta - z}d\zeta \qquad (3.13)$$

$$\frac{u}{U_\infty}: \qquad \varphi_x = \frac{Q_{xx}(x)}{2\pi}\ln[s(x)\sqrt{(1-(\frac{z}{s(x)})^2)}] - \frac{1}{2\pi}\int_{-s(x)}^{+s(x)}\frac{P_{xx}(x,\zeta)}{\zeta - z}d\zeta \qquad (3.14)$$

$$\frac{v}{U_\infty}: \qquad \varphi_y = h_x(x,z) \qquad (3.15)$$

$$\frac{w}{U_\infty}: \qquad \varphi_z = -\frac{1}{\pi}\int_{-s(x)}^{+s(x)}\frac{h_x(x,\zeta)}{\zeta - z}d\zeta \qquad (3.16)$$

The u component in the above equation (phi_x) can also be expressed the following non-dimensional manner:

$$\frac{\varphi_x(x,\bar{z})}{\sigma\delta} = \frac{\bar{Q}_{xx}(x)}{2\pi}[\ln\sigma + \ln\bar{s}(x) + \ln\sqrt{(1-(\frac{\bar{z}}{\bar{s}(x)})^2)}] - \frac{\bar{P}_{xx}(x,\bar{z})}{2\pi}\ln\left|\frac{1-\frac{\bar{z}}{\bar{s}(x)}}{1+\frac{\bar{z}}{\bar{s}(x)}}\right| - \frac{1}{\pi}\int_0^{\bar{s}(x)}\frac{\bar{P}_{xx}(x,\bar{\zeta}) - \bar{P}_{xx}(x,\bar{z})}{\bar{\zeta} - \bar{z}}d\bar{\zeta} \qquad (3.17)$$

$$P(x,z) = 2\int_0^z h(x,\zeta)\, d\zeta \qquad (3.18)$$

The spatial influence is represened by:

$$\frac{\Phi}{U_\infty}: \qquad \Omega = \frac{1}{4\pi} Q_x(x)[ln2x+ln2(x_o-x)] + \frac{1}{4\pi}\int_0^{x_o} \frac{Q_x(x)-Q_x(\xi)}{|x-\xi|} d\xi \tag{3.19}$$

$$\frac{u}{U_\infty}: \qquad \Omega_x = \frac{1}{4\pi}[-\frac{Q_x(0)}{x}+\frac{Q_x(x_o)}{x_o-x}] - \frac{1}{4\pi} Q_{xx}(x) ln4x(x_o-x) + \frac{1}{4\pi}\int_0^{x_o} \frac{Q_{xx}(x)-Q_{xx}(\xi)}{|x-\xi|} d\xi \tag{3.20}$$

$$\frac{v}{U_\infty}: \qquad \Omega_y = 0 \tag{3.21}$$

$$\frac{w}{U_\infty}: \qquad \Omega_z = 0 \tag{3.22}$$

The u component in the above equation ($omega_x$) can also be written:

$$\Omega_x = \frac{1}{4\pi}[-\frac{Q_x(0)}{x}+\frac{Q_x(x_o)}{x_o-x}] - \frac{1}{4\pi}[Q_{xx}(0)ln2x+Q_{xx}(x_o)ln2(x_o-x)]$$

$$-\frac{1}{4\pi}\int_0^x Q_{xxx}(\xi)ln2(x-\xi)d\xi + \frac{1}{4\pi}\int_x^{x_o} Q_{xxx}(\xi)ln2(\xi-x)d\xi \tag{3.23}$$

One marked particularity of this theory is that the spatial influence (axisymmetric flow) is only a function of the cross-sectional area. Therefore the wing can be represented by a simpler geometry with equivalent sectional area (like its equivalent body of revolution) in order to simplify the calculations

b. Analytical Application Example Using The Triangular Wing

Using a computer analytical solver (Ref. [16]), the u component of both terms of the flow were separately computed for the triangular wing described at the beginning of this section. For this wing, the segment of the cross-sectional area for positive ordinates z is:

$$P(x,z) = 4\delta\sigma(1-x)(x-\frac{|z|}{2\sigma})\frac{|z|}{\sigma} \tag{3.24}$$

and the cross-sectional area is given by:

$$Q(x) = 4\delta\sigma x^2(1-x) \tag{3.25}$$

(1) Spatial Influence. The u component of the spatial influence was computed using two equations. The first one is the general equation (Equation (3.23)) and the second one is the specific equation for the triangular wing (Equation (3.26)) as given by Ref. [15].

$$\frac{\Omega_x}{\delta\sigma} = -\frac{1}{\pi}\frac{1}{1-x} + \frac{6}{\pi}(1-2x) - \frac{2}{\pi}(1-3x)ln4x(1-x) \tag{3.26}$$

Both equations would be expected to produce the same results as Equation (3.26) is directly derived from Equation (3.23). As Figure 3.57 shows however, small disparities are observed, especially past the mid-chord point. These differences are explained by the accuracy of the integration methods used. But more importantly, the figure also indicates that we were able to exactly reproduce the results of Ref. [15] using the general Equation (3.23). Appendix **B** presents the Equations (3.21) and (3.26) at different stages of their solution.

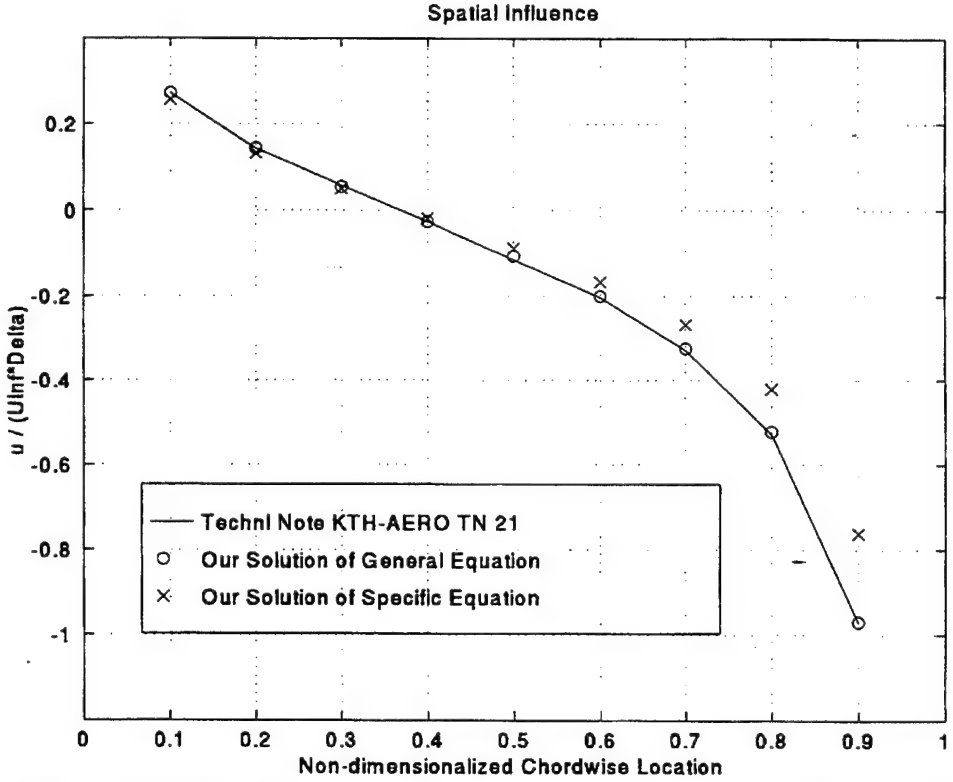

Figure 3.57 Comparison of Spatial Influence u-Component of The Velocity Potential as a Function of Chord Location. Triangular Wing, Parabolic Arc Spanwise Section, AR=2/3, AOA=0 Degree.

(2) Cross-sectional flow. Once again, two equations were solved for comparison purposes. The specific equation (Equation (3.27)) as given in Ref. [15] and the general equation (Equation (3.17)). Appendix **C** presents the equations at different stages of their solution. The results were identical and in good agreement with those obtained by Ref. [15]. Figure 3.58 presents these results.

$$\frac{\varphi_x}{\sigma\delta} = \frac{4}{\pi}(1-3x)[\ln\sigma+\ln x+\ln\sqrt{(1-\frac{z^2}{\sigma^2x^2})}] + \frac{8}{\pi}x + \frac{4}{\pi}\frac{z}{\sigma}\ln\left|\frac{1-\frac{z}{\sigma x}}{1+\frac{z}{\sigma x}}\right| \qquad (3.27)$$

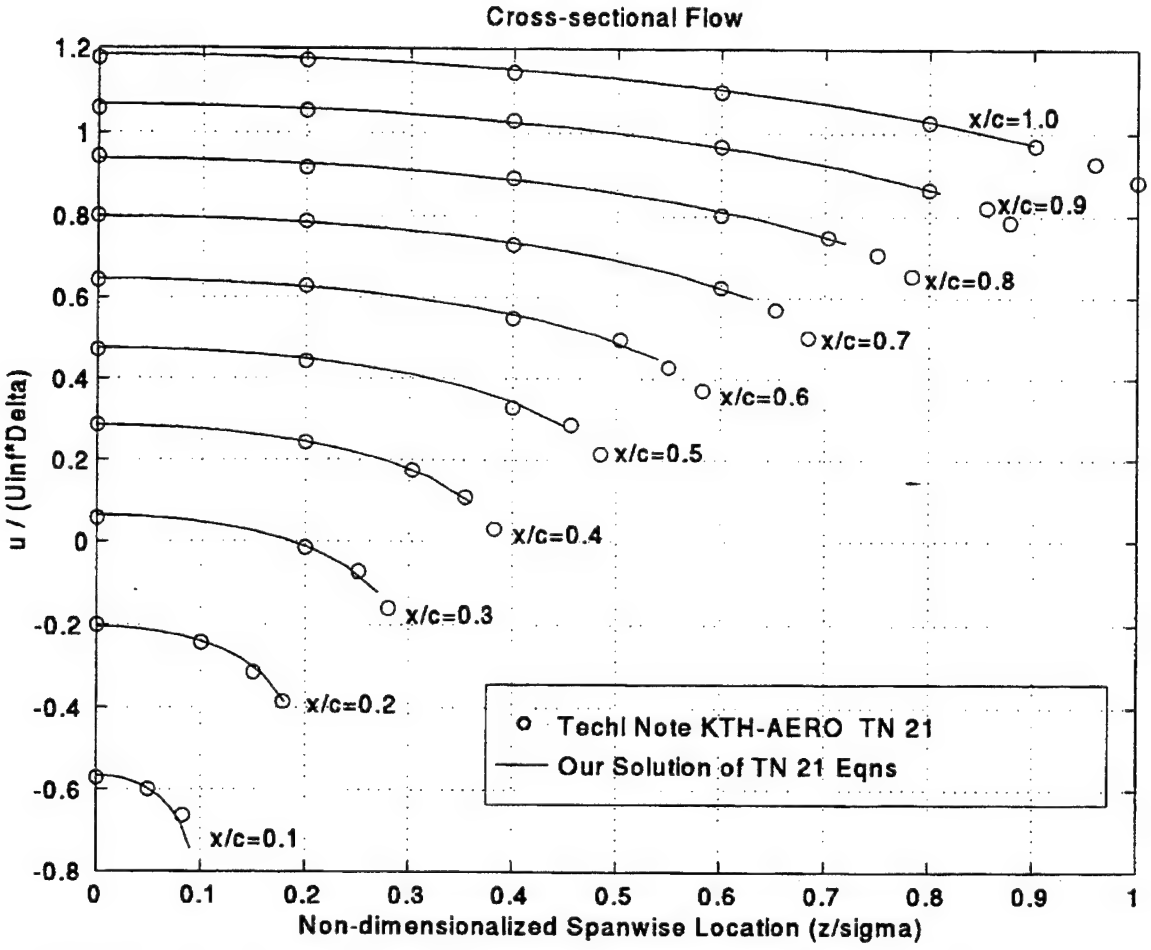

Figure 3.58 Comparison of The Chordwise Cross-Sectional Flow u-Component Velocity Potential as a Function of Non-Dimensionalized Spanwise Location. Triangular Wing, Parabolic Arc Section, AR=2/3, AOA=0 Degree.

(3) Total Flow. When the spatial influence and the cross-sectional flow results are added up, we obtain the curves depicted in Figure 3.59, which correspond very well to those computed by Ref. [15].

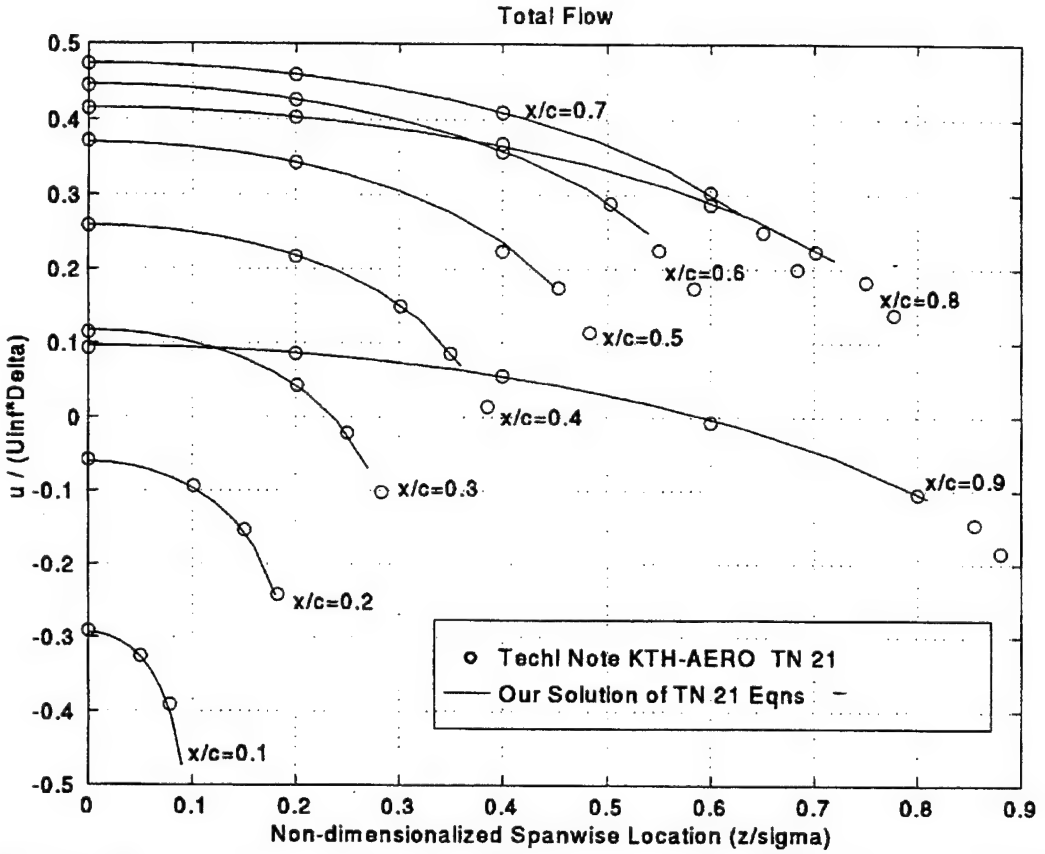

Figure 3.59 Comparison of The Combined u-Components of The Chordwise Basic Flow as a Function of Non-Dimensionalized Spanwise Location. Triangular Wing, Parabolic Arc Spanwise Section, AR=2/3, AOA=0 Degree.

2. Results and Discussion

As for the F5 wing, PMARC seems not capable of recreating a realistic x-component velocity distribution on the triangular wing. Figure 3.60 once again shows velocity peaks that increase as the spanwise location gets towards the tip. This is a behavior that would be more representative of a wing of constant thickness. In our case, the tip is modelled to be of virtually zero

thickness, therefore the velocity perturbation should approach zero as we get closer to the tip. On Figure 3.60, zbar is the non-dimensional spanwise location divided by the dimensionless semi-span. As mentioned before, z corresponds to the y axis in the PMARC notation and was left as is to match our reference notation (Ref. [15]).

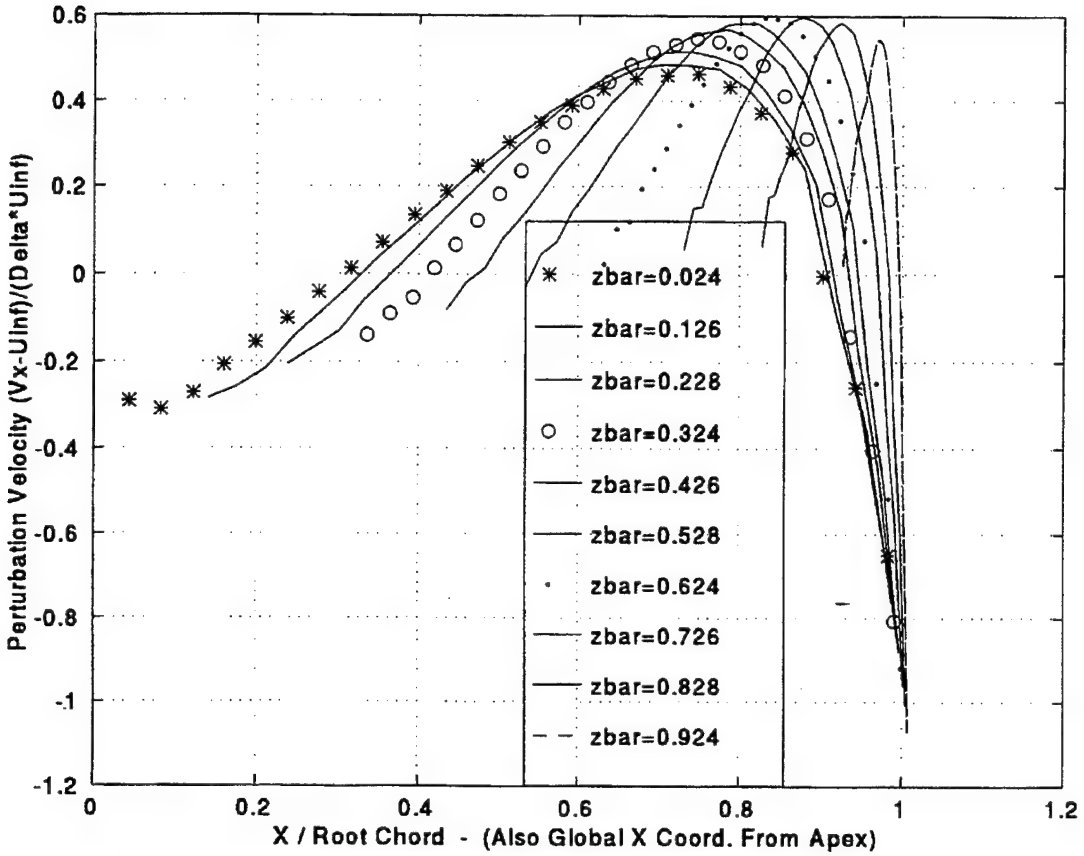

Figure 3.60 Spanwise Perturbation Velocity as a Function of Chord Location. Triangular Wing, Parabolic Arc Spanwise Section, AR=2/3, AOA=0 Degree.

In order for the reader to better appreciate what behavior is expected, we extracted a figure from Ref. [15] which shows the perturbation velocity distribution on the triangular wing. Interpretation of this figure corroborates the intuitive expectation of progressively smaller perturbation velocity from root to tip. See Figure 3.61 below.

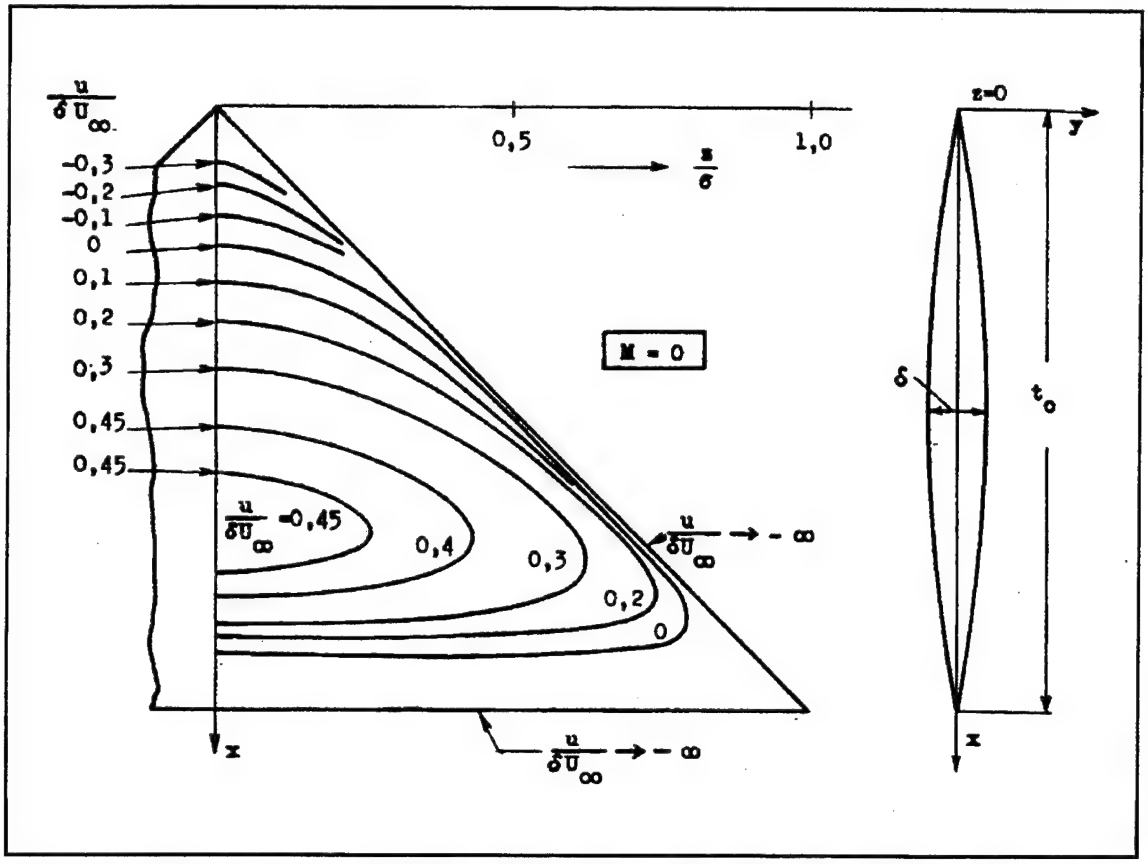

Figure 3.61 Isotaches in The Wing Plane. Triangular Wing, Parabōlic Arc Spanwise Section, AR=2/3, AOA=0 Degree. z/x Proportions Not to Scale. (From Ref. [15])

To ensure that the erroneous results were not due to our geometry which in turn could have caused matrix singularities, a series of variation of our triangular wing were modeled. The tips were truncated, the leading and trailing edges were rounded, and the panel density and distribution were varied. Larger aspect ratio delta wings were also modelled and all without any positive effect. The same erroneous behavior was always present.

Interestingly however, the problem is not apparent in the case of rectangular geometries. As shown in Appendix **D**, a thickness tapered rectangular wing was modelled and the velocity perturbation decreases towards the tips, as it should.

3. PMARC Input Instructions

The input file for the triangular wing is no different than any of the delta wings previously studied. Only the airfoil section, the tip location, the geometric fields, and the scaling vary. The points defining the airfoil cross-section were separately obtained substituting chordwise locations in the triangular wing expression of thickness distribution (Equation (3.5)). In the following paragraphs, one of the above differences will be discussed, the tip scaling, and an important observation will be brought to light regarding the spanwise cross-section definition in PMARC.

a. The Tip Scaling

As it can be observed in the triangular wing input file (Figure 3.62), the tip scaling was made smaller than what was done for the delta wings. It was mentioned then that we wanted as small a tip as we could get without creating too many panels with virtually zero area. In the case of the delta wings, SCALE=0.05 was an optimum value which would generate a relatively low number of zero area panels . With the triangular wing, this scaling would change the aspect ratio of the wing as it corresponds to a larger proportion of the root chord. We then had to go down as low as SCALE=0.01 to conserve the triangular shape, although that increased the number of zero area panels. However, these panels account for a small proportion of the total number of panels, still allowing for a good flow solution.

b. Spanwise Cross-Section Definition

The spanwise cross-section of the wing as defined in the input file of Figure 3.62 has a linearly decreasing thickness. The cross-section would then have a diamond shape. This is due to the fact that we prescribed the coordinates for the origin of the root chordwise cross-section and also for the tip cross-section and from there, PMARC seems to linearly interpolate all the origin coordinates of all chordwise cross-sections in between. The delta wings studied earlier also had this diamond shape spanwise cross-section.

If the spanwise cross-section has a non-linearly decreasing thickness from root to tip creating an oval shape or double parabolic arc shape, then the PMARC construction

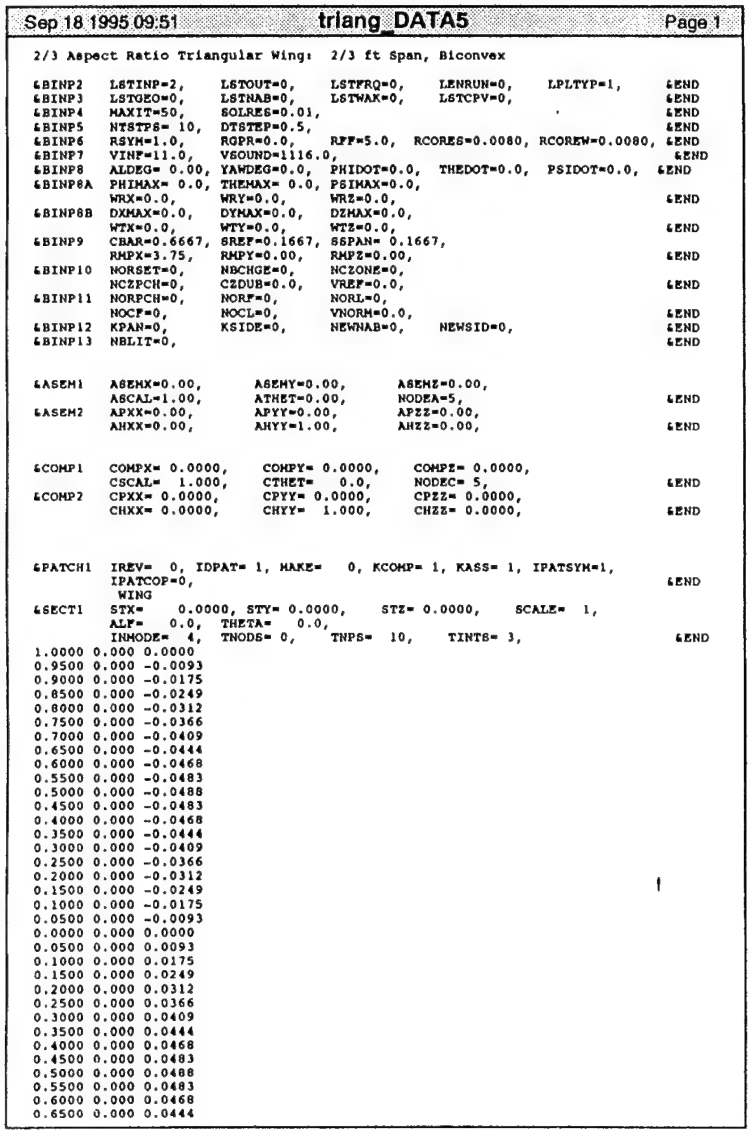

Sep 18 1995 09:51 triang_DATA5 Page 1

```
2/3 Aspect Ratio Triangular Wing:  2/3 ft Span, Biconvex

&BINP2    LSTINP=2,     LSTOUT=0,     LSTFRQ=0,     LENRUN=0,     LPLTYP=1,     &END
&BINP3    LSTGEO=0,     LSTNAB=0,     LSTWAK=0,     LSTCPV=0,                   &END
&BINP4    MAXIT=50,     SOLRES=0.01,                                            &END
&BINP5    NTSTPS= 10,   DTSTEP=0.5,                                             &END
&BINP6    RSYM=1.0,     RGPR=0.0,     RFF=5.0,   RCORES=0.0080, RCOREW=0.0080, &END
&BINP7    VINF=11.0,    VSOUND=1116.0,                                          &END
&BINP8    ALDEG= 0.00, YAWDEG=0.0,  PHIDOT=0.0,  THEDOT=0.0,  PSIDOT=0.0,   &END
&BINP8A   PHIMAX= 0.0, THEMAX= 0.0, PSIMAX=0.0,
          WRX=0.0,      WRY=0.0,      WRZ=0.0,                                  &END
&BINP8B   DXMAX=0.0,    DYMAX=0.0,    DZMAX=0.0,
          WTX=0.0,      WTY=0.0,      WTZ=0.0,                                  &END
&BINP9    CBAR=0.6667, SREF=0.1667, SSPAN= 0.1667,
          RMPX=3.75,    RMPY=0.00,    RMPZ=0.00,                                &END
&BINP10   NORSET=0,     NBCHGE=0,     NCZONE=0,
          NCZPCH=0,     CZDUB=0.0,    VREF=0.0,                                 &END
&BINP11   NORPCH=0,     NORF=0,       NORL=0,
          NOCF=0,       NOCL=0,       VNORM=0.0,                                &END
&BINP12   KPAN=0,       KSIDE=0,      NEWNAB=0,     NEWSID=0,                   &END
&BINP13   NBLIT=0,                                                              &END


&ASEM1    ASEMX=0.00,       ASEMY=0.00,       ASEMZ=0.00,
          ASCAL=1.00,       ATHET=0.00,       NODEA=5,                        &END
&ASEM2    APXX=0.00,        APYY=0.00,        APZZ=0.00,
          AHXX=0.00,        AHYY=1.00,        AHZZ=0.00,                      &END


&COMP1    COMPX= 0.0000,    COMPY= 0.0000,    COMPZ= 0.0000,
          CSCAL=  1.000,    CTHET=   0.0,     NODEC= 5,                       &END
&COMP2    CPXX= 0.0000,     CPYY= 0.0000,     CPZZ= 0.0000,
          CHXX= 0.0000,     CHYY=  1.000,     CHZZ= 0.0000,                   &END



&PATCH1   IREV=  0, IDPAT= 1, MAKE=   0, KCOMP= 1, KASS= 1, IPATSYM=1,
          IPATCOP=0,                                                          &END
           WING
&SECT1    STX=    0.0000, STY= 0.0000,    STZ= 0.0000,    SCALE=  1,
          ALF=   0.0,  THETA=   0.0,
          INMODE=  4,  TNODS= 0,    TNPS=  10,    TINTS= 3,                    &END
1.0000 0.000 0.0000
0.9500 0.000 -0.0093
0.9000 0.000 -0.0175
0.8500 0.000 -0.0249
0.8000 0.000 -0.0312
0.7500 0.000 -0.0366
0.7000 0.000 -0.0409
0.6500 0.000 -0.0444
0.6000 0.000 -0.0468
0.5500 0.000 -0.0483
0.5000 0.000 -0.0488
0.4500 0.000 -0.0483
0.4000 0.000 -0.0468
0.3500 0.000 -0.0444
0.3000 0.000 -0.0409
0.2500 0.000 -0.0366
0.2000 0.000 -0.0312
0.1500 0.000 -0.0249
0.1000 0.000 -0.0175
0.0500 0.000 -0.0093
0.0000 0.000 0.0000
0.0500 0.000 0.0093
0.1000 0.000 0.0175
0.1500 0.000 0.0249
0.2000 0.000 0.0312
0.2500 0.000 0.0366
0.3000 0.000 0.0409
0.3500 0.000 0.0444
0.4000 0.000 0.0468
0.4500 0.000 0.0483
0.5000 0.000 0.0488
0.5500 0.000 0.0483
0.6000 0.000 0.0468
0.6500 0.000 0.0444
```

Sep 18 1995 09:51 triang_DATA5 Page 2

```
0.7000 0.000 0.0409
0.7500 0.000 0.0366
0.8000 0.000 0.0312
0.8500 0.000 0.0249
0.9000 0.000 0.0175
0.9500 0.000 0.0093
1.0000 0.000 0.0000
&BPNODE   TNODE=3     TNPC=30     TINTC=0     &END
&SECT1    STX=   1.00, STY= 0.1667,    STZ= 0.0000,    SCALE=  0.01,
          ALF=   0.0,  THETA=   0.0,
          INMODE=  0,  TNODS= 3,    TNPS= 10,    TINTS= 3,                    &END

&PATCH1   IREV=  0, IDPAT= 1, MAKE=   1, KCOMP= 1, KASS= 1, IPATSYM=1,
          IPATCOP=0,                                                          &END
           WING_TIP
&PATCH2   ITYP=  2,    TNODS= 5,    TNPS=   1,   TINTS= 3,                   &END


&WAKE1    IDWAK=1,        IFLXW=1,        ITRFTZ= 0,      INTRW= 0,          &END
 WING_WAKE
&WAKE2    KWPACH=2,       KWSIDE=4,       KWLINE=0,       KWPAN1=0,
          KWPAN2=0,       NODEW=0,        INITIAL=0,                         &END
&WAKE2    KWPACH=1,       KWSIDE=2,       KWLINE=0,       KWPAN1=0,
          KWPAN2=0,       NODEW=5,        INITIAL=0,                         &END


&ONSTRM   NONSL =0,  KPSL = 20,                                               &END


&BLPARAM RN =35755000,    VISC = 0.000157, NSLBL = 1,                          &END


&VS1      NVOLR= 0,       NVOLC= 0,                                           &END
&VS2      X0=    -0.1000, Y0=     1.5000, Z0=    -0.1000, INTVSR= 1,          &END
&VS3      X1=    -0.1000, Y1=     1.5000, Z1=     0.1000, NPT1=  0,           &END
&VS4      X2=    -0.1000, Y2=     1.5000, Z2=     0.1000, NPT2= 20,           &END
&VS5      X3=     1.1000, Y3=     1.5000, Z3=    -0.1000, NPT3= 25,           &END

&VS6      XR0=    2.0000, YR0=    2.0000, ZR0=    0.0000, INTVSC= 1,          &END
&VS7      XR1=    4.0000, YR1=    2.0000, ZR1=    0.0000,
          XR2=    2.0000, YR2=    2.0000, ZR2=    1.0000,                     &END
&VS8      R1=     0.1000, R2=     1.0000, PHI1=  0.0,     PHI2=360.0,         &END
&VS9      NRAD=   5,      NPHI=   12,     NLEN=  3,                          &END


&SLIN1    NSTLIN=0,                                                           &END
&SLIN2    SX0=   -2.0000, SY0=     1.0000, SZ0=   -0.5000,
          SU=     0.0000, SD=    10.0000, DS=     0.2500, INTSL= 1,           &END
&SLIN2    SX0=   -2.0000, SY0=     1.0000, SZ0=   -0.4000,
          SU=     0.0000, SD=    10.0000, DS=     0.2500, INTSL= 1,           &END
&SLIN2    SX0=   -2.0000, SY0=     1.0000, SZ0=   -0.3000,
          SU=     0.0000, SD=    10.0000, DS=     0.2500, INTSL= 1,           &END
&SLIN2    SX0=   -2.0000, SY0=     1.0000, SZ0=   -0.2000,
          SU=     0.0000, SD=    10.0000, DS=     0.2500, INTSL= 1,           &END
&SLIN2    SX0=   -2.0000, SY0=     1.0000, SZ0=   -0.1000,
          SU=     0.0000, SD=    10.0000, DS=     0.2500, INTSL= 1,           &END
&SLIN2    SX0=   -2.0000, SY0=     1.0000, SZ0=    0.0000,
          SU=     0.0000, SD=    10.0000, DS=     0.2500, INTSL= 1,           &END
```

Figure 3.62 PMARC Input File for Triangular Wing, Parabolic Arc Spanwise Section, AR=2\3.

would be more intricate. Although not tried, it is suspected that several different airfoil section definitions would be required at various spanwise locations, each showing a different thickness to chord ratio. Enough of these intermediate section definitions would be required to create a smooth spanwise cross-section.

4. PMARC Output - Data Retrieval

a. Direct Method

In order to reproduce the format of the results presented in our reference literature (Figure 3.63), an intricate data retrieval is required. As can be seen from that figure, we need arrays of velocities taken at constant x values, for various increasing z values (y in PMARC). To do that, we need to find the beginning of the steady state results in DATA6. Then, for each block of results (which corresponds to columns, or strips of panels) the velocity Vx at x=0.1 is recorded. The same process is repeated for x=0.2 and all other chordwise locations desired.

Unless the panel density is very high, one won't find in the output the chordwise locations that exactly correspond to locations plotted in Figure 3.63, (x=0.1, 0.2, 0.3, 0.4 ...). Therefore, an interpolation will be required. In that regard, it was observed that quadratic interpolations produce slightly different results than linear interpolations. The difference being small, the latter method would be acceptable for the type of comparative study in question.

b. Indirect Method

Another data retrieval technique is a lot simpler but some interpretation of the resulting plots is needed to compare with the reference plots. All that is required here is to plot the x column against the Vx column for selected blocks of data (or panel strips). This produces plots as presented in Figure 3.60. The difference is that instead of dealing with perturbation velocities as a function of spanwise stations for fixed chordwise locations, we deal with perturbation velocities as a function of chordwise stations for fixed spanwise locations.

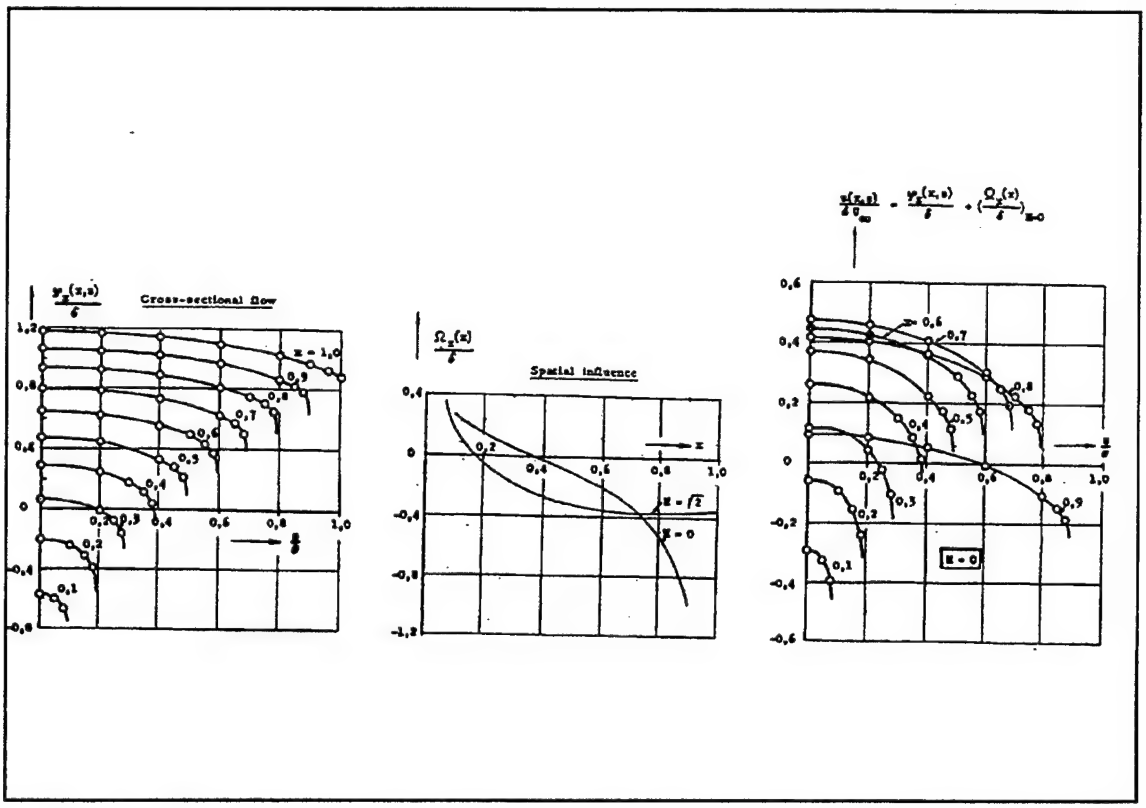

Figure 3.63 Flow Results From F. Keune in The Plane y=0 (PMARC *z*). Triangular Wing, Parabolic Arc Spanwise Section, AR=2/3, AOA=0 Degree. (From Ref. [15]).

c. Perturbation Velocity

The data retrieved in DATA6 are *x*-component velocities. Plotting these values instead of those shown in the reference plots (perturbation velocities) would only make a difference in the abscissa and ordinate; the behavior of the curves would be the same. However, we were interested in the perturbation velocities which are simply the velocities found in the DATA6 minus the freestream velocity, all divided by the product of the freestream velocity and the dimensionless maximum thickness.

$$u = \frac{V_x - U_\infty}{U_\infty \delta} \tag{3.4}$$

H. CONCLUSION

In this chapter, we demonstrated that lift and pressure coefficients generated by PMARC accurately compare with the wide range of experimental and theoretical results consulted, or with higher order panel code results. However, disparities were found in the area of velocity distribution as the PMARC results showed increasing velocity perturbation towards the tips of the triangular wing whose thickness actually decreases towards the tips. On the other hand, it was also shown that the perturbation velocity behavior was adequate in the case of a thickness tapered rectangular wing. Another area that requires more attention is the wing tip modelling. It would have to be ascertain that panels with virtually no area indeed do not corrupt any of the output.

The cases studied in this chapter include swept back wings, delta wings, rectangular wings and the F5 wing. Instructions were given on how to build each model and make the input file. Also, details on data retrieval from the PMARC output file were provided for each case studied.

IV. SOFTWARE VALIDATION - BODIES OF REVOLUTION

A. INTRODUCTION

The previous chapter studied the PMARC capability to recreate existing aerodynamic parameters of standard shape wings in steady state. This chapter has the same objective for bodies of revolution. The body of revolution is the longitudinal integration of circular cross-sections. Computational advantages are associated with this technique as was introduced earlier.The body of revolution can be one of independent shape or one which is an equivalent representation of the spanwise cross-sectional area of a given wing. The two types will be treated here. More specifically, the equivalent area body of revolution for the F5 wing and the triangular wing studied previously will be modelled. A spindle will also be analyzed. The spindle is a body of revolution symmetric about all axes originating at the mid-chord point. In all cases, the emphasis will be on the pressure distributions. It is because there exist important relationships between the aerodynamic coefficients of a wing and those of its equivalent body of revolution that we will build and analyze the latter. Note that the demonstration of the above mentioned relationships and their utilities will be the subject of follow-up work. For now, we will only present and discuss the chordwise pressure distribution at various circumferential locations for angles of attack of zero and five degrees, which will be compared against the outcome of the slender body theory.

Based on the format of the previous chapter, each body of revolution will have a dedicated section. The respective bodies will first be described, followed by an overview of the applicable theory serving as reference. Then, the results as obtained by PMARC will be presented and discussed. Also, the specific PMARC input steps for modeling the subject body of revolution will be explained. Finally, the output data retrieval techniques are presented.

B. F5 WING - EQUIVALENT AREA BODY OF REVOLUTION

The F5 wing was modelled earlier in this paper and several pressure distributions were obtained for some specific conditions of flight. The correspondent equivalent area body of revolution will have the same main chord length of 0.6439 unit. Figure 4.1 shows the F5 wing superposed to its equivalent body of revolution. The spanwise cross-sectional areas of the wing needed to build the body of revolution were obtained using an indepth computer program designed by the author and presented later in this section.

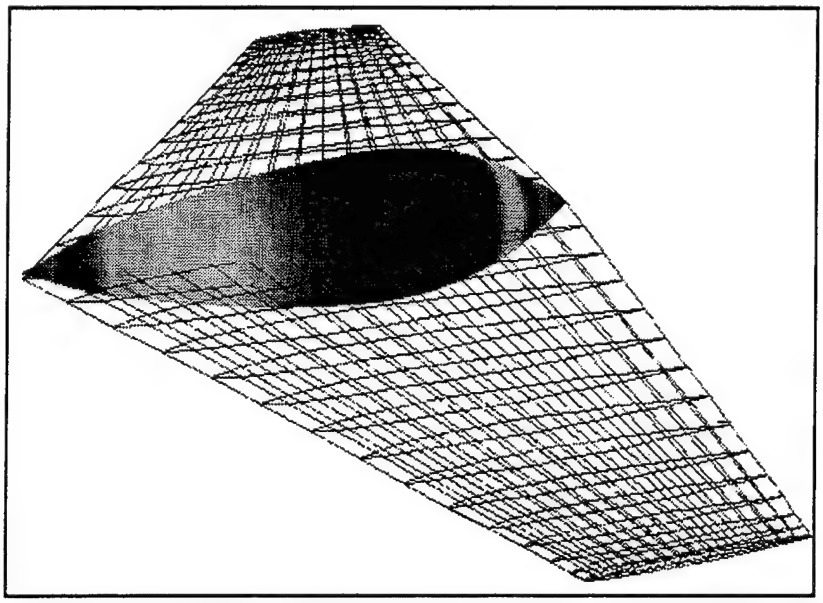

Figure 4.1 F5 Wing With Corresponding Equivalent Area Body of Revolution.

1. Theory, Background and Reference Data

In order to validate the PMARC results of pressure distribution for the F5 equivalent body of revolution, we will rely on past experience for the general expected behavior, and on the approximate slender body theory for the magnitude of the pressures. Our chordwise pressure distribution analysis will be performed at several circumferential locations to ensure consistency in the expected trends.

a. Expected General Behavior

As a general behavior, the total lift on a body of revolution should be zero as the upward lift on the front portion of the body is cancelled by the downward lift on the rear portion. In terms of pressure distribution, it will be observed that for a change of angle of attack from zero to an arbitrary value, the pressure differential (from zero to a new value of angle of attack) at a specific aft chordwise location will be equal in magnitude but in the reverse direction than that of a related rearward location. This means that somewhere along the chord there is a point where this differential is bound to be zero. This point is not at the mid-chord, except for a symmetrical body of revolution like the spindle, as we will see later.

The behavior described above would be modified for the chordwise distributions that lie along the 0 and 270 degree circumferential positions. Not only is the magnitude of the pressure differential for a zero to five degrees shift in angle of attack expected to be the same at two related forward and rearward positions, but also the direction of the pressure.

b. Slender Body Theory

According to the slender body theory, the pressure on a body at angle of attack is approximated by the pressure at zero angle of attack plus the pressure differential between its value at zero and at the new angle of attack. This differential can be calculated using the following slender body theory derivation in which R is the radius distribution and Q the cross-sectional area distribution.

$$Cp = Cp_{\alpha\text{-}0} + Cp_{d\alpha} \tag{4.1}$$

$$Cp_{d\alpha} = 2\alpha R'(x)\cos\theta \tag{4.2}$$

where:

$$R(x) = \sqrt{(\frac{Q(x)}{\pi})} \tag{4.3}$$

$$R'(x) = \frac{1}{2\pi} Q'(x) \sqrt{(\frac{Q(x)}{\pi})} \tag{4.4}$$

$$Q(x) = 71.3x^{10} - 352.00x^{9} + 743.17x^{8} - 875.60x^{7} + 630.85x^{6}$$

$$-286.66x^{5} + 81.70x^{4} - 14.13x^{3} + 1.42x^{2} - 0.04x \tag{4.5}$$

Using the expected behavior description given above and the numerical results of the slender body theory applied to the F5 wing equivalent body of revolution, we will now present the PMARC results.

2. Results and Discussion

Figures 4.3 to 4.8 presented below display the chordwise pressure distribution at various circumferential positions for two angles of attack, which will allow comparison with intuitive expectations . Figures 4.9 to 4.12 show the pressure perturbation when going from zero angle of attack to 5 degrees, as calculated by PMARC and the slender body theory. It should be noted that the circumferential positions of the chordwise body line of analysis were chosen to correspond with the control point coordinates of the chordwise strips of panels which were the closest to the points separating the body cross-section in 12 pie sections (Figure4.2). Finally, although the first and last point on all the figures were plotted, they should be disregarded. The reasons are not well understood but PMARC has difficulty with the pointy nose and tail when the model is built by

repetitive scaling like for the F5 and triangular wing equivalent bodies of revolution, by opposition to individual cross-section definition like for the spindle. These two methods will be reviewed later.

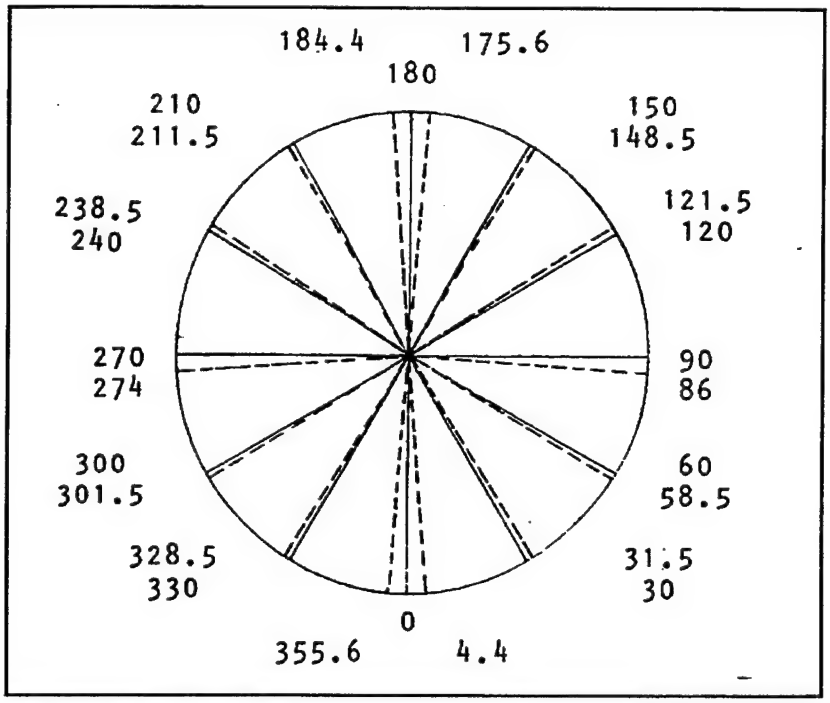

Figure 4.2 Circumferential Angular Locations Studied on The F5 Wing Equivalent Body of Revolution Cross-Sections. (Dotted Lines)

a. Chordwise Pressure Distributions

The first figure (Figure 4.3) shows the expected results that the pressure distribution will be the same for any circumferential position when the body of revolution is at zero angle of attack. Figure 4.4 presents the same parameters but with the body at five degrees angle of attack. We now observe the progression in pressure from top to bottom at a particular aft section and regression at a particular rear section. This plot also shows the relative chordwise position of the minimum pressure for each chordwise distribution.

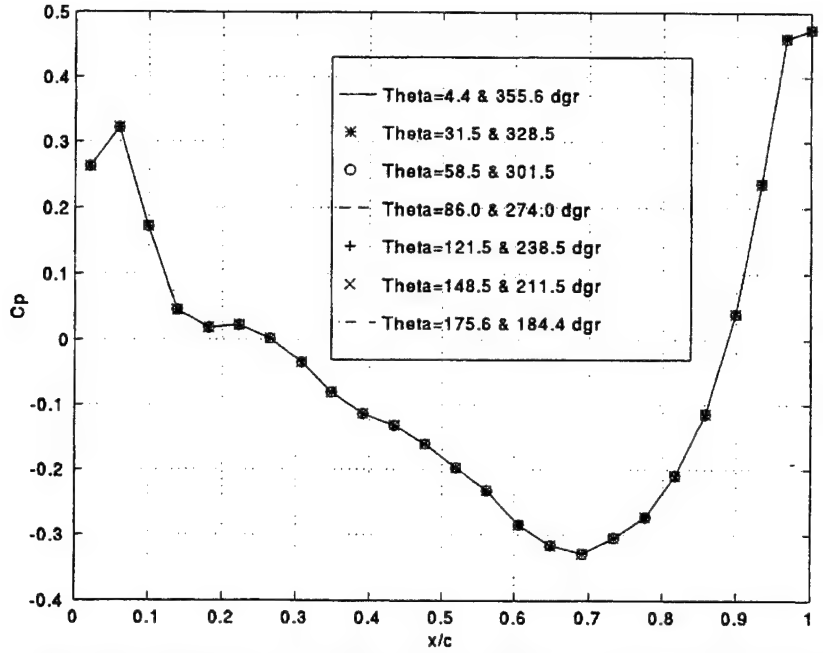

Figure 4.3 Chordwise Pressure Distribution for Various Circumferential Angles. F5 Wing Equivalent Body of Revolution. AOA=0 Degree.

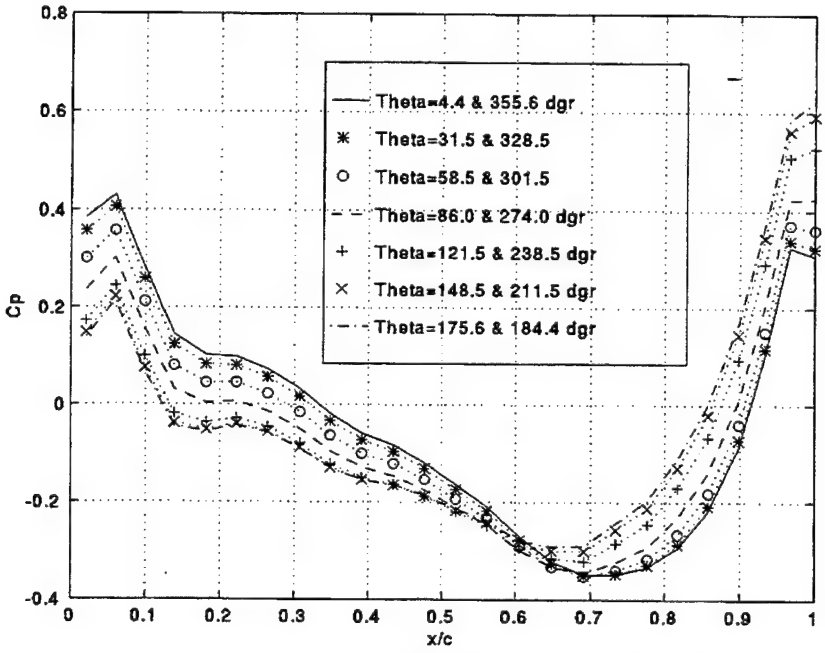

Figure 4.4 Chordwise Pressure Distribution for Various Circumferential Angles. F5 Wing Equivalent Body of Revolution, AOA=5 Degrees.

Figures 4.5 to 4.8 compare the chordwise pressure distribution at various circumferential positions for zero and five degrees angle of attack. Each figure displays the variation for two corresponding circumferential positions (longitudinal mirror image) of the body. In all cases, the leeward pressure perturbation is equal and opposite to the windward pressure perturbation, as expected. At theta in the vicinity of 90 degrees, a pressure perturbation exists but remains approximatively constant along the chord.

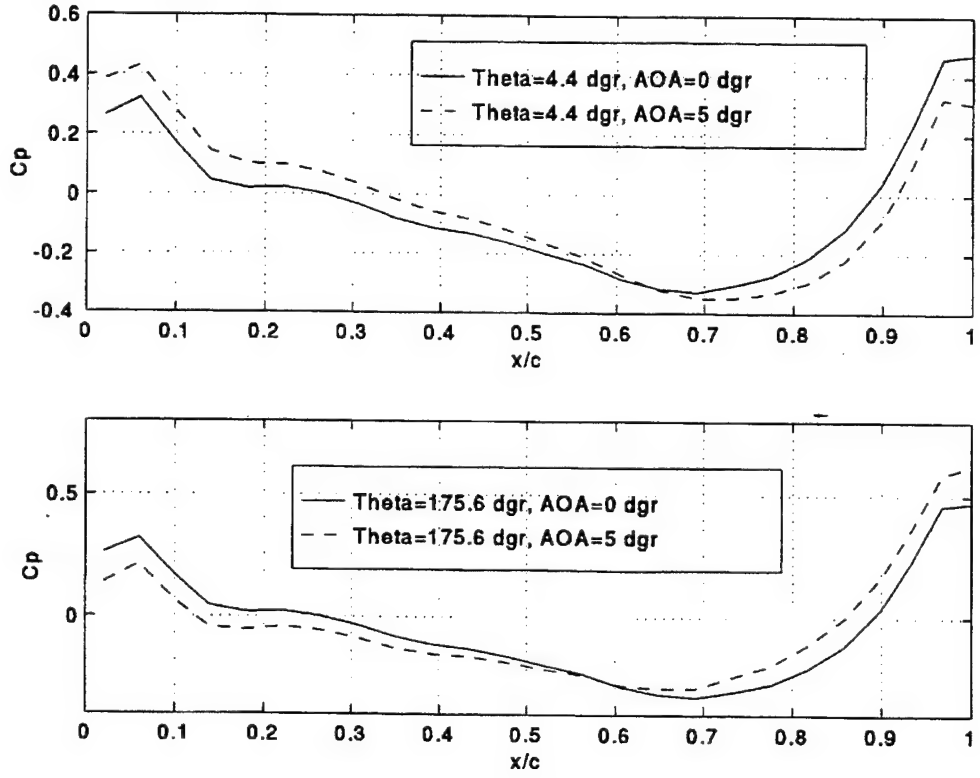

Figure 4.5 Comparison of Chordwise Pressure Distribution Along Selected Circumferential Angular Positions for Two Angles of Attack. F5 Wing Equivalent Body of Revolution.

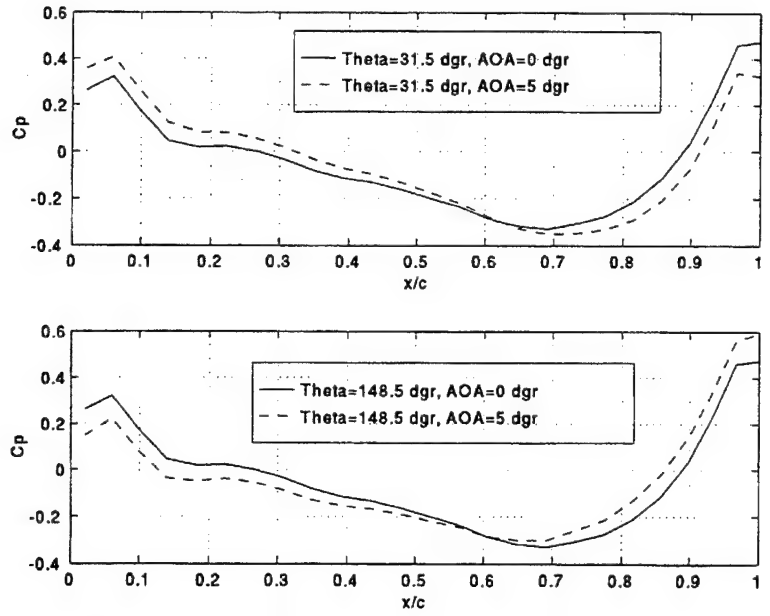

Figure 4.6 Comparison of Chordwise Pressure Distribution Along Selected Circumferential Angular Positions for Two Angles of Attack. F5 Wing Equivalent Body of Revolution.

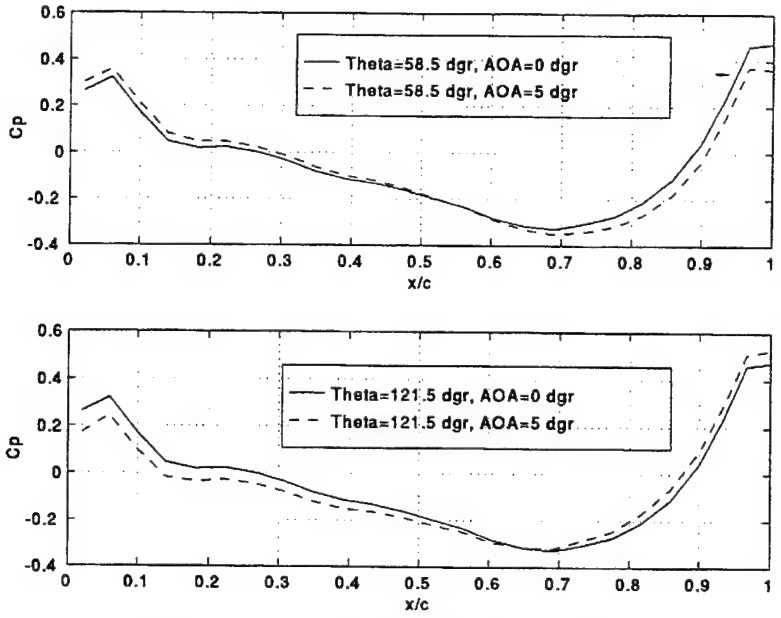

Figure 4.7 Comparison of Chordwise Pressure Distribution Along Selected Circumferential Angular Positions for Two Angles of Attack. F5 Wing Equivalent Body of Revolution.

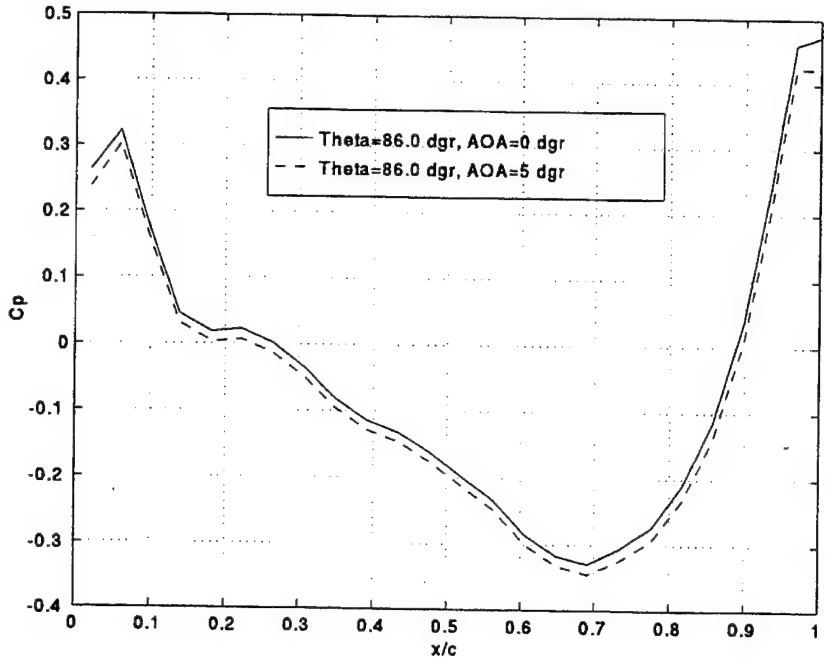

Figure 4.8 Comparison of Chordwise Pressure Distribution Along a Selected Circumferential Angular Position for Two Angles of Attack. F5 Wing Equivalent Body of Revolution.

b. Pressure Perturbations

Using the PMARC results on Figures 4.5 to 4.8 above, the difference in pressure between the body at zero and five degrees angle of attack was calculated for various circumferential positions and plotted against the pressure perturbation as computed with the slender body theory at the same respective circumferential positions and the same change of angle of attack (Figures 4.9 to 4.12).

For reasons given in the previous subsection, the extremities of these plots should be discarded. However, this restriction still leaves relatively large disparities between the two perturbation calculations for all the cases considered. These disparities are larger towards the nose and the tail and progressively reduce to zero towards the shifting point.

The shifting point is defined as the chordwise location where there is no pressure perturbation following the change of angle of attack. Ahead of the shifting point the pressure perturbations will be in the opposite direction than those after. It can be observed that the shifting points as calculated with the slender body theory do not always correspond to those obtained by PMARC. The differences for the theta angles 4.4, 31.5, 58.5, 121.5, 148.5, and 175.6 degrees are 1.5%, 0.0%, 12.7%, 3.1%, 3.3%, and 6.9% respectively.

For the theta position of 86 degrees, we observe that the perturbations are close to zero. A reading at exactly 90 degrees would in fact reveal zero perturbation when computed with the slender body theory.

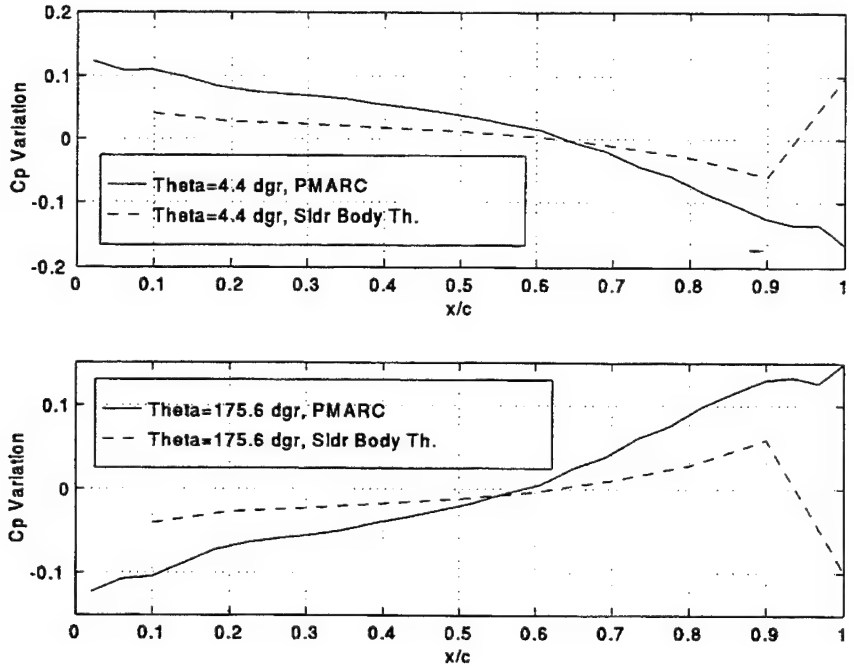

Figure 4.9 Comparison of Chordwise Pressure Perturbation at Selected Circumferential Angular Positions for a 0 to 5 Degree Change in AOA. F5 Wing Equivalent Body of Revolution.

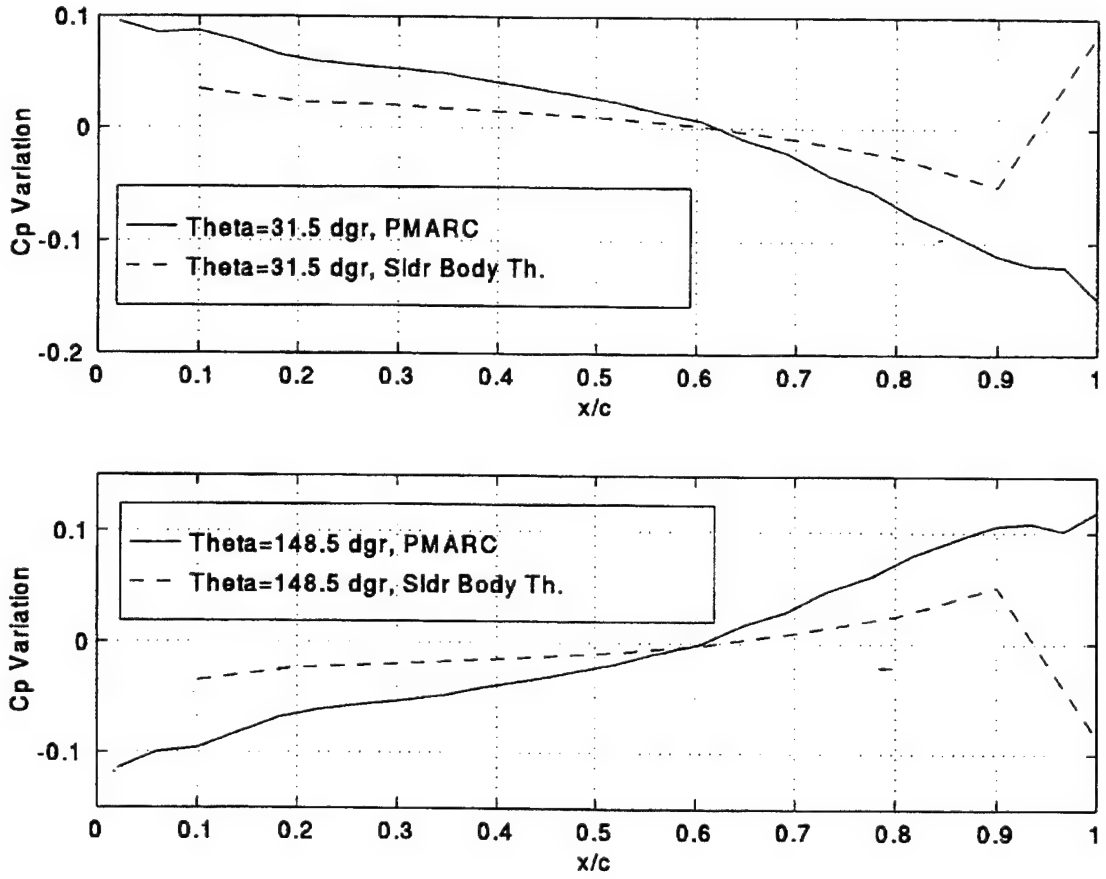

Figure 4.10 Comparison of Chordwise Pressure Perturbation at Selected Circumferential Angular Positions for a 0 to 5 Degree Change in AOA. F5 Wing Equivalent Body of Revolution.

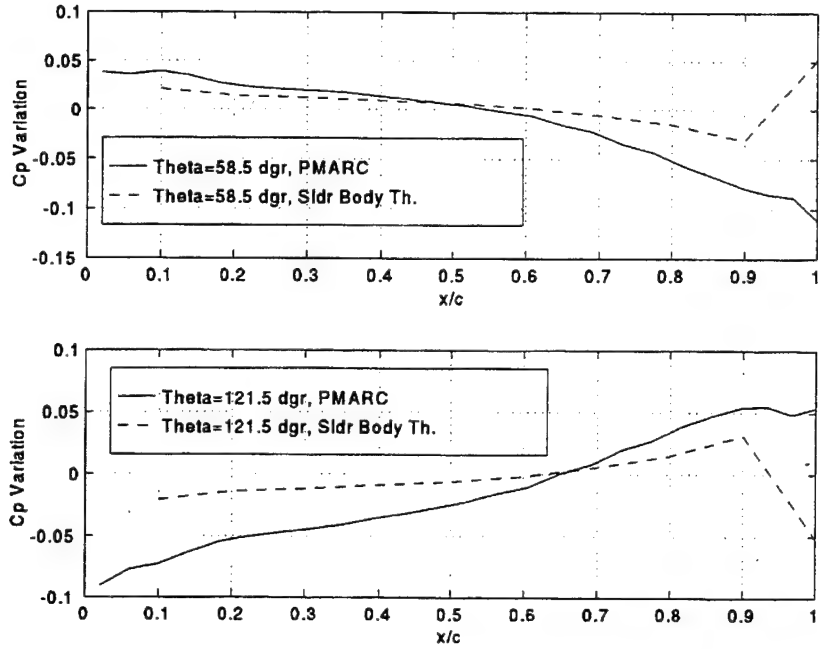

Figure 4.11 Comparison of Chordwise Pressure Perturbation at Selected Circumferential Angular Positions for a 0 to 5 Degree Change in AOA. F5 Wing Equivalent Body of Revolution.

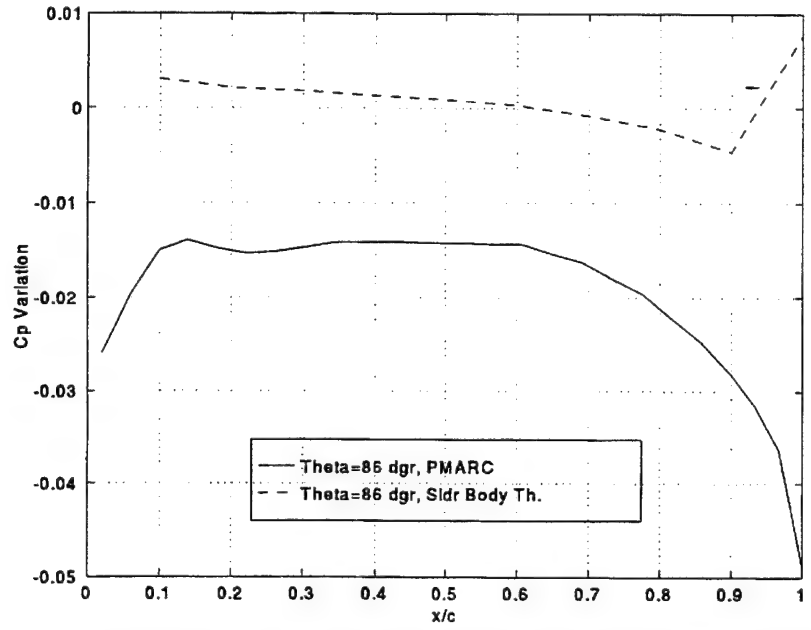

Figure 4.12 Comparison of Chordwise Pressure Perturbation at Selected Circumferential Angular Positions for a 0 to 5 Degree Change in AOA. F5 Wing Equivalent Body of Revolution.

3. PMARC Input Instructions

The basic steps to construct a body of revolution are very similar from those required for a wing. The main difference resides in the section definition of the circles distributed along the longitudinal axis. There exists more than one way to construct a body of revolution. One will be presented here and a second when introducing the spindle in a later section. A common requirement for each method is a set of spanwise cross-sectional areas sufficiently dense to properly define the body of revolution. Section **6** will present a computer program designed by the author that generates 41 cross-sectional areas and the chordwise locations of their centroids from the geometry of the F5 wing. Each of the two body-of-revolution construction methods presented have advantages and disadvantages which will be discussed at the end of each section. Figure 4.13 presents the input file for the first method and the next paragraphs discusses it.

a. Basic Input Section

The only fields which may differ from the standard wings studied so far are CBAR, SREF, and SSPAN. CBAR is taken to be the length of the longitudinal axis of the body or revolution. SREF is the reference area upon which all the coefficients are calculated, and therefore its selection could be different depending on the analysis performed or the results desired. In our case, it was the area of the largest cross-section. Finally, for the pressure and lift coefficient analysis we did up to now, the SSPAN field did not seem to be a useful factor. For completeness, we selected it to be half the diameter of the largest cross-section.

b. Assembly and Component Coordinate System Information

Nothing is different from the standard wings studied so far.

c. Patch and Section Coordinate System Information

This section is significantly different from what we have seen so far. This section also offers some flexibility which we will demonstrate by building the F5 wing body of revolution one way, and later the spindle using another way.

```
F5 Wing: NACA-65A004.8  -EQUIVALENT BODY OF REVOLUTION-

&BINP2   LSTINP=2,    LSTOUT=0,    LSTFRQ=0,    LENRUN=0,    LPLTYP=1,     &END
&BINP3   LSTGEO=0,    LSTNAB=0,    LSTWAK=0,    LSTCPV=0,                  &END
&BINP4   MAXIT=50,    SOLRES=0.01,                                         &END
&BINP5   NTSTPS= 10,   DTSTEP=0.5,                                         &END
&BINP6   RSYM=1.0,    RGPR=0.0,    RFF=5.0,  RCORES=0.0080, RCOREW=0.0080, &END
&BINP7   VINF=11.0,   VSOUND=1116.0,                                       &END
&BINP8   ALDEG= 5.00, YAWDEG=0.0,  PHIDOT=0.0,  THEDOT=0.0,  PSIDOT=0.0,   &END
&BINP8A  PHIMAX= 0.0, THEMAX= 0.0, PSIMAX=0.0,
         WRX=0.0,     WRY=0.0,     WRZ=0.0,                                 &END
&BINP8B  DXMAX=0.0,   DYMAX=0.0,   DZMAX=0.0,
         WTX=0.0,     WTY=0.0,     WTZ=0.0,                                 &END
&BINP9   CBAR=0.1712, SREF=0.0230, SSPAN= 0.0856,
         RMPX=0.00,   RMPY=0.00,   RMPZ=0.00,                               &END
&BINP10  NORSET=0,    NBCHGE=0,    NCZONE=0,
         NCZPCH=0,    CZDUB=0.0,   VREF=0.0,                               &END
&BINP11  NORPCH=0,    NORF=0,      NORL=0,
         NOCF=0,      NOCL=0,      VNORM=0.0,                               &END
&BINP12  KPAN=0,      KSIDE=0,     NEWNAB=0,    NEWSID=0,                  &END
&BINP13  NBLIT=0,                                                          &END

&ASEM1   ASEMX=0.00,       ASEMY=0.00,       ASEMZ=0.00,
         ASCAL=1.00,       ATHET=0.00,       NODEA=5,                     &END
&ASEM2   APXX=0.00,        APYY=0.00,        APZZ=0.00,
         AHXX=0.00,        AHYY=1.00,        AHZZ=0.00,                   &END


&COMP1   COMPX= 0.0000,    COMPY= 0.0000,    COMPZ= 0.0000,
         CSCAL=  1.000,    CTHET=   0.0,     NODEC= 5,                    &END
&COMP2   CPXX= 0.0000,     CPYY= 0.0000,     CPZZ= 0.0000,
         CHXX= 0.0000,     CHYY=  1.000   ,  CHZZ= 0.0000,                &END



&PATCH1  IREV=  0, IDPAT= 2, MAKE=   0, KCOMP= 1, KASS= 1, IPATSYM=1,
         IPATCOP=0,                                                        &END
          EQUIVALENT BODY
&SECT1   STX=    0.0000, STY= 0.0000,    STZ= 0.0000,    SCALE= 0.0000,
         ALF=   0.0,  THETA=   0.0,
         INMODE=  1,  TNODS= 0,    TNPS=  0,    TINTS= 0,                 &END
 0.0000  -1.0000  0.0000
 0.1735  -0.9845  0.0000
 0.3420  -0.9395  0.0000
 0.5000  -0.8660  0.0000
 0.6425  -0.7660  0.0000
 0.7660  -0.6425  0.0000
 0.8660  -0.5000  0.0000
 0.9395  -0.3420  0.0000
 0.9845  -0.1735  0.0000
 1.0000   0.0000  0.0000
 0.9845   0.1735  0.0000
 0.9395   0.3420  0.0000
 0.8660   0.5000  0.0000
 0.7660   0.6425  0.0000
 0.6425   0.7660  0.0000
 0.5000   0.8660  0.0000
 0.3420   0.9395  0.0000
 0.1735   0.9845  0.0000
 0.0000   1.0000  0.0000
&BPNODE   TNODE=3,    TNPC=20,  TINTC=3,    &END
&SECT1   STX= 0.0422, STY= 0.0000,    STZ= 0.0000,    SCALE= 0.0178,
         ALF=   0.0,  THETA=   0.0,
         INMODE=  0,  TNODS= 0,    TNPS=  0,    TINTS= 0,                 &END
&SECT1   STX= 0.0819, STY= 0.0000,    STZ= 0.0000,    SCALE= 0.0339,
         ALF=   0.0,  THETA=   0.0,
         INMODE=  0,  TNODS= 0,    TNPS=  0,    TINTS= 0,                 &END
&SECT1   STX= 0.1241, STY= 0.0000,    STZ= 0.0000,    SCALE= 0.0451,
         ALF=   0.0,  THETA=   0.0,
         INMODE=  0,  TNODS= 0,    TNPS=  0,    TINTS= 0,                 &END
&SECT1   STX= 0.1612, STY= 0.0000,    STZ= 0.0000,    SCALE= 0.0535,
         ALF=   0.0,  THETA=   0.0,
         INMODE=  0,  TNODS= 0,    TNPS=  0,    TINTS= 0,                 &END
&SECT1   STX= 0.1995, STY= 0.0000,    STZ= 0.0000,    SCALE= 0.0618,
         ALF=   0.0,  THETA=   0.0,
```



```
         INMODE=  0,  TNODS= 0,    TNPS=  0,    TINTS= 0,                 &END
&SECT1   STX= 0.2341, STY= 0.0000,    STZ= 0.0000,    SCALE= 0.0686,
         ALF=   0.0,  THETA=   0.0,
         INMODE=  0,  TNODS= 0,    TNPS=  0,    TINTS= 0,                 &END
&SECT1   STX= 0.2660, STY= 0.0000,    STZ= 0.0000,    SCALE= 0.0736,
         ALF=   0.0,  THETA=   0.0,
         INMODE=  0,  TNODS= 0,    TNPS=  0,    TINTS= 0,                 &END
&SECT1   STX= 0.2967, STY= 0.0000,    STZ= 0.0000,    SCALE= 0.0778,
         ALF=   0.0,  THETA=   0.0,
         INMODE=  0,  TNODS= 0,    TNPS=  0,    TINTS= 0,                 &END
&SECT1   STX= 0.3210, STY= 0.0000,    STZ= 0.0000,    SCALE= 0.0806,
         ALF=   0.0,  THETA=   0.0,
         INMODE=  0,  TNODS= 0,    TNPS=  0,    TINTS= 0,                 &END
&SECT1   STX= 0.3453, STY= 0.0000,    STZ= 0.0000,    SCALE= 0.0829,
         ALF=   0.0,  THETA=   0.0,
         INMODE=  0,  TNODS= 0,    TNPS=  0,    TINTS= 0,                 &END
&SECT1   STX= 0.3633, STY= 0.0000,    STZ= 0.0000,    SCALE= 0.0841,
         ALF=   0.0,  THETA=   0.0,
         INMODE=  0,  TNODS= 0,    TNPS=  0,    TINTS= 0,                 &END
&SECT1   STX= 0.3786, STY= 0.0000,    STZ= 0.0000,    SCALE= 0.0848,
         ALF=   0.0,  THETA=   0.0,
         INMODE=  0,  TNODS= 0,    TNPS=  0,    TINTS= 0,                 &END
&SECT1   STX= 0.3901, STY= 0.0000,    STZ= 0.0000,    SCALE= 0.0852,
         ALF=   0.0,  THETA=   0.0,
         INMODE=  0,  TNODS= 0,    TNPS=  0,    TINTS= 0,                 &END
&SECT1   STX= 0.3952, STY= 0.0000,    STZ= 0.0000,    SCALE= 0.0856,
         ALF=   0.0,  THETA=   0.0,
         INMODE=  0,  TNODS= 0,    TNPS=  0,    TINTS= 0,                 &END
&SECT1   STX= 0.3991, STY= 0.0000,    STZ= 0.0000,    SCALE= 0.0856,
         ALF=   0.0,  THETA=   0.0,
         INMODE=  0,  TNODS= 0,    TNPS=  0,    TINTS= 0,                 &END
&SECT1   STX= 0.4156, STY= 0.0000,    STZ= 0.0000,    SCALE= 0.0852,
         ALF=   0.0,  THETA=   0.0,
         INMODE=  0,  TNODS= 0,    TNPS=  0,    TINTS= 0,                 &END
&SECT1   STX= 0.4321, STY= 0.0000,    STZ= 0.0000,    SCALE= 0.0844,
         ALF=   0.0,  THETA=   0.0,
         INMODE=  0,  TNODS= 0,    TNPS=  0,    TINTS= 0,                 &END
&SECT1   STX= 0.4486, STY= 0.0000,    STZ= 0.0000,    SCALE= 0.0833,
         ALF=   0.0,  THETA=   0.0,
         INMODE=  0,  TNODS= 0,    TNPS=  0,    TINTS= 0,                 &END
&SECT1   STX= 0.4652, STY= 0.0000,    STZ= 0.0000,    SCALE= 0.0810,
         ALF=   0.0,  THETA=   0.0,
         INMODE=  0,  TNODS= 0,    TNPS=  0,    TINTS= 0,                 &END
&SECT1   STX= 0.4817, STY= 0.0000,    STZ= 0.0000,    SCALE= 0.0782,
         ALF=   0.0,  THETA=   0.0,
         INMODE=  0,  TNODS= 0,    TNPS=  0,    TINTS= 0,                 &END
&SECT1   STX= 0.4982, STY= 0.0000,    STZ= 0.0000,    SCALE= 0.0748,
         ALF=   0.0,  THETA=   0.0,
         INMODE=  0,  TNODS= 0,    TNPS=  0,    TINTS= 0,                 &END
&SECT1   STX= 0.5147, STY= 0.0000,    STZ= 0.0000,    SCALE= 0.0714,
         ALF=   0.0,  THETA=   0.0,
         INMODE=  0,  TNODS= 0,    TNPS=  0,    TINTS= 0,                 &END
&SECT1   STX= 0.5313, STY= 0.0000,    STZ= 0.0000,    SCALE= 0.0658,
         ALF=   0.0,  THETA=   0.0,
         INMODE=  0,  TNODS= 0,    TNPS=  0,    TINTS= 0,                 &END
&SECT1   STX= 0.5478, STY= 0.0000,    STZ= 0.0000,    SCALE= 0.0602,
         ALF=   0.0,  THETA=   0.0,
         INMODE=  0,  TNODS= 0,    TNPS=  0,    TINTS= 0,                 &END
&SECT1   STX= 0.5643, STY= 0.0000,    STZ= 0.0000,    SCALE= 0.0529,
         ALF=   0.0,  THETA=   0.0,
         INMODE=  0,  TNODS= 0,    TNPS=  0,    TINTS= 0,                 &END
&SECT1   STX= 0.5808, STY= 0.0000,    STZ= 0.0000,    SCALE= 0.0444,
         ALF=   0.0,  THETA=   0.0,
         INMODE=  0,  TNODS= 0,    TNPS=  0,    TINTS= 0,                 &END
&SECT1   STX= 0.5974, STY= 0.0000,    STZ= 0.0000,    SCALE= 0.0339,
         ALF=   0.0,  THETA=   0.0,
         INMODE=  0,  TNODS= 0,    TNPS=  0,    TINTS= 0,                 &END
&SECT1   STX= 0.5968, STY= 0.0000,    STZ= 0.0000,    SCALE= 0.0348,
         ALF=   0.0,  THETA=   0.0,
         INMODE=  0,  TNODS= 0,    TNPS=  0,    TINTS= 0,                 &END
&SECT1   STX= 0.5974, STY= 0.0000,    STZ= 0.0000,    SCALE= 0.0339,
         ALF=   0.0,  THETA=   0.0,
         INMODE=  0,  TNODS= 0,    TNPS=  0,    TINTS= 0,                 &END
&SECT1   STX= 0.5988, STY= 0.0000,    STZ= 0.0000,    SCALE= 0.0329,
         ALF=   0.0,  THETA=   0.0,
         INMODE=  0,  TNODS= 0,    TNPS=  0,    TINTS= 0,                 &END
```

Figure 4.13 PMARC Input File for The F5 Wing Equivalent Area Body of Revolution.

```
&SECT1   STX= 0.6006, STY= 0.0000,    STZ= 0.0000,    SCALE= 0.0329,
         ALF=   0.0,  THETA=   0.0,
         INMODE=  0,  TNODS= 0,    TNPS= 0,    TINTS= 0,                 &END
&SECT1   STX= 0.6028, STY= 0.0000,    STZ= 0.0000,    SCALE= 0.0299,
         ALF=   0.0,  THETA=   0.0,
         INMODE=  0,  TNODS= 0,    TNPS= 0,    TINTS= 0,                 &END
&SECT1   STX= 0.6057, STY= 0.0000,    STZ= 0.0000,    SCALE= 0.0276,
         ALF=   0.0,  THETA=   0.0,
         INMODE=  0,  TNODS= 0,    TNPS= 0,    TINTS= 0,                 &END
&SECT1   STX= 0.6086, STY= 0.0000,    STZ= 0.0000,    SCALE= 0.0252,
         ALF=   0.0,  THETA=   0.0,
         INMODE=  0,  TNODS= 0,    TNPS= 0,    TINTS= 0,                 &END
&SECT1   STX= 0.6122, STY= 0.0000,    STZ= 0.0000,    SCALE= 0.0226,
         ALF=   0.0,  THETA=   0.0,
         INMODE=  0,  TNODS= 0,    TNPS= 0,    TINTS= 0,                 &END
&SECT1   STX= 0.6160, STY= 0.0000,    STZ= 0.0000,    SCALE= 0.0195,
         ALF=   0.0,  THETA=   0.0,
         INMODE=  0,  TNODS= 0,    TNPS= 0,    TINTS= 0,                 &END
&SECT1   STX= 0.6201, STY= 0.0000,    STZ= 0.0000,    SCALE= 0.0195,
         ALF=   0.0,  THETA=   0.0,
         INMODE=  0,  TNODS= 0,    TNPS= 0,    TINTS= 0,                 &END
&SECT1   STX= 0.6247, STY= 0.0000,    STZ= 0.0000,    SCALE= 0.0138,
         ALF=   0.0,  THETA=   0.0,
         INMODE=  0,  TNODS= 0,    TNPS= 0,    TINTS= 0,                 &END
&SECT1   STX= 0.6291, STY= 0.0000,    STZ= 0.0000,    SCALE= 0.0113,
         ALF=   0.0,  THETA=   0.0,
         INMODE=  0,  TNODS= 0,    TNPS= 0,    TINTS= 0,                 &END
&SECT1   STX= 0.6341, STY= 0.0000,    STZ= 0.0000,    SCALE= 0.0080,
         ALF=   0.0,  THETA=   0.0,
         INMODE=  0,  TNODS= 0,    TNPS= 0,    TINTS= 0,                 &END
&SECT1   STX= 0.6389, STY= 0.0000,    STZ= 0.0000,    SCALE= 0.0002,
         ALF=   0.0,  THETA=   0.0,
         INMODE=  0,  TNODS= 0,    TNPS= 0,    TINTS= 0,                 &END
&SECT1   STX= 0.6439, STY= 0.0000,    STZ= 0.0000,    SCALE= 0.0000,
         ALF=   0.0,  THETA=   0.0,
         INMODE=  0,  TNODS= 5,    TNPS= 25,    TINTS= 3,                &END
&BPNODE   TNODE=3,    TNPC=0,   TINTC=0,    &END

&WAKE1   IDWAK=0,        IFLXW=1,        ITRFTZ= 0,      INTRW= 0,        &END
 WING_WAKE
&WAKE2   KWPACH=2,       KWSIDE=4,       KWLINE=0,       KWPAN1=0,
         KWPAN2=0,       NODEW=0,        INITIAL=0,                       &END
&WAKE2   KWPACH=1,       KWSIDE=2,       KWLINE=0,       KWPAN1=0,
         KWPAN2=0,       NODEW=5,        INITIAL=0,                       &END


&ONSTRM  NONSL =0,  KPSL =                                                &END


&BLPARAM RN =37210000,    VISC = 0.000157, NSLBL = 1,                     &END


&VS1     NVOLR= 0,       NVOLC= 0,                                        &END
&VS2     X0=    -0.1000, Y0=     1.5000, Z0=    -0.1000, INTVSR= 1,       &END
&VS3     X1=    -0.1000, Y1=     1.5000, Z1=     0.1000, NPT1=  0,        &END
&VS4     X2=    -0.1000, Y2=     1.5000, Z2=     0.1000, NPT2= 20,        &END
&VS5     X3=     1.1000, Y3=     1.5000, Z3=    -0.1000, NPT3= 25,        &END

&VS6     XR0=    2.0000, YR0=    2.0000, ZR0=    0.0000, INTVSC= 1,       &END
&VS7     XR1=    4.0000, YR1=    2.0000, ZR1=    0.0000,
         XR2=    2.0000, YR2=    2.0000, ZR2=    1.0000,                  &END
&VS8     R1=     0.1000, R2=     1.0000, PHI1=  0.0,     PHI2=360.0,      &END
&VS9     NRAD=   5,      NPHI=   12,     NLEN=  3,                        &END


&SLIN1   NSTLIN=0,                                                        &END
&SLIN2   SX0=   -2.0000, SY0=    1.0000, SZ0=   -0.5000,
         SU=     0.0000, SD=    10.0000, DS=     0.2500, INTSL= 1,        &END
&SLIN2   SX0=   -2.0000, SY0=    1.0000, SZ0=   -0.4000,
         SU=     0.0000, SD=    10.0000, DS=     0.2500, INTSL= 1,        &END
&SLIN2   SX0=   -2.0000, SY0=    1.0000, SZ0=   -0.3000,
         SU=     0.0000, SD=    10.0000, DS=     0.2500, INTSL= 1,        &END
&SLIN2   SX0=   -2.0000, SY0=    1.0000, SZ0=   -0.2000,
         SU=     0.0000, SD=    10.0000, DS=     0.2500, INTSL= 1,        &END
&SLIN2   SX0=   -2.0000, SY0=    1.0000, SZ0=   -0.1000,
         SU=     0.0000, SD=    10.0000, DS=     0.2500, INTSL= 1,        &END
```

Figure 4.13 (Cont'd) PMARC Input File for The F5 Wing Equivalent Area Body of Revolution.

The patch fields are not varying from before. It is the section fields that do. In the first method, a circle of radius one is defined by 19 points. As shown on Figure 4.13, that circle is then scaled to correspond to the cross-section radius at a particular chordwise location of the body of revolution. Thus, we scale the circle to zero at the nose tip and progressively augment and then reduce the scaling back to zero along the longitudinal axis. This process is done by repeating the SECT1 block as many times as we have cross-section definitions.

The number of panels on the circumference is prescribed in the first break point node (BPNODE) following the initial circle definition. The value attributed to TNPC with this method determines the number of panels on one half of the circumference, as the model is built by joining two patches (Fig 4.14). The number of panels longitudinally from nose to tail is prescribed in the last SECT1 block by the TNPS value. The panel distribution is selected as before with the TINTC and TINTS fields next to the respective panel fields.

One last note is that the TNODS value is set at 0 in all the SECT1 blocks to indicate that they constitute the first or an intermediate section of the patch. SECT1 of the last block is set to 5 to indicate the last section definition.

d. Wake and Streamlines

It is important for a body of revolution to turn the wake option off. That is done by setting IDWAK to 0 in the WAKE1 block. Indeed, the body of revolution theoretically does not generate a wake.

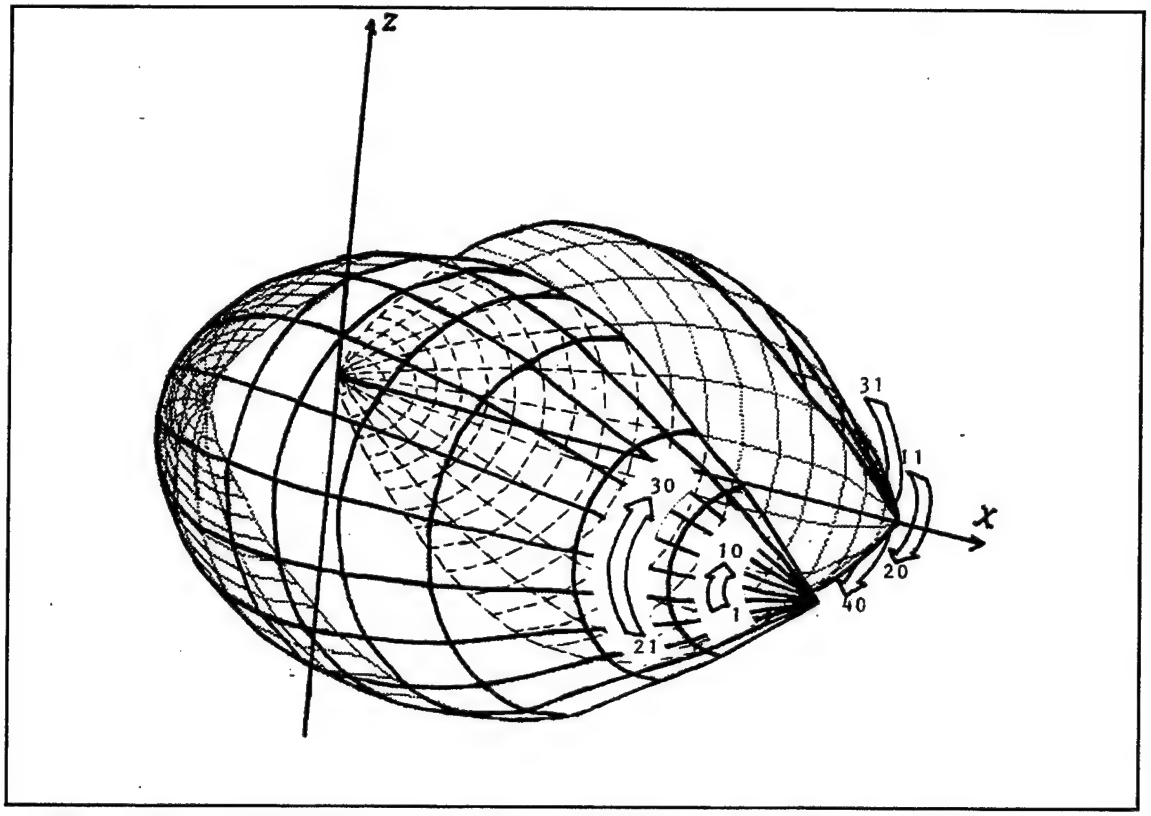

Figure 4.14 PMARC Panels and Patches Definition for The Body of Revolution.

4. Scaled Circles Model Construction Method Characteristics

The main advantage of this method is its ease of programing. The input file is no longer than for a simple wing. A circle is defined once and it is scaled at will. PMARC will create two patches to model the body of revolution which are mirror images of each other. One drawback when compared to the next method is the apparent difficulty with the pointed nose and tail. Even with a low number of panels which allow a finite panel area at the nose and tail, the same erratic behavior is present in the output as the pressures at the nose and tail break down. The rest of the results however are good.

5. PMARC Output - Data Retrieval

For the purpose of our study, only the pressure coefficient distributions at various circumferential positions were required. Since patch one and two generate the same results for the control points in mirror image positions, only the Cp from patch one were extracted. In order to obtain a Cp distribution all along the chord for the theta position selected, one reading per column of data is required. One or more columns of data can be skipped but care should be exercised as to conserve the proper smoothness of the distribution. In the DATA6 output file, one column of data details the coordinates and aerodynamic parameters of one circumferential strip of panels running from bottom to top for patch one, and from top to bottom for patch two, as shown on Figure 4.14.

The circumferential position theta is translated to a panel number on the output file by looking through one column of data for the arctangent of the y over -z ratio which will give the angle needed. Once the position of the panel relative to the first panel of that column is determined, the corresponding panel in each column of data will be approximatively at the same angle theta. In our case, we wanted to study the pressure distribution at seven different circumferential positions: 0, 30, 60, 90, 120, 150, and 180 degrees. As mentioned earlier, we did not have to study the mirror image position of these angles (0, 330, 300, 270, 240, 210 and 180 degrees) as the results would be identical. Because of the automatic panel distribution option used in PMARC, there was virtually no way to make the control points correspond with the theta desired. Consequently, we had to select values close to the ones above: 4.4, 31.5, 58.5, 86, 121.5, 148.5, and 175.6 degrees. But that did not matter for our analytical comparison as we used the same values in the slender body theory application. It should be noted however, that by varying the number of panels around the body, one would eventually find the divisions that best suit the requirements.

6. Computing The Cross-Sectional Area of The Body of Revolution

The following subsections will review the method employed to build the F5 wing equivalent body of revolution using the F5 wing PMARC output, which is our only source of data. We will first go through the steps indicating what data are required from DATA6, and how this selection can

become tremendously complicated for some types of wing, like the F5 wing, compared to simple rectangular wings. We will then discuss the program that was written to assist in the construction of the body of revolution, along with some of its output.

a. Using The PMARC Output to Build The Body Of Revolution - Code

The first objective while building an equivalent body of revolution is to obtain the section definition of the many spanwise cross-sections needed. Once the cross-sectional spanwise surface coordinates are identified for each 'cut', all that is left is to calculate their respective area. In the case of the rectangular wing, constructing spanwise cross-sections using the PMARC output is very easy and can be done in a matter of minutes. That is so because all the panel rows are parallel to the leading edge and the output provides the coordinates for each panel control point (Figure 4.15). It then becomes very simple to use the coordinates of the top and bottom row of panels to define the spanwise cross-section of this wing. In cases where the rows of panels are not parallel to the leading edge, like for the F5 wing, it becomes more complicated as the panel rows do not match with the spanwise cross-section anymore (Figure 4.15).

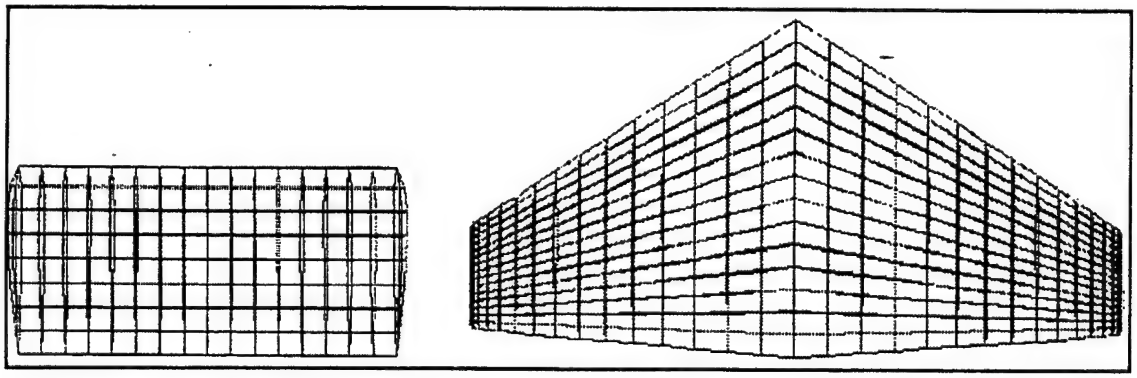

Figure 4.15 PMARC Panel Distributions for The Rectangular and The F5 Wings.

A series of steps is then required to create the data points for spanwise cross-sections from the panel control points provided by the output file (DATA6) of PMARC. These steps are summarized below and each corresponds to a section of the MATLAB code written to digitally perform them. The

code is presented in Appendix **E**. It is to be noted that steps (1) to (5) were built to simplify the data retrieval required for this process. These first few steps reconstruct the chordwise airfoil cross-section along the span; an operation already performed by PMARC. The advantage of our method is that we only need to input the general non-dimensional airfoil cross-sectional definition once instead of having to input the several cross-sectional definitions required along the span in order to proceed with the determination of the spanwise cross-sections.

(1) Chordwise Section Definition. The first step is to define the airfoil cross-section in three dimensions. The x and z coordinates (in the PMARC axis definition) are in this case taken from the input file (DATA5), themselves taken from the literature. The y coordinates (spanwise locations of the various two-dimensional airfoil sections) is taken in the PMARC output file, DATA6. They correspond to the coordinates of the chordwise panel control points calculated by PMARC from the prescribed airfoil section and wing geometry. Strictly on the basis of the above coordinates, all the following operations will be performed.

(2) Chordwise Panel Width. Because the spanwise panels are not always the same width, we needed a routine that calculates the width of each chordwise strip of panels. This information is later used along with the sweep angle to determine the chordwise origin of the airfoil cross-sections covering the control points of each strip of panels.

(3) Origin Of The Chordwise Panel Control Point Cross-Section. Trigonometric operations on the sweep angle and the width and cumulative width of the columns allow to determine the origin in global coordinates of each of the chordwise cross-sections that cover the control points of each strip of panels.

(4) Non-Translated Coordinates Of The Control Points Cross-Sections. This step constructs fifteen coordinate sets of airfoil chordwise cross-section. Each cross-section is the representation of the corresponding panel strip control points. At this stage, all the sections constructed have their leading edge x value at zero. However, all y and z values are representative of the actual wing proportional geometry.

(5) Translating The Cross-Sections. Using the results of step *c,* each cross-section is now translated to its actual relative position, completing the chordwise cross-sectional definition of the wing. As mentioned earlier, these coordinates are available in DATA6, but the data management required to isolate the points needed is by far more tedious than using a single non-dimensional airfoil cross-section definition along with this program.

(6) Fitting the Chordwise Sections Along The Span. In order to create spanwise cross-sections, we needed to have a means to identify the coordinates of any surface locations on a chordwise cross-section instead of only the coordinates of the panel control points. To achieve this goal, we fitted the top and bottom surface of each chordwise cross-sections with high order polynomials. This resulted in thirty-two polynomial expressions for one half wing.

(7) Creating the Spanwise Cross-Sections. For different chordwise locations (forty-three in this case) and using the polynomials obtained above, we now determine different z coordinates for selected y locations (fifteen). This will create a series of data points defining forty-three spanwise cross-sections. Each of these spanwise cross-sections then was fitted with a polynomial in order to smooth out some small irregularities introduced by the previous curve fitting.

(8) Plotting the Results. This step helps visualize the spanwise cross-sections from leading edge apex to trailing edge apex. Some of these plots are shown below. Figure 4.16 shows eight of the forty-one spanwise cross-sections for one half wing. Figure 4.17 presents seven cross-sections that end at the wing tip parallel to the chord. The flat look of that tip reflects reality as this geometry allows for the mounting of a tip tank or missile. Figure 4.18 illustrates a selection of cross-sections located in the back portion of the wing past the tips. The curvature of some of these cross-sections is due to the very high order polynomial used in the program which were required to get convergence at the extremity between the top and bottom curves. These tortuous curves could in fact be replaced by straight lines.

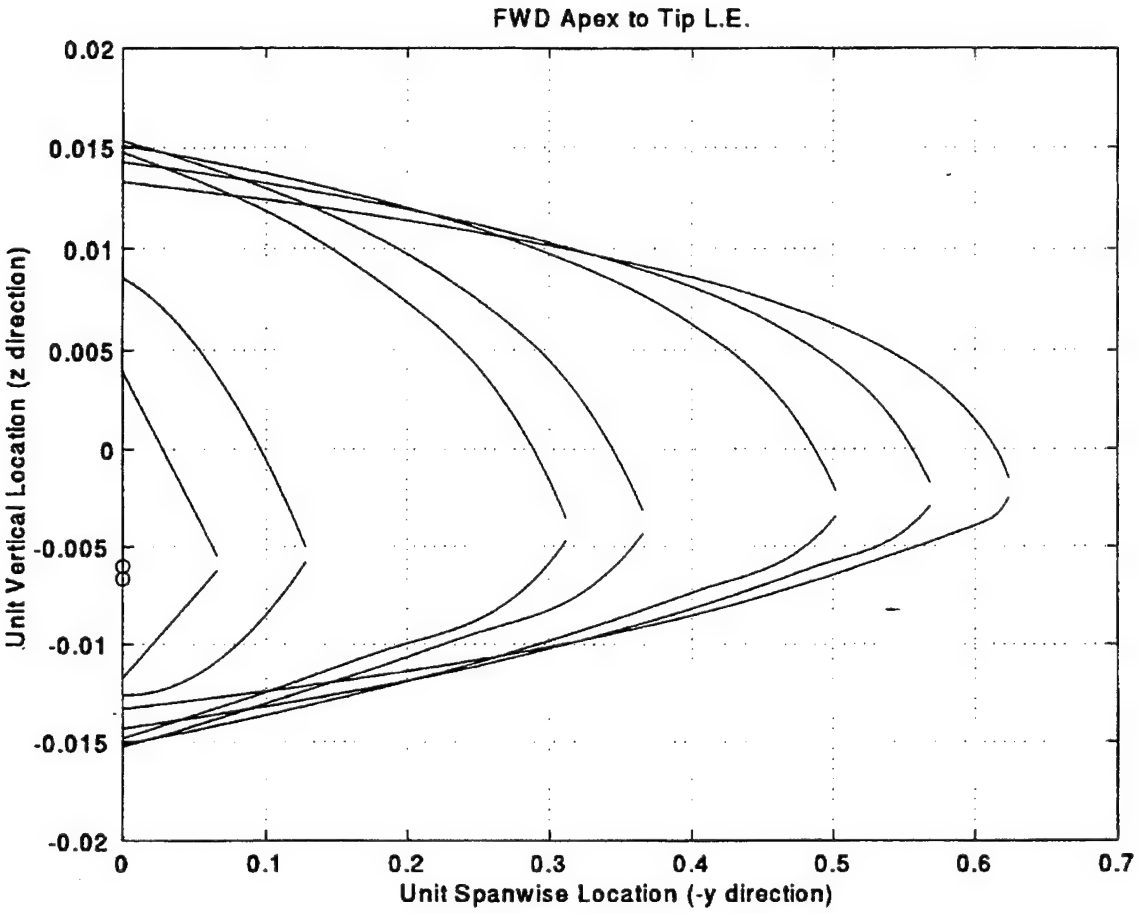

Figure 4.16 Selected F5 Wing Spanwise Cross-Sections From Apex to Tip Leading Edge. (Half Wing).

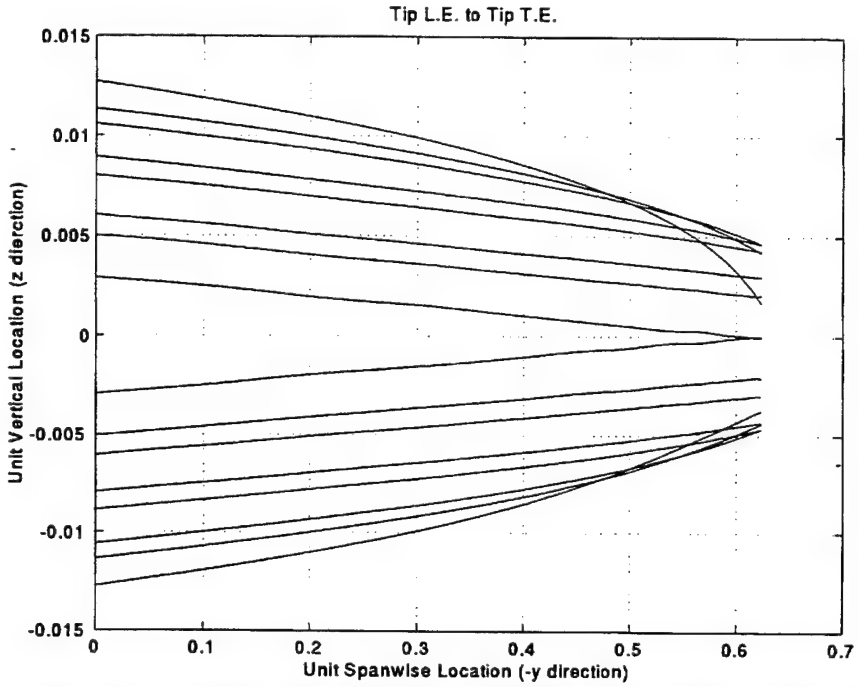

Figure 4.17 Selected F5 Wing Spanwise Cross-Sections From Tip Leading Edge to Tip Trailing Edge. (Half Wing).

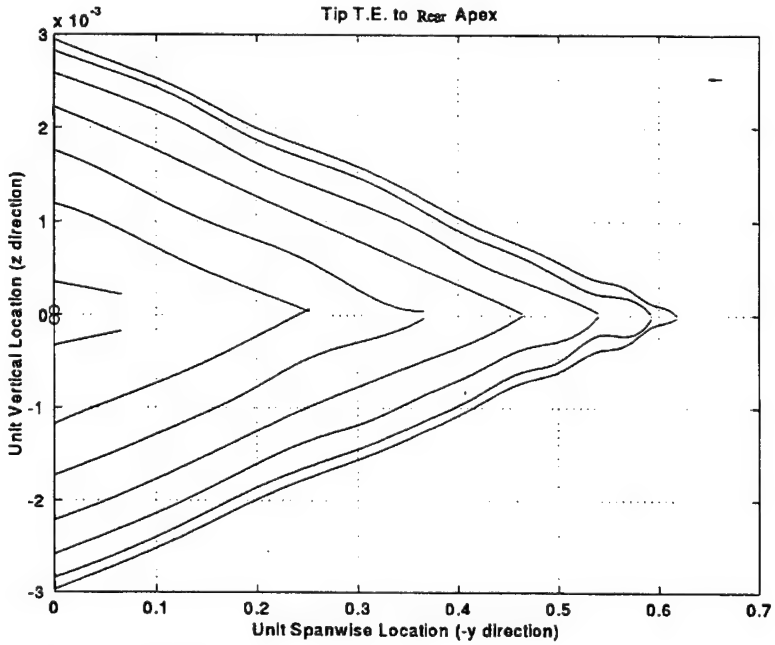

Figure 4.18 Selected F5 Wing Spanwise Cross-Sections From Tip Trailing Edge to Rear Apex. (Half Wing).

(9) Calculating the Area of Each Spanwise Cross-Section. The final step before constructing the equivalent body of revolution is to obtain the area of each spanwise cross-section. Two methods were used in order to ascertain the results. The first one calculated the area between the curves representing the spanwise cross-sections (top and bottom surface respectively) and the abscissa by integrating the polynomials describing each curve. A translation of these curves was necessary before the integration was performed in order to eliminate any intersection with the abscissa which would have rendered erroneous areas. The second method used a trapezoid approach to directly get the area between the two curves defining each spanwise cross-sections. Both methods gave the same results, as expected. Appendix **F** summarizes these results.

(10) Constructing the Equivalent Body of Revolution. Now that all spanwise cross-sectional areas are known, the radius of the related equivalent area circles can be determined and located at the corresponding chordwise locations, thus producing the wing equivalent body of revolution (Figure 4.19).

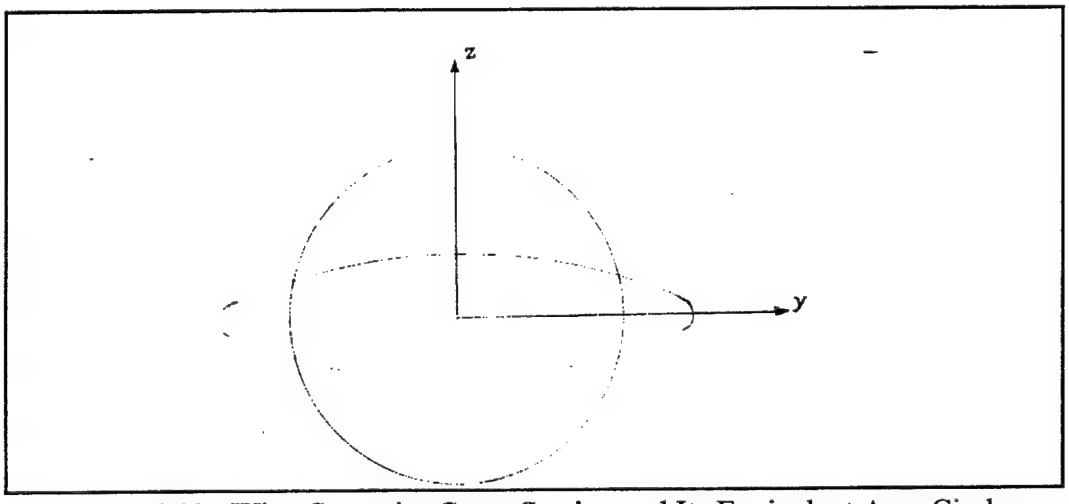

Figure 4.19 Wing Spanwise Cross-Section and Its Equivalent Area Circle.

(11) Cross-Sectional Area Distribution It is possible now to establish an expression describing the distribution of the spanwise cross-sectional area. All we need to do is to find the best fit for the arrays of data points defining the area as a function of chordwise locations. In the case of the F5 wing, this expression is the tenth order polynomial shown in Equation (4.5).

b. Note on the Equivalent Body of Revolution Computer Code

In the conceptual phase of the program described above, several data management complications arose that needed additional sub-routines that kept adding to its length and complexity. However, as this program was initially intended for a one-time use tool, no effort was expended in trying to keep it computationally efficient as the subroutines were getting added. The end result is a program that requires a relatively long running time, and experiences difficulty in plotting certain three-dimensional representations.

This program is now thought to be an excellent tool for the application at hand. Providing some spanwise locations are prescribed as well as the sweep angle and the chordwise cross-sections scaling , this program will produce forty-three spanwise cross-sections. If it is to be used extensively in the future, it could be modified to operate more efficiently, therefore becoming quicker. The modification required is to combine all arrays of data produced by the code into a large matrix. All the variables would then hold double indices instead of one. This program could also work for any other types of wing for which the general non-dimensional chordwise cross-sectional coordinates are known. However, it would first have to be carefully reviewed in order to customize it to the wing under study.

c. Camber of The Body of Revolution

One aspect still needing some investigation is the question of the camber. If the wing camber needs to be reflected in the body of revolution, one possibility is to place the centroid of each spanwise cross-section equivalent area circles along the mean camber line of the wing.

C. TRIANGULAR WING - EQUIVALENT AREA BODY OF REVOLUTION

The body of revolution making the subject of this section is made out of equivalent spanwise cross-sections of the triangular wing studied in Chapter **III**, section **G**. The longitudinal axis of the body of revolution will then correspond to the root chord of the wing which was made unity through non-dimensionalization. The spanwise cross-sectional area of the wing was a lot easier than for the F5 wing as an analytical expression for the cross-sectional area was given in Ref. [15] and reproduced in Equation (4.6) below.

$$Q(x) = 4\delta\sigma x^2(1-x) \tag{4.6}$$

Sigma is the dimensionless semi-span and is equal to 1/6. *Delta* is the dimensionless maximum thickness and will be set at 0.098. Figure 4.20 shows the PMARC representation of the body of revolution with its parent wing.

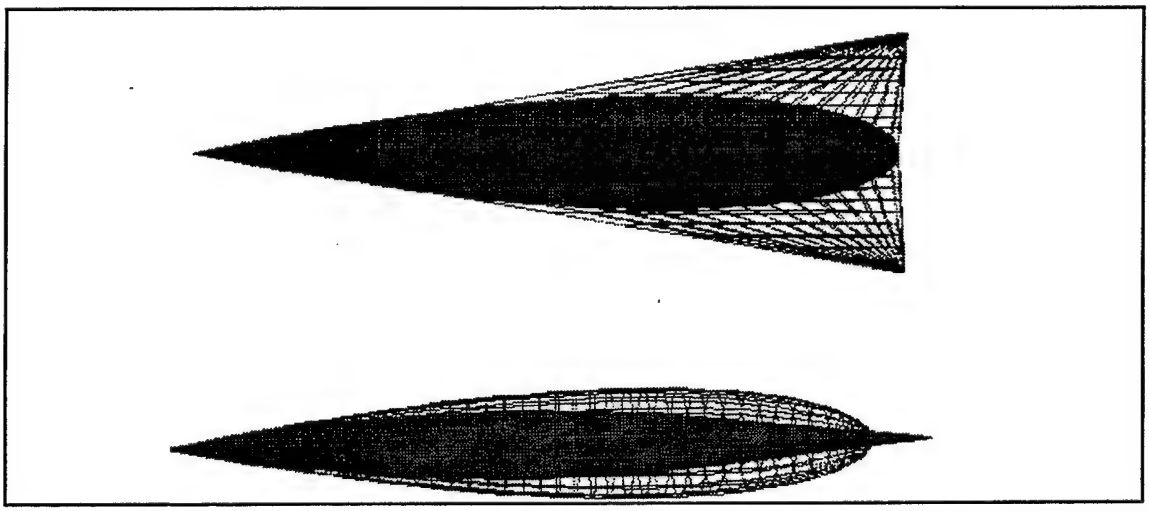

Figure 4.20 PMARC Top and Side Representation of The Triangular Wing Equivalent Area Body of Revolution and its Parent Wing. Maximum Thickness. Ratio = 0.09. (Two Figures not at Same Scale).

1. Theory, Background and Reference Data

In order to validate the PMARC results of pressure distribution for the triangular wing equivalent body of revolution, we will once again rely on past experience for the general expected behavior, and on the approximate slender body theory for the magnitude of the pressures. Like for the F5 equivalent body of revolution, our chordwise pressure distribution analysis will be performed at several circumferential locations to ensure consistency in the expected trends.

a. Expected General Behavior

As for the F5 equivalent body of revolution, the total lift on the triangular wing body of revolution should be zero as the upward lift on the front portion of the body is cancelled by the downward lift on the rear portion. In terms of pressure distribution, it will once again be observed that for a change of angle of attack from zero to 5 degrees, the pressure differential at a specific aft chordwise location will be equal in magnitude but in the reverse direction than that of a related rearward location. This means that somewhere along the chord there is a point where this differential is zero. This point is not at the mid-chord, except for a symmetrical body of revolution like the spindle, as we will see later.

As for the F5 equivalent body of revolution, the behavior described above would be modified for the chordwise distributions that lie along the 90 and 270 degree circumferential positions. Not only is the magnitude of the pressure differential for a zero to five degrees shift in angle of attack expected to be the same at two related forward and rearward positions, but also the direction of the pressure.

b. Slender Body Theory

As already mentioned in the previous section, the slender body theory dictates that the pressure on a body at angle of attack is approximated by the pressure at zero angle of attack plus the pressure differential between its value at zero and at the new angle of attack. This differential can be calculated using the following slender body theory derivation in which R is the radius distribution and Q the cross-sectional area distribution.

$$Cp = Cp_{\alpha=0} + Cp_{d\alpha} \tag{4.1}$$

$$Cp_{d\alpha} = 2\alpha R'(x)\cos\theta \tag{4.2}$$

$$R(x) = \sqrt{(\frac{Q(x)}{\pi})} \tag{4.3}$$

$$R'(x) = \frac{1}{2\pi} Q'(x)\sqrt{(\frac{Q(x)}{\pi})} \tag{4.4}$$

$$Q(x) = 4\delta\sigma x^2(1-x) \tag{4.6}$$

Using the expected behavior description given above and the numerical results of the slender body theory applied to the triangular wing equivalent body of revolution, we will now present the PMARC results.

2. Results and Discussion

Figures 4.22 to 4.27 presented below display the chordwise pressure distribution at various circumferential positions for two angles of attack, which will allow comparison with intuitive expectations . Figures 4.28 to 4.31 show the pressure perturbation when going from zero angle of attack to a higher value, as calculated by PMARC and the slender body theory. It should be noted that the circumferential positions of the chordwise body line of analysis were chosen to correspond

with the control point coordinates of the chordwise strips of panels which were the closest to the points separating the body cross-section in 12 pie sections (Figure4.21). Finally, although the first point on all the figures was plotted, it should be disregarded. As mentioned earlier, the reasons are not well understood why PMARC has difficulty with the pointed nose and tail when the model is built by repetitive scaling like for the F5 and the triangular wing equivalent bodies of revolution, as opposed to individual cross-section definition like for the spindle.

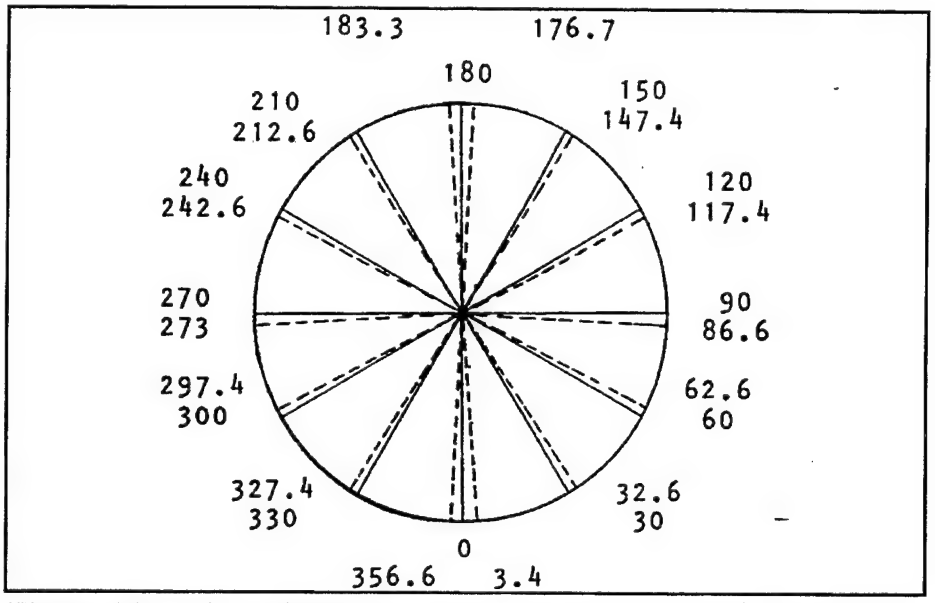

Figure 4.21 Circumferential Angular Locations Studied on The Triangular Wing Equivalent Body of Revolution Cross-Sections (Dotted Lines).

a. Chordwise Pressure Distributions

The first figure (Figure 4.22) shows the expected results that the pressure distribution will be the same for any circumferential position when the body of revolution is at zero angle of attack. Figure 4.23 presents the same parameters but with the body at five degrees angle of attack. We now observe the progression in pressure from top to bottom at a particular aft section and regression at a particular rear section. This plot also shows the relative chordwise position of the minimum pressure for each chordwise distribution.

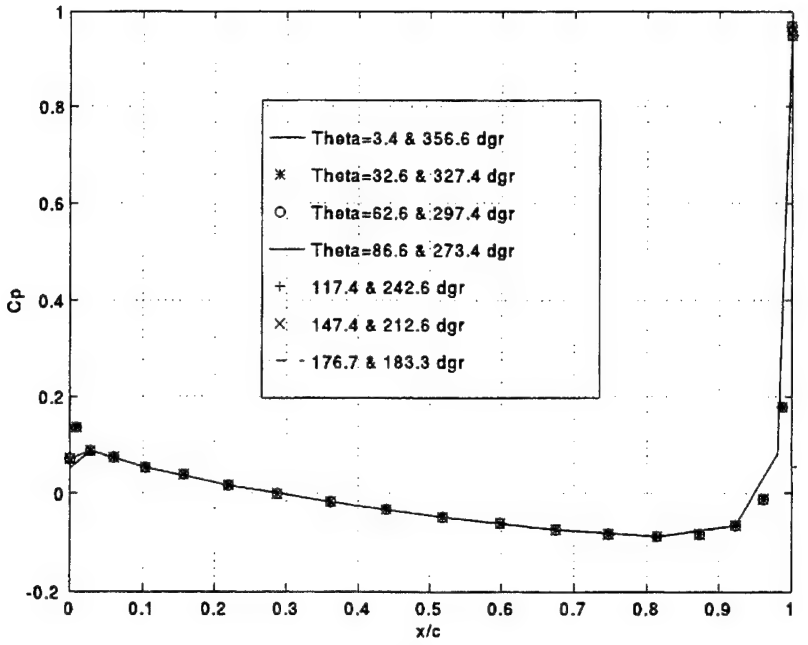

Figure 4.22 Chordwise Pressure Distribution for Various Circumferential Angles. Triangular Wing Equivalent Body of Revolution, Delta=0.098, AOA=0 Degree.

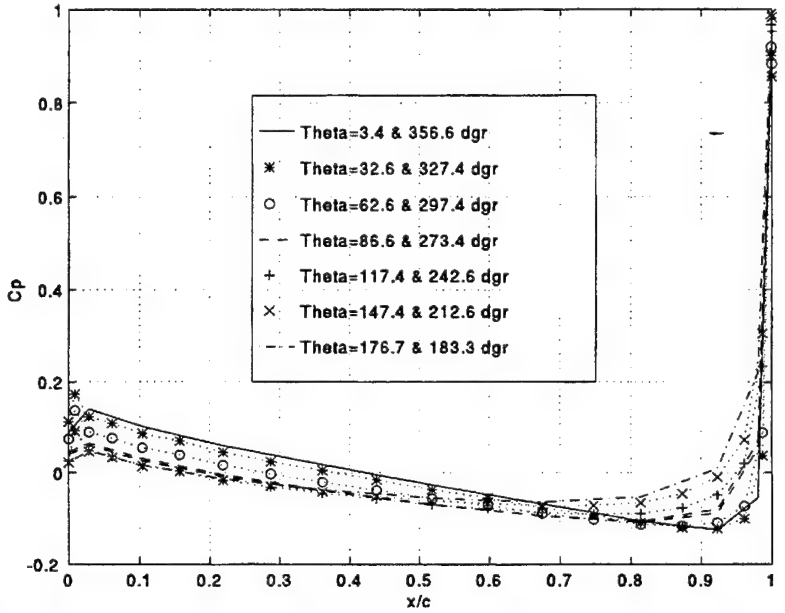

Figure 4.23 Chordwise Pressure Distribution for Various Circumferential Angles. Triangular Wing Equivalent Body of Revolution, Delta=0.098, AOA=5 Degrees.

Figures 4.24 to 4.27 compare the chordwise pressure distribution at various circumferential positions for zero and five degrees angle of attack. Each figure displays the variation for two corresponding circumferential positions (longitudinal mirror image) of the body. In all cases, the leeward pressure perturbation is equal and opposite to the windward pressure perturbation, as expected. At theta in the vicinity of 90 degrees, a pressure perturbation exists but remains approximately constant along the chord.

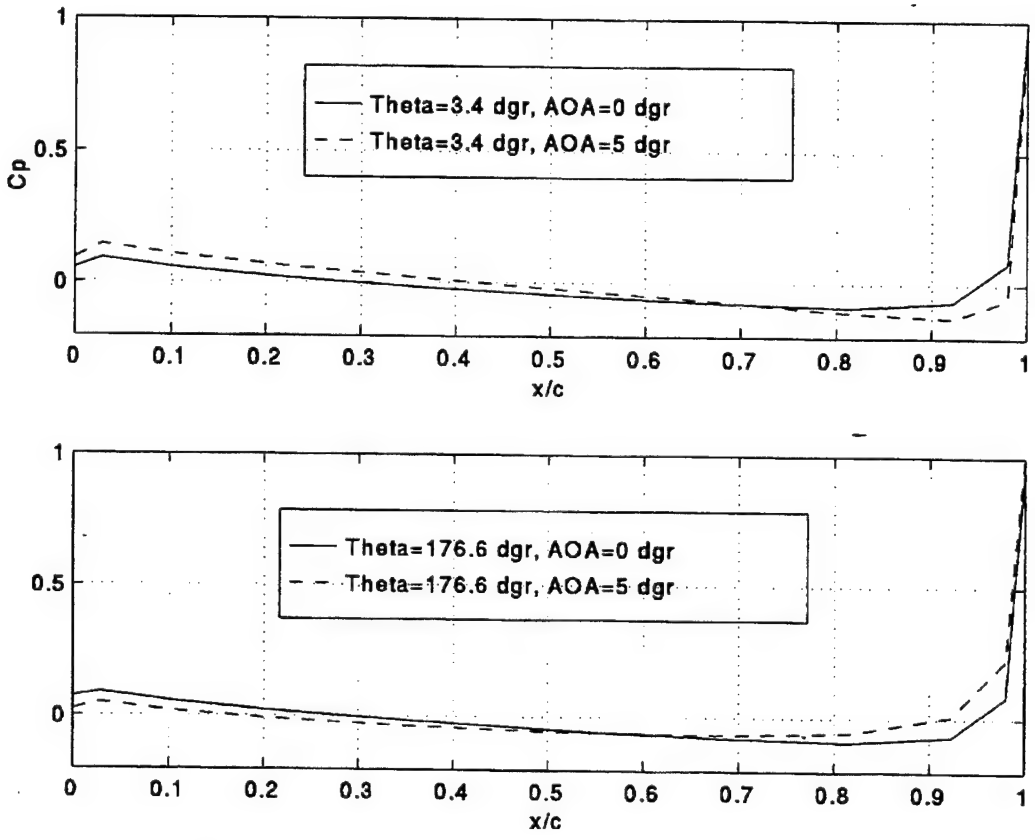

Figure 4.24 Comparison of Chordwise Pressure Distribution Along Selected Circumferential Angular Positions for Two Angles of Attack. Triangular Wing Equivalent Body of Revolution, Delta=0.098.

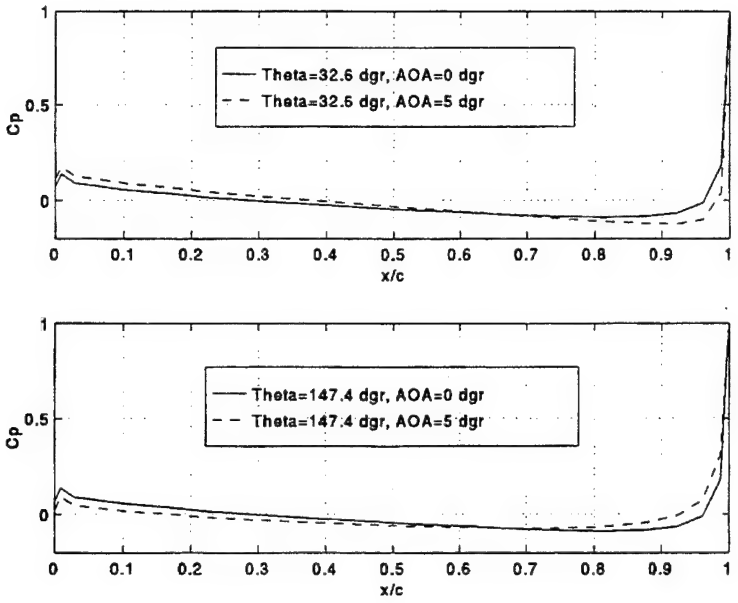

Figure 4.25 Comparison of Chordwise Pressure Distribution Along Selected Circumferential Angular Positions for Two Angles of Attack. Triangular Wing Equivalent Body of Revolution, Delta=0.098.

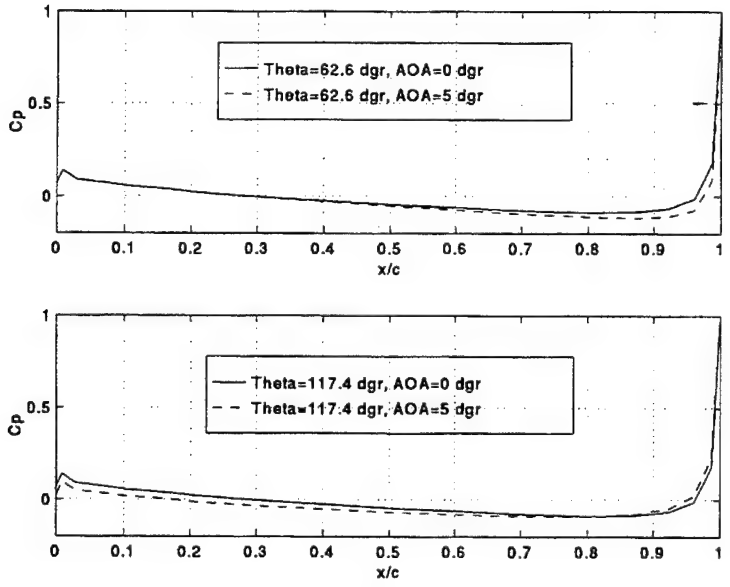

Figure 4.26 Comparison of Chordwise Pressure Distribution Along Selected Circumferential Angular Positions for Two Angles of Attack. Triangular Wing Equivalent Body of Revolution, Delta=0.098.

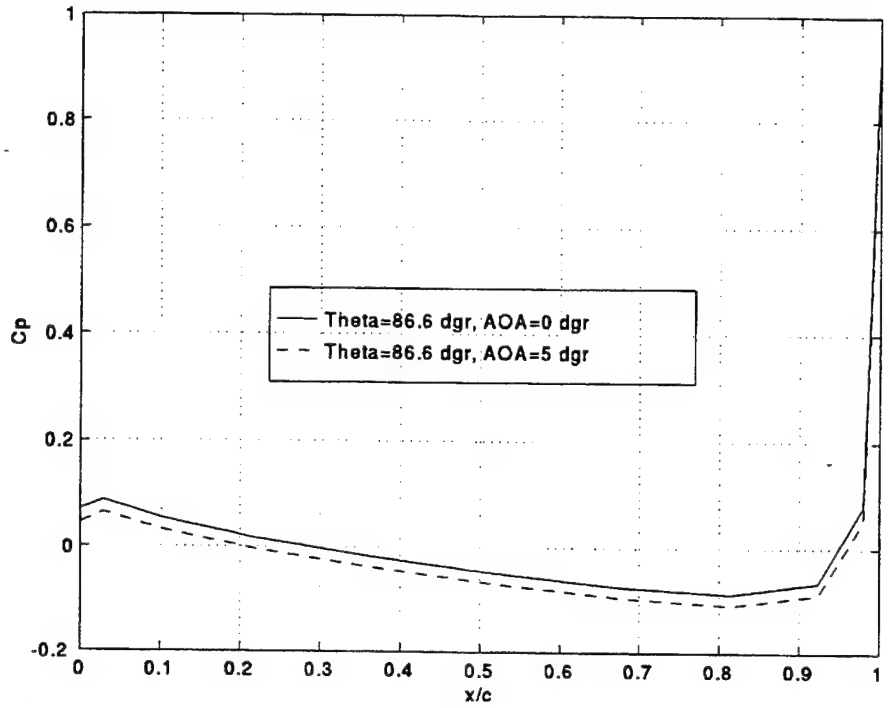

Figure 4.27 Comparison of Chordwise Pressure Distribution Along a Selected Circumferential Angular Position for Two Angles of Attack. Triangular Wing Equivalent Body of Revolution, Delta=0.098.

b. Pressure Perturbations

Using the PMARC results on Figures 4.24 to 4.27 above, the difference in pressure between the body at zero and five degrees angle of attack was calculated for various circumferential positions and plotted against the pressure perturbation as computed with the slender body theory at the same respective circumferential positions and the same change of angle of attack (Figures 4.28 to 4.31).

For reasons given in the previous subsection, the nose results of these plots should be discarded. However, this restriction still leaves relatively large disparities between the two perturbation calculations for all the cases considered. These disparities are larger towards the nose and the tail and progressively reduce to zero towards the shifting point.

As described before, the shifting point is defined as the chordwise location where there is no pressure perturbation following the change of angle of attack. Ahead of the shifting point the pressure perturbations will be in the opposite direction than those after. It can be observed that the shifting points as calculated with the slender body theory do not always correspond to those obtained by PMARC. The differences for the theta angles 3.4, 32.6, 62.6, 117.4, 147.4, and 176.6 degrees are 8.5%, 0.0%, 225.0%, 17.0%, 0.0%, and 13.8% respectively. Unlike the F5 wing equivalent body of revolution where all the differences were within acceptable range, we now observe complete disagreement for the theta angle of 62.6 degrees. As before, the 30 degree range shows perfect agreement. For the theta position of 87 degrees, we observe that the perturbations are close to zero. A reading at exactly 90 degrees would in fact reveal zero perturbation when computed with the slender body theory.

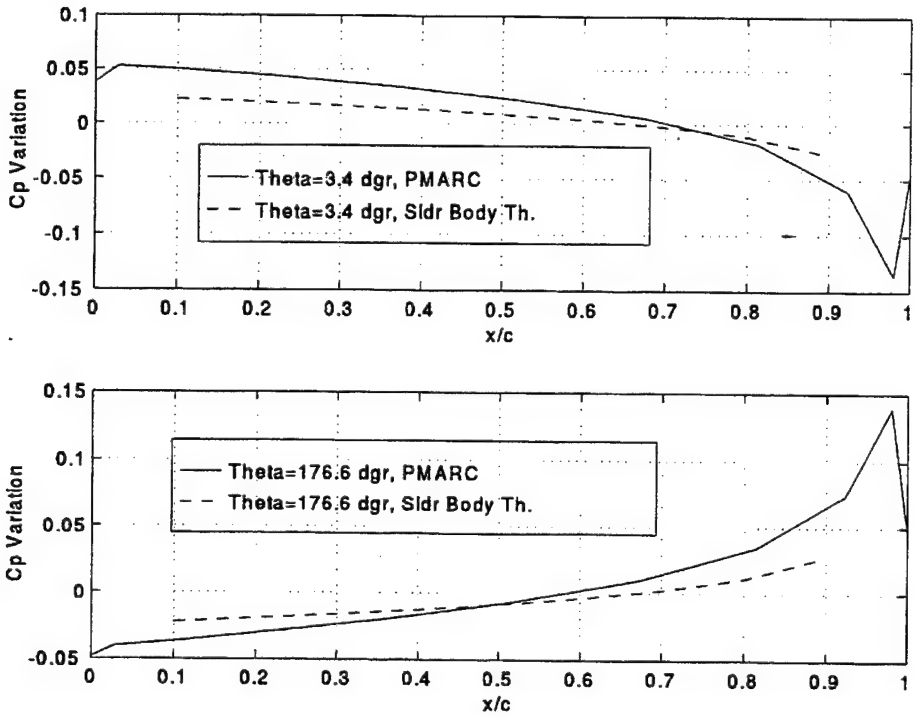

Figure 4.28 Comparison of Chordwise Pressure Perturbation at Selected Circumferential Angular Positions for a 0 to 5 Degree Change in AOA. Triangular Wing Equivalent Body of Revolution, Delta=0.098.

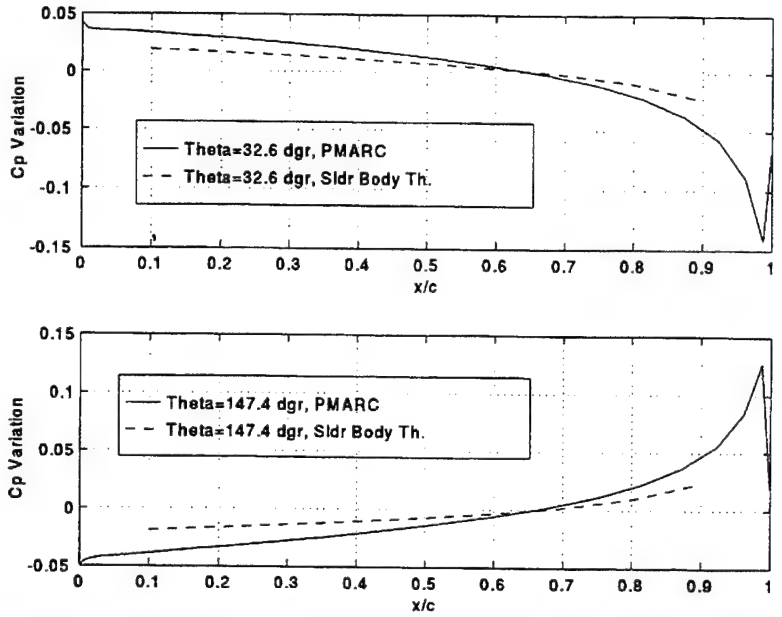

Figure 4.29 Comparison of Chordwise Pressure Perturbation at Selected Circumferential Angular Positions for a 0 to 5 Degree Change in AOA. Triangular Wing Equivalent Body of Revolution, Delta=0.098.

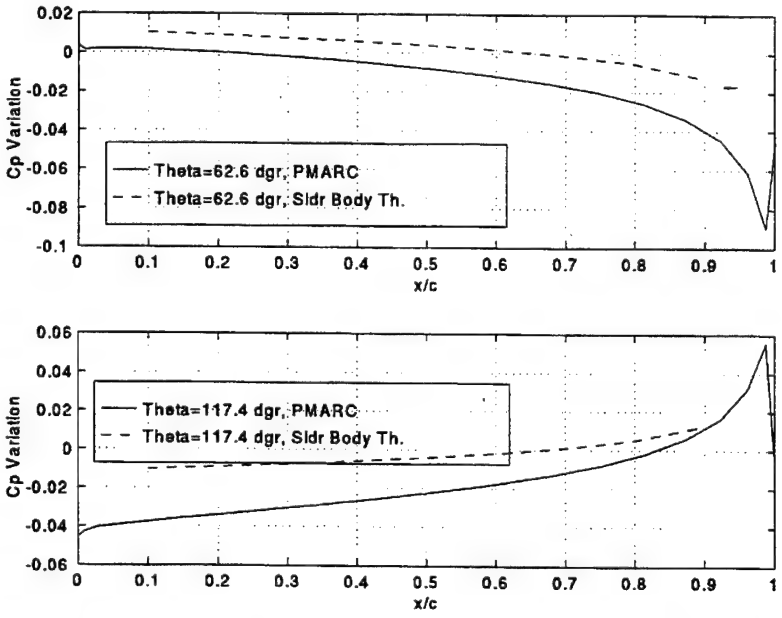

Figure 4.30 Comparison of Chordwise Pressure Perturbation at Selected Circumferential Angular Positions for a 0 to 5 Degree Change in AOA. Triangular Wing Equivalent Body of Revolution, Delta=0.098.

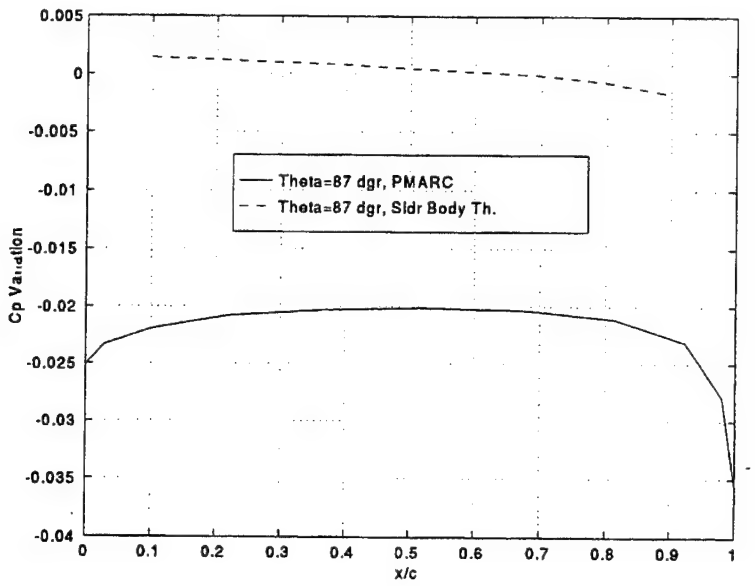

Figure 4.31 Comparison of Chordwise Pressure Perturbation at a Selected Circumferential Angular Position for a 0 to 5 Degree Change in AOA. Triangular Wing Equivalent Body of Revolution, Delta=0.098

3. PMARC Input Instructions

The steps used to construct the PMARC model of the triangular wing equivalent body of revolution are the same as for the F5 wing equivalent body of revolution. The reader should refer to the previous section for the details. The only difference is in the acquisition of the spanwise cross-sectional areas. Unlike for the F5 wing, we did not need the assistance of a computer program to get them as an analytical expression was available (Equation (4.6)). Appendix **G** shows the results of the analytical expression at various chord location for use in the slender body theory. Figure 4.32 presents the input file for the triangular wing equivalent body of revolution.

4. Scaled Circles Model Construction Method Characteristics

The same advantages and disadvantages of the method used for the construction of the F5 wing equivalent body of revolution discussed in the previous section stand for the triangular wing equivalent body of revolution.

```
Oct 23 1995 10:25          triBofR0d_098.in                Page 1

 2/3 AR, Delta=0.098, Bicvex Triang Wing -EQUIV BODY OF REVOL'N- Steady
 &BINP2    LSTINP=2,     LSTOUT=0,     LSTFRQ=0,     LENRUN=0,     LPLTYP=1,     &END
 &BINP3    LSYSEO=0,     LSTNAB=0,     LSTWAK=0,     LSTOPV=0,                   &END
 &BINP4    MAXITR=200,   SOLRES=0.0005,                                          &END
 &BINP5    NTSTPS=58,    DTSTEP=0.2,                                             &END
 &BINP6    RSYM=1.0,     RGPR=0.0,     RFF=5.0,  RCORES=0.0080, RCOREW=0.0080, &END
 &BINP7    VINF=11.0,    VSOUND=1116.0,                                          &END
 &BINP8    ALDEG= 0.00,  YAWDEG=0.0,   PHIDOT=0.0,  THEDOT=0.0,  PSIDOT=0.0,    &END
 &BINP8A   PHIMAX= 0.0,  THEMAX= 0.0,  PSIMAX=0.0,
           WRX=0.0,      WRY=0.0,      WRZ=0.0,                                  &END
 &BINP8B   DXMAX=0.0,    DYMAX=0.0,    DZMAX=0.0,
           WTX=0.0,      WTY=0.0,      WTZ=0.0,                                  &END
 &BINP9    CBAR=0.1111,  SREF=0.0097,  SSPAN= 0.0555,
           RMPX=0.00,    RMPY=0.00,    RMPZ=0.00,                                &END
 &BINP10   NORSET=0,     NBCHGE=0,     NCZONE=0,
           NC2PCH=0,     CZDUB=0.0,    VREF=0.0,                                 &END
 &BINP11   NORPCH=0,     NORF=0,       NORL=0,
           NOCF=0,       NOCL=0,       VNORM=0.0,                                &END
 &BINP12   KFAN=0,       KSIDE=0,      NEWNAB=0,     NEWBID=0,                   &END
 &BINP13   NBLIT=0,                                                              &END

 &ASEM1    ASEMX=0.0,    ASEMY=0.00,   ASEMZ=0.00,
           ASCAL=1.00,   ATHET=0.00,   NODEA=5,                                  &END
 &ASEM2    APXX=0.00,    APYY=0.00,    APZZ=0.00,
           AHXX=0.00,    AHYY=1.00,    AHZZ=0.00,                                &END

 &COMP1    COMPX= 0.0000,  COMPY= 0.0000,  COMPZ= 0.0000,
           CSCAL= 1.000,   CTHET=  0.0,    NODEC= 5,                             &END
 &COMP2    CPXX= 0.0000,   CPYY= 0.0000,   CPZZ= 0.0000,
           CHXX= 0.0000,   CHYY=  1.000,   CHZZ= 0.0000,                         &END

 &PATCH1   IREV=  0, IDPAT= 2, MAKE=   0, KCONP= 1, KASS= 1, IPATSYM=1,
           IPATCOP=0,                                                          &END
     EQUIVALENT BODY
 &SECT1    STX=    0.0000, STY= 0.0000,   STZ= 0.0000,   SCALE=  0.0000,
           ALF=    0.0,  THETA=   0.0,
           INNODE=   1,  TNODS= 0,   TNPS=  0,   TINTS= 0,                       &END
      0.0000   -1.0000    0.0000
      0.1735   -0.9845    0.0000
      0.3420   -0.9395    0.0000
      0.5000   -0.8660    0.0000
      0.6425   -0.7660    0.0000
      0.7660   -0.6425    0.0000
      0.8660   -0.5000    0.0000
      0.9395   -0.3420    0.0000
      0.9845   -0.1735    0.0000
      1.0000    0.0000    0.0000
      0.9845    0.1735    0.0000
      0.9395    0.3420    0.0000
      0.8660    0.5000    0.0000
      0.7660    0.6425    0.0000
      0.6425    0.7660    0.0000
      0.5000    0.8660    0.0000
      0.3420    0.9395    0.0000
      0.1735    0.9845    0.0000
      0.0000    1.0000    0.0000
 &BPNODE   TNPOINT=3   TNPC=10   TINTC=3   &END
 &SECT1    STX= 0.0250, STY= 0.0000, STZ= 0.0000,   SCALE= 0.0016,
           ALF=   0.0,  THETA=   0.0,
           INNODE=   1,  TNODS= 0,   TNPS=  0,   TINTS= 0,                       &END
 &SECT1    STX= 0.0500, STY= 0.0000, STZ= 0.0000,   SCALE= 0.0070,
           ALF=   0.0,  THETA=   0.0,
           INNODE=   1,  TNODS= 0,   TNPS=  0,   TINTS= 0,                       &END
 &SECT1    STX= 0.0750, STY= 0.0000, STZ= 0.0000,   SCALE= 0.0104,
           ALF=   0.0,  THETA=   0.0,
           INNODE=   1,  TNODS= 0,   TNPS=  0,   TINTS= 0,                       &END
 &SECT1    STX= 0.1000, STY= 0.0000, STZ= 0.0000,   SCALE= 0.0137,
           ALF=   0.0,  THETA=   0.0,
           INNODE=   0,  TNODS= 0,   TNPS=  0,   TINTS= 0,                       &END
 &SECT1    STX= 0.1250, STY= 0.0000, STZ= 0.0000,   SCALE= 0.0169,
           ALF=   0.0,  THETA=   0.0,
```

```
Oct 23 1995 10:25          triBofR0d_098.in                Page 2

           INNODE=   0,  TNODS= 0,   TNPS=  0,   TINTS= 0,
 &SECT1    STX= 0.1500, STY= 0.0000, STZ= 0.0000,   SCALE= 0.0199,
           ALF=   0.0,  THETA=   0.0,
           INNODE=   0,  TNODS= 0,   TNPS=  0,   TINTS= 0,                       &END
 &SECT1    STX= 0.1750, STY= 0.0000, STZ= 0.0000,   SCALE= 0.0229,
           ALF=   0.0,  THETA=   0.0,
           INNODE=   0,  TNODS= 0,   TNPS=  0,   TINTS= 0,                       &END
 &SECT1    STX= 0.2000, STY= 0.0000, STZ= 0.0000,   SCALE= 0.0258,
           ALF=   0.0,  THETA=   0.0,
           INNODE=   0,  TNODS= 0,   TNPS=  0,   TINTS= 0,                       &END
 &SECT1    STX= 0.2250, STY= 0.0000, STZ= 0.0000,   SCALE= 0.0286,
           ALF=   0.0,  THETA=   0.0,
           INNODE=   0,  TNODS= 0,   TNPS=  0,   TINTS= 0,                       &END
 &SECT1    STX= 0.2500, STY= 0.0000, STZ= 0.0000,   SCALE= 0.0312,
           ALF=   0.0,  THETA=   0.0,
           INNODE=   0,  TNODS= 0,   TNPS=  0,   TINTS= 0,                       &END
 &SECT1    STX= 0.2750, STY= 0.0000, STZ= 0.0000,   SCALE= 0.0338,
           ALF=   0.0,  THETA=   0.0,
           INNODE=   0,  TNODS= 0,   TNPS=  0,   TINTS= 0,                       &END
 &SECT1    STX= 0.3000, STY= 0.0000, STZ= 0.0000,   SCALE= 0.0362,
           ALF=   0.0,  THETA=   0.0,
           INNODE=   0,  TNODS= 0,   TNPS=  0,   TINTS= 0,                       &END
 &SECT1    STX= 0.3250, STY= 0.0000, STZ= 0.0000,   SCALE= 0.0385,
           ALF=   0.0,  THETA=   0.0,
           INNODE=   0,  TNODS= 0,   TNPS=  0,   TINTS= 0,                       &END
 &SECT1    STX= 0.3500, STY= 0.0000, STZ= 0.0000,   SCALE= 0.0407,
           ALF=   0.0,  THETA=   0.0,
           INNODE=   0,  TNODS= 0,   TNPS=  0,   TINTS= 0,                       &END
 &SECT1    STX= 0.3750, STY= 0.0000, STZ= 0.0000,   SCALE= 0.0428,
           ALF=   0.0,  THETA=   0.0,
           INNODE=   0,  TNODS= 0,   TNPS=  0,   TINTS= 0,                       &END
 &SECT1    STX= 0.4000, STY= 0.0000, STZ= 0.0000,   SCALE= 0.0447,
           ALF=   0.0,  THETA=   0.0,
           INNODE=   0,  TNODS= 0,   TNPS=  0,   TINTS= 0,                       &END
 &SECT1    STX= 0.4250, STY= 0.0000, STZ= 0.0000,   SCALE= 0.0465,
           ALF=   0.0,  THETA=   0.0,
           INNODE=   0,  TNODS= 0,   TNPS=  0,   TINTS= 0,                       &END
 &SECT1    STX= 0.4500, STY= 0.0000, STZ= 0.0000,   SCALE= 0.0481,
           ALF=   0.0,  THETA=   0.0,
           INNODE=   0,  TNODS= 0,   TNPS=  0,   TINTS= 0,                       &END
 &SECT1    STX= 0.4750, STY= 0.0000, STZ= 0.0000,   SCALE= 0.0496,
           ALF=   0.0,  THETA=   0.0,
           INNODE=   0,  TNODS= 0,   TNPS=  0,   TINTS= 0,                       &END
 &SECT1    STX= 0.5000, STY= 0.0000, STZ= 0.0000,   SCALE= 0.0510,
           ALF=   0.0,  THETA=   0.0,
           INNODE=   0,  TNODS= 0,   TNPS=  0,   TINTS= 0,                       &END
 &SECT1    STX= 0.5250, STY= 0.0000, STZ= 0.0000,   SCALE= 0.0522,
           ALF=   0.0,  THETA=   0.0,
           INNODE=   0,  TNODS= 0,   TNPS=  0,   TINTS= 0,                       &END
 &SECT1    STX= 0.5500, STY= 0.0000, STZ= 0.0000,   SCALE= 0.0532,
           ALF=   0.0,  THETA=   0.0,
           INNODE=   0,  TNODS= 0,   TNPS=  0,   TINTS= 0,                       &END
 &SECT1    STX= 0.5750, STY= 0.0000, STZ= 0.0000,   SCALE= 0.0541,
           ALF=   0.0,  THETA=   0.0,
           INNODE=   0,  TNODS= 0,   TNPS=  0,   TINTS= 0,                       &END
 &SECT1    STX= 0.6000, STY= 0.0000, STZ= 0.0000,   SCALE= 0.0547,
           ALF=   0.0,  THETA=   0.0,
           INNODE=   0,  TNODS= 0,   TNPS=  0,   TINTS= 0,                       &END
 &SECT1    STX= 0.6250, STY= 0.0000, STZ= 0.0000,   SCALE= 0.0552,
           ALF=   0.0,  THETA=   0.0,
           INNODE=   0,  TNODS= 0,   TNPS=  0,   TINTS= 0,                       &END
 &SECT1    STX= 0.6500, STY= 0.0000, STZ= 0.0000,   SCALE= 0.0555,
           ALF=   0.0,  THETA=   0.0,
           INNODE=   0,  TNODS= 0,   TNPS=  0,   TINTS= 0,                       &END
 &SECT1    STX= 0.6750, STY= 0.0000, STZ= 0.0000,   SCALE= 0.0555,
           ALF=   0.0,  THETA=   0.0,
           INNODE=   0,  TNODS= 0,   TNPS=  0,   TINTS= 0,                       &END
 &SECT1    STX= 0.7000, STY= 0.0000, STZ= 0.0000,   SCALE= 0.0553,
           ALF=   0.0,  THETA=   0.0,
           INNODE=   0,  TNODS= 0,   TNPS=  0,   TINTS= 0,                       &END
 &SECT1    STX= 0.7250, STY= 0.0000, STZ= 0.0000,   SCALE= 0.0548,
           ALF=   0.0,  THETA=   0.0,
           INNODE=   0,  TNODS= 0,   TNPS=  0,   TINTS= 0,                       &END
 &SECT1    STX= 0.7500, STY= 0.0000, STZ= 0.0000,   SCALE= 0.0541,
           ALF=   0.0,  THETA=   0.0,
           INNODE=   0,  TNODS= 0,   TNPS=  0,   TINTS= 0,                       &END
```

Figure 4.32 PMARC Input File for The Triangular Wing Equivalent Area Body of Revolution, Maximum Thickness Ratio = 0.098.

```
&SECT1   STX= 0.7750, STY= 0.0000,    STZ= 0.0000,    SCALE= 0.0530,
         ALF=   0.0,  THETA=   0.0,
         INMODE=  0,  TNODS= 0,    TNPS= 0,    TINTS= 0,                 &END
&SECT1   STX= 0.8000, STY= 0.0000,    STZ= 0.0000,    SCALE= 0.0516,
         ALF=   0.0,  THETA=   0.0,
         INMODE=  0,  TNODS= 0,    TNPS= 0,    TINTS= 0,                 &END
&SECT1   STX= 0.8250, STY= 0.0000,    STZ= 0.0000,    SCALE= 0.0498,
         ALF=   0.0,  THETA=   0.0,
         INMODE=  0,  TNODS= 0,    TNPS= 0,    TINTS= 0,                 &END
&SECT1   STX= 0.8500, STY= 0.0000,    STZ= 0.0000,    SCALE= 0.0475,
         ALF=   0.0,  THETA=   0.0,
         INMODE=  0,  TNODS= 0,    TNPS= 0,    TINTS= 0,                 &END
&SECT1   STX= 0.8750, STY= 0.0000,    STZ= 0.0000,    SCALE= 0.0446,
         ALF=   0.0,  THETA=   0.0,
         INMODE=  0,  TNODS= 0,    TNPS= 0,    TINTS= 0,                 &END
&SECT1   STX= 0.9000, STY= 0.0000,    STZ= 0.0000,    SCALE= 0.0410,
         ALF=   0.0,  THETA=   0.0,
         INMODE=  0,  TNODS= 0,    TNPS= 0,    TINTS= 0,                 &END
&SECT1   STX= 0.9250, STY= 0.0000,    STZ= 0.0000,    SCALE= 0.0365,
         ALF=   0.0,  THETA=   0.0,
         INMODE=  0,  TNODS= 0,    TNPS= 0,    TINTS= 0,                 &END
&SECT1   STX= 0.9500, STY= 0.0000,    STZ= 0.0000,    SCALE= 0.0306,
         ALF=   0.0,  THETA=   0.0,
         INMODE=  0,  TNODS= 0,    TNPS= 0,    TINTS= 0,                 &END
&SECT1   STX= 0.9625, STY= 0.0000,    STZ= 0.0000,    SCALE= 0.0269,
         ALF=   0.0,  THETA=   0.0,
         INMODE=  0,  TNODS= 0,    TNPS= 0,    TINTS= 0,                 &END
&SECT1   STX= 0.9750, STY= 0.0000,    STZ= 0.0000,    SCALE= 0.0222,
         ALF=   0.0,  THETA=   0.0,
         INMODE=  0,  TNODS= 0,    TNPS= 0,    TINTS= 0,                 &END
&SECT1   STX= 0.9813, STY= 0.0000,    STZ= 0.0000,    SCALE= 0.0194,
         ALF=   0.0,  THETA=   0.0,
         INMODE=  0,  TNODS= 0,    TNPS= 0,    TINTS= 0,                 &END
&SECT1   STX= 0.9876, STY= 0.0000,    STZ= 0.0000,    SCALE= 0.0159,
         ALF=   0.0,  THETA=   0.0,
         INMODE=  0,  TNODS= 0,    TNPS= 0,    TINTS= 0,                 &END
&SECT1   STX= 0.9938, STY= 0.0000,    STZ= 0.0000,    SCALE= 0.0113,
         ALF=   0.0,  THETA=   0.0,
         INMODE=  0,  TNODS= 0,    TNPS= 0,    TINTS= 0,                 &END
&SECT1   STX= 0.9969, STY= 0.0000,    STZ= 0.0000,    SCALE= 0.0080,
         ALF=   0.0,  THETA=   0.0,
         INMODE=  0,  TNODS= 0,    TNPS= 0,    TINTS= 0,                 &END
&SECT1   STX= 1.0000, STY= 0.0000,    STZ= 0.0000,    SCALE= 0.0000,
         ALF=   0.0,  THETA=   0.0,
         INMODE=  0,  TNODS= 5,    TNPS= 22,    TINTS= 2,                &END
&BPNODE   TNODE=3,    TNPC=0,   TINTC=0,    &END

&WAKE1   IDWAK=0,        IFLXW=1,        ITRFTZ= 0,      INTRW= 0,        &END
 WING_WAKE
&WAKE2   KWPACH=2,       KWSIDE=4,       KWLINE=0,       KWPAN1=0,
         KWPAN2=0,       NODEW=0,        INITIAL=0,                       &END
&WAKE2   KWPACH=1,       KWSIDE=2,       KWLINE=0,       KWPAN1=0,
         KWPAN2=0,       NODEW=5,        INITIAL=0,                       &END


&ONSTRM  NONSL =0,  KPSL =                                                &END


&BLPARAM RN =35755000,    VISC = 0.000157, NSLBL = 1,                     &END


                                                                          &END
&VS1     NVOLR= 0,       NVOLC= 0,                                        &END
&VS2     X0=    -0.1000, Y0=    1.5000, Z0=    -0.1000, INTVSR= 1,       &END
&VS3     X1=    -0.1000, Y1=    1.5000, Z1=     0.1000, NPT1=  0,        &END
&VS4     X2=    -0.1000, Y2=    1.5000, Z2=     0.1000, NPT2= 20,        &END
&VS5     X3=     1.1000, Y3=    1.5000, Z3=    -0.1000, NPT3= 25,        &END

&VS6     XR0=    2.0000, YR0=    2.0000, ZR0=    0.0000, INTVSC= 1,       &END
&VS7     XR1=    4.0000, YR1=    2.0000, ZR1=    0.0000,
         XR2=    2.0000, YR2=    2.0000, ZR2=    1.0000,                  &END
&VS8     R1=     0.1000, R2=     1.0000, PHI1=  0.0,     PHI2=360.0,      &END
&VS9     NRAD=   5,      NPHI=  12,      NLEN=  3,                        &END


&SLIN1   NSTLIN=0,                                                        &END
&SLIN2   SX0=   -2.0000, SY0=    1.0000, SZ0=   -0.5000,
```

Figure 4.32 Cont'd PMARC Input File for The Triangular Wing Equivalent Area Body of Revolution, Maximum Thickness Ratio = 0.098.

5. PMARC Output - Data Retrieval

The data retrieval techniques used here to obtain the pressure coefficient distribution at different circumferential theta angles are the same as for the F5 wing body of revolution studied in the previous section.

D. THE SPINDLE

The body of revolution making the subject of this section is symmetrical about the longitudinal axis and its mid-chord. The length of the longitudinal axis was made unity through non-dimensionalization. The thickness distribution represented by the radius distribution is shown in Equation (4.7) below.

$$R(x) = 2\tau(x-x^2) \tag{4.7}$$

where *tau* is the maximum thickness. Figure 4.33 shows the PMARC representation of the spindle.

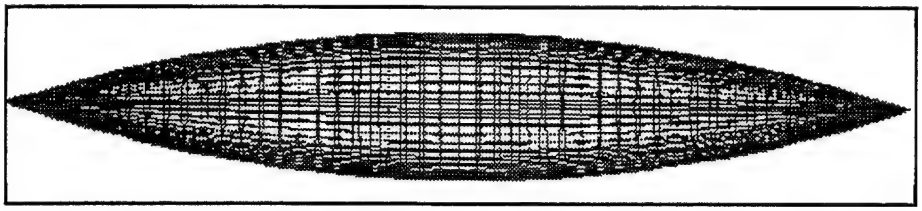

Figure 4.33 PMARC Representation of The Spindle.

1. Theory, Background and Reference Data

In order to validate the PMARC results of pressure distribution for the spindle, we will once again rely on past experience for the general expected behavior, and on the approximate slender body theory for the magnitude of the pressures. Like for the F5 and the triangular wing equivalent body of revolutions, our chordwise pressure distribution analysis will be performed at several circumferential locations to ensure consistency in the expected trends.

a. Expected General Behavior

As for the F5 and the triangular wing equivalent body of revolutions, the total lift on the spindle should be zero as the upward lift on the front portion of the body is cancelled by the

downward lift on the rear portion. In term of pressure distribution, it will once again be observed that for a change of angle of attack from zero to 5 degrees, the pressure differential at a specific aft chordwise location will be equal in magnitude but in the reverse direction than that of the corresponding rearward location (mirror image from mid-chord). This means that this differential will be zero exactly at the mid-chord point, unlike for the F5 and triangular wing equivalent body of revolutions where it was further back.

The behavior described above would be modified for the chordwise distributions that lie along the 90 and 270 degree circumferential positions. Not only is the magnitude of the pressure differential for a zero to five degrees shift in angle of attack expected to be the same at two related forward and rearward positions, but also the direction of the pressure.

b. Slender Body Theory

As already mentioned in the previous sections, the slender body theory dictates that the pressure on a body at angle of attack is approximated by the pressure at zero angle of attack plus the pressure differential between its value at zero and at the new angle of attack. Recall that this differential can be calculated using the following slender body theory derivation in which R is the radius distribution and *tau* the maximum thickness.

$$Cp = Cp_{\alpha=0} + Cp_{d\alpha} \tag{4.1}$$

$$Cp_{d\alpha} = 2\alpha R'(x)\cos\theta \tag{4.2}$$

$$R(x) = 2\tau(x-x^2) \tag{4.8}$$

$$R'(x) = 2\tau(1-2x) \tag{4.9}$$

Using the expected behavior description given above and the numerical results of the slender body theory applied to the spindle, we will now present the PMARC results.

2. Results and Discussion

Figures 4.35 to 4.40 presented below display the chordwise pressure distribution at various circumferential positions for two angles of attack, which will allow comparison with intuitive expectations . Figures 4.41 to 4.44 show the pressure perturbation when going from zero angle of attack to a higher value, as calculated by PMARC and the slender body theory.

It should be noted that the circumferential positions of the chordwise body line of analysis were chosen to exactly correspond with the control point coordinates of the chordwise strips of panels which separate the body cross-section in 12 pie sections (Figure4.34).

This exact selection was not possible in the two previous cases. It was made possible here due to the method employed to build the model as will be discussed in the next subsection. Also as a result of that particular method, the end points (nose and tail) were not corrupted and generated valid results.

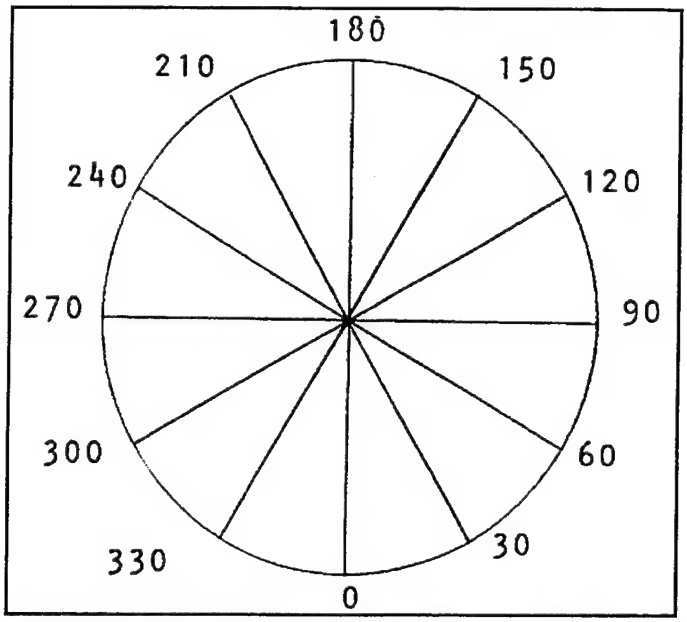

Figure 4.34 Circumferential Angular Locations Studied on The Spindle Cross-Sections.

a. Chordwise Pressure Distributions

The first figure (Figure 4.35) shows the expected results that the pressure distribution will be the same for any circumferential position when the body of revolution is at zero angle of attack. Figure 4.36 presents the same parameters but with the body at five degrees angle of attack. We now observe the progression in pressure from top to bottom at a particular section aft of the shifting point and regression at a particular section rearward of the shifting point. This plot also shows the relative chordwise position of the minimum pressure for each chordwise distribution.

Figures 4.37 to 4.40 compare the chordwise pressure distribution at various circumferential positions for zero and five degrees angle of attack. Each figure displays the variation for two corresponding circumferential positions (longitudinal mirror image) of the body. In all cases, the leeward pressure perturbation is equal and opposite to the windward pressure perturbation, as expected. At 90 degrees, a pressure perturbation exist but remains approximately constant along the chord.

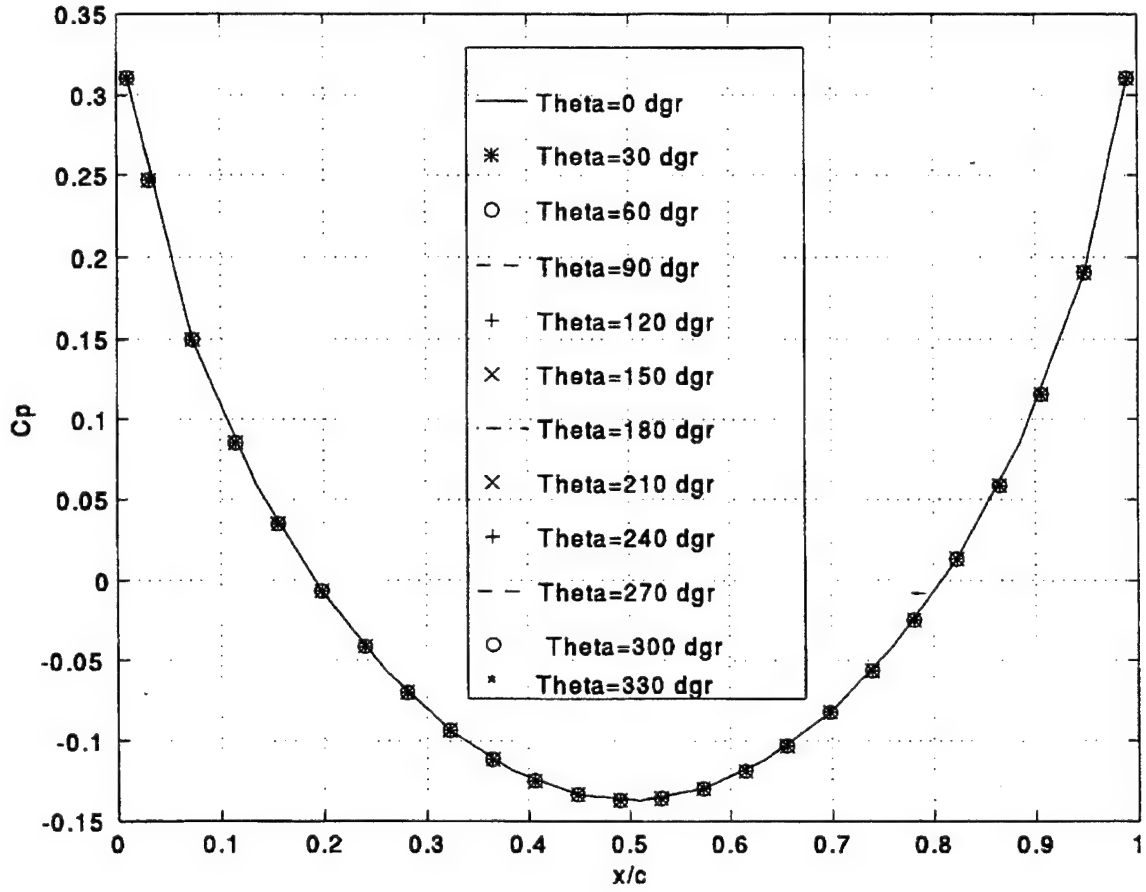

Figure 4.35 Chordwise Pressure Distribution for Various Circumferential Angles. Spindle, Delta=0.160, AOA=0 Degree.

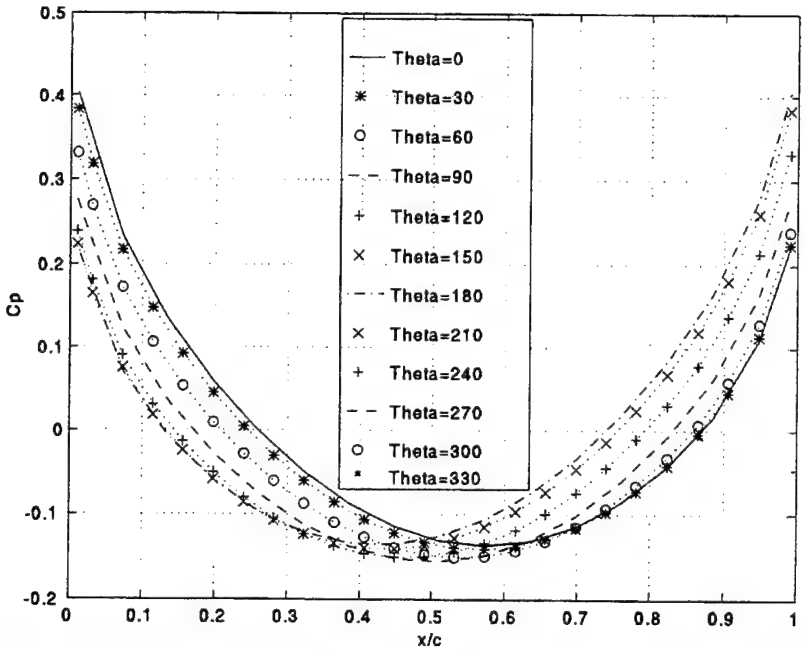

Figure 4.36 Chordwise Pressure Distribution for Various Circumferential Angles. Spindle, Delta=0.160, AOA=5 Degrees.

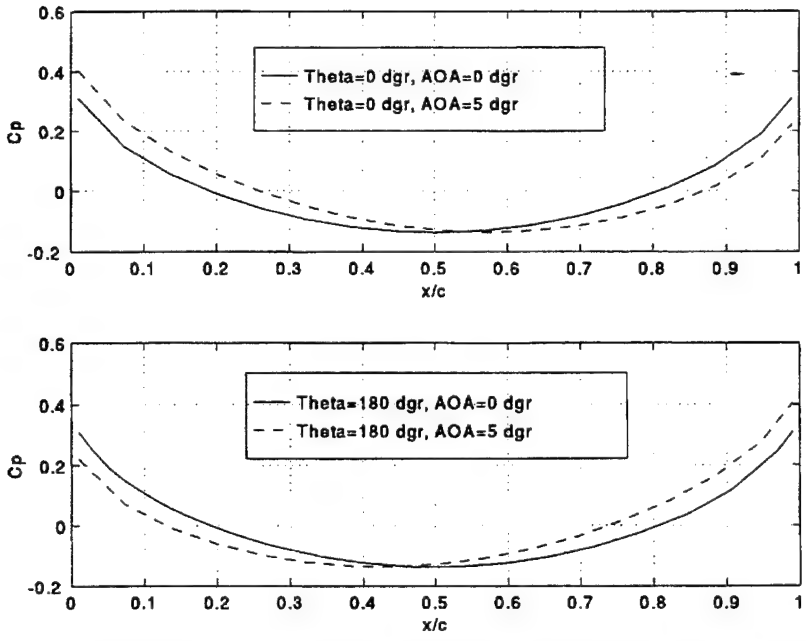

Figure 4.37 Comparison of Chordwise Pressure Distribution Along Selected Circumferential Angular Positions for Two Angles of Attack. Spindle, Delta=0.160.

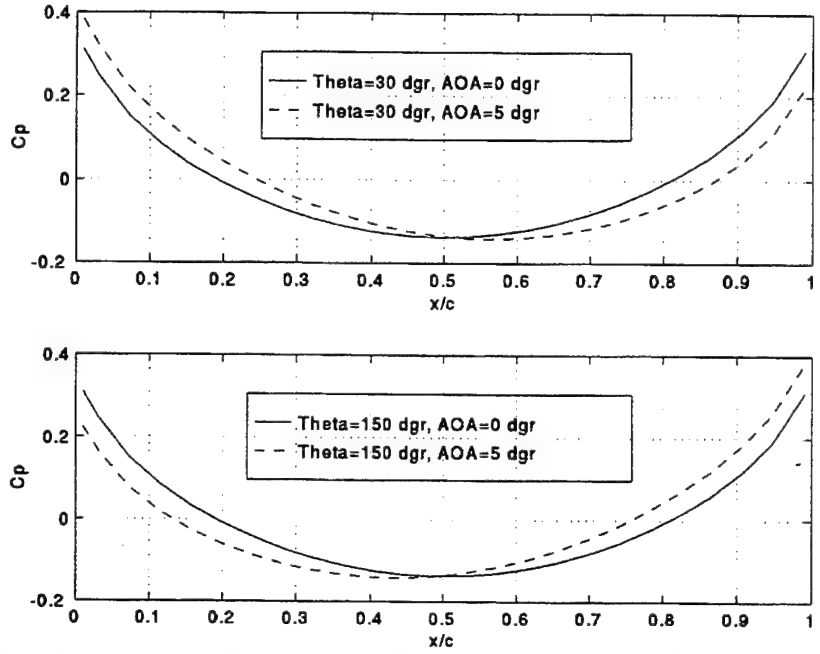

Figure 4.38 Comparison of Chordwise Pressure Distribution Along Selected Circumferential Angular Positions for Two Angles of Attack. Spindle, Delta=0.160.

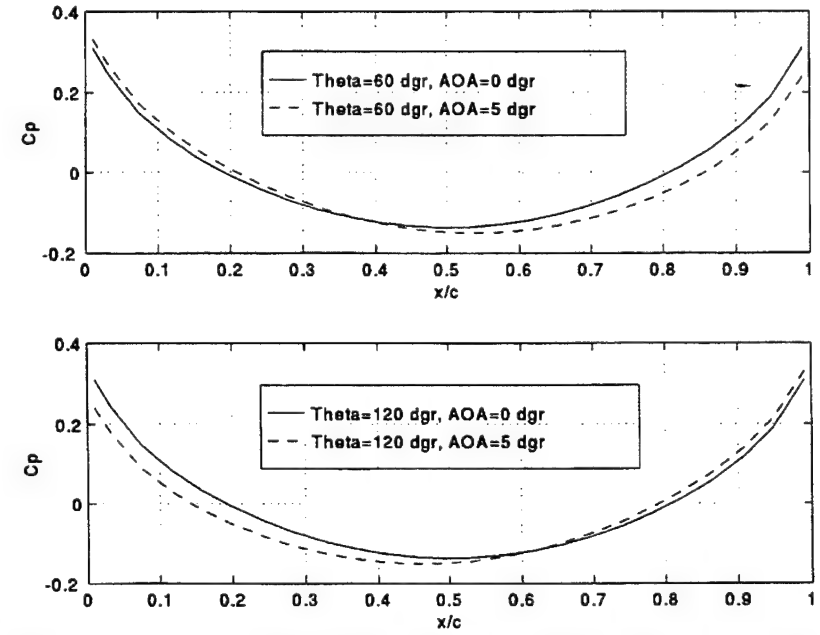

Figure 4.39 Comparison of Chordwise Pressure Distribution Along Selected Circumferential Angular Positions for Two Angles of Attack. Spindle, Delta=0.160.

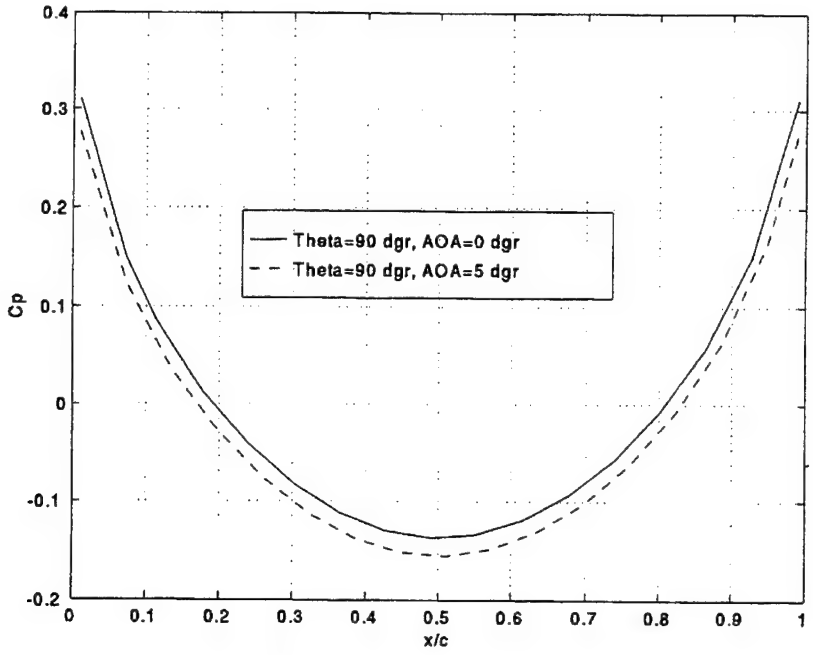

Figure 4.40 Comparison of Chordwise Pressure Distribution Along a Selected Circumferential Angular Position for Two Angles of Attack. Spindle, Delta=0.160.

b. Pressure Perturbations

Using the PMARC results on Figures 4.37 to 4.40 above, the difference in pressure between the body at zero and five degrees angle of attack was calculated for various circumferential positions and plotted against the pressure perturbation as computed with the slender body theory at the same respective circumferential positions and the same change of angle of attack (Figures 4.41 to 4.44).

Like for the F5 and triangular wing equivalent body of revolution, there exist for the spindle some disparities between the two perturbation calculations for almost all the cases considered. These disparities are larger towards the nose and the tail and progressively reduce to zero towards the shifting point.

Once again, it can be observed that the shifting points as calculated with the slender body theory do not always correspond to those obtained by PMARC. The differences for the theta angles 0, 30, 60, 120, 150, and 180 degrees are 6.0%, 3.0%, 28.0%, 19.0%, 4.0%, and 8.0% respectively. Here, we observe the largest deviation at a theta of 60 degrees. It appears like the deviation gets larger as theta approaches 90 degrees from either side.

For the theta position of 90 degrees, we observe that the perturbations are zero when computed with the slender body theory, but the PMARC results follow an elliptic distribution.

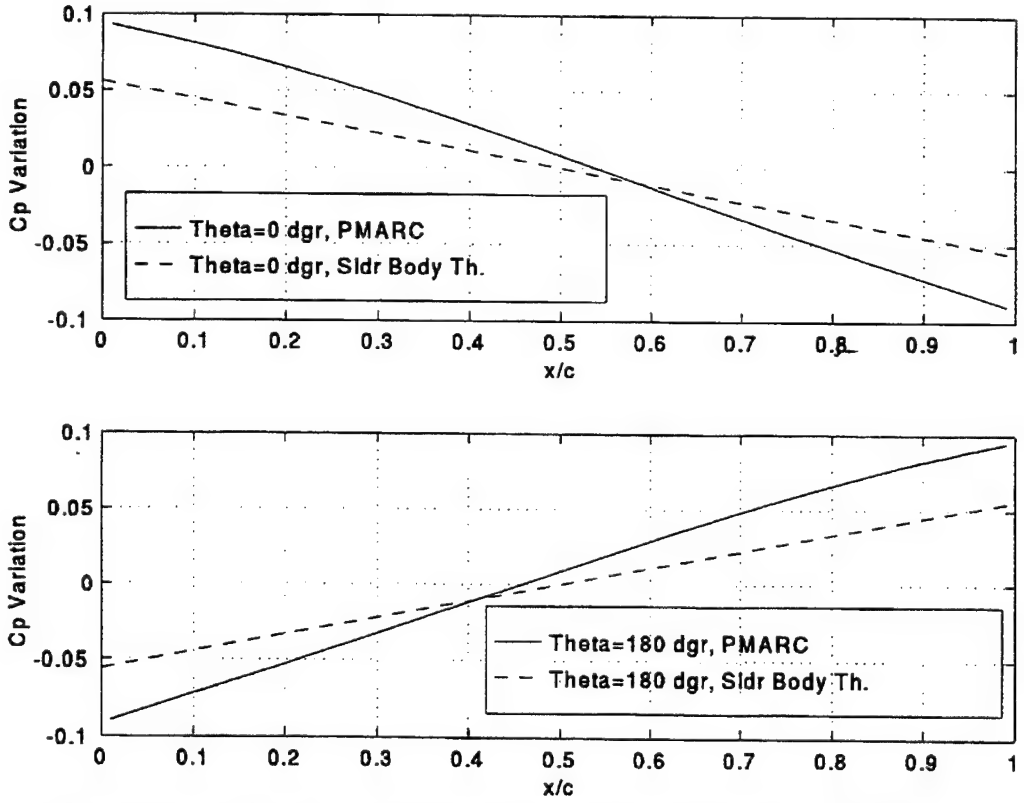

Figure 4.41 Comparison of Chordwise Pressure Perturbation at Selected Circumferential Angular Positions for a 0 to 5 Degree Change in AOA. Spindle, Maximum Thickness Ratio = 0.160.

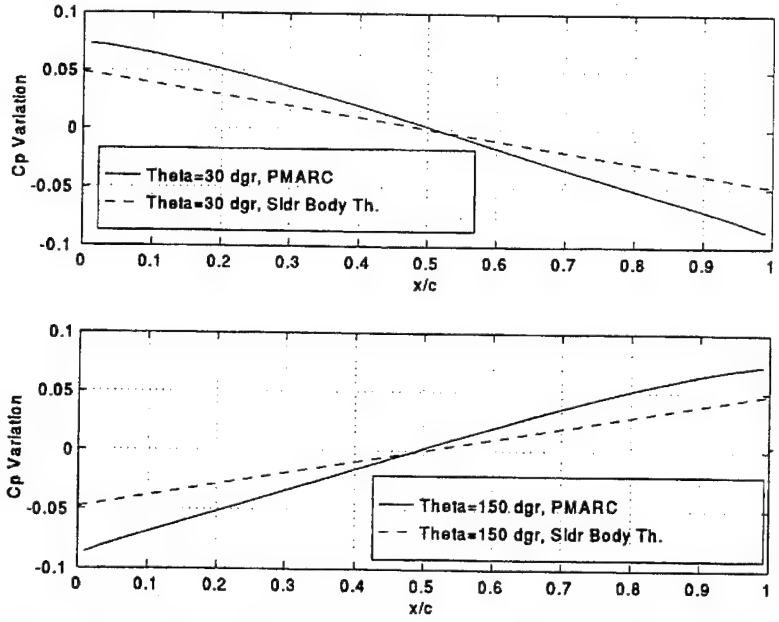

Figure 4.42 Comparison of Chordwise Pressure Perturbation at Selected Circumferential Angular Positions for a 0 to 5 Degree Change in AOA. Spindle, Maximum Thickness Ratio = 0.160.

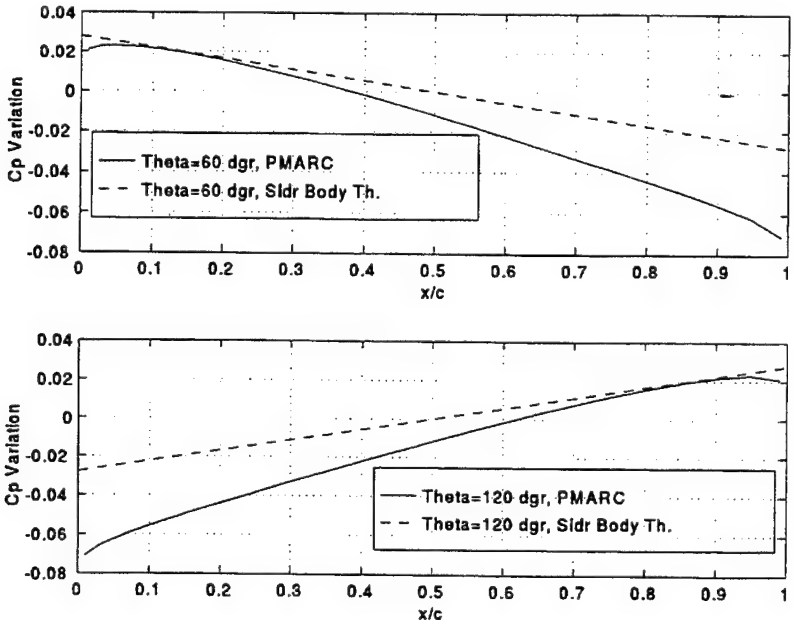

Figure 4.43 Comparison of Chordwise Pressure Perturbation at Selected Circumferential Angular Positions for a 0 to 5 Degree Change in AOA. Spindle, Maximum Thickness Ratio = 0.160.

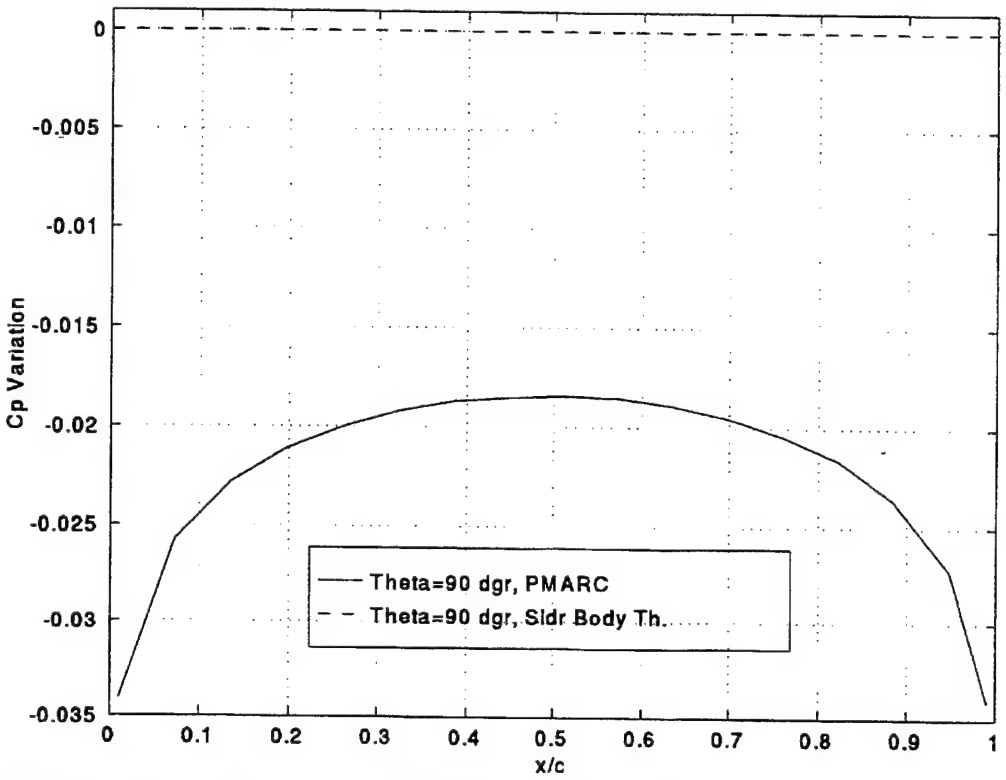

Figure 4.44 Comparison of Chordwise Pressure Perturbation at a Selected Circumferential Angular Position for a 0 to 5 Degree Change in AOA. Spindle, Maximum Thickness Ratio = 0.160.

3. PMARC Input Instructions

The steps used to construct the PMARC model of the spindle significantly vary from those used for the F5 and triangular wing equivalent body of revolution. We will present here the second method of modelling a body of revolution in PMARC. One similarity however is the acquisition of the cross-sectional areas. Although we did not need the assistance of the computer program as with the F5 wing, an analytical expression was available (Equation (4.7)). Figure 4.45 presents an extract of the input file for the spindle. The following subsections will review this second approach.

Figure 4.45 Extract of The PMARC Input File for The Spindle, Maximum Thickness Ratio = 0.160.

a. Basic Input Section

No differences exist in the format and content of the basic input section of this method and the first one used for the F5 and triangular wing equivalent body of revolution.

b. Assembly and Components System Information

Once again, the two methods present no differences in this area of the input file.

c. Patch and Section Coordinate System Information

This section is the one that differs for the two methods. Instead of defining the coordinates of one circle and scaling the latter to the dimensions corresponding to the area at a prescribed chord location, this method redefines new circle coordinates at each of these chord locations. Like for the first method, the SECT1 block is repeated each time a circle is defined. However, the reader will recall that in that method the field INMODE was set to zero in all succeeding blocks to indicate that the circle section defined in the first block was to be copied. It was then scaled by changing the SCALE field.

In the second method, INMODE is set at four in all blocks to indicate that the x, y, z coordinates of each circle will be inputted. In this case the field SCALE is always set to zero since the circles are defined in global coordinates.

In the approach presented above, all the panel fields (TNPS and TNPC) were set to zero. This tells PMARC to use the input section definitions to define the panel edges, longitudinally and along the circumference. This was possible here because all the circle points were generated so they longitudinally corresponded to each other. Otherwise, TNPS and TNPC can be prescribed and PMARC disregards the points coordinates.

d. Wake and Streamlines

As for the previous method, the wake shall be turned off for the spindle. As for the streamlines, they are not required.

4. Global Coordinate Circles Model Construction Method Characteristics

For the studies performed in this paper, the only advantage that this method seems to present is that it allows PMARC to compute more easily the flow at the pointed ends. This is said with some reservation because until we understand why the behavior of the first method is encountered in the vicinity of the pointed ends, there is no certitude about the actual superiority of the second method. Maybe it is possible to correct the input file in the first method to allow for a smoother computation at the ends. That would make the first method better all around for the type of studies performed because the input file for the spindle method is about thirty times longer. Despite this apparent disadvantage, this approach could however be necessary in some other configurations.

5. PMARC Output - Data Retrieval

For the purpose of our study, only the pressure coefficient distributions at various circumferential positions were required. In order to obtain a Cp distribution all along the chord for the theta positions selected, one reading per column of data is required. One or more columns of data can be skipped but care should be exercised as to conserve the proper smoothness of the distribution. In the DATA6 output file, one column of data details the coordinates and aerodynamic parameters of one circumferential strip of panels running all around the body from bottom to bottom as shown on Figure 4.46.

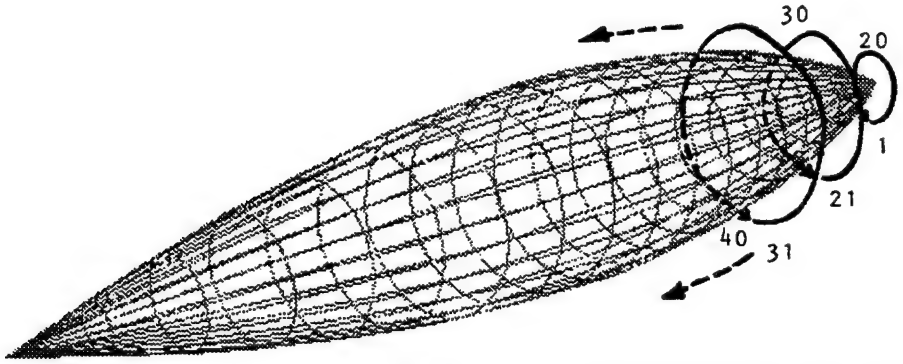

Figure 4.46 PMARC Panel Distribution on The Spindle Single Patch Model.

The circumferential position theta which need a pressure distribution analysis is translated to a panel number on the output file by looking through one column of data for the arctangent of the y over -z ratio which will give the angle needed. Once the position of the panel relative to the first panel of that column is determined, the corresponding panel in each column of data will be approximately at the same angle theta. In this case, we were able to study the pressure distribution at circumferential positions dividing the half body in six exact parts: 0, 30, 60, 90, 120, 150, and 180 degrees. As mentioned earlier, we did not have to study the mirror image position of these angles (0, 330, 300, 270, 240, 210 and 180 degrees) as the results would be identical. Recall that it is the cross-section point definitions that were judiciously made so that we ended up with control points exactly at these theta angles.

E. CONCLUSION

From our study of three different bodies of revolution, it became apparent that PMARC generates pressure distributions that match the expected trends. When compared to the slender body theory, our results indicate good agreement near the chordwise location where the pressure differential between the zero and five degrees angle of attack switches sign. As we proceed towards either end of the body, the difference between PMARC results and the slender body theory in the computation of these pressure differentials (or perturbations) progressively gets larger to an unacceptable level at the ends.

Interpretation of the plots presented also reveals that the shifting point is different depending on the method of calculation (PMARC or slender body theory). The differences however are in most cases in the vicinity of 5%. In all cases, PMARC is expected to be more precise than the slender body theory.

V. UNSTEADY CASE - OSCILLATION

A. INTRODUCTION

The intent for this chapter is to validate the PMARC results for wings and bodies of revolution in oscillation. Time constraint prevented a complete analysis of the unsteady case. It was possible to obtain results for the F5 and the triangular wings and their respective equivalent bodies of revolution as well as for the spindle for ten-degree amplitude oscillations about their mid-chord at various reduced frequencies. The results will be presented with a warning to the reader about their validity. It is left for future work to analytically or experimentally verify these results.

B. F5 WING AND EQUIVALENT BODY OF REVOLUTION

The F5 wing was shown and described in section **F** of Chapter **III,** and its equivalent body of revolution in section **B** of Chapter **IV**. Recall that for the purpose of the PMARC modelling, the main chord was set at 0.6439 unit and the corresponding maximum thickness was 0.0309 unit. The dimensionless maximum thickness ratio is then 0.0480. The wing and its equivalent body of revolution are reproduced below in Figure 5.1.

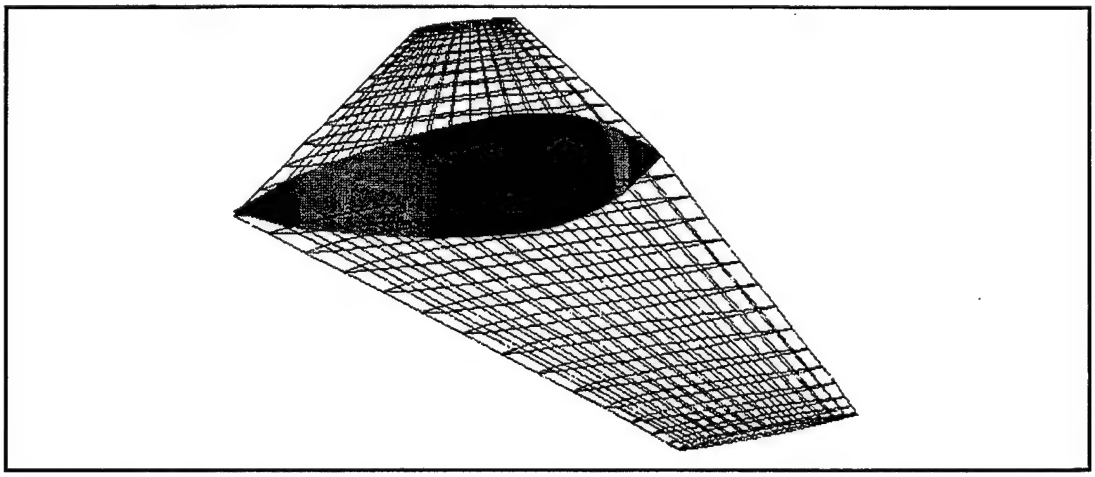

Figure 5.1 F5 Wing and its Corresponding Equivalent Area Body of Revolution.

This section will first lead the reader through the various calculations of frequency, time-stepping and other parameters related to each oscillatory case. The results will then be presented with the lift and moment coefficients plotted for two cycles of oscillation. Following the results, the specific input instructions to run an oscillatory case in PMARC will be described. Finally, a technique will be shown to retrieve the numerous data required from DATA6.

1. Oscillatory Frequency and Time-Stepping Calculations

Three reduced frequencies (k) were selected for the oscillations: 0.1, 0.5, and 1.0. The oscillations had an amplitude of plus and minus five degrees about the mid-chord. Two full oscillatory cycles were required. Here is a sample calculation for k=0.1 and the results for the other cases. All parameters shown below apply for both the wing and the equivalent body of revolution.

In the following equations, c was taken to be the root chord, and the freestream velocity was arbitrarily selected at 11 units per second. *Omega* is the oscillatory frequency in rad/sec and its PMARC notation is WRY. T is the period, N the number of time-steps and dt the size of the time-step in seconds. The PMARC notations of the last two parameters are NTSTPS and DTSTEP respectively.

$$k=0.1rad=\frac{\omega c}{U_\infty}=\frac{\omega*0.6439}{11}\Rightarrow\omega=WRY=1.7083rad/s \tag{5.1}$$

$$T=\frac{2\pi}{\omega}=\frac{2\pi}{1.7083}=3.6780\text{sec}/cycle \tag{5.2}$$

$$t=N*dt=NTSTPS*DTSTEP\Rightarrow 3.6780=NTSTPS*0.1\Rightarrow NTSTPS=36.78steps/cycle \tag{5.3}$$

NTSTPS=73.56 time-steps for two cycles

As noticed, the number of time-steps (NTSTPS) times the size of each time-step (DTSTEP) must equal the period (T). The combination selected is the one which will render a smooth distribution. In PMARC, this becomes a trial and error exercise. The following table provides the values of the above parameters for all values of reduced frequency studied.

k	Amplitude	Osc. About...	Omega (WRY)	NTSTPS	DTSTEP
0.1	+- 5 Degrees	Mid-Chord	1.7083 rad/s	74	0.1 sec
0.5	+- 5 Degrees	Mid-Chord	8.5417 rad/s	30	0.05 sec
1.0	+- 5 Degrees	Mid-Chord	17.0834 rad/s	37	0.02 sec

Table 5.1 Test Parameters for The Oscillation of The F5 Wing Equivalent Body of Revolution.

2. Results

Figures 5.3 to 5.5 below show the combined CL and CM results of the wing and the equivalent body of revolution in oscillation at the three reduced frequencies listed in Table 5.1. The analysis of the relative maximums and minimums of the CL and CM curves as a function of the reduced frequency, as well as the general behavior will be left to future work. It will only be said that the lift and moment coefficients for the body of revolution seem to behave as expected. The lift vectors aft of the pivot point are balanced by those behind it (Figure 5.2). This causes the net value of the lift to be close to zero (zero in steady state) and the moments to increasingly become larger with angle of attack as larger forces each side of the pivot point and in opposite directions torque the body. Some lift is expected due to oscillation effects. All the oscillation figures are plotted against reduced time (*tbar*) which is obtained as follows:

$$t(i) = NTSTPS(i) * DTSTEP$$

$$\bar{t}(i) = \frac{U_\infty * t(i)}{c}$$

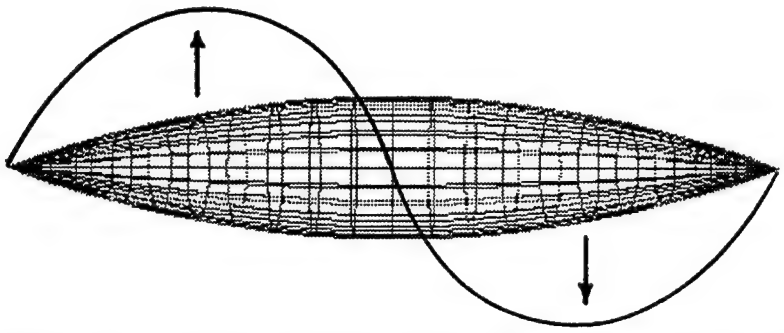

Figure 5.2 Typical Balanced Pressure Distribution Along The Longitudinal Camber of a Body of Revolution.

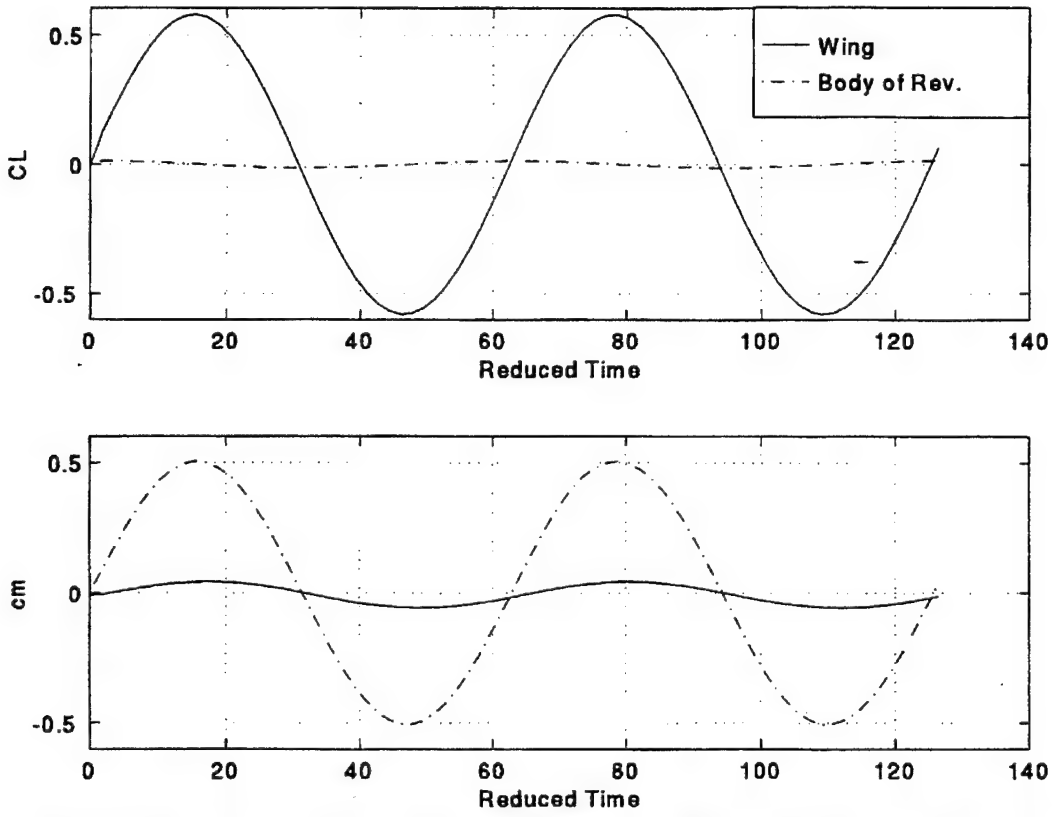

Figure 5.3 Comparison of The Lift and Moment Coefficients in Unsteady State as a Function of Reduced Time. F5 Wing and Equivalent Body of Revolution, Oscillation Amplitude=10 Degrees About c/2, U_{inf}=11, Omega=1.7083 rad/s, k=0.1.

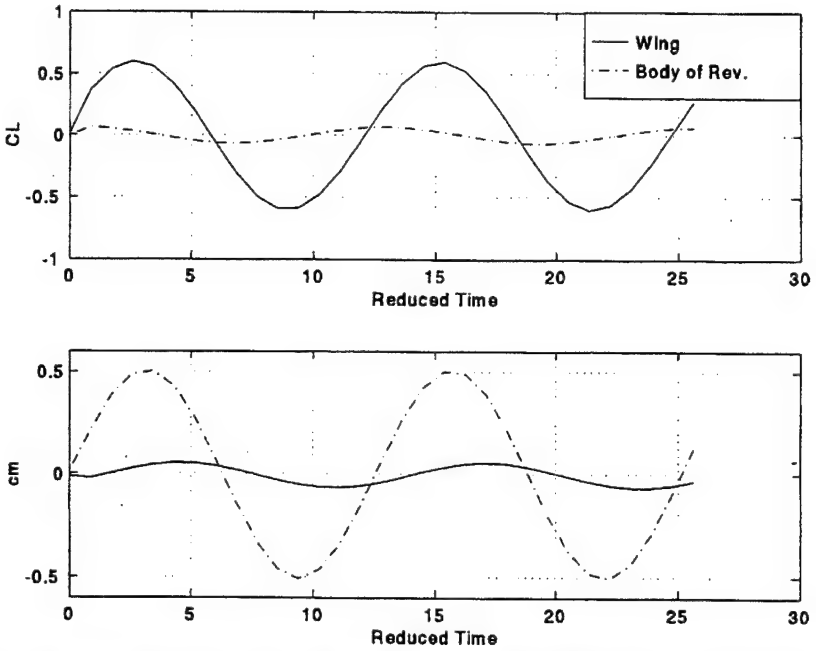

Figure 5.4 Comparison of The Lift and Moment Coefficients in Unsteady State as a Function of Reduced Time. F5 Wing and Equivalent Body of Revolution, Oscillation Amplitude=10 Degrees About c/2, U_{inf}=11, Omega=8.5417 rad/s, k=0.5.

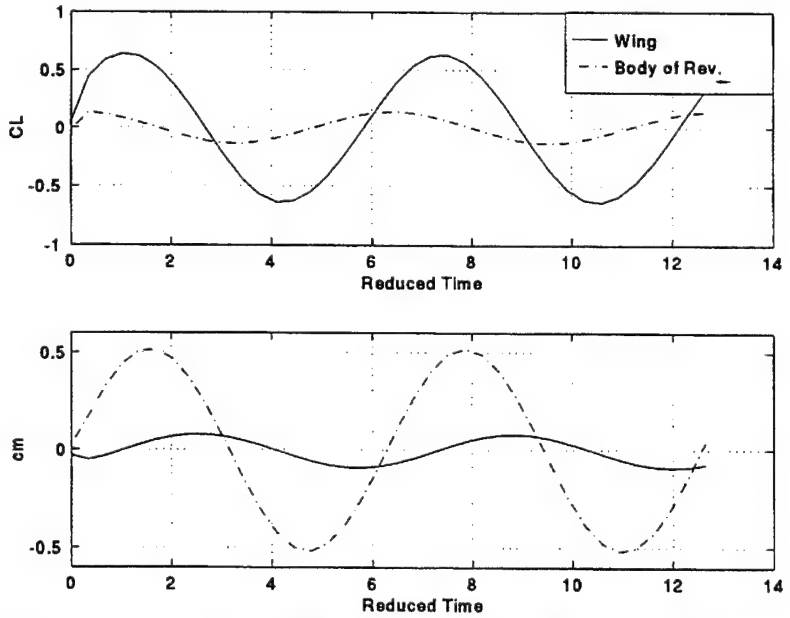

Figure 5.5 Comparison of The Lift and Moment Coefficients in Unsteady State as a Function of Reduced Time. F5 Wing and Equivalent Body of Revolution, Oscillation Amplitude=10 Degrees About c/2, U_{inf}=11, Omega=17.0834 rad/s, k=1.0.

3. PMARC Input Instructions

In the unsteady case like in the steady case, the most difficult part about the conception of the input file is the geometry modelling. Throughout this paper we reviewed most of the techniques for simple wings and bodies of revolution. With this background, we got virtually all that it needed to run an unsteady case in PMARC. Only a few fields have to be changed to reflect the oscillation parameters. Theses fields are concentrated in the first two major sections of the input file: the Basic Input Section, and the Assembly and Component Coordinate Section. Figures 5.6 and 5.7 show these sections extracted from the input file of the F5 wing and its equivalent body of revolution respectively. The fields modified to run the oscillations are boxed. The following paragraphs will review these fields. The rest of the input file won't be discussed as there is no difference with the input file of the steady cases we ran previously.

a. Basic Input Section

In this section, four fields are directly related to the oscillatory case. They are: NTSTPS, DTSTEP, THEMAX, and WRY. Except for THEMAX, definitions and calculation methods for these fields were given in subsection **1** above. THEMAX is simply the amplitude of the oscillatory rotation about the PMARC global Y axis, in degree. Two other fields are not inherent to the oscillation but may need adjustment to allow a successful run. They are: MAXIT and SOLRES. The first one is the limit on number of solver iterations. The second is the convergence criteria for the matrix solver. The recommended setting are 150 to 200 for MAXIT and 0.0005 for SOLRES.

b. Assembly and Component Coordinate System Information

In this section of the input file, only one field requires to be changed from the steady case: ASEMX. That indicates in PMARC the axis of rotation for the oscillation. As can be noticed on Figures 5.6 and 5.7, this value needs to be negative in order to have the rotation axis on the body. That is because the body is defined in assembly coordinates and by putting a negative value to ASEMX we are prescribing the origin of the assembly coordinates to begin somewhere behind the global coordinates origin, the latter being taken for the axis of rotation.

```
Oct 16 1995 13:20              osc1F5wing.in                    Page 1

F5 Wing: NACA-65A004.8  Sweep angle=32.6 def, AR=2.98, Ct/Cr=0.31

&BINP2    LSTINP=2,     LSTOUT=0,     LSTFRQ=0,     LENRUN=2,     LPLTYP=1,        &END
&BINP3    LSTGEO=0,     LSTNAB=0,     LSTWAK=0,     LSTCPV=0,                      &END
&BINP4    MAXIT=200,    SOLRES=0.0005,                                             &END
&BINP5    NTSTPS=74,    DTSTEP=0.1,                                                &END
&BINP6    RSYM=1.0,     RGPR=0.0,     RFF=5.0,   RCORES=0.0080,  RCOREW=0.0080,    &END
&BINP7    VINF=11.0,    VSOUND=1116.0,                                             &END
&BINP8    ALDEG= 0.00,  YAWDEG=0.0,   PHIDOT=0.0,   THEDOT=0.0,   PSIDOT=0.0,      &END
&BINP8A   PHIMAX= 0.0,  THEMAX= 10.0  PSIMAX=0.0,
          WRX=0.0,      WRY=1.7083,   WRZ=0.0,                                     &END
&BINP8B   DXMAX=0.0,    DYMAX=0.0,    DZMAX=0.0,
          WTX=0.0,      WTY=0.0,      WTZ=0.0,                                     &END
&BINP9    CBAR=0.4577,  SREF=0.5209,  SSPAN= 0.6226,
          RMPX=0.00,    RMPY=0.00,    RMPZ=0.00,                                   &END
&BINP10   NORSET=0,     NBCHGE=0,     NCZONE=0,
          NCZPCH=0,     CZDUB=0.0,    VREF=0.0,                                    &END
&BINP11   NORPCH=0,     NORF=0,       NORL=0,
          NOCF=0,       NOCL=0,       VNORM=0.0,                                   &END
&BINP12   KPAN=0,       KSIDE=0,      NEWNAB=0,     NEWSID=0,                      &END
&BINP13   NBLIT=0,                                                                 &END


&ASEM1    ASEMX=-0.3220,    ASEMY=0.00,       ASEMZ=0.00,
          ASCAL=1.00,       ATHET=0.00,       NODEA=5,                             &END
&ASEM2    APXX=0.00,        APYY=0.00,        APZZ=0.00,
          AHXX=0.00,        AHYY=1.00,        AHZZ=0.00,                           &END


&COMP1    COMPX= 0.0000,    COMPY= 0.0000,    COMPZ= 0.0000,
          CSCAL=  1.000,    CTHET=   0.0,     NODEC= 5,                            &END
&COMP2    CPXX= 0.0000,     CPYY= 0.0000,     CPZZ= 0.0000,
          CHXX= 0.0000,     CHYY=  1.000   ,  CHZZ= 0.0000,                        &END



&PATCH1   IREV=  0, IDPAT= 1, MAKE=   0, KCOMP= 1, KASS= 1, IPATSYM=1,
          IPATCOP=0,                                                               &END
           WING
&SECT1    STX=     0.0000, STY= 0.0000,     STZ= 0.0000,     SCALE= 0.6439,
          ALF=    0.0,   THETA=   0.0,
          INMODE=  4,   TNODS= 0,     TNPS=  15,     TINTS= 2,                    &END
1.00000   0.000   0.00001
0.99327   0.000   -0.00038
0.97340   0.000   -0.00165
0.95354   0.000   -0.00292
0.92870   0.000   -0.00451
0.90387   0.000   -0.00608
0.87407   0.000   -0.00795
0.84428   0.000   -0.00977
0.81448   0.000   -0.01154
0.78468   0.000   -0.01323
0.75488   0.000   -0.01483
0.72508   0.000   -0.01633
0.69529   0.000   -0.01772
0.66549   0.000   -0.01898
0.63569   0.000   -0.02011
0.60589   0.000   -0.02110
0.57609   0.000   -0.02195
0.54630   0.000   -0.02264
0.51650   0.000   -0.02318
0.48670   0.000   -0.02356
0.45690   0.000   -0.02379
0.42710   0.000   -0.02388
0.39731   0.000   -0.02384
0.36751   0.000   -0.02366
0.33771   0.000   -0.02337
0.30791   0.000   -0.02299
0.27811   0.000   -0.02252
0.24832   0.000   -0.02199
0.21852   0.000   -0.02141
0.18872   0.000   -0.02082
0.15892   0.000   -0.02021
0.12913   0.000   -0.01960
0.09933   0.000   -0.01897
0.07946   0.000   -0.01851
```

```
Oct 16 1995 13:20              osc1F5wing.in                    Page 2

0.05960   0.000   -0.01796
0.04470   0.000   -0.01742
0.03476   0.000   -0.01695
0.02483   0.000   -0.01631
0.01490   0.000   -0.01537
0.00497   0.000   -0.01360
0.00000   0.000   -0.00990
0.00497   0.000   -0.00568
0.01490   0.000   -0.00305
0.02483   0.000   -0.00088
0.03476   0.000    0.00104
0.04470   0.000    0.00279
0.05960   0.000    0.00517
0.07946   0.000    0.00796
0.09933   0.000    0.01039
0.12913   0.000    0.01349
0.15892   0.000    0.01603
0.18872   0.000    0.01810
0.21852   0.000    0.01977
0.24832   0.000    0.02111
0.27811   0.000    0.02214
0.30791   0.000    0.02292
0.33771   0.000    0.02348
0.36751   0.000    0.02384
0.39731   0.000    0.02401
0.42710   0.000    0.02402
0.45690   0.000    0.02387
0.48670   0.000    0.02358
0.51650   0.000    0.02315
0.54630   0.000    0.02258
0.57609   0.000    0.02187
0.60589   0.000    0.02103
0.63569   0.000    0.02006
0.66549   0.000    0.01895
0.69529   0.000    0.01771
0.72508   0.000    0.01635
0.75488   0.000    0.01487
0.78468   0.000    0.01327
0.81448   0.000    0.01158
0.84428   0.000    0.00980
0.87407   0.000    0.00795
0.90387   0.000    0.00605
0.92870   0.000    0.00446
0.95354   0.000    0.00288
0.97340   0.000    0.00164
0.99327   0.000    0.00043
1.00000   0.000    0.00001
&BPNODE   TNODE=3     TNPC=30     TINTC=3     &END
&SECT1    STX= 0.3982, STY= 0.6226,     STZ= 0.0000,     SCALE= 0.1983 ,
          ALF=   0.0,   THETA=   0.0,
          INMODE=  0,   TNODS= 3,     TNPS= 15,     TINTS= 2,                    &END
&BPNODE   TNODE=3     TNPC=30     TINTC=3     &END


&PATCH1   IREV=  0, IDPAT= 1, MAKE=   1, KCOMP= 1, KASS= 1, IPATSYM=1,
          IPATCOP=0,                                                               &END
           WING TIP
&PATCH2   ITYP=  2,     TNODS= 5,     TNPS=   1,    TINTS= 3,                     &END


&WAKE1    IDWAK=1,          IFLXW=1,          ITRFTZ= 0,        INTRW= 0,          &END
 WING_WAKE
&WAKE2    KWPACH=2,         KWSIDE=4,         KWLINE=0,         KWPAN1=0,
          KWPAN2=0,         NODEW=0,          INITIAL=0,                           &END
&WAKE2    KWPACH=1,         KWSIDE=2,         KWLINE=0,         KWPAN1=0,
          KWPAN2=0,         NODEW=5,          INITIAL=0,                           &END


&ONSTRM   NONSL =0,  KPSL =                                                        &END


&BLPARAM  RN =37210000,     VISC = 0.000157,  NSLBL = 1,                           &END


&VS1      NVOLR= 0,         NVOLC= 0,                                              &END
&VS2      XO=     -0.1000, YO=      1.5000, ZO=     -0.1000, INTVSR= 1,            &END
```

Figure 5.6 Top Portion of a PMARC Input File for The Oscillation Case of The F5 Wing.

Figure 5.7 Top Portion of a PMARC Input File for The Oscillation Case of The F5 Wing Equivalent Body of Revolution.

c. Customizing The Source Code If Failure to Run

Two other parameters require attention. However, they are not found in the input file. They are in the parameter file of the source code (PARAM.DAT). One is the number of surface panels allowed (NSPDIM) and the other one is the number of wake panels allowed (NWPDIM). NSPDIM should at least be set to the number of panels covering the surface studied. NWPDIM was boosted up form 1900 to 5000 in order to get a successful run. Although it has not yet been confirmed or scientifically explained, it appears like this latter parameter should be set at a value at least equal to the product of the total number of spanwise panels and the number of time-steps. When the parameter file is modified, the source code has to be recompiled.

4. PMARC Output - Data Retrieval

In the oscillatory case, large files of output data are created; sometimes up to 6 Megabytes. Unless the number of time-steps is very small, the data retrieval should not be done manually as it would become very time consuming. The output file for the oscillation case follows the same format as for the steady case. At time-step zero and at the very last time-step, the x, y, z coordinates, the Cp, Vx, Vy, Vz, V, DUB, DPHI/DT and MACH number are provided for the control points of all panels. For the intermediate time-steps, the control point coordinates from the leading edge are given with the section chord, CL, CD, CY, Cm, Cn, and Cl. Figure 5.8 shows selected portions of a thirty page output file.

Not shown on Figure 5.8 are the total coefficients for each time-steps. These are the values we needed in our study. More specifically CL and CM. In order to efficiently extract them, small programs written in the UNIX operating system AWK language were written. The data retrieval becomes relatively simple as the output file repeats the total coefficient block under the same format after each time-step. Thus, these programs look for a prescribed recurring feature, and from it counts an indicated number of lines and then take the desired value in the prescribed field of that line. In our case, the program was searching for the words WIND AXES from which it counted 32 lines and then stored the first field for the CL value or the fourth for the CM value. This process was repeated at each time-step. These geometry specific programs can be found in Appendix **H**.

Nov 1 1995 11:52 maxplat Page 1

TIME STEP 0
AERODYNAMIC DATA FOR PATCH 1 WING

COLUMN 1 VINF = 11.0000

PANEL	Z	X	Y	DPHI/DT	CP	VX	VY	V
			DUB		MACH			
1		0.299	0.033	-0.001	0.0458	10.6494	-0.0271	0.674
1	10.6708	-0.0802		-0.0133	0.0096			
2		0.257	0.033	-0.004	0.0071	10.8597	-0.0160	0.683
5	10.8812	-0.0888		-0.0147	0.0098			
3		0.216	0.033	-0.006	-0.0264	11.0468	-0.0185	0.656
7	11.0664	-0.0887		-0.0147	0.0099			
4		0.174	0.033	-0.009	-0.0513	11.1926	-0.0303	0.595
9	11.2085	-0.0822		-0.0136	0.0100			
5		0.133	0.033	-0.011	-0.0699	11.3071	-0.0479	0.509
2	11.3187	-0.0706		-0.0117	0.0101			
6		0.092	0.033	-0.012	-0.0821	11.3907	-0.0680	0.399
5	11.3979	-0.0552		-0.0091	0.0102			
7		0.050	0.033	-0.014	-0.0878	11.4404	-0.0868	0.274
6	11.4440	-0.0374		-0.0062	0.0103			
8		0.009	0.033	-0.014	-0.0868	11.4541	-0.1005	0.140
6	11.4554	-0.0185		-0.0031	0.0103			
9		-0.033	0.033	-0.015	-0.0801	11.4356	-0.1069	0.016
8	11.4361	0.0001		0.0000	0.0102			
10		-0.074	0.033	-0.015	-0.0689	11.3914	-0.1044	-0.094
5	11.3921	0.0173		0.0029	0.0102			
11		-0.116	0.033	-0.014	-0.0560	11.3348	-0.0963	-0.173
2	11.3366	0.0322		0.0053	0.0102			
12		-0.157	0.033	-0.013	-0.0454	11.2881	-0.0913	-0.219
3	11.2906	0.0449		0.0074	0.0101			
13		-0.199	0.033	-0.013	-0.0448	11.2945	-0.1136	-0.233
3	11.2975	0.0561		0.0093	0.0101			
14		-0.240	0.033	-0.012	-0.0683	11.4286	-0.2133	-0.268
5	11.4338	0.0693		0.0115	0.0102			
15		-0.281	0.033	-0.008	-0.1589	11.7936	-0.4671	-1.674
2	11.9210	0.0914		0.0151	0.0107			
16		-0.281	0.033	-0.001	0.1902	9.7821	0.7580	2.180
2	10.0508	0.1511		0.0250	0.0090			
17		-0.240	0.033	0.006	-0.0148	11.1350	-0.0231	1.257
5	11.2103	0.1456		0.0241	0.0100			
18		-0.199	0.033	0.010	-0.0690	11.4480	-0.1596	0.859
0	11.4813	0.1267		0.0209	0.0103			

TIME STEP 1

SECTION PARAMETERS

XLE	YLE	ZLE	CHORD	CIRC	YLE/SSPAN
-0.301	0.033	-0.006	0.621	0.273	0.052

	CL	CD	CY	C_m	C_n	C_l
WING	0.1095	0.0016	0.0028	0.0072	-0.0007	0.0057
BODY	0.1095	-0.0017	0.0028	0.0072	-0.0005	0.0057

SECTION PARAMETERS

XLE	YLE	ZLE	CHORD	CIRC	YLE/SSPAN
-0.260	0.097	-0.005	0.574	0.269	0.156

	CL	CD	CY	C_m	C_n	C_l
WING	0.1155	0.0009	0.0033	0.0049	-0.0008	0.0180
BODY	0.1155	-0.0025	0.0033	0.0049	-0.0002	0.0180

SECTION PARAMETERS

XLE	YLE	ZLE	CHORD	CIRC	YLE/SSPAN
-0.219	0.161	-0.005	0.529	0.264	0.258

	CL	CD	CY	C_m	C_n	C_l
WING	0.1210	0.0005	0.0037	0.0015	-0.0007	0.0312
BODY	0.1210	-0.0030	0.0037	0.0015	0.0002	0.0312

Nov 1 1995 11:52 maxplat Page 2

SECTION PARAMETERS

XLE	YLE	ZLE	CHORD	CIRC	YLE/SSPAN
-0.179	0.223	-0.004	0.484	0.255	0.358

TIME STEP 74
AERODYNAMIC DATA FOR PATCH 1 WING

COLUMN 1 VINF = 11.0000

PANEL	Z	X	Y	DPHI/DT	CP	VX	VY	V
		V	DUB		MACH			
1		0.299	0.033	-0.001	0.0897	10.6085	-0.0266	0.671
6	10.6298	-0.0303		0.0232	0.0095			
2		0.257	0.033	0.004	0.0501	10.8299	-0.0128	0.681
6	10.8513	-0.0404		0.0288	0.0097			
3		0.216	0.033	0.006	0.0152	11.0231	-0.0139	0.655
3	11.0426	-0.0420		0.0244	0.0099			
4		0.174	0.033	0.009	-0.0113	11.1683	-0.0245	0.594
7	11.1842	-0.0367		0.0289	-0.0100			
5		0.133	0.033	0.011	-0.0318	11.2793	-0.0406	0.508
0	11.2908	-0.0265		0.0311	-0.0101			
6		0.092	0.033	0.012	-0.0463	11.3572	-0.0588	0.398
4	11.3644	-0.0126		0.0203	-0.0102			
7		0.050	0.033	0.014	-0.0545	11.3998	-0.0751	0.273
8	11.4033	0.0036		0.0194	-0.0102			
8		0.009	0.033	0.014	-0.0561	11.4052	-0.0856	0.140
2	11.4064	0.0206		0.0184	-0.0102			
9		-0.033	0.033	0.015	-0.0519	11.3775	-0.0879	0.016
9	11.3778	0.0369		0.0172	-0.0102			
10		-0.074	0.033	0.015	-0.0431	11.3228	-0.0803	-0.093
4	11.3235	0.0516		0.0159	-0.0101			
11		-0.116	0.033	0.014	-0.0319	11.2541	-0.0657	-0.171
3	11.2556	0.0636		0.0144	-0.0101			
12		-0.157	0.033	0.013	-0.0224	11.1928	-0.0519	-0.216
5	11.1950	0.0728		0.0127	-0.0100			
13		-0.199	0.033	0.013	-0.0221	11.1798	-0.0614	-0.229
6	11.1823	0.0798		0.0108	-0.0100			
14		-0.240	0.033	0.012	-0.0440	11.2832	-0.1394	-0.263
2	11.2871	0.0880		0.0084	-0.0101			
15		-0.281	0.033	0.008	-0.0920	11.4112	-0.2402	-1.599
8	11.5253	0.1015		0.0055	-0.0103			
16		-0.281	0.033	0.001	0.0950	10.1641	0.5304	2.302
2	10.4351	0.1397		-0.0050	-0.0101			
17		-0.240	0.033	-0.006	0.0954	11.2887	-0.1017	1.321
2	11.3662	0.1277		-0.0079	-0.0102			

Figure 5.8 Selected Portion of a PMARC Unsteady Case Output File Showing The Data Produced at The Initial, First and Last Time-Step.

C. TRIANGULAR WING AND EQUIVALENT BODY OF REVOLUTION

The triangular wing was shown and described in section **G** of Chapter **III**, and its equivalent body of revolution in section **C** of Chapter **IV.** For these cases, the main chord and longitudinal axis respectively were made unity. Like for the steady case, two thickness ratios will be treated in oscillation: 0.098, and 0.196. The wing and its equivalent body of revolution are reproduced below in Figure 5.9. Then the oscillation parameter calculations, the oscillation results, and the PMARC specifics are presented.

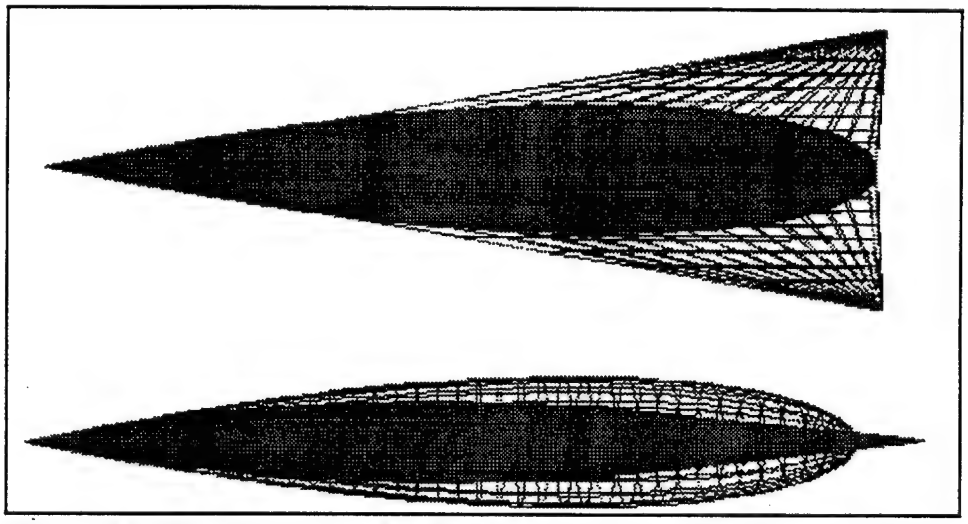

Figure 5.9 PMARC Top and Side Representation of The Triangular Wing and Its Corresponding Equivalent Area Body of Revolution. Maximum Thickness Ratio = 0.098. (Each View Not at Same Scale).

1. Oscillatory Frequency and Time-Stepping Calculations

The same three reduced frequencies (k) as for the F5 were selected for these oscillation runs: 0.1, 0.5, and 1.0. The movement had the same plus and minus five degrees amplitude about the mid-chord, and two full oscillatory cycles were operated. Again, here is a sample parameters calculation for k=0.1 and the results for the other cases. All parameters shown below apply for both the wing

and the equivalent body of revolution. c is the root chord (or longitudinal axis), *omega* is the oscillatory frequency in rad/sec (WRY in PMARC), T is the period, N the number of time-steps and dt the size of the time-steps in seconds. The PMARC notations for the last two parameters are NTSTPS and DTSTEP respectively. The freestream velocity was arbitrarily selected at 11 unit per second.

$$k=0.1 rad=\frac{\omega c}{U_\infty}=\frac{\omega * 1.0}{11} \quad \Rightarrow \quad \omega=WRY=1.1 \ rad/s \tag{5.4}$$

$$T=\frac{2\pi}{\omega}=\frac{2\pi}{1.1}=5.71 \ \text{sec/}cycle \tag{5.5}$$

$$T=N*dt=NTSTPS*DTSTEP \quad \Rightarrow \quad 5.71=NTSTPS*0.2 \quad \Rightarrow \quad NTSTPS=28.55 \ steps/cycle \tag{5.6}$$

NTSTPS=57.1 time-steps for two cycles

As mentioned in the previous section, the number of time-steps (NTSTPS) times the size of each time-step (DTSTEP) must equal the period (T). The combination selected is the one which will render a smooth distribution in the PMARC output. The following table now provides the value of the parameters shown above for all values of reduced frequency studied. Note that all the parameters not only apply for both the wing and the equivalent body of revolution, but also for the two thickness distributions considered.

k	Amplitude	Osc. About...	Omega (WRY)	NTSTPS	DTSTEP
0.1	+- 5 Degrees	Mid-Chord	1.1 rad/s	58	0.2 sec
0.5	+- 5 Degrees	Mid-Chord	5.5 rad/s	23	0.1 sec
1.0	+- 5 Degrees	Mid-Chord	11.0 rad/s	23	0.05 sec

Table 5.2 Test Parameters for The Oscillation of The Triang. Wing Equivalent Body of Revolution.

2. Results

Figures 5.10 to 5.12 below show the combined CL and CM results of the wing and the equivalent body of revolution of thickness ratio 0.098 in oscillation at the three reduced frequencies listed in Table 5.2. Figures 5.13 to 5.15 do the same thing for a thickness ratio of 0.196. The analysis of the relative maximums and minimums of the CL and CM curves as a function of the reduced frequency, as well as the general behavior will be left to future work. It will only be said that the lift coefficients for the body of revolution seem to behave as expected only for the low reduced frequency, contrary to the F5 where their behavior seemed legitimate for all reduced frequencies. As illustrated in section **B-2** of this chapter, the lift vectors in front of the pivot point are theoretically balanced by those behind it (Figure 5.2). This should cause the net value of the lift to be close to zero at any angle of attack. Some lift is expected due to the oscillation effects. Also, as observed in our results, the moments should increasingly become larger with angle of attack. As detailed in the previous section, all the figures are plotted against the reduced time which is the ratio of the product of freestream velocity and time over the main chord.

3. PMARC Input Instructions

Except for the values of the parameters, there is no difference between the input files for the oscillations of the triangular wing and its equivalent body of revolution and those of the F5 wing and its equivalent body of revolution studied in the previous section. One input file for the triangular wing and one for its equivalent body of revolution for the reduced frequency of 0.1 are presented below. The reader should consult section **B-3** of this chapter for details.

4. PMARC Output- Data Retrieval

As no difference exists with the data retrieval techniques used in the previous section, the reader should refer to the latter for details on the program required to extract the data off DATA6.

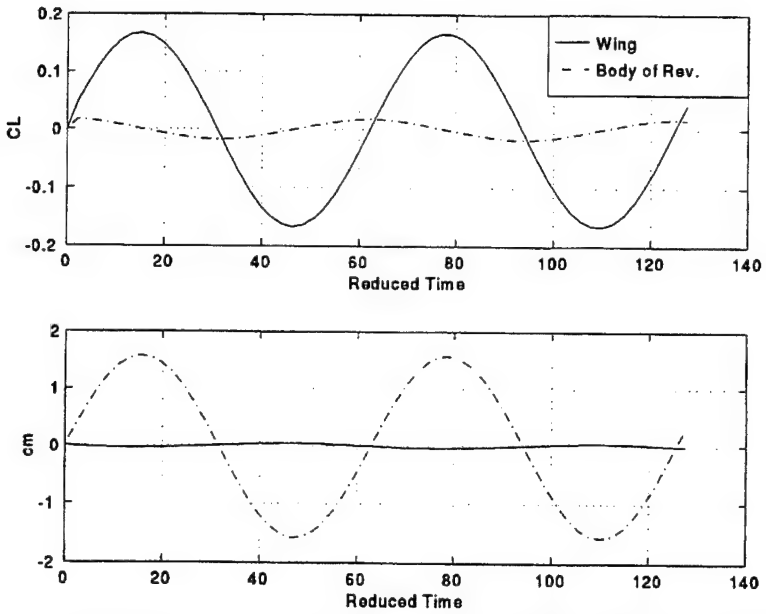

Figure 5.10 Comparison of The Lift and Moment Coefficients in Unsteady State as a Function of Reduced Time. Triangular Wing of AR=2/3 and Equivalent Body of Revolution of Delta=0.098, Oscillation Amplitude=10 Degrees About c/2, U_{inf}=11, Omega=1.1 rad/s, k=0.1.

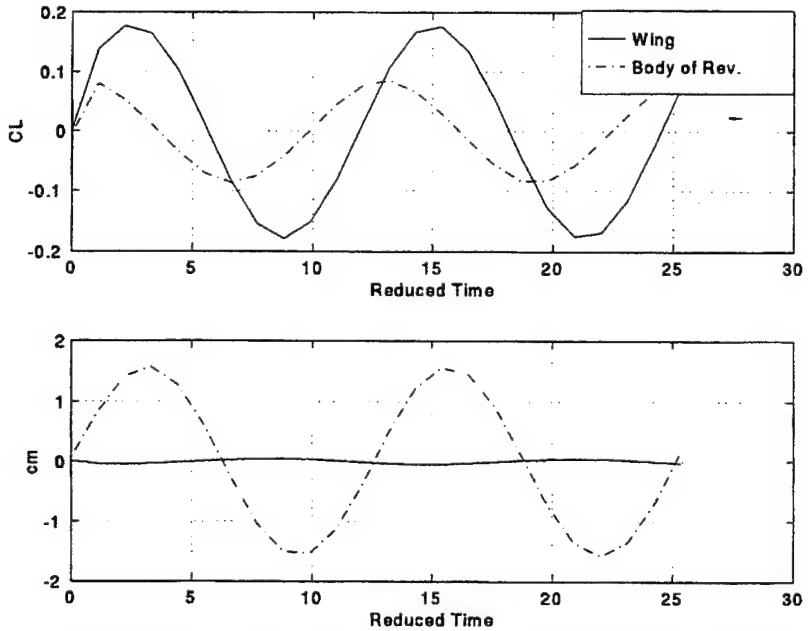

Figure 5.11 Comparison of The Lift and Moment Coefficients in Unsteady State as a Function of Reduced Time. Triangular Wing of AR=2/3 and Equivalent Body of Revolution of Delta=0.098, Oscillation Amplitude=10 Degrees About c/2, U_{inf}=11, Omega=5.5 rad/s, k=0.5.

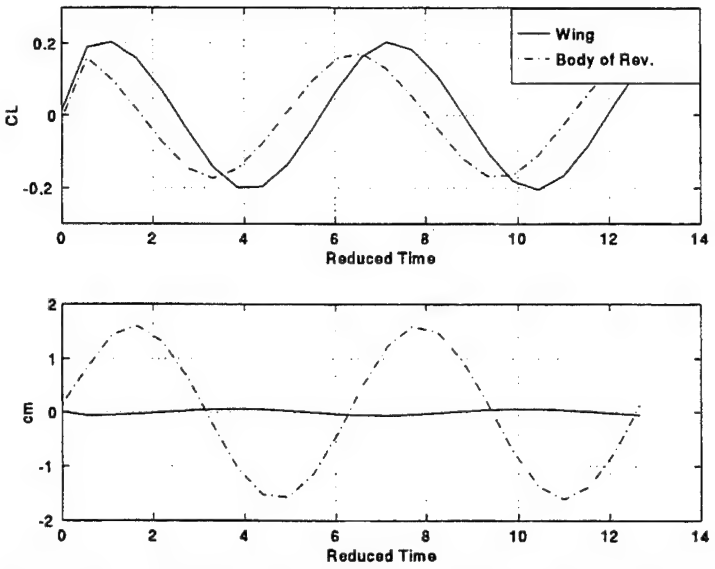

Figure 5.12 Comparison of The Lift and Moment Coefficients in Unsteady State as a Function of Reduced Time. Triangular Wing of AR=2/3 and Equivalent Body of Revolution of Delta=0.098, Oscillation Amplitude=10 Degrees About c/2, U_{inf}=11, Omega=11.0 rad/s, k=1.0.

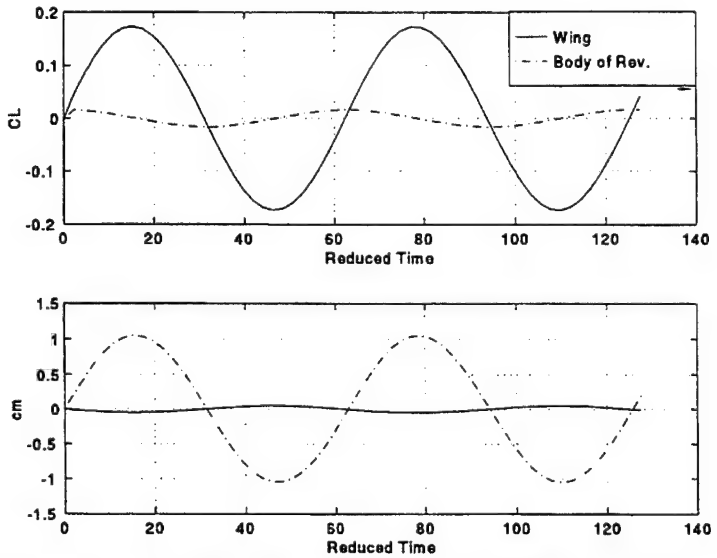

Figure 5.13 Comparison of The Lift and Moment Coefficients in Unsteady State as a Function of Reduced Time. Triangular Wing of AR=2/3 and Equivalent Body of Revolution of Delta=0.196, Oscillation Amplitude=10 Degrees About c/2, U_{inf}=11, Omega=1.1 rad/s, k=0.1.

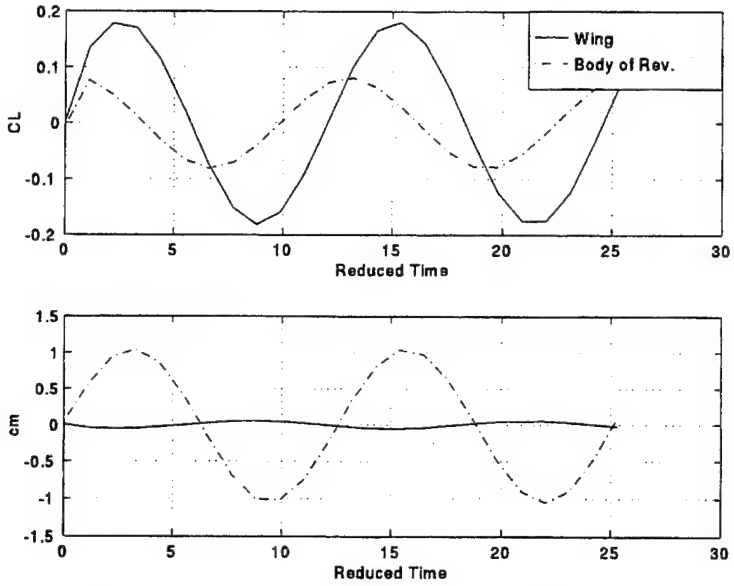

Figure 5.14 Comparison of The Lift and Moment Coefficients in Unsteady State as a Function of Reduced Time. Triangular Wing of AR=2/3 and Equivalent Body of Revolution of Delta=0.196, Oscillation Amplitude=10 Degrees About c/2, U_{inf}=11, Omega=5.5 rad/s, k=0.5.

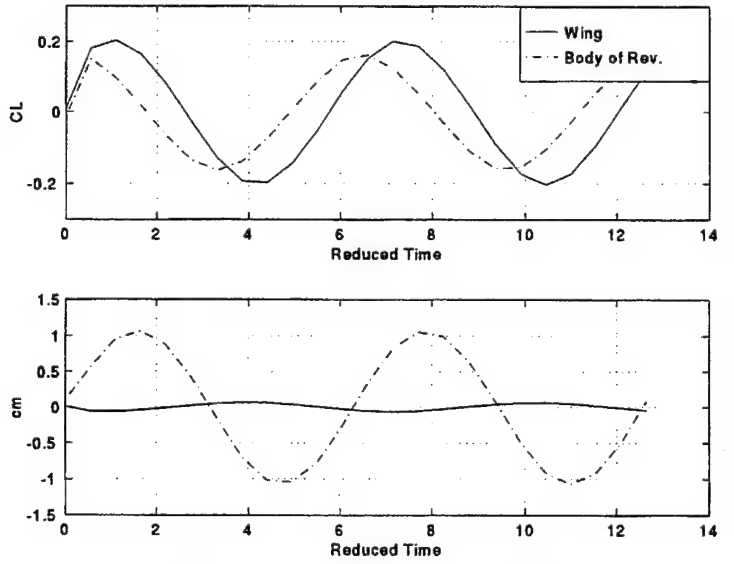

Figure 5.15 Comparison of The Lift and Moment Coefficients in Unsteady State as a Function of Reduced Time. Triangular Wing of AR=2/3 and Equivalent Body of Revolution of Delta=0.196, Oscillation Amplitude=10 Degrees About c/2, U_{inf}=11, Omega=11.0 rad/s, k=1.0.

Figure 5.16 PMARC Input File for The Triangular Wing in Oscillation About The Mid-Chord for k=0.1.

Oct 18 1995 20:34 osc1triBofR_098.in Page 1

```
 2/3 AR, Delta=0.098, Bicvex Triang Wing -EQUIV BODY OF REVOL'N- (No Tip)
 &BINP2    LSTINP=2,     LSTOUT=0,     LSTFRQ=0,     LENRUN=0,     LPLTYP=1,     &END
 &BINP3    LSTGEO=0,     LSTNAB=0,     LSTWAK=0,     LSTCPV=0,                   &END
 &BINP4    MAXIT=200,    SOLRES=0.0005,                                          &END
 &BINP5    NTSTPS=58,    DTSTEP=0.2,                                             &END
 &BINP6    RSYM=1.0,     RGPR=0.0,     RFF=5.0,  RCORZS=0.0080, RCOREW=0.0080,   &END
 &BINP7    VINF=11.0,    VSOUND=1116.0,                                          &END
 &BINP8    ALDEG= 0.00,  YAWDEG=0.0,   PHIDOT=0.0,  THEDOT=0.0,  PSIDOT=0.0,    &END
 &BINP8A   PHIMAX= 0.0,  THEMAX= 10.0, PSIMAX=0.0,
           WRX=0.0,      WRY=1.1,      WRZ=0.0,                                  &END
 &BINP8B   DXMAX=0.0,    DYMAX=0.0,    DZMAX=0.0,
           WTX=0.0,      WTY=0.0,      WTZ=0.0,                                  &END
 &BINP9    CBAR=0.111,   SREF=0.0097,  SSPAN= 0.0555,
           RMPX=0.00,    RMPY=0.00,    RMPZ=0.00,                                &END
 &BINP10   NORSET=0,     NBCHGE=0,     NCZONE=0,
           NC2PCH=0,     C2DUB=0.0,    VREF=0.0,                                 &END
 &BINP11   NORPCH=0,     NORF=0,       NORL=0,
           NOCP=0,       NOCI=0,       VNORM=0.0,                                &END
 &BINP12   KPAN=0,       KSIDE=0,      NEWNAB=0,     NEWSID=0,                   &END
 &BINP13   NBLIT=0,                                                              &END

 &ASEM1    ASEMX=-0.5,   ASEMY=0.00,   ASEMZ=0.00,
           ASCAL=1.00,   ATHET=0.00,   NODEA=5,                                  &END
 &ASEM2    APXX=0.00,    APYY=0.00,    APZZ=0.00,
           AHXX=0.00,    AHYY=1.00,    AHZZ=0.00,                                &END

 &COMP1    COMPX= 0.0000,  COMPY= 0.0000,  COMPZ= 0.0000,
           CSCAL= 1.000,   CTHET= 0.0,     NODEA=5,                              &END
 &COMP2    CPXX= 0.0000,   CPYY= 0.0000,   CPZZ= 0.0000,
           CHXX= 0.0000,   CHYY= 1.000,    CHZZ= 0.0000,                         &END

 &PATCH1   IREV=  0, IDPAT= 2, MAXE=   0, KCONP= 1, KASS= 1, IPATSYM=1,
           IPATCOP=0,                                                          &END
           EQUIVALENT BODY
 &SECT1    STX=  0.0000, STY= 0.0000,  STZ= 0.0000,  SCALE=  0.0000,
           ALF=   0.0,   THETA=  0.0,
           INNODE=  1,   TNODS= 0,   TNPS=  0,   TINTS= 0,                     &END
    0.0000   -1.0000   0.0000
    0.1735   -0.9845   0.0000
    0.3420   -0.9395   0.0000
    0.5000   -0.8660   0.0000
    0.6425   -0.7660   0.0000
    0.7660   -0.6425   0.0000
    0.8660   -0.5000   0.0000
    0.9395   -0.3420   0.0000
    0.9845   -0.1735   0.0000
    1.0000    0.0000   0.0000
    0.9845    0.1735   0.0000
    0.9395    0.3420   0.0000
    0.8660    0.5000   0.0000
    0.7660    0.6425   0.0000
    0.6425    0.7660   0.0000
    0.5000    0.8660   0.0000
    0.3420    0.9395   0.0000
    0.1735    0.9845   0.0000
    0.0000    1.0000   0.0000
 &BPNODE   TNODE=3   TNPC=10   TINTC=3   &END
 &SECT1    STX= 0.0250, STY= 0.0000,  STZ= 0.0000,   SCALE= 0.0036,
           ALF=   0.0,   THETA=  0.0,
           INNODE=  0,   TNODS= 0,   TNPS=  0,   TINTS= 0,                     &END
 &SECT1    STX= 0.0500, STY= 0.0000,  STZ= 0.0000,   SCALE= 0.0070,
           ALF=   0.0,   THETA=  0.0,
           INNODE=  0,   TNODS= 0,   TNPS=  0,   TINTS= 0,                     &END
 &SECT1    STX= 0.0750, STY= 0.0000,  STZ= 0.0000,   SCALE= 0.0104,
           ALF=   0.0,   THETA=  0.0,
           INNODE=  0,   TNODS= 0,   TNPS=  0,   TINTS= 0,                     &END
 &SECT1    STX= 0.1000, STY= 0.0000,  STZ= 0.0000,   SCALE= 0.0137,
           ALF=   0.0,   THETA=  0.0,
           INNODE=  0,   TNODS= 0,   TNPS=  0,   TINTS= 0,                     &END
 &SECT1    STX= 0.1250, STY= 0.0000,  STZ= 0.0000,   SCALE= 0.0169,
           ALF=   0.0,   THETA=  0.0,
```


Oct 18 1995 20:34 osc1triBofR_098.in Page 2

```
 &SECT1    INNODE=  0,   TNODS= 0,   TNPS= 0,   TINTS= 0,
           STX= 0.1500, STY= 0.0000,  STZ= 0.0000,   SCALE= 0.0199,
           ALF=   0.0,   THETA=  0.0,
           INNODE=  0,   TNODS= 0,   TNPS= 0,   TINTS= 0,                      &END
 &SECT1    STX= 0.1750, STY= 0.0000,  STZ= 0.0000,   SCALE= 0.0229,
           ALF=   0.0,   THETA=  0.0,
           INNODE=  0,   TNODS= 0,   TNPS= 0,   TINTS= 0,                      &END
 &SECT1    STX= 0.2000, STY= 0.0000,  STZ= 0.0000,   SCALE= 0.0258,
           ALF=   0.0,   THETA=  0.0,
           INNODE=  0,   TNODS= 0,   TNPS= 0,   TINTS= 0,                      &END
 &SECT1    STX= 0.2250, STY= 0.0000,  STZ= 0.0000,   SCALE= 0.0286,
           ALF=   0.0,   THETA=  0.0,
           INNODE=  0,   TNODS= 0,   TNPS= 0,   TINTS= 0,                      &END
 &SECT1    STX= 0.2500, STY= 0.0000,  STZ= 0.0000,   SCALE= 0.0312,
           ALF=   0.0,   THETA=  0.0,
           INNODE=  0,   TNODS= 0,   TNPS= 0,   TINTS= 0,                      &END
 &SECT1    STX= 0.2750, STY= 0.0000,  STZ= 0.0000,   SCALE= 0.0338,
           ALF=   0.0,   THETA=  0.0,
           INNODE=  0,   TNODS= 0,   TNPS= 0,   TINTS= 0,                      &END
 &SECT1    STX= 0.3000, STY= 0.0000,  STZ= 0.0000,   SCALE= 0.0362,
           ALF=   0.0,   THETA=  0.0,
           INNODE=  0,   TNODS= 0,   TNPS= 0,   TINTS= 0,                      &END
 &SECT1    STX= 0.3250, STY= 0.0000,  STZ= 0.0000,   SCALE= 0.0385,
           ALF=   0.0,   THETA=  0.0,
           INNODE=  0,   TNODS= 0,   TNPS= 0,   TINTS= 0,                      &END
 &SECT1    STX= 0.4000, STY= 0.0000,  STZ= 0.0000,   SCALE= 0.0447,
           ALF=   0.0,   THETA=  0.0,
           INNODE=  0,   TNODS= 0,   TNPS= 0,   TINTS= 0,                      &END
 &SECT1    STX= 0.4250, STY= 0.0000,  STZ= 0.0000,   SCALE= 0.0465,
           ALF=   0.0,   THETA=  0.0,
           INNODE=  0,   TNODS= 0,   TNPS= 0,   TINTS= 0,                      &END
 &SECT1    STX= 0.4500, STY= 0.0000,  STZ= 0.0000,   SCALE= 0.0481,
           ALF=   0.0,   THETA=  0.0,
           INNODE=  0,   TNODS= 0,   TNPS= 0,   TINTS= 0,                      &END
 &SECT1    STX= 0.4750, STY= 0.0000,  STZ= 0.0000,   SCALE= 0.0496,
           ALF=   0.0,   THETA=  0.0,
           INNODE=  0,   TNODS= 0,   TNPS= 0,   TINTS= 0,                      &END
 &SECT1    STX= 0.5000, STY= 0.0000,  STZ= 0.0000,   SCALE= 0.0510,
           ALF=   0.0,   THETA=  0.0,
           INNODE=  0,   TNODS= 0,   TNPS= 0,   TINTS= 0,                      &END
 &SECT1    STX= 0.5250, STY= 0.0000,  STZ= 0.0000,   SCALE= 0.0522,
           ALF=   0.0,   THETA=  0.0,
           INNODE=  0,   TNODS= 0,   TNPS= 0,   TINTS= 0,                      &END
 &SECT1    STX= 0.5500, STY= 0.0000,  STZ= 0.0000,   SCALE= 0.0532,
           ALF=   0.0,   THETA=  0.0,
           INNODE=  0,   TNODS= 0,   TNPS= 0,   TINTS= 0,                      &END
 &SECT1    STX= 0.5750, STY= 0.0000,  STZ= 0.0000,   SCALE= 0.0541,
           ALF=   0.0,   THETA=  0.0,
           INNODE=  0,   TNODS= 0,   TNPS= 0,   TINTS= 0,                      &END
 &SECT1    STX= 0.6000, STY= 0.0000,  STZ= 0.0000,   SCALE= 0.0547,
           ALF=   0.0,   THETA=  0.0,
           INNODE=  0,   TNODS= 0,   TNPS= 0,   TINTS= 0,                      &END
 &SECT1    STX= 0.6250, STY= 0.0000,  STZ= 0.0000,   SCALE= 0.0552,
           ALF=   0.0,   THETA=  0.0,
           INNODE=  0,   TNODS= 0,   TNPS= 0,   TINTS= 0,                      &END
 &SECT1    STX= 0.6500, STY= 0.0000,  STZ= 0.0000,   SCALE= 0.0555,
           ALF=   0.0,   THETA=  0.0,
           INNODE=  0,   TNODS= 0,   TNPS= 0,   TINTS= 0,                      &END
 &SECT1    STX= 0.6750, STY= 0.0000,  STZ= 0.0000,   SCALE= 0.0555,
           ALF=   0.0,   THETA=  0.0,
           INNODE=  0,   TNODS= 0,   TNPS= 0,   TINTS= 0,                      &END
 &SECT1    STX= 0.7000, STY= 0.0000,  STZ= 0.0000,   SCALE= 0.0553,
           ALF=   0.0,   THETA=  0.0,
           INNODE=  0,   TNODS= 0,   TNPS= 0,   TINTS= 0,                      &END
 &SECT1    STX= 0.7250, STY= 0.0000,  STZ= 0.0000,   SCALE= 0.0548,
           ALF=   0.0,   THETA=  0.0,
           INNODE=  0,   TNODS= 0,   TNPS= 0,   TINTS= 0,                      &END
 &SECT1    STX= 0.7500, STY= 0.0000,  STZ= 0.0000,   SCALE= 0.0541,
           ALF=   0.0,   THETA=  0.0,
           INNODE=  0,   TNODS= 0,   TNPS= 0,   TINTS= 0,                      &END
```

Figure 5.17 PMARC Input File for The Triangular Wing Equivalent Body of Revolution in Oscillation About The Mid-Chord for k=0.1.

```
 &SECT1   STX= 0.7750, STY= 0.0000,    STZ= 0.0000,    SCALE= 0.0530,
          ALF=   0.0,  THETA=   0.0,
          INMODE=  0,  TNODS= 0,    TNPS= 0,    TINTS= 0,               &END
 &SECT1   STX= 0.8000, STY= 0.0000,    STZ= 0.0000,    SCALE= 0.0516,
          ALF=   0.0,  THETA=   0.0,
          INMODE=  0,  TNODS= 0,    TNPS= 0,    TINTS= 0,               &END
 &SECT1   STX= 0.8250, STY= 0.0000,    STZ= 0.0000,    SCALE= 0.0498,
          ALF=   0.0,  THETA=   0.0,
          INMODE=  0,  TNODS= 0,    TNPS= 0,    TINTS= 0,               &END
 &SECT1   STX= 0.8500, STY= 0.0000,    STZ= 0.0000,    SCALE= 0.0475,
          ALF=   0.0,  THETA=   0.0,
          INMODE=  0,  TNODS= 0,    TNPS= 0,    TINTS= 0,               &END
 &SECT1   STX= 0.8750, STY= 0.0000,    STZ= 0.0000,    SCALE= 0.0446,
          ALF=   0.0,  THETA=   0.0,
          INMODE=  0,  TNODS= 0,    TNPS= 0,    TINTS= 0,               &END
 &SECT1   STX= 0.9000, STY= 0.0000,    STZ= 0.0000,    SCALE= 0.0410,
          ALF=   0.0,  THETA=   0.0,
          INMODE=  0,  TNODS= 0,    TNPS= 0,    TINTS= 0,               &END
 &SECT1   STX= 0.9250, STY= 0.0000,    STZ= 0.0000,    SCALE= 0.0365,
          ALF=   0.0,  THETA=   0.0,
          INMODE=  0,  TNODS= 0,    TNPS= 0,    TINTS= 0,               &END
 &SECT1   STX= 0.9500, STY= 0.0000,    STZ= 0.0000,    SCALE= 0.0306,
          ALF=   0.0,  THETA=   0.0,
          INMODE=  0,  TNODS= 0,    TNPS= 0,    TINTS= 0,               &END
 &SECT1   STX= 0.9625, STY= 0.0000,    STZ= 0.0000,    SCALE= 0.0269,
          ALF=   0.0,  THETA=   0.0,
          INMODE=  0,  TNODS= 0,    TNPS= 0,    TINTS= 0,               &END
 &SECT1   STX= 0.9750, STY= 0.0000,    STZ= 0.0000,    SCALE= 0.0222,
          ALF=   0.0,  THETA=   0.0,
          INMODE=  0,  TNODS= 0,    TNPS= 0,    TINTS= 0,               &END
 &SECT1   STX= 0.9813, STY= 0.0000,    STZ= 0.0000,    SCALE= 0.0194,
          ALF=   0.0,  THETA=   0.0,
          INMODE=  0,  TNODS= 0,    TNPS= 0,    TINTS= 0,               &END
 &SECT1   STX= 0.9876, STY= 0.0000,    STZ= 0.0000,    SCALE= 0.0159,
          ALF=   0.0,  THETA=   0.0,
          INMODE=  0,  TNODS= 0,    TNPS= 0,    TINTS= 0,               &END
 &SECT1   STX= 0.9938, STY= 0.0000,    STZ= 0.0000,    SCALE= 0.0113,
          ALF=   0.0,  THETA=   0.0,
          INMODE=  0,  TNODS= 0,    TNPS= 0,    TINTS= 0,               &END
 &SECT1   STX= 0.9969, STY= 0.0000,    STZ= 0.0000,    SCALE= 0.0080,
          ALF=   0.0,  THETA=   0.0,
          INMODE=  0,  TNODS= 0,    TNPS= 0,    TINTS= 0,               &END
 &SECT1   STX= 1.0000, STY= 0.0000,    STZ= 0.0000,    SCALE= 0.0000,
          ALF=   0.0,  THETA=   0.0,
          INMODE=  0,  TNODS= 5,    TNPS= 22,    TINTS= 2,              &END
 &BPNODE   TNODE=3,    TNPC=0,   TINTC=0,    &END

 &WAKE1   IDWAK=0,        IFLXW=1,        ITRFTZ= 0,      INTRW= 0,  —     &END
  WING_WAKE
 &WAKE2   KWPACH=2,       KWSIDE=4,       KWLINE=0,       KWPAN1=0,
          KWPAN2=0,       NODEW=0,        INITIAL=0,                       &END
 &WAKE2   KWPACH=1,       KWSIDE=2,       KWLINE=0,       KWPAN1=0,
          KWPAN2=0,       NODEW=5,        INITIAL=0,                       &END


 &ONSTRM  NONSL =0,  KPSL =                                                &END


 &BLPARAM RN =35755000,    VISC = 0.000157, NSLBL = 1,                     &END


 &VS1     NVOLR= 0,       NVOLC= 0,                                        &END
 &VS2     X0=    -0.1000, Y0=     1.5000, Z0=    -0.1000, INTVSR= 1,       &END
 &VS3     X1=    -0.1000, Y1=     1.5000, Z1=     0.1000, NPT1=  0,        &END
 &VS4     X2=    -0.1000, Y2=     1.5000, Z2=     0.1000, NPT2= 20,        &END
 &VS5     X3=     1.1000, Y3=     1.5000, Z3=    -0.1000, NPT3= 25,        &END

 &VS6     XR0=    2.0000, YR0=    2.0000, ZR0=    0.0000, INTVSC= 1,       &END
 &VS7     XR1=    4.0000, YR1=    2.0000, ZR1=    0.0000,
          XR2=    2.0000, YR2=    2.0000, ZR2=    1.0000,                  &END
 &VS8     R1=     0.1000, R2=     1.0000, PHI1=  0.0,     PHI2=360.0,      &END
 &VS9     NRAD=   5,      NPHI=  12,      NLEN=  3,                        &END


 &SLIN1   NSTLIN=0,                                                        &END
 &SLIN2   SX0=   -2.0000, SY0=    1.0000, SZ0=   -0.5000,
```

Figure 5.17 Cont'd PMARC Input File for The Triangular Wing Equivalent Body of Revolution in Oscillation About The Mid-Chord for k=0.1.

D. SPINDLE

The spindle was shown and described in section **D** of Chapter **IV**. The main chord (or longitudinal axis) was made unity. The thickness ratio considered is 0.160. The spindle is reproduced below in Figure 5.18. Then the oscillation parameter calculations, the oscillation results, and the PMARC specifics are presented.

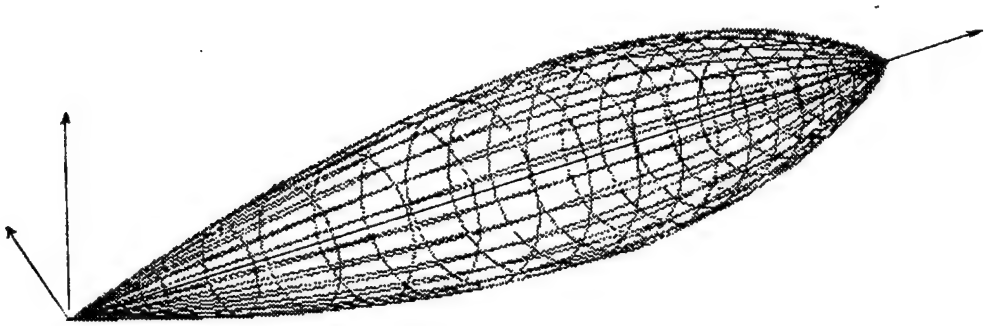

Figure 5.18 PMARC Representation of The Spindle.

1. Oscillatory Frequency and Time-Stepping Calculations

This time, only two reduced frequencies (k) will be studied: 0.1 and 0.5. The oscillation had the same plus and minus five degrees amplitude about the mid-chord, and two full oscillatory cycles were also computed. Again, here is a sample parameters calculation for k=0.1 and the results for the other case. c is the root chord (or longitudinal axis), *omega* is the oscillatory frequency in rad/sec (WRY in PMARC), T is the period, N the number of time-steps and dt the size of the time-steps in seconds. The PMARC notations for the last two parameters are NTSTPS and DTSTEP respectively. The freestream velocity was arbitrarily selected at 100 unit per second for the case of $k=0.1$ and at 11 for the case of $k=0.5$.

$$k=0.1rad=\frac{\omega c}{U_\infty}=\frac{\omega*1.0}{100} \quad \Rightarrow \quad \omega=WRY=10.0 \ rad/s \tag{5.7}$$

$$T=\frac{2\pi}{\omega}=\frac{2\pi}{10}=0.6283 \ \text{sec/}cycle \tag{5.8}$$

$$T=N*dt=NTSTPS*DTSTEP \Rightarrow 0.6283=NTSTPS*0.025 \Rightarrow NTSTPS=25.13 \ steps/cycle \tag{5.9}$$

NTSTPS=50.27 time-steps for two cycles

As mentioned before, the number of time-steps (NTSTPS) times the size of each time-step (DTSTEP) must equal the period (T). The combination selected is the one which will render a smooth distribution in the PMARC output. The following table now provides the value of the parameters shown above for the two values of reduced frequency studied. Recall that the freestream velocity was 100 unit per second for k=0.1 and 11 unit per second for k=0.5̄. This selection was necessary in order to keep the time step size from getting too small.

k	Amplitude	Osc. About...	Omega (WRY)	NTSTPS	DTSTEP
0.1	+- 5 Degrees	Mid-Chord	10.0 rad/s	51	0.025 sec
0.5	+- 5 Degrees	Mid-Chord	5.5 rad/s	115	0.02 sec

Table 5.3 Test Parameters for The Oscillation of The Spindle.

2. Results

Figures 5.19 and 5.20 below show the combined CL and CM results for the two reduced frequencies considered. The analysis of the relative maximums and minimums of the CL and CM

curves as a function of the reduced frequency, as well as the general behavior will be left to future work. It can be said however that the behavior of the lift and moment coefficients warrants interrogation as to their validity. As illustrated in the section **B-2** of this chapter, the lift vectors in front of the pivot point are theoretically balanced by those behind it (Figure 5.2). This should cause the net value of the lift to be close to zero at any angle of attack and the moment to vary over wider ranges. Some lift is expected due to the oscillation effects. Although the scaling of the plot varies widely, we still observe some lift, but more importantly, an equal moment variation. As detailed in section **B** of this chapter, all the oscillation figures are plotted against the reduced time which is the ratio of the product of the freestream velocity and time over the main chord.

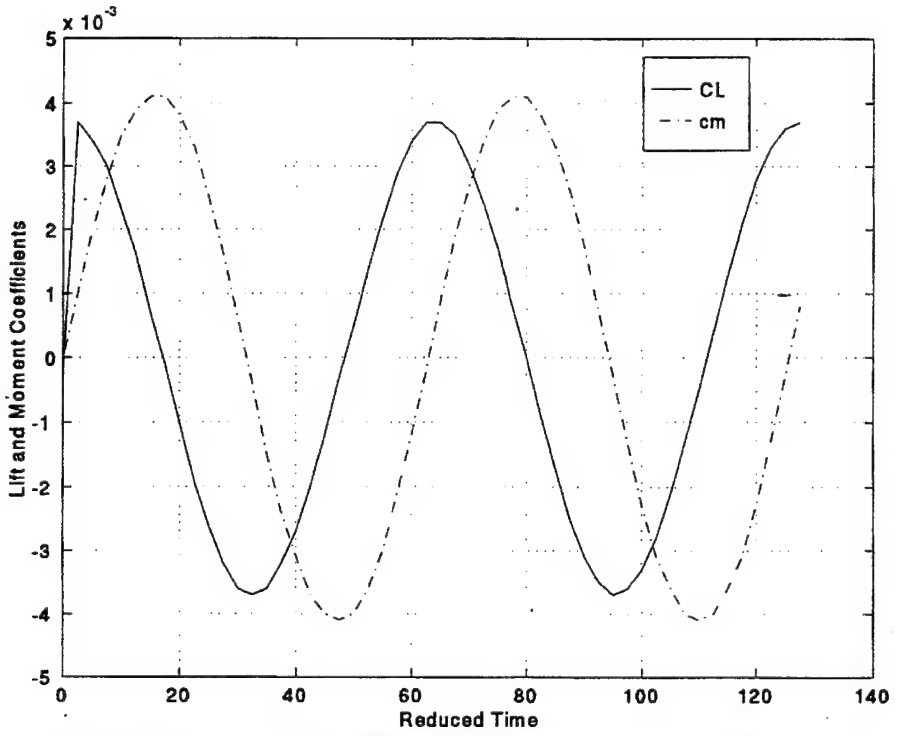

Figure 5.19 Lift and Moment Coefficient in Unsteady State as a Function of Reduced Time. Spindle, Delta=0.160, Oscillation Amplitude = 10 Degrees About c/2, U_{inf}=100, Omega=10.0 rad/s, k=0.1.

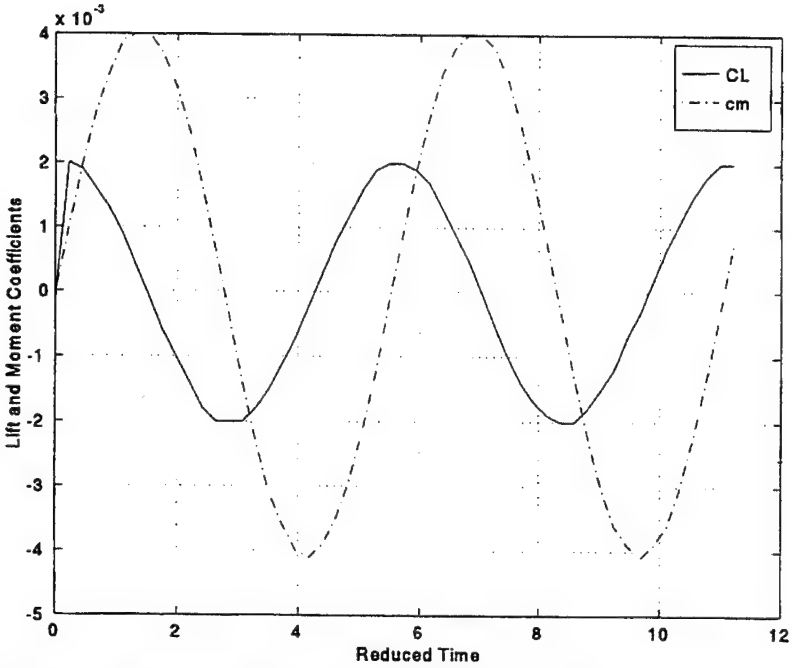

Figure 5.20 Lift and Moment Coefficient in Unsteady State as a Function of Reduced Time. Spindle, Delta=0.160, Oscillation Amplitude = 10 Degrees About c/2, U_{inf}=11, Omega=5.5 rad/s, k=0.5.

3. PMARC Input Instructions

Except for the values of the parameters, there is no difference between the input files for the oscillations of the spindle and those of the previous cases. An extract from one input file for the spindle is presented below. The reader should consult section **B-3** of this chapter for further details.

4. PMARC Output - Data Retrieval

As no difference exists with the data retrieval techniques used in the previous oscillation sections, the reader should refer to the latter for details on the program required to extract the data off DATA6.

Nov 17 1995 13:00 **osc1spdl160_shrt.in** Page 1

```
SPINDLE BODY (OSCILLATION CASE, PANELS=2304 )
&BINP2    LSTINP= 2,   LSTOUT= 0,   LSTFRQ= 0,  LENRUN= 0,LPLTYP=1,      &END
&BINP3    LSTGEO= 1,   LSTNAB= 1,   LSTWAK=0,   LSTCPV=0,               &END
&BINP4    MAXIT=200,  SOLRES=0.0005,                                    &END
&BINP5    NTSTPS= 51,   DTSTEP= 0.025,                                  &END
&BINP6    RSYM= 1.0,   RGPR=0.0,   RFF=5.0, RCORES=0.0080 RCOREW=0.0080, &END
&BINP7    VINF= 100.0,  VSOUND= 1117.3,                                 &END
&BINP8    ALDEG= 0.0,  YAWDEG=0.0,  PHIDOT=0.0, THEDOT=0.0,  PSIDOT=0.0, &END
&BINP8A   PHIMAX=0.0, THEMAX=10.0,  PSIMAX=0.0,
           WRX=0.0,    WRY=10.0,    WRZ=0.0                             &END
&BINP8B   DXMAX=0.0,  DYMAX=0.0,   DZMAX=0.0,
          WTX=0.0,    WTY=0.0,     WTZ=0.0,                             &END
&BINP9    CBAR=       1.00,  SREF=    0.7854   SSPAN=      1.00,
          RMPX= 0.0,  RMPY=0.00,   RMPZ=0.00,                           &END
&BINP10    NORSET=0,   NBCHGE=0,    NCZONE=0,
           NCZPCH=0,   CZDUB=0.0,   VREF=0.0,                           &END
&BINP11    NORPCH=0,
           NORF=0,     NORL=0,
           NOCF=0,     NOCL=0,
           VNORM=0.0,                                                  &END
&BINP12    KPAN=0,     KSIDE=0,    NEWNAB=0,   NEWSID=0,               &END
&BINP13    NBLIT= 0,                                                   &END
&ASEM1    ASEMX=-0.50,     ASEMY=0.00,     ASEMZ=0.00,
          ASCAL=1.00,     ATHET=0.00,     NODEA= 5,                    &END
&ASEM2    APXX=0.00,      APYY=0.00,      APZZ=0.00,
          AHXX=0.00,      AHYY=1.00,      AHZZ=0.00,                   &END
&COMP1    COMPX= 0.0000,   COMPY= 0.0000,   COMPZ= 0.0000,
          CSCAL=  1.000,   CTHET=   0.0,    NODEC= 5,                  &END
&COMP2    CPXX= 0.0000,    CPYY= 0.0000,    CPZZ= 0.0000,
          CHXX= 0.0000,    CHYY=  1.000,    CHZZ= 0.0000,              &END
&PATCH1   IREV=  0, IDPAT= 2, MAKE=   0, KCOMP= 1, KASS= 1, IPATSYM=0,
          IPATCOP=0,                                                   &END
      BODY ( only patch # 1 )
&SECT1    STX=  0.000000E+00, STY= 0.0,    STZ= 0.0,    SCALE=  0.0,
      ALF=   0.0,  THETA=   0.0,
      INMODE=  4,  TNODS= 0,    TNPS= 0,    TINTS= 3,                  &END
 0.000000E+00   0.426937E-03  -0.651380E-02
 0.000000E+00   0.127351E-02  -0.640235E-02
 0.000000E+00   0.209829E-02  -0.618135E-02
 0.000000E+00   0.288716E-02  -0.585459E-02
 0.000000E+00   0.362664E-02  -0.542765E-02
 0.000000E+00   0.430406E-02  -0.490784E-02
 0.000000E+00   0.490784E-02  -0.430406E-02
 0.000000E+00   0.542765E-02  -0.362664E-02
 0.000000E+00   0.585459E-02  -0.288716E-02
 0.000000E+00   0.618135E-02  -0.209829E-02
 0.000000E+00   0.640235E-02  -0.127351E-02
 0.000000E+00   0.651380E-02  -0.426938E-03
 0.000000E+00   0.651380E-02   0.426937E-03
 0.000000E+00   0.640235E-02   0.127351E-02
 0.000000E+00   0.618135E-02   0.209829E-02
 0.000000E+00   0.585459E-02   0.288716E-02
 0.000000E+00   0.542765E-02   0.362664E-02
 0.000000E+00   0.490784E-02   0.430406E-02
 0.000000E+00   0.430406E-02   0.490784E-02
 0.000000E+00   0.362664E-02   0.542765E-02
 0.000000E+00   0.288716E-02   0.585459E-02
 0.000000E+00   0.209829E-02   0.618135E-02
 0.000000E+00   0.127351E-02   0.640235E-02
 0.000000E+00   0.426937E-03   0.651380E-02
 0.000000E+00  -0.426937E-03   0.651380E-02
 0.000000E+00  -0.127351E-02   0.640235E-02
 0.000000E+00  -0.209828E-02   0.618135E-02
 0.000000E+00  -0.288716E-02   0.585459E-02
 0.000000E+00  -0.362664E-02   0.542765E-02
 0.000000E+00  -0.430406E-02   0.490784E-02
 0.000000E+00  -0.490784E-02   0.430406E-02
 0.000000E+00  -0.542765E-02   0.362664E-02
 0.000000E+00  -0.585459E-02   0.288716E-02
 0.000000E+00  -0.618135E-02   0.209828E-02
 0.000000E+00  -0.640235E-02   0.127351E-02
 0.000000E+00  -0.651380E-02   0.426936E-03
 0.000000E+00  -0.651380E-02  -0.426936E-03
 0.000000E+00  -0.640235E-02  -0.127351E-02
 0.000000E+00  -0.618135E-02  -0.209828E-02
 0.000000E+00  -0.585459E-02  -0.288716E-02
```

Nov 17 1995 13:00 **osc1spdl160_shrt.in** Page 2

```
 0.000000E+00  -0.542765E-02  -0.362664E-02
 0.000000E+00  -0.490784E-02  -0.430406E-02
 0.000000E+00  -0.430406E-02  -0.490784E-02
 0.000000E+00  -0.362664E-02  -0.542765E-02
 0.000000E+00  -0.288716E-02  -0.585459E-02
 0.000000E+00  -0.209829E-02  -0.618135E-02
 0.000000E+00  -0.127351E-02  -0.640235E-02
 0.000000E+00  -0.426938E-03  -0.651380E-02
 0.000000E+00   0.426937E-03  -0.651380E-02
&BPNODE   TNODE=3,   TNPC= 0,    TINTC= 3,                             &END
.
.
.
 0.000000E+00  -0.542775E-02   0.362671E-02
 0.000000E+00  -0.585470E-02   0.288722E-02
 0.000000E+00  -0.618147E-02   0.209832E-02
 0.000000E+00  -0.640247E-02   0.127353E-02
 0.000000E+00  -0.651392E-02   0.426944E-03
 0.000000E+00  -0.651392E-02  -0.426944E-03
 0.000000E+00  -0.640247E-02  -0.127353E-02
 0.000000E+00  -0.618147E-02  -0.209832E-02
 0.000000E+00  -0.585470E-02  -0.288722E-02
 0.000000E+00  -0.542775E-02  -0.362671E-02
 0.000000E+00  -0.490794E-02  -0.430414E-02
 0.000000E+00  -0.430415E-02  -0.490793E-02
 0.000000E+00  -0.362671E-02  -0.542775E-02
 0.000000E+00  -0.288722E-02  -0.585470E-02
 0.000000E+00  -0.209833E-02  -0.618147E-02
 0.000000E+00  -0.127353E-02  -0.640247E-02
 0.000000E+00  -0.426946E-03  -0.651392E-02
 0.000000E+00   0.426945E-03  -0.651392E-02
&BPNODE   TNODE=3,   TNPC= 0,    TINTC= 3,                             &END
&WAKE1    IDWAK= 0,    IFLXW= 0,      ITRFTZ= 0,   INTRW= 0,           &END
 BODY WAKE
&WAKE2    KWPACH= 1,   KWSIDE= 3,     KWLINE=   48,  KWPAN1= 0,
          KWPAN2= 0,   NODEW=  5,     INITIAL= 0,                      &END
&ONSTRM   NONSL = 0,   KPSL = 0,                                       &END
&BLPARAM RN = 200000, VISC = 0.00335, NSLBL = 0,                       &END
&VS1      NVOLR= 0,    NVOLC= 0,                                       &END
&SLIN1    NSTLIN= 0,                                                   &END
```

Figure 5.21 Extract From The PMARC Input File for a Spindle in Oscillation About The Mid-Chord, Amplitude=10 Degrees, Omega=10.0 rad/s, k=0.1.

E. CONCLUSION

In this section, the lift and moment coefficients variations at different reduced frequencies were presented for the F5 wing, the triangular wing, their respective equivalent body of revolution, and the spindle. The magnitude and relative behavior of the results seem legitimate in some cases but require more study in others.

In the event that the results are indeed erratic, one should not exclude the software as a potential source of error. However, the input files could also be introducing unrealistic behavior. One should then look for fields not yet discussed, or in the source code and its parameter sub-routines.

VI. SUMMARY AND CONCLUSION

It was the objective of this thesis to contribute to the development of a new approach to determine the steady and unsteady airloads on missiles and on low-aspect ratio aircraft configurations typically used for high-performance fighter aircraft. This approach uses a second-order approximation to the steady and oscillatory lifting flow past low aspect ratio wings which exhibits the same fundamental division as the slender-body/slender-wing theory: incompressible cross-flow and a Mach-number dependent spatial influence. To test the range of validity of this second-order theory, it was necessary to compare it with an exact three-dimensional flow solution, and a low speed three-dimensional flow panel code named PMARC developed by NASA-Ames was selected for that goal.

Therefore, PMARC was first validated by comparing it with other known solutions. For this purpose lifting flow over swept back, rectangular, and delta wings was studied and the PMARC predictions were found to be in good agreement. A detailed analysis of the F5 wing was then performed, and a program was written to compute its equivalent area body of revolution. The lifting pressure distributions were again found to agree well with the measured ones. However, a discrepancy was detected where the PMARC predictions of the non-lifting pressure distributions on delta wings at zero angle of attack were compared with linearized theory and with the Oswatitsch-Keune low aspect ratio wing theory. PMARC predicts velocity perturbations which do not decrease with decreasing local chordwise thickness ratio of the wing. Interestingly, no similar discrepancy was found on lifting and non-lifting rectangular wings when thickness ratio decreases toward the tips. Similarly, the PMARC predictions for lifting and non-lifting bodies of revolution generally compare well with slender body theory. Some differences in the magnitude of the pressure perturbation exist towards the tips of the bodies of revolution, which are in some cases larger than 10 percent. The chordwise location where the pressure perturbation switches sign also varies from the PMARC to the slender body theory, but never by more than 5 percent. Finally, PMARC was applied to the computation of the forces and moments generated on oscillatory wings and bodies of revolution. However, time constraint prevented any analytical or experimental comparison.

In light of the above summary, our contribution to the development of a second-order approximation to the steady and oscillatory lifting flow past low aspect ratio wings may appear dim as we were not able to obtain correct velocity distributions around delta wings at zero angle of attack using PMARC. However, through this difficulty we fulfilled one of our objectives which was to validate the software. It proved good in all other areas. It remains to work towards correcting PMARC or the procedure that lead to the erroneous results. Otherwise it will be necessary to establish the validity of another software.

APPENDIX A. F5 WING SPATIAL INFLUENCE FLOW CALCULATION

This appendix shows all the intermediate calculations leading to the solution of the spatial influence incompressible flow for the F5 wing studied in section **F** of chapter **III**. The form of the spatial influence flow equation solved is introduced as Equation (3.23) and is reproduced below. The solution was obtained for nine equally spaced chord locations. The software utilized to perform the analytical calculations is called MAPLE (Ref. [16]).

$$\Omega_x = \frac{1}{4\pi}\left[-\frac{Q_x(0)}{x}+\frac{Q_x(x_o)}{x_o-x}\right] - \frac{1}{4\pi}\left[Q_{xx}(0)ln2x+Q_{xx}(x_o)ln2(x_o-x)\right]$$

$$-\frac{1}{4\pi}\int_0^x Q_{xxx}(\xi)ln2(x-\xi)d\xi + \frac{1}{4\pi}\int_x^{x_o} Q_{xxx}(\xi)ln2(\xi-x)d\xi \qquad (3.23)$$

```
> Q:=71.2901*xi^10-352.0008*xi^9+743.1697*xi^8-875.6007*xi^7+630.8471*xi^6-2
  86.6580*xi^5+81.7019*xi^4-14.1307*xi^3+1.4169*xi^2-0.0348*xi;
```

$$Q := 71.2901\,\xi^{10} - 352.0008\,\xi^{9} + 743.1697\,\xi^{8} - 875.6007\,\xi^{7} + 630.8471\,\xi^{6} - 286.6580\,\xi^{5} + 81.7019\,\xi^{4} - 14.1307\,\xi^{3} + 1.4169\,\xi^{2} - .0348\,\xi$$

```
> dQ1:=diff(Q,xi);
```

$$dQ1 := 712.9010\,\xi^{9} - 3168.0072\,\xi^{8} + 5945.3576\,\xi^{7} - 6129.2049\,\xi^{6} + 3785.0826\,\xi^{5} - 1433.2900\,\xi^{4} + 326.8076\,\xi^{3} - 42.3921\,\xi^{2} + 2.8338\,\xi - .0348$$

```
> dQ2:=diff(dQ1,xi);
```

$$dQ2 := 6416.1090\,\xi^{8} - 25344.0576\,\xi^{7} + 41617.5032\,\xi^{6} - 36775.2294\,\xi^{5} + 18925.4130\,\xi^{4} - 5733.1600\,\xi^{3} + 980.4228\,\xi^{2} - 84.7842\,\xi + 2.8338$$

```
> dQ3:=diff(dQ2,xi);
```

$$dQ3 := 51328.8720\,\xi^{7} - 177408.4032\,\xi^{6} + 249705.0192\,\xi^{5} - 183876.1470\,\xi^{4} + 75701.6520\,\xi^{3} - 17199.4800\,\xi^{2} + 1960.8456\,\xi - 84.7842$$

```
> ans:=subs(xi=0,dQ1);
```

$$ans := -.0348$$

```
> ans:=subs(xi=1,dQ1);
```

$$ans := .0536$$

```
> ans:=subs(xi=0,dQ2);
```

$$ans := 2.8338$$

```
> ans:=subs(xi=1,dQ2);
```

$$ans := 5.0506$$

```
> term1:=(1/(4*Pi))*((0.0348/x)+(0.0536)/(1-x));
```

$$term1 := \frac{1}{4} \frac{.0348 \frac{1}{x} + .0536 \frac{1}{1 - x}}{\pi}$$

```
> term2:=(1/(4*Pi))*(2.8338*(ln(2*x))+5.0506*ln(2*(1-x)));
```

$$term2 := \frac{1}{4} \frac{2.8338 \ln(2\,x) + 5.0506 \ln(2 - 2\,x)}{\pi}$$

```
> term3:=dQ3*ln(2*(x-xi));
```

$$term3 := \left(51328.8720\,\xi^7 - 177408.4032\,\xi^6 + 249705.0192\,\xi^5 - 183876.1470\,\xi^4 + 75701.6520\,\xi^3 - 17199.4800\,\xi^2 + 1960.8456\,\xi - 84.7842\right) \ln(2\,x - 2\,\xi)$$

```
> term4:=dQ3*ln(2*(xi-x));
```

$$term4 := \left(51328.8720\,\xi^7 - 177408.4032\,\xi^6 + 249705.0192\,\xi^5 - 183876.1470\,\xi^4 + 75701.6520\,\xi^3 - 17199.4800\,\xi^2 + 1960.8456\,\xi - 84.7842\right) \ln(2\,\xi - 2\,x)$$

```
> term5:=(1/(4*Pi))*Int(term3,xi=0.0..x);
```

$$term5 := \frac{1}{4} \left(\int_0^x \left(51328.8720\,\xi^7 - 177408.4032\,\xi^6 + 249705.0192\,\xi^5 - 183876.1470\,\xi^4 + 75701.6520\,\xi^3 - 17199.4800\,\xi^2 + 1960.8456\,\xi - 84.7842\right) \ln(2\,x - 2\,\xi)\, d\xi \right.$$

$$\Big)\Big/\pi$$

```
> term5:=(1/(4*Pi))*int(term3,xi=0.0..x);
```

$$term5 := \frac{1}{4}(84.78420000\,x + 83970.10713\,x^5 - 1470.634200\,x^2$$
$$+ 10510.79333\,x^3 - 39427.94375\,x^4$$
$$- 36775.22940\ln(2.\,x)\,x^5 - 101962.8828\,x^6$$
$$+ 65713.52078\,x^7 - 25344.05760\ln(2.\,x)\,x^7$$
$$- 84.78420000\ln(2.\,x)\,x + 41617.50320\ln(2.\,x)\,x^6$$
$$- 17438.06768\,x^8 + 980.4228000\ln(2.\,x)\,x^2$$
$$- 5733.160000\ln(2.\,x)\,x^3 + 6416.109000\ln(2.\,x)\,x^8$$
$$+ 18925.41300\ln(2.\,x)\,x^4)\Big/\pi$$

```
> term6:=(1/(4*Pi))*Int(term4,xi=x..1);
```

$$term6 := \frac{1}{4}\left(\int_x^1 \left(51328.8720\,\xi^7 - 177408.4032\,\xi^6\right.\right.$$
$$+ 249705.0192\,\xi^5 - 183876.1470\,\xi^4 + 75701.6520\,\xi^3$$
$$\left.\left. - 17199.4800\,\xi^2 + 1960.8456\,\xi - 84.7842\right)\ln(2\,\xi - 2\,x)\,d\xi\right)\Big/\pi$$

```
> term6:=(1/(4*Pi))*int(term4,xi=x..1);
```

$$term6 := \frac{1}{4}(-6416.109000 \ln(2. - 2.x)x^8 + 17438.06768 x^8$$
$$- 329.3686900 x - 41617.50320 \ln(2. - 2.x)x^6$$
$$+ 3594.581720 x^2 - 980.4228000 \ln(2. - 2.x)x^2$$
$$+ 62238.41350 x^4 - 115054.2845 x^5 + 124098.8859 x^6$$
$$- 19868.30010 x^3 - 18925.41300 \ln(2. - 2.x)x^4$$
$$+ 36775.22940 \ln(2. - 2.x)x^5$$
$$+ 5733.160000 \ln(2. - 2.x)x^3 - 72129.62978 x^7$$
$$+ 84.78420000 \ln(2. - 2.x)x + 11.63426214$$
$$+ 2.216800000 \ln(2. - 2.x) + 25344.05760 \ln(2. - 2.x)x^7$$
$$)/\pi$$

```
> uoverUinf:=term1-term2-term5+term6;
```

$$uoverUinf := \frac{1}{4}\frac{.0348\frac{1}{x} + .0536\frac{1}{1-x}}{\pi}$$
$$- \frac{1}{4}\frac{2.8338\ln(2x) + 5.0506\ln(2-2x)}{\pi} - \frac{1}{4}($$
$$84.78420000 x + 83970.10713 x^5 - 1470.634200 x^2$$
$$+ 10510.79333 x^3 - 39427.94375 x^4$$
$$- 36775.22940 \ln(2.x)x^5 - 101962.8828 x^6$$
$$+ 65713.52078 x^7 - 25344.05760 \ln(2.x)x^7$$
$$- 84.78420000 \ln(2.x)x + 41617.50320 \ln(2.x)x^6$$

$$
\begin{aligned}
&- 17438.06768\, x^8 + 980.4228000 \ln(2.\, x)\, x^2 \\
&- 5733.160000 \ln(2.\, x)\, x^3 + 6416.109000 \ln(2.\, x)\, x^8 \\
&+ 18925.41300 \ln(2.\, x)\, x^4 \Big)\Big/ \pi + \frac{1}{4} \Big(\\
&-6416.109000 \ln(2. - 2.\, x)\, x^8 + 17438.06768\, x^8 \\
&- 329.3686900\, x - 41617.50320 \ln(2. - 2.\, x)\, x^6 \\
&+ 3594.581720\, x^2 - 980.4228000 \ln(2. - 2.\, x)\, x^2 \\
&+ 62238.41350\, x^4 - 115054.2845\, x^5 + 124098.8859\, x^6 \\
&- 19868.30010\, x^3 - 18925.41300 \ln(2. - 2.\, x)\, x^4 \\
&+ 36775.22940 \ln(2. - 2.\, x)\, x^5 \\
&+ 5733.160000 \ln(2. - 2.\, x)\, x^3 - 72129.62978\, x^7 \\
&+ 84.78420000 \ln(2. - 2.\, x)\, x + 11.63426214 \\
&+ 2.216800000 \ln(2. - 2.\, x) + 25344.05760 \ln(2. - 2.\, x)\, x^7 \\
\Big)\Big/ \pi
\end{aligned}
$$

```
> xvec:=array(1 .. 10);
```

$$xvec := \text{array}(1 .. 10, [\ ])$$

```
> for i to 10 do xvec[i]:=i/10 od;
```

$$xvec_{[1]} := \frac{1}{10}$$

$$xvec_{[2]} := \frac{1}{5}$$

$$xvec_{[3]} := \frac{3}{10}$$

$$xvec_{[4]} := \frac{2}{5}$$

$$xvec_{[5]} := \frac{1}{2}$$

$$xvec_{[6]} := \frac{3}{5}$$

$$xvec_{[7]} := \frac{7}{10}$$

$$xvec_{[8]} := \frac{4}{5}$$

$$xvec_{[9]} := \frac{9}{10}$$

$$xvec_{[10]} := 1$$

```
> for i from 1 to 10 do uovrUinf[i]:=evalf(subs(x=xvec[i],uoverUinf)) od;
```

$$uovrUinf_{[1]} := -.0573921826$$

$$uovrUinf_{[2]} := .0346121370$$

$$uovrUinf_{[3]} := .0017849588$$

$$uovrUinf_{[4]} := -.00548285722$$

$$uovrUinf_{[5]} := -.01293665332$$

$$uovrUinf_{[6]} := -.08484371084$$

$$uovrUinf_{[7]} := -.1297571415$$

$$uovrUinf_{[8]} := -.1189657140$$

$$uovrUinf_{[9]} := -.0926006053$$

```
Error, division by zero
```

```
>
```

APPENDIX B. TRIANGULAR WING SPATIAL INFLUENCE FLOW CALCULATION

This appendix shows all the intermediate calculations leading to the solution of the spatial influence incompressible flow for the triangular wing studied in section **G** of chapter **III**. Two forms of the spatial influence flow equations were solved and were introduced as Equation (3.23) and Equation (3.26). They are respectively reproduced below. Equation (3.23) is the general analytical expression, and Equation (3.26) is a specific Equation derived from Equation (3.23) for the triangular wing. The solutions were obtained for nine equally spaced chord locations. The expression for the wing cross-sectional area was provided in Ref. [15].The software utilized to perform the analytical calculations is called MAPLE (Ref. [16]).

$$\Omega_x = \frac{1}{4\pi}\left[-\frac{Q_x(0)}{x}+\frac{Q_x(x_o)}{x_o-x}\right] - \frac{1}{4\pi}\left[Q_{xx}(0)ln2x+Q_{xx}(x_o)ln2(x_o-x)\right]$$

$$-\frac{1}{4\pi}\int_0^x Q_{xxx}(\xi)ln2(x-\xi)d\xi + \frac{1}{4\pi}\int_x^{x_o} Q_{xxx}(\xi)ln2(\xi-x)d\xi \qquad (3.23)$$

$$\frac{\Omega_x}{\delta\sigma} = -\frac{1}{\pi}\frac{1}{1-x} + \frac{6}{\pi}(1-2x) - \frac{2}{\pi}(1-3x)ln4x(1-x) \qquad (3.26)$$

```
> Q:=4*delta*sigma*xi^2*(1-xi);
```

$$Q := 4\,\delta\,\sigma\,\xi^2\,(1 - \xi)$$

```
> dQ1:=diff(Q,xi);
```

$$dQ1 := 8\,\delta\,\sigma\,\xi\,(1 - \xi) - 4\,\delta\,\sigma\,\xi^2$$

```
> dQ2:=diff(dQ1,xi);
```

$$dQ2 := 8\,\delta\,\sigma\,(1 - \xi) - 16\,\delta\,\sigma\,\xi$$

```
> dQ3:=diff(dQ2,xi);
```

$$dQ3 := -24\,\delta\,\sigma$$

```
> ans:=subs(xi=1,dQ2);
```

$$ans := -16\,\delta\,\sigma$$

```
> term1:=(1/(4*Pi))*((-4*delta*sigma)/(1-x));
```

$$term1 := -\frac{\delta\,\sigma}{\pi\,(1 - x)}$$

```
> term2:=(1/(4*Pi))*(8*delta*sigma*(ln(2*x))-16*delta*sigma*ln(2*(1-x)));
```

$$term2 := \frac{1}{4}\,\frac{8\,\delta\,\sigma\,\ln(2\,x) - 16\,\delta\,\sigma\,\ln(2 - 2\,x)}{\pi}$$

```
> term3:=dQ3*ln(2*(x-xi));
```

$$term3 := -24\,\delta\,\sigma\,\ln(2\,x - 2\,\xi)$$

```
> term4:=dQ3*ln(2*(xi-x));
```

$$term4 := -24\,\delta\,\sigma\,\ln(2\,\xi - 2\,x)$$

```
> term5:=(1/(4*Pi))*int(term3,xi=0.0..x);
```

$$term5 := \frac{1}{4}\,\frac{-24\,\delta\,\sigma\,\ln(2\,x)\,x + 24\,\delta\,\sigma\,x}{\pi}$$

```
> term6:=(1/(4*Pi))*int(term4,xi=x..1);
```

$$term6 := \frac{1}{4}(-24\,\delta\,\sigma\ln(2-2x) + 24\,\delta\,\sigma + 24\,\delta\,\sigma\ln(2-2x)\,x - 24\,\delta\,\sigma\,x)/\pi$$

```
> sigma:=1/6:
> uoverUinf:=term1-term2-term5+term6;
```

$$uoverUinf := -\frac{1}{6}\frac{\delta}{\pi(1-x)} - \frac{1}{4}\frac{\frac{4}{3}\delta\ln(2x) - \frac{8}{3}\delta\ln(2-2x)}{\pi} - \frac{1}{4}\frac{-4\,\delta\ln(2x)\,x + 4\,\delta\,x}{\pi} + \frac{1}{4}\frac{-4\,\delta\ln(2-2x) + 4\,\delta + 4\,\delta\ln(2-2x)\,x - 4\,\delta\,x}{\pi}$$

```
> xvec:=array(1 .. 10);
```

$$xvec := \text{array}(1 .. 10, [\ ])$$

```
> for i to 10 do xvec[i]:=i/10 od;
```

$$xvec_{[1]} := \frac{1}{10}$$

$$xvec_{[2]} := \frac{1}{5}$$

$$xvec_{[3]} := \frac{3}{10}$$

$$xvec_{[4]} := \frac{2}{5}$$

$$xvec_{[5]} := \frac{1}{2}$$

$$xvec_{[6]} := \frac{3}{5}$$

$$xvec_{[7]} := \frac{7}{10}$$

$$xvec_{[8]} := \frac{4}{5}$$

$$xvec_{[9]} := \frac{9}{10}$$

$$xvec_{[10]} := 1$$

```
> for i from 1 to 10 do uvel[i]:=evalf(subs(x=xvec[i],uoverUinf)) od;
```

$$uvel_{[1]} := .2715820284\ \delta$$

$$uvel_{[2]} := .1436123850\ \delta$$

$$uvel_{[3]} := .05338583318\ \delta$$

$$uvel_{[4]} := -.02562370518\ \delta$$

$$uvel_{[5]} := -.1061032954\ \delta$$

$$uvel_{[6]} := -.1997561750\ \delta$$

$$uvel_{[7]} := -.3245121960\ \delta$$

$$uvel_{[8]} := -.5225377152\ \delta$$

$$uvel_{[9]} := -.9694453447\ \delta$$

```
Error, division by zero
```

```
> uoverUinf:=-(1/(1-x)/Pi)+6*(1-2*x)/Pi-2*(1-3*x)*ln(4*x)*(1-x)/Pi;
```

$$uoverUinf := -\frac{1}{(1-x)\,\pi} + 6\,\frac{1-2\,x}{\pi} - 2\,\frac{(1-3\,x)\,\ln(4\,x)\,(1-x)}{\pi}$$

```
> xvec:=array(1 .. 10);
```

$$xvec := \mathrm{array}(1 \,..\, 10, [\ ])$$

```
> for i to 10 do xvec[i]:=i/10 od;
```

$$xvec_{[1]} := \frac{1}{10}$$

$$xvec_{[2]} := \frac{1}{5}$$

$$xvec_{[3]} := \frac{3}{10}$$

$$xvec_{[4]} := \frac{2}{5}$$

$$xvec_{[5]} := \frac{1}{2}$$

$$xvec_{[6]} := \frac{3}{5}$$

$$xvec_{[7]} := \frac{7}{10}$$

$$xvec_{[8]} := \frac{4}{5}$$

$$xvec_{[9]} := \frac{9}{10}$$

$$xvec_{[10]} := 1$$

> for i from 1 to 10 do uvel[i]:=evalf(subs(x=xvec[i],uoverUinf)) od;

$$uvel_{[1]} := 1.541706944$$

$$uvel_{[2]} := .7934866633$$

$$uvel_{[3]} := .3010904523$$

$$uvel_{[4]} := -.1126389811$$

$$uvel_{[5]} := -.5263019721$$

$$uvel_{[6]} := -.9993975524$$

$$uvel_{[7]} := -1.608669574$$

$$uvel_{[8]} := -2.530129275$$

$$uvel_{[9]} := -4.572356786$$

```
Error, division by zero
```

>

APPENDIX C. TRIANGULAR WING CROSS-SECTIONAL FLOW CALCULATION

This appendix shows all the intermediate calculations leading to the solution of the cross-sectional incompressible flow for the triangular wing studied in section **G** of chapter **III**. The form of the spatial influence flow equation solved is introduced as Equation (3.17) and is reproduced below. The solution was obtained for nine equally spaced chord locations and the process repeated for two spanwise locations (near the root and near the tip). For conciseness, the intermediate spanwise locations although calculated in our study are not presented because of their repetitive character. The software utilized to perform the analytical calculations is called MAPLE (Ref. [16]).

$$\frac{\varphi_x(x,\bar{z})}{\sigma\delta} = \frac{\bar{Q}_{xx}(x)}{2\pi}\left[\ln\sigma+\ln\bar{s}(x)+\ln\sqrt{\left(1-\left(\frac{\bar{z}}{\bar{s}(x)}\right)^2\right)}\right] - \frac{\bar{P}_{xx}(x,\bar{z})}{2\pi}\ln\left|\frac{1-\frac{\bar{z}}{\bar{s}(x)}}{1+\frac{\bar{z}}{\bar{s}(x)}}\right| - \frac{1}{\pi}\int_0^{\bar{s}(x)}\frac{\bar{P}_{xx}(x,\bar{\zeta})-\bar{P}_{xx}(x,\bar{z})}{\bar{\zeta}-\bar{z}}d\bar{\zeta} \tag{3.17}$$

```
> Q:=4*delta*sigma*x^2*(1-x);
```

$$Q := 4\,\delta\,\sigma\,x^2\,(1 - x)$$

```
> Qbar:=Q/(sigma*delta);
```

$$Qbar := 4\,x^2\,(1 - x)$$

```
> dQbar1:=diff(Qbar,x);
```

$$dQbar1 := 8\,x\,(1 - x) - 4\,x^2$$

```
> dQbar2:=diff(dQbar1,x);
```

$$dQbar2 := 8 - 24\,x$$

```
> dPbar2:=-8*zbar;
```

$$dPbar2 := -8\,zbar$$

```
> dPzetabar2:=-8*zetabar;
```

$$dPzetabar2 := -8\,zetabar$$

```
> term1:=(dQbar2/(2*Pi))*(ln((1/6))+ln(x)+ln(sqrt(1-(zbar/x)^2)));
```

$$term1 := \frac{1}{2}\,\frac{(8 - 24\,x)\left(-\ln(6) + \ln(x) + \ln\left(\sqrt{1 - \frac{zbar^2}{x^2}}\right)\right)}{\pi}$$

```
> term2:=(dPbar2/(2*Pi))*ln(abs((1-(zbar/x))/(1+(zbar/x))));
```

$$term2 := -4\,\frac{zbar\,\ln\left(\left|\frac{1 - \frac{zbar}{x}}{1 + \frac{zbar}{x}}\right|\right)}{\pi}$$

```
> term3:=(dPzetabar2-dPbar2)/(zetabar-(zbar));
```

$$term3 := \frac{-8\,zetabar + 8\,zbar}{zetabar - zbar}$$

```
> term4:=(1/Pi)*Int(term3,zeta=0.0..(x));
```

$$term4 := \frac{\int_0^x \frac{-8\ zetabar + 8\ zbar}{zetabar - zbar}\, d\zeta}{\pi}$$

```
> term4:=(1/Pi)*int(term3,zeta=0.0..(x));
```

$$term4 := -8\,\frac{x}{\pi}$$

```
> sigma:=1/6:
> phi:=term1-term2-term4;
```

$$\phi := \frac{1}{2}\,\frac{(8 - 24\,x)\left(-\ln(6) + \ln(x) + \ln\left(\sqrt{1 - \frac{zbar^2}{x^2}}\right)\right)}{\pi} + 4\,\frac{zbar\,\ln\left(\frac{\left|1 - \frac{zbar}{x}\right|}{\left|1 + \frac{zbar}{x}\right|}\right)}{\pi} + 8\,\frac{x}{\pi}$$

```
>
> # CALCULATIONS FOR X=1/10
> phianaly1:=subs(x=1/10,phi);
```

$$phianaly1 := \frac{14}{5}\,\frac{-\ln(6) + \ln\left(\frac{1}{10}\right) + \ln\left(\sqrt{1 - 100\,zbar^2}\right)}{\pi} + 4\,\frac{zbar\,\ln\left(\frac{\left|1 - 10\,zbar\right|}{\left|1 + 10\,zbar\right|}\right)}{\pi} + \frac{4}{5}\,\frac{1}{\pi}$$

```
> zvec:=array(1 .. 10);
```

$$zvec := \mathrm{array}(1 \,..\, 10, [\ ])$$

```
> for i to 10 do zvec[i]:=6*i/600 od;
```

$$zvec_{[1]} := \frac{1}{100}$$

$$zvec_{[2]} := \frac{1}{50}$$

$$zvec_{[3]} := \frac{3}{100}$$

$$zvec_{[4]} := \frac{1}{25}$$

$$zvec_{[5]} := \frac{1}{20}$$

$$zvec_{[6]} := \frac{3}{50}$$

$$zvec_{[7]} := \frac{7}{100}$$

$$zvec_{[8]} := \frac{2}{25}$$

$$zvec_{[9]} := \frac{9}{100}$$

$$zvec_{[10]} := \frac{1}{10}$$

```
> # the division by 6 is to get the form of the answers which has no sigma (1/6) a
  t the denominator
> ans:=subs(zbar=1/100,phianaly1);
```

$$ans := \frac{14}{5}\,\frac{-\ln(6) - \ln(10) + \ln\left(\frac{1}{100}\sqrt{99}\,\sqrt{100}\right)}{\pi} + \frac{1}{25}\,\frac{\ln\left(\left|\frac{\frac{9}{10}}{\frac{11}{10}}\right|\right)}{\pi} + \frac{4}{5}\,\frac{1}{\pi}$$

```
> final:=evalf(ans)/6;
```

$$final := -.5669238108$$

```
>
> ans:=subs(zbar=1/50,phianaly1):
> final:=evalf(ans)/6;
```

$$final := -.5705043033$$

```
>
> ans:=subs(zbar=3/100,phianaly1):
> final:=evalf(ans)/6;
```

$$final := -.5766971103$$

```
>
> ans:=subs(zbar=1/25,phianaly1):
> final:=evalf(ans)/6;
```

$$final := -.5858932281$$

```
>
> ans:=subs(zbar=1/20,phianaly1);
```

$$ans := \frac{14}{5}\,\frac{-\ln(6) - \ln(10) + \ln\left(\frac{1}{4}\sqrt{3}\,\sqrt{4}\right)}{\pi} + \frac{1}{5}\,\frac{\ln\left(\left|\frac{\frac{1}{2}}{\frac{3}{2}}\right|\right)}{-\pi} + \frac{4}{5}\,\frac{1}{\pi}$$

```
> final:=evalf(ans)/6;
```

$$final := -.5987749621$$

```
>
> ans:=subs(zbar=3/50,phianaly1);
```

$$ans :=$$

$$\frac{14}{5}\,\frac{-\ln(6) - \ln(10) + \ln\left(\frac{1}{25}\sqrt{16}\,\sqrt{25}\right)}{\pi} + \frac{6}{25}\,\frac{\ln\left(\left|\frac{\frac{2}{5}}{\frac{8}{5}}\right|\right)}{\pi} + \frac{4}{5}\,\frac{1}{\pi}$$

```
> final:=evalf(ans)/6;
```

$$final := -.6165491328$$

```
>
> ans:=subs(zbar=7/100,phianaly1);
```

$$ans := \frac{14}{5}\,\frac{-\ln(6) - \ln(10) + \ln\left(\frac{1}{100}\sqrt{51}\,\sqrt{100}\right)}{\pi} + \frac{7}{25}\,\frac{\ln\left(\left|\frac{\frac{3}{10}}{\frac{17}{10}}\right|\right)}{\pi} + \frac{4}{5}\,\frac{1}{\pi}$$

```
> final:=evalf(ans)/6;
```

$$final := -.6415289300$$

```
>
> ans:=subs(zbar=2/25,phianaly1);
```

$$ans := \frac{14}{5}\,\frac{-\ln(6) - \ln(10) + \ln\left(\frac{1}{25}\sqrt{9}\,\sqrt{25}\right)}{\pi} + \frac{8}{25}\,\frac{\ln\left(\left|\frac{\frac{1}{5}}{\frac{9}{5}}\right|\right)}{\pi} + \frac{4}{5}\,\frac{1}{\pi}$$

```
> final:=evalf(ans)/6;
```

$$final := -.6789331503$$

```
>
> ans:=subs(zbar=9/100,phianaly1);
```

$$ans := \frac{14}{5}\,\frac{-\ln(6) - \ln(10) + \ln\left(\frac{1}{100}\sqrt{19}\,\sqrt{100}\right)}{\pi} + \frac{9}{25}\,\frac{\ln\left(\frac{\left|\frac{1}{10}\right|}{\left|\frac{19}{10}\right|}\right)}{\pi} + \frac{4}{5}\,\frac{1}{\pi}$$

```
> final:=evalf(ans)/6;
```

$$final := -.7453324925$$

```
>
> ans:=subs(zbar=1/10,phianaly1);
```

$$ans := \frac{14}{5}\,\frac{-\ln(6) - \ln(10) + \ln(0)}{\pi} + \frac{2}{5}\,\frac{\ln\left(\frac{|0|}{|2|}\right)}{\pi} + \frac{4}{5}\,\frac{1}{\pi}$$

```
> final:=evalf(ans)/6;
Error, (in ln) singularity encountered
```

```
>
> # CALCULATIONS FOR X=1
> phianaly10:=subs(x=1,phi);
```

$$phianaly10 := -8\,\frac{-\ln(6)+\ln(1)+\ln\left(\sqrt{1-zbar^2}\right)}{\pi} + 4\,\frac{zbar\,\ln\left(\frac{|1-zbar|}{|1+zbar|}\right)}{\pi} + 8\,\frac{1}{\pi}$$

```
> for i to 10 do zvec[i]:=6*i*10/600 od:
>
> ans:=subs(zbar=1/10,phianaly10);
```

$$ans := -8\,\frac{-\ln(6)+\ln\left(\frac{1}{100}\sqrt{99}\,\sqrt{100}\right)}{\pi} + \frac{2}{5}\,\frac{\ln\left(\frac{\left|\frac{9}{10}\right|}{\left|\frac{11}{10}\right|}\right)}{\pi} + 8\,\frac{1}{\pi}$$

```
> final:=evalf(ans)/6;
```

$$final := 1.182733902$$

```
>
> ans:=subs(zbar=1/5,phianaly10);
```

$$ans := -8\,\frac{-\ln(6)+\ln\left(\frac{1}{25}\sqrt{24}\,\sqrt{25}\right)}{\pi} + \frac{4}{5}\,\frac{\ln\left(\frac{\left|\frac{4}{5}\right|}{\left|\frac{6}{5}\right|}\right)}{\pi} + 8\,\frac{1}{\pi}$$

```
> final:=evalf(ans)/6;
```

$$final := 1.176313741$$

```
>
> ans:=subs(zbar=3/10,phianaly10);
```

$$ans := -8\,\frac{-\ln(6) + \ln\left(\frac{1}{100}\sqrt{91}\,\sqrt{100}\right)}{\pi} + \frac{6}{5}\,\frac{\ln\left(\frac{\left|\frac{7}{10}\right|}{\left|\frac{13}{10}\right|}\right)}{\pi} + 8\,\frac{1}{\pi}$$

```
> final:=evalf(ans)/6;
```

$$final := 1.165463606$$

```
>
> ans:=subs(zbar=2/5,phianaly10);
```

$$ans := -8\,\frac{-\ln(6) + \ln\left(\frac{1}{25}\sqrt{21}\,\sqrt{25}\right)}{\pi} + \frac{8}{5}\,\frac{\ln\left(\frac{\left|\frac{3}{5}\right|}{\left|\frac{7}{5}\right|}\right)}{\pi} + 8\,\frac{1}{\pi}$$

```
> final:=evalf(ans)/6;
```

$$final := 1.149937580$$

```
>
> ans:=subs(zbar=1/2,phianaly10);
```

$$ans := -8\,\frac{-\ln(6) + \ln\left(\frac{1}{4}\sqrt{3}\,\sqrt{4}\right)}{\pi} + 2\,\frac{\ln\left(\frac{\left|\frac{1}{2}\right|}{\left|\frac{3}{2}\right|}\right)}{\pi} + 8\,\frac{1}{\pi}$$

```
> final:=evalf(ans)/6;
```

$$final := 1.129341166$$

```
>
> ans:=subs(zbar=3/5,phianaly10);
```

$$ans := -8\,\frac{-\ln(6)+\ln\left(\frac{1}{25}\sqrt{16}\,\sqrt{25}\right)}{\pi}+\frac{12}{5}\,\frac{\ln\left(\left|\frac{\frac{2}{5}}{\frac{8}{5}}\right|\right)}{\pi}+8\,\frac{1}{\pi}$$

```
> final:=evalf(ans)/6;
```

$$final := 1.103056103$$

```
>
> ans:=subs(zbar=7/10,phianaly10);
```

$$ans := -8\,\frac{-\ln(6)+\ln\left(\frac{1}{100}\sqrt{51}\,\sqrt{100}\right)}{\pi}+\frac{14}{5}\,\frac{\ln\left(\left|\frac{\frac{3}{10}}{\frac{17}{10}}\right|\right)}{\pi}+8\,\frac{1}{\pi}$$

```
> final:=evalf(ans)/6;
```

$$final := 1.070082027$$

```
>
> ans:=subs(zbar=4/5,phianaly10);
```

$$ans := -8\,\frac{-\ln(6)+\ln\left(\frac{1}{25}\sqrt{9}\,\sqrt{25}\right)}{\pi}+\frac{16}{5}\,\frac{\ln\left(\left|\frac{\frac{1}{5}}{\frac{9}{5}}\right|\right)}{\pi}+8\,\frac{1}{\pi}$$

> final:=evalf(ans)/6;

$$final := 1.028648218$$

>

> ans:=subs(zbar=9/10,phianaly10);

$$ans := -8\,\frac{-\ln(6)+\ln\left(\frac{1}{100}\sqrt{19}\sqrt{100}\right)}{\pi}+\frac{18}{5}\,\frac{\ln\left(\frac{\left|\frac{1}{10}\right|}{\left|\frac{19}{10}\right|}\right)}{\pi}+8\,\frac{1}{\pi}$$

> final:=evalf(ans)/6;

$$final := .9749312040$$

>

> ans:=subs(zbar=1,phianaly10);

$$ans := -8\,\frac{-\ln(6)+\ln(0)}{\pi}+4\,\frac{\ln\left(\frac{|0|}{|2|}\right)}{\pi}+8\,\frac{1}{\pi}$$

> final:=evalf(ans)/6;

> h:=2*delta*(x-abs(z)/sigma)*(1-x);

$$h := 2\,\delta\left(x - \frac{|z|}{\sigma}\right)(1 - x)$$

> hzeta:=2*delta*(x-abs(zeta)/sigma)*(1-x);

$$hzeta := 2\,\delta\left(x - \frac{|\zeta|}{\sigma}\right)(1 - x)$$

> P:=2*Int(hzeta,zeta=0..z);

$$P := 2\int_0^z 2\,\delta\left(x - \frac{|\zeta|}{\sigma}\right)(1 - x)\,d\zeta$$

> P:=2*int(hzeta,zeta=0..z);

$$P := -2\,\frac{z\,(2\,x\,\sigma - z\,\mathrm{signum}(z))\,\delta\,(-1 + x)}{\sigma}$$

> dP1:=diff(P,x);

$$dP1 := -4\,z\,\delta\,(-1 + x) - 2\,\frac{z\,(2\,x\,\sigma - z\,\mathrm{signum}(z))\,\delta}{\sigma}$$

> dP2:=diff(dP1,x);

$$dP2 := -8\,z\,\delta$$

> dP2bar:=dP2/(delta*sigma);

$$dP2bar := -8\,\frac{z}{\sigma}$$

> dP2bar:=-8*zbar;

$$dP2bar := -8\,zbar$$

APPENDIX D. STREAMWISE VELOCITY DISTRIBUTION TEST ON THE RECTANGULAR WING

This appendix is related to the discussion in section **G-2** of chapter **III** about the velocity perturbation distribution in the streamwise direction on the triangular wing. It was said for this case that PMARC produces erroneous results. This appendix shows that for the rectangular wing the streamwise velocity distribution seems to present a proper behavior. The appendix is broken down as follows.

a. Application of the slender body theory perturbation expression to corroborate the results subsequently obtained with PMARC,

b. Plot showing the streamwise velocity as a function of chordwise location for various spanwise locations, in the case of a rectangular wing of aspect ratio 20 with a biconvex cross-section which thickness is tapered from root to tip.

c. Plot showing the streamwise velocity as a function of chordwise location for various spanwise locations, in the case of a rectangular wing of aspect ratio 7 with a biconvex cross-section which thickness is tapered from root to tip..

d. Plot showing the streamwise velocity as a function of chordwise location for various spanwise locations, in the case of a rectangular wing of aspect ratio 4.5 with a biconvex cross-section which thickness is tapered from root to tip..

e. Plot showing the streamwise velocity as a function of chordwise location for various spanwise locations, in the case of a rectangular wing of aspect ratio 4.5 with a NACA 0012 cross-section which thickness is tapered from root to tip..

As can be observed, the PMARC results for the biconvex cross-section cases show similar behavior than the one predicted by the slender body theory. Furthermore, all the distributions shown are legitimate as the velocities (or perturbations) become smaller toward the tip, as expected.

```
> u:=((4*tau/Pi)*(1-(0.5-x)*ln(abs((1-x)/x)))*Vinf)+Vinf;
```

$$u := 4\,\frac{\tau\left(1 - (.5 - x)\ln\left(\frac{|1 - x|}{|x|}\right)\right)Vinf}{\pi} + Vinf$$

```
> xvec:=array(1..10);
```

$$xvec := \mathrm{array}(1 .. 10, [\ ])$$

```
> for i to 10 do xvec[i]:=i/10 od;
```

$$xvec_{[1]} := \frac{1}{10}$$

$$xvec_{[2]} := \frac{1}{5}$$

$$xvec_{[3]} := \frac{3}{10}$$

$$xvec_{[4]} := \frac{2}{5}$$

$$xvec_{[5]} := \frac{1}{2}$$

$$xvec_{[6]} := \frac{3}{5}$$

$$xvec_{[7]} := \frac{7}{10}$$

$$xvec_{[8]} := \frac{4}{5}$$

$$xvec_{[9]} := \frac{9}{10}$$

$$xvec_{[10]} := 1$$

```
> tau:=0.098:
> Vinf:=11:
> for i from 1 to 10 do uvel[i]:=evalf(subs(x=xvec[i],u)) od;
```

$$uvel_{[1]} := 11.16623003$$

$$uvel_{[2]} := 11.80172380$$

$$uvel_{[3]} := 12.13996012$$

$$uvel_{[4]} := 12.31690003$$

$$uvel_{[5]} := 12.37255223$$

$$uvel_{[6]} := 12.31690003$$

$$uvel_{[7]} := 12.13996012$$

$$uvel_{[8]} := 11.80172380$$

$$uvel_{[9]} := 11.16623003$$

```
Error, (in evalf/ln) singularity encountered
```

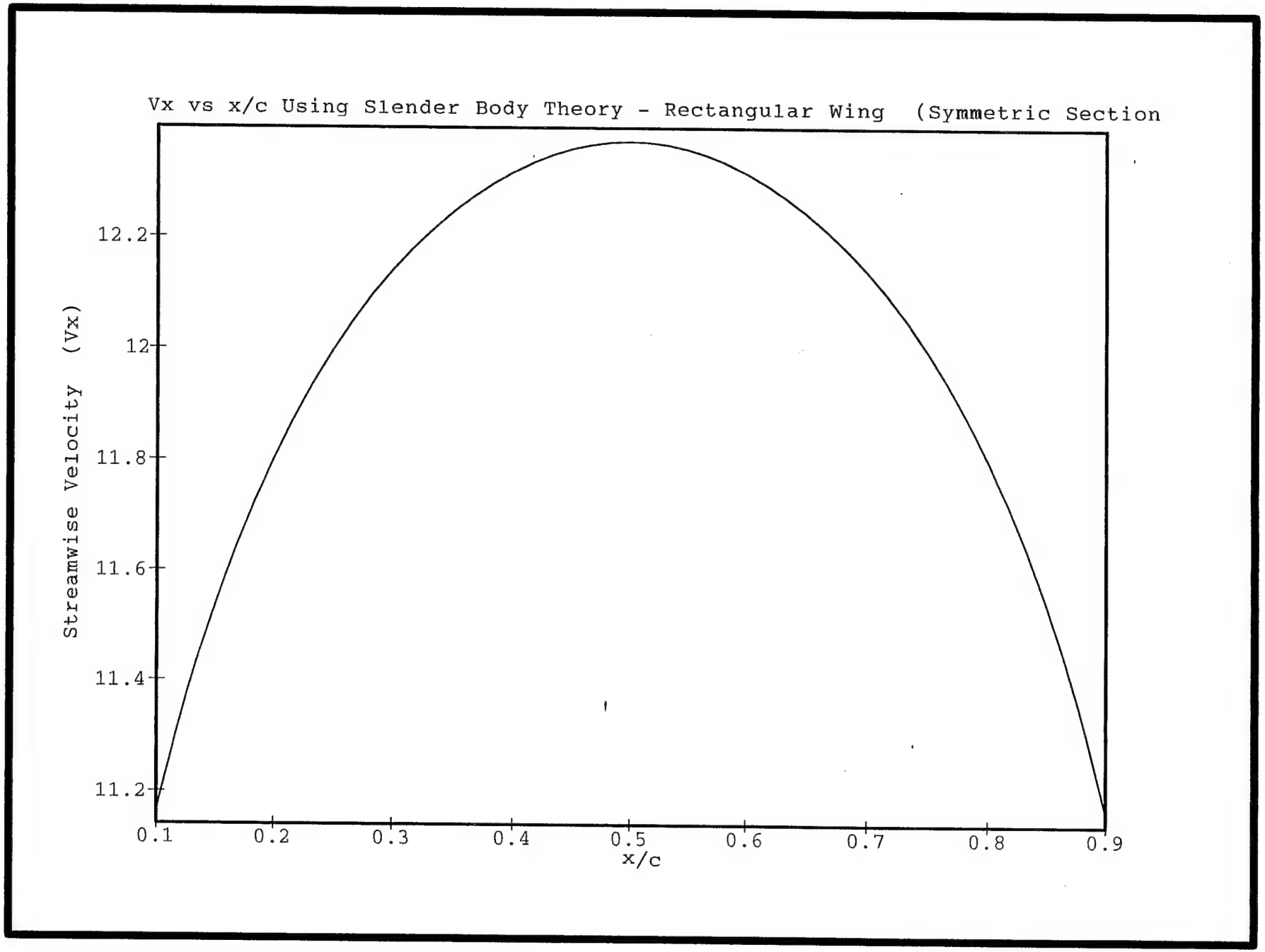
Vx vs x/c Using Slender Body Theory - Rectangular Wing (Symmetric Section
Streamwise Velocity (Vx)
12.2
12
11.8
11.6
11.4
11.2
0.1
0.2
0.3
0.4
0.5
0.6
0.7
0.8
0.9
x/c

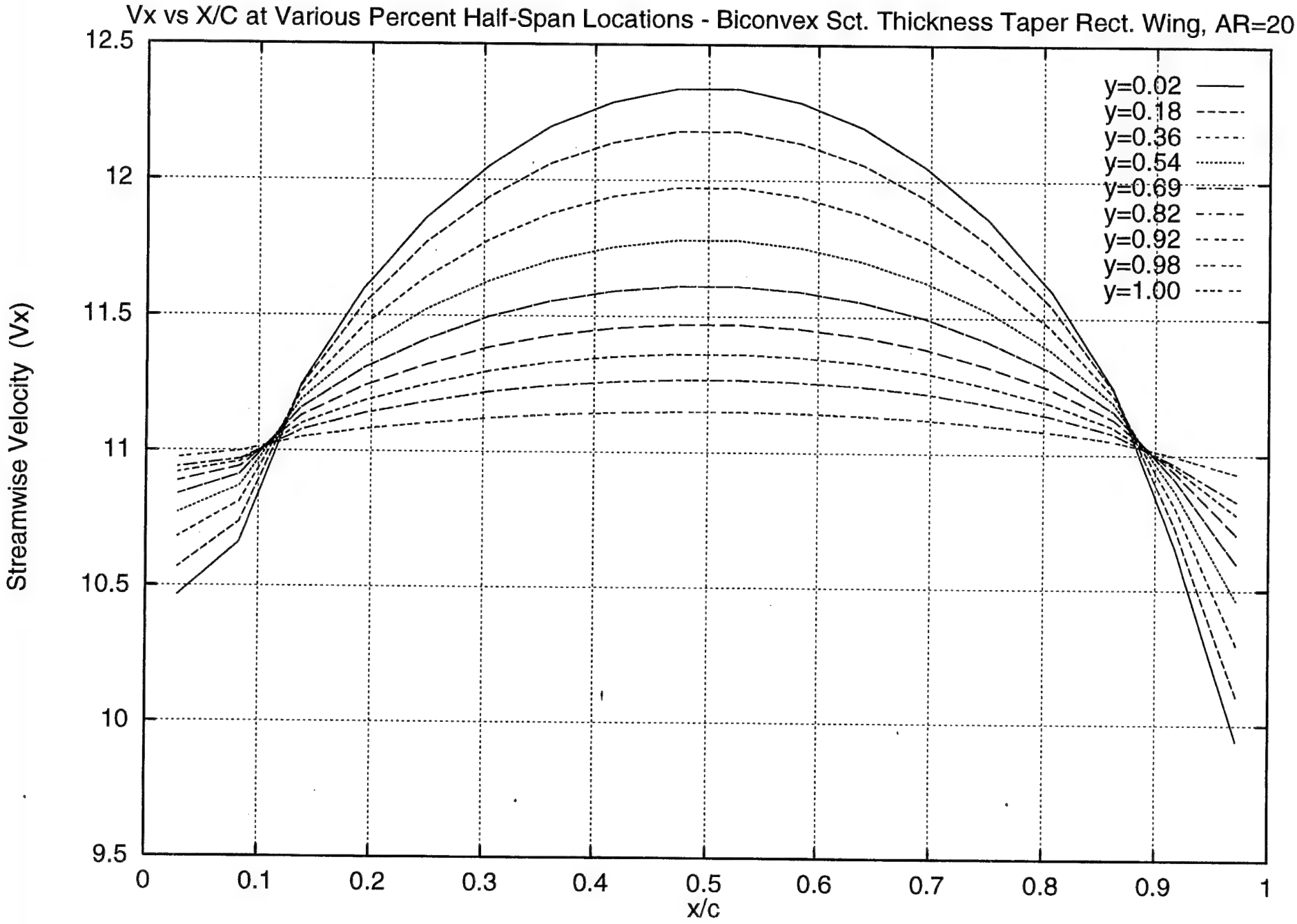
Vx vs X/C at Various Percent Half-Span Locations - Biconvex Sct. Thickness Taper Rect. Wing, AR=20
Streamwise Velocity (Vx)
x/c
y=0.02
y=0.18
y=0.36
y=0.54
y=0.69
y=0.82
y=0.92
y=0.98
y=1.00
12.5
12
11.5
11
10.5
10
9.5
0
0.1
0.2
0.3
0.4
0.5
0.6
0.7
0.8
0.9
1

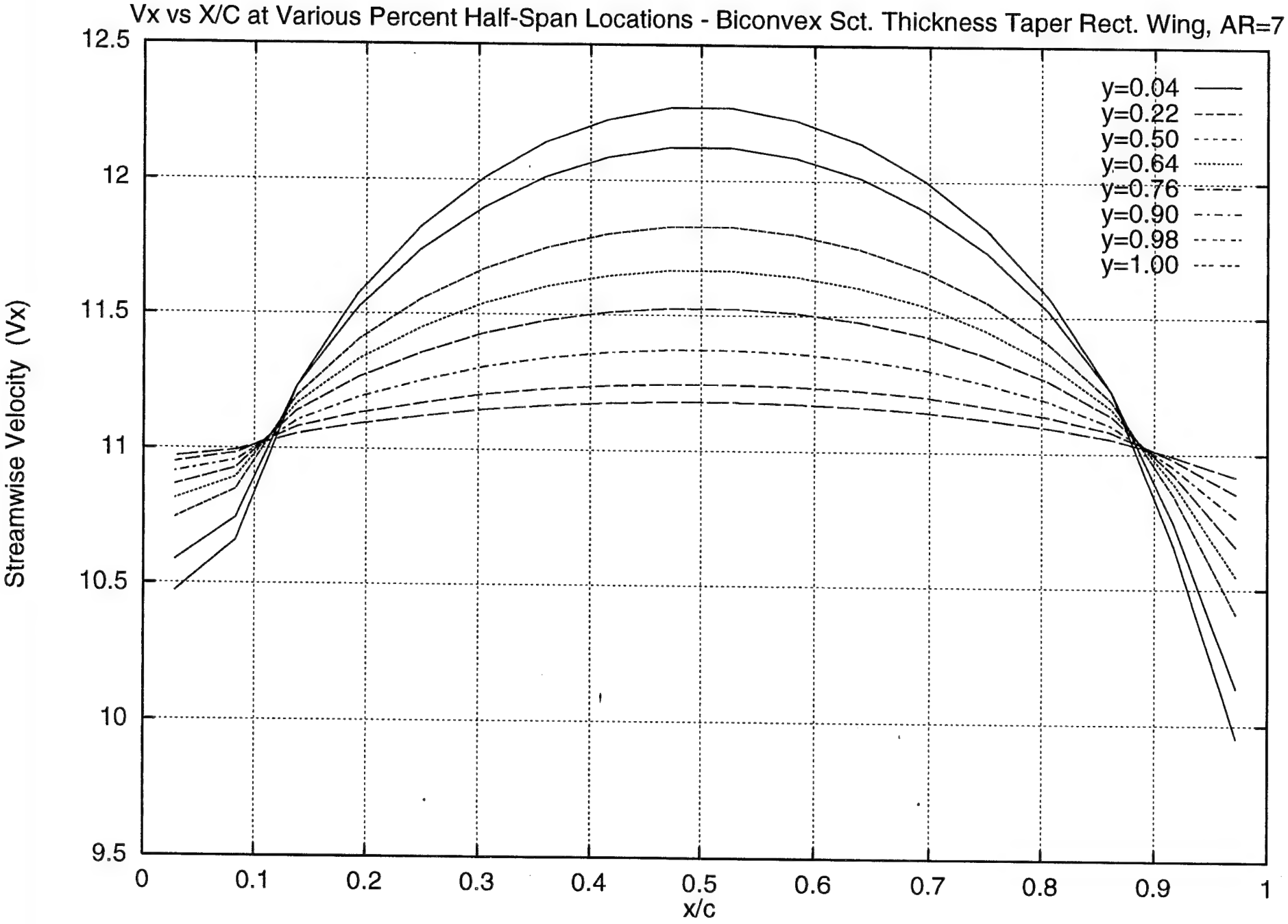
Vx vs X/C at Various Percent Half-Span Locations - Biconvex Sct. Thickness Taper Rect. Wing, AR=7
Streamwise Velocity (Vx)
x/c
12.5
12
11.5
11
10.5
10
9.5
0
0.1
0.2
0.3
0.4
0.5
0.6
0.7
0.8
0.9
1
y=0.04
y=0.22
y=0.50
y=0.64
y=0.76
y=0.90
y=0.98
y=1.00

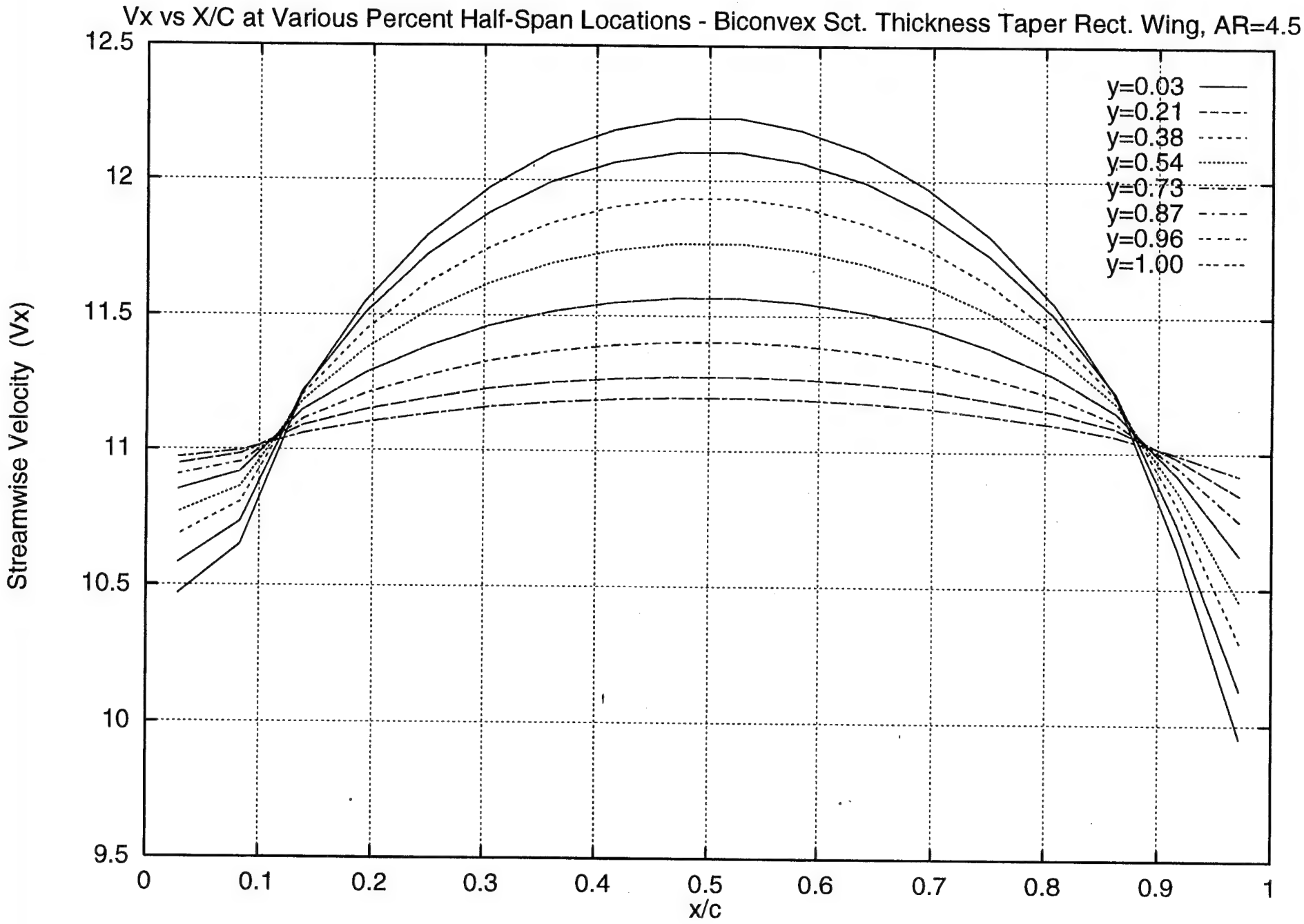
Vx vs X/C at Various Percent Half-Span Locations - Biconvex Sct. Thickness Taper Rect. Wing, AR=4.5
Streamwise Velocity (Vx)
x/c
y=0.03
y=0.21
y=0.38
y=0.54
y=0.73
y=0.87
y=0.96
y=1.00
12.5
12
11.5
11
10.5
10
9.5
0
0.1
0.2
0.3
0.4
0.5
0.6
0.7
0.8
0.9
1

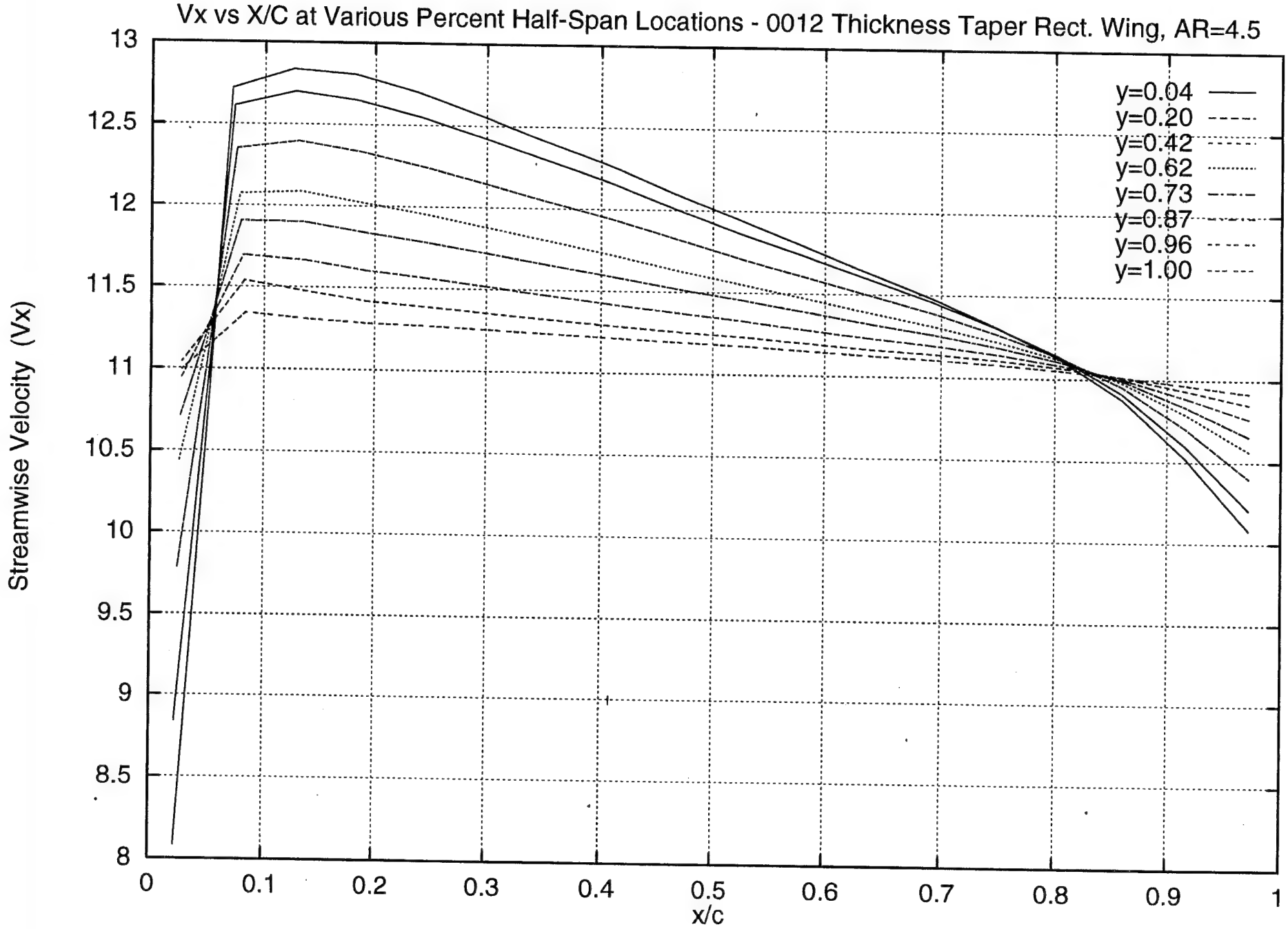
Vx vs X/C at Various Percent Half-Span Locations - 0012 Thickness Taper Rect. Wing, AR=4.5
Streamwise Velocity (Vx)
x/c
y=0.04
y=0.20
y=0.42
y=0.62
y=0.73
y=0.87
y=0.96
y=1.00
13
12.5
12
11.5
11
10.5
10
9.5
9
8.5
8
0
0.1
0.2
0.3
0.4
0.5
0.6
0.7
0.8
0.9
1

APPENDIX E. SPANWISE CROSS-SECTIONAL AREA CODE

This appendix present the MATLAB computer code created to transform the chordwise section definition of the F5 wing into 41 spanwise cross-sectional areas. As can be seen, the program 's input requirements are the x, y, and z coordinates of the cross-sections. The y coordinates can be taken from the PMARC output file, which by virtue of its construction delineate some of the geometry parameters. Also required in the input are the sweep angle and span. Section **B-6-a** of chapter **IV** details how the code operates.

This code could be used on other wings than the F5 providing the input data mentioned above is updated as well as some other parameters scattered within the code. It could become advantageous to bring all variables that are now scattered in the code at the beginning of the file so it is a lot easier to adapt to other wings. Section **B-6-b** of chapter **IV** explains why the program is presently geared more towards the F5 wing.

```
%       This MATLAB program tranforms the chordwise coordinates of a F5 wing
% into the spanwise coordinates in an effort to calculate the area of specified
% spanwise sections. The latter will be used in an area rule/body of revolution
% study using the PMARC and NAVIER-STOKES softwares.
%
% By Alain Carrier. Start : 10 Jul 1995
%                   Finish: 19 Jul 1995
%
%_____________________________________________________________________

% MISC VARIABLES
% --------------

lambda=32.6*pi/180;

% CHORDWISE SECTION DEFINITION IN PERCENTAGE OF CHORD
% ---------------------------------------------------
% (x & z from 'F5wing_ShpTE.in', y from 'F5wing_ShpTE.DATA6')

x =      [0.0000    0.0050    0.0149    0.0248    0.0348    0.0447    0.0596 ...
          0.0795    0.0993    0.1291    0.1589    0.1887    0.2185    0.2483 ...
          0.2781    0.3079    0.3377    0.3675    0.3973    0.4271    0.4569 ...
          0.4867    0.5165    0.5463    0.5761    0.6059    0.6357    0.6655 ...
          0.6953    0.7251    0.7549    0.7847    0.8145    0.8443    0.8741 ...
          0.9039    0.9287    0.9535    0.9734    0.9933    1.0000];

y =      [0.0330    0.0970    0.1610    0.2230    0.2820    0.3390    0.3910 ...
          0.4400    0.4830    0.5210    0.5540    0.5800    0.6010    0.6140 ...
          0.6210];

zbot = [-0.0099   -0.0136   -0.0154   -0.0163   -0.0169   -0.0174   -0.0180 ...
         -0.0185   -0.0190   -0.0196   -0.0202   -0.0208   -0.0214   -0.0220 ...
         -0.0225   -0.0230   -0.0234   -0.0237   -0.0238   -0.0239   -0.0238 ...
         -0.0236   -0.0232   -0.0226   -0.0220   -0.0211   -0.0201   -0.0190 ...
         -0.0177   -0.0163   -0.0148   -0.0132   -0.0115   -0.0098   -0.0080 ...
         -0.0061   -0.0045   -0.0029   -0.0016   -0.0004    0.0000];

ztop = [-0.0099   -0.0057   -0.0031   -0.0009    0.0010    0.0028    0.0052 ...
          0.0080    0.0104    0.0135    0.0160    0.0181    0.0198    0.0211 ...
          0.0221    0.0229    0.0235    0.0238    0.0240    0.0240    0.0239 ...
          0.0236    0.0232    0.0226    0.0219    0.0210    0.0201    0.0190 ...
          0.0177    0.0163    0.0149    0.0133    0.0116    0.0098    0.0080 ...
          0.0060    0.0045    0.0029    0.0016    0.0004    0.0000];

% CHORDWISE PANEL WIDTH
% ---------------------

colwidth(1)=y(1)*2;
colwidth(2)=(y(2)-colwidth(1))*2;
for i=3:15
 colwidth(i)=(y(i)-(y(i-1)+colwidth(i-1)/2))*2;
end

% CHORDWISE STARTING POINT OF PANEL STRIP EDGES
% ---------------------------------------------

xtransl(1)=colwidth(1)*tan(lambda);
for i=2:15
 xtransl(i)=colwidth(i)*tan(lambda)+xtransl(i-1);
end                                    % NOTE: xtransl(15) should=0.3982


% CHORDWISE PANEL STRIP EDGES COORDINATES - NON TRANSLATED
% --------------------------------------------------------
% (Non translated means all sections strarting points are at x=0)

% ...FOR ROOT AND TIP
% ~~~~~~~~~~~~~~~~~~~

chsct_xroot=0.6439*x;
chsct_yroot=0;
chsct_zbotroot=0.6439*zbot;
chsct_ztoproot=0.6439*ztop;

chsct_x15=0.1983*x;
chsct_y15=0.6226;
```



```
chsct_zbot15=0.1983*zbot;
chsct_ztop15=0.1983*ztop;

% ...FOR WING SECTIONS BETWEEN ROOT AND TIP
% ~~~~~~~~~~~~~~~~~~~~~~~~~~~~~~~~~~~~~~~~~

chsct_y(1)=colwidth(1);
for i=2:14
 chsct_y(i)=chsct_y(i-1)+colwidth(i);
end

for i=1:14
 scale(i)=0.1983+0.7157*(0.6226-chsct_y(i));
end
%diff=0.1983-scale(15)   % Check to see if Diff is zero as it should.


chsct_x1=scale(1)*x;
chsct_x2=scale(2)*x;
chsct_x3=scale(3)*x;
chsct_x4=scale(4)*x;
chsct_x5=scale(5)*x;
chsct_x6=scale(6)*x;
chsct_x7=scale(7)*x;
chsct_x8=scale(8)*x;
chsct_x9=scale(9)*x;
chsct_x10=scale(10)*x;
chsct_x11=scale(11)*x;
chsct_x12=scale(12)*x;
chsct_x13=scale(13)*x;
chsct_x14=scale(14)*x;

chsct_zbot1=scale(1)*zbot;
chsct_zbot2=scale(2)*zbot;
chsct_zbot3=scale(3)*zbot;
chsct_zbot4=scale(4)*zbot;
chsct_zbot5=scale(5)*zbot;
chsct_zbot6=scale(6)*zbot;
chsct_zbot7=scale(7)*zbot;
chsct_zbot8=scale(8)*zbot;
chsct_zbot9=scale(9)*zbot;
chsct_zbot10=scale(10)*zbot;
chsct_zbot11=scale(11)*zbot;
chsct_zbot12=scale(12)*zbot;
chsct_zbot13=scale(13)*zbot;
chsct_zbot14=scale(14)*zbot;

chsct_ztop1=scale(1)*ztop;
chsct_ztop2=scale(2)*ztop;
chsct_ztop3=scale(3)*ztop;
chsct_ztop4=scale(4)*ztop;
chsct_ztop5=scale(5)*ztop;
chsct_ztop6=scale(6)*ztop;
chsct_ztop7=scale(7)*ztop;
chsct_ztop8=scale(8)*ztop;
chsct_ztop9=scale(9)*ztop;
chsct_ztop10=scale(10)*ztop;
chsct_ztop11=scale(11)*ztop;
chsct_ztop12=scale(12)*ztop;
chsct_ztop13=scale(13)*ztop;
chsct_ztop14=scale(14)*ztop;


% TRANSLATING THE 'X' COORDINATES TO ACTUAL LOCATIONS
% ---------------------------------------------------

chsctAct_xroot=chsct_xroot;
chsctAct_x1=chsct_x1+xtransl(1);
chsctAct_x2=chsct_x2+xtransl(2);
chsctAct_x3=chsct_x3+xtransl(3);
chsctAct_x4=chsct_x4+xtransl(4);
chsctAct_x5=chsct_x5+xtransl(5);
chsctAct_x6=chsct_x6+xtransl(6);
chsctAct_x7=chsct_x7+xtransl(7);
chsctAct_x8=chsct_x8+xtransl(8);
```

```
chsctAct_x9=chsct_x9+xtransl(9);
chsctAct_x10=chsct_x10+xtransl(10);
chsctAct_x11=chsct_x11+xtransl(11);
chsctAct_x12=chsct_x12+xtransl(12);
chsctAct_x13=chsct_x13+xtransl(13);
chsctAct_x14=chsct_x14+xtransl(14);
chsctAct_x15=chsct_x15+xtransl(15);

% FITTING THE CHORDWISE SECTIONS ALONG THE SPAN
% ---------------------------------------------
% (xz plane - top and bottom)


xi=chsctAct_xroot(1):0.0001:chsctAct_xroot(41);
zibot=spline(chsctAct_xroot,chsct_zbotroot,xi);
zitop=spline(chsctAct_xroot,chsct_ztoproot,xi);
xzrootbot_crv=polyfit(xi,zibot,25);
xzrootop_crv=polyfit(xi,zitop,25);
%plot(chsctAct_xroot,chsct_zbotroot,'o',xi,zibot)
%plot(chsctAct_xroot,chsct_ztoproot,'o',xi,zitop)

xi=chsctAct_x1(1):0.0001:chsctAct_x1(41);
zibot=spline(chsctAct_x1,chsct_zbot1,xi);
zitop=spline(chsctAct_x1,chsct_ztop1,xi);
xz1bot_crv=polyfit(xi,zibot,35);
xz1top_crv=polyfit(xi,zitop,35);
%plot(chsctAct_x1,chsct_zbot1,'o',xi,zibot)
%plot(chsctAct_x1,chsct_ztop1,'o',xi,zitop)

xi=chsctAct_x2(1):0.0001:chsctAct_x2(41);
zibot=spline(chsctAct_x2,chsct_zbot2,xi);
zitop=spline(chsctAct_x2,chsct_ztop2,xi);
xz2bot_crv=polyfit(xi,zibot,50);
xz2top_crv=polyfit(xi,zitop,50);
%plot(chsctAct_x2,chsct_zbot2,'o',xi,zibot)
%plot(chsctAct_x2,chsct_ztop2,'o',xi,zitop)

xi=chsctAct_x3(1):0.0001:chsctAct_x3(41);
zibot=spline(chsctAct_x3,chsct_zbot3,xi);
zitop=spline(chsctAct_x3,chsct_ztop3,xi);
xz3bot_crv=polyfit(xi,zibot,20);
xz3top_crv=polyfit(xi,zitop,20);
%plot(chsctAct_x3,chsct_zbot3,'o',xi,zibot)
%plot(chsctAct_x3,chsct_ztop3,'o',xi,zitop)

xi=chsctAct_x4(1):0.0001:chsctAct_x4(41);
zibot=spline(chsctAct_x4,chsct_zbot4,xi);
zitop=spline(chsctAct_x4,chsct_ztop4,xi);
xz4bot_crv=polyfit(xi,zibot,25);
xz4top_crv=polyfit(xi,zitop,25);
%plot(chsctAct_x4,chsct_zbot4,'o',xi,zibot)
%plot(chsctAct_x4,chsct_ztop4,'o',xi,zitop)

xi=chsctAct_x5(1):0.0001:chsctAct_x5(41);
zibot=spline(chsctAct_x5,chsct_zbot5,xi);
zitop=spline(chsctAct_x5,chsct_ztop5,xi);
xz5bot_crv=polyfit(xi,zibot,35);
xz5top_crv=polyfit(xi,zitop,35);
%plot(chsctAct_x5,chsct_zbot5,'o',xi,zibot)
%plot(chsctAct_x5,chsct_ztop5,'o',xi,zitop)

xi=chsctAct_x6(1):0.0001:chsctAct_x6(41);
zibot=spline(chsctAct_x6,chsct_zbot6,xi);
zitop=spline(chsctAct_x6,chsct_ztop6,xi);
xz6bot_crv=polyfit(xi,zibot,25);
xz6top_crv=polyfit(xi,zitop,25);
%plot(chsctAct_x6,chsct_zbot6,'o',xi,zibot)
%plot(chsctAct_x6,chsct_ztop6,'o',xi,zitop)

xi=chsctAct_x7(1):0.0001:chsctAct_x7(41);
zibot=spline(chsctAct_x7,chsct_zbot7,xi);
zitop=spline(chsctAct_x7,chsct_ztop7,xi);
xz7bot_crv=polyfit(xi,zibot,25);
xz7top_crv=polyfit(xi,zitop,25);
%plot(chsctAct_x7,chsct_zbot7,'o',xi,zibot)
%plot(chsctAct_x7,chsct_ztop7,'o',xi,zitop)
```



```
xi=chsctAct_x8(1):0.0001:chsctAct_x8(41);
zibot=spline(chsctAct_x8,chsct_zbot8,xi);
zitop=spline(chsctAct_x8,chsct_ztop8,xi);
xz8bot_crv=polyfit(xi,zibot,20);
xz8top_crv=polyfit(xi,zitop,20);
%plot(chsctAct_x8,chsct_zbot8,'o',xi,zibot)
%plot(chsctAct_x8,chsct_ztop8,'o',xi,zitop)

xi=chsctAct_x9(1):0.0001:chsctAct_x9(41);
zibot=spline(chsctAct_x9,chsct_zbot9,xi);
zitop=spline(chsctAct_x9,chsct_ztop9,xi);
xz9bot_crv=polyfit(xi,zibot,30);
xz9top_crv=polyfit(xi,zitop,30);
%plot(chsctAct_x9,chsct_zbot9,'o',xi,zibot)
%plot(chsctAct_x9,chsct_ztop9,'o',xi,zitop)

xi=chsctAct_x10(1):0.0001:chsctAct_x10(41);
zibot=spline(chsctAct_x10,chsct_zbot10,xi);
zitop=spline(chsctAct_x10,chsct_ztop10,xi);
xz10bot_crv=polyfit(xi,zibot,40);
xz10top_crv=polyfit(xi,zitop,40);
%plot(chsctAct_x10,chsct_zbot10,'o',xi,zibot)
%plot(chsctAct_x10,chsct_ztop10,'o',xi,zitop)

xi=chsctAct_x11(1):0.0001:chsctAct_x11(41);
zibot=spline(chsctAct_x11,chsct_zbot11,xi);
zitop=spline(chsctAct_x11,chsct_ztop11,xi);
xz11bot_crv=polyfit(xi,zibot,25);
xz11top_crv=polyfit(xi,zitop,25);
%plot(chsctAct_x11,chsct_zbot11,'o',xi,zibot)
%plot(chsctAct_x11,chsct_ztop11,'o',xi,zitop)

xi=chsctAct_x12(1):0.0001:chsctAct_x12(41);
zibot=spline(chsctAct_x12,chsct_zbot12,xi);
zitop=spline(chsctAct_x12,chsct_ztop12,xi);
xz12bot_crv=polyfit(xi,zibot,15);
xz12top_crv=polyfit(xi,zitop,15);
%plot(chsctAct_x12,chsct_zbot12,'o',xi,zibot)
%plot(chsctAct_x12,chsct_ztop12,'o',xi,zitop)

xi=chsctAct_x13(1):0.0001:chsctAct_x13(41);
zibot=spline(chsctAct_x13,chsct_zbot13,xi);
zitop=spline(chsctAct_x13,chsct_ztop13,xi);
xz13bot_crv=polyfit(xi,zibot,20);
xz13top_crv=polyfit(xi,zitop,20);
%plot(chsctAct_x13,chsct_zbot13,'o',xi,zibot)
%plot(chsctAct_x13,chsct_ztop13,'o',xi,zitop)

xi=chsctAct_x14(1):0.0001:chsctAct_x14(41);
zibot=spline(chsctAct_x14,chsct_zbot14,xi);
zitop=spline(chsctAct_x14,chsct_ztop14,xi);
xz14bot_crv=polyfit(xi,zibot,15);
xz14top_crv=polyfit(xi,zitop,15);
%plot(chsctAct_x14,chsct_zbot14,'o',xi,zibot)
%plot(chsctAct_x14,chsct_ztop14,'o',xi,zitop)

xi=chsctAct_x15(1):0.0001:chsctAct_x15(41);
zibot=spline(chsctAct_x15,chsct_zbot15,xi);
zitop=spline(chsctAct_x15,chsct_ztop15,xi);
xz15bot_crv=polyfit(xi,zibot,10);
xz15top_crv=polyfit(xi,zitop,10);
%plot(chsctAct_x15,chsct_zbot15,'o',xi,zibot)
%plot(chsctAct_x15,chsct_ztop15,'o',xi,zitop)

% CREATING AND FITTING THE SPANWISE SECTIONS ALONG THE CHORD
% ----------------------------------------------------------
% (41 sections + root LE & TE points for one side of 'x' axis)

% ...AT THE ROOT LEADING EDGE (ONE POINT)
% ---------------------------------------

spsct_xbotLE=0;
spsct_ybotLE=0;
spsct_zbotLE=polyval(xzrootbot_crv,0);
```

```
spsct_xtopLE=0;
spsct_ytopLE=0;
spsct_ztopLE=polyval(xzroottop_crv,0);

% ...FOR SECTION 1 (TWO POINTS)
% ~~~~~~~~~~~~~~~~~~~~~~~~~~~~~

 spsct_xbot1(1)=xtransl(1);
 spsct_xbot1(2)=xtransl(1);

 spsct_ybot1(1)=0;
 spsct_ybot1(2)=colwidth(1);

 spsct_zbot1(1)=polyval(xzrootbot_crv,spsct_xbot1(1));
 spsct_zbot1(2)=polyval(xz1bot_crv,spsct_xbot1(2));

%................................................

 spsct_xtop1(1)=xtransl(1);
 spsct_xtop1(2)=xtransl(1);

 spsct_ytop1(1)=0;
 spsct_ytop1(2)=colwidth(1);

 spsct_ztop1(1)=polyval(xzroottop_crv,spsct_xtop1(1));
 spsct_ztop1(2)=polyval(xz1top_crv,spsct_xtop1(2));


% ...FOR SECTION 2 (THREE POINTS)
% ~~~~~~~~~~~~~~~~~~~~~~~~~~~~~~~

spsct_xbot2(1)=xtransl(2);
spsct_xbot2(2)=xtransl(2);
spsct_xbot2(3)=xtransl(2);

spsct_ybot2(1)=0;
spsct_ybot2(2)=colwidth(1);
spsct_ybot2(3)=spsct_ybot2(2)+colwidth(2);

spsct_zbot2(1)=polyval(xzrootbot_crv,spsct_xbot2(1));
spsct_zbot2(2)=polyval(xz1bot_crv,spsct_xbot2(2));
spsct_zbot2(3)=polyval(xz2bot_crv,spsct_xbot2(3));

%................................................

spsct_xtop2(1)=xtransl(2);
spsct_xtop2(2)=xtransl(2);
spsct_xtop2(3)=xtransl(2);

spsct_ytop2(1)=0;
spsct_ytop2(2)=colwidth(1);
spsct_ytop2(3)=spsct_ytop2(2)+colwidth(2);

spsct_ztop2(1)=polyval(xzroottop_crv,spsct_xtop2(1));
spsct_ztop2(2)=polyval(xz1top_crv,spsct_xtop2(2));
spsct_ztop2(3)=polyval(xz2top_crv,spsct_xtop2(3));

% ...FOR SECTION 3 (FOUR POINTS)
% ~~~~~~~~~~~~~~~~~~~~~~~~~~~~~~

for i=1:4
 spsct_xbot3(i)=xtransl(3);
end

spsct_ybot3(1)=0;
spsct_ybot3(2)=colwidth(1);
for i=3:4
 spsct_ybot3(i)=spsct_ybot3(i-1)+colwidth(i-1);
end

spsct_zbot3(1)=polyval(xzrootbot_crv,spsct_xbot3(1));
spsct_zbot3(2)=polyval(xz1bot_crv,spsct_xbot3(2));
spsct_zbot3(3)=polyval(xz2bot_crv,spsct_xbot3(3));
spsct_zbot3(4)=polyval(xz3bot_crv,spsct_xbot3(4));

%................................................
```



```
for i=1:4
 spsct_xtop3(i)=xtransl(3);
end

spsct_ytop3(1)=0;
spsct_ytop3(2)=colwidth(1);
for i=3:4
 spsct_ytop3(i)=spsct_ytop3(i-1)+colwidth(i-1);
end

spsct_ztop3(1)=polyval(xzroottop_crv,spsct_xtop3(1));
spsct_ztop3(2)=polyval(xz1top_crv,spsct_xtop3(2));
spsct_ztop3(3)=polyval(xz2top_crv,spsct_xtop3(3));
spsct_ztop3(4)=polyval(xz3top_crv,spsct_xtop3(4));

% ...FOR SECTION 4 (FIVE POINTS)
% ~~~~~~~~~~~~~~~~~~~~~~~~~~~~~~

for i=1:5
 spsct_xbot4(i)=xtransl(4);
end

spsct_ybot4(1)=0;
spsct_ybot4(2)=colwidth(1);
for i=3:5
 spsct_ybot4(i)=spsct_ybot4(i-1)+colwidth(i-1);
end

spsct_zbot4(1)=polyval(xzrootbot_crv,spsct_xbot4(1));
spsct_zbot4(2)=polyval(xz1bot_crv,spsct_xbot4(2));
spsct_zbot4(3)=polyval(xz2bot_crv,spsct_xbot4(3));
spsct_zbot4(4)=polyval(xz3bot_crv,spsct_xbot4(4));
spsct_zbot4(5)=polyval(xz4bot_crv,spsct_xbot4(5));

%................................................

for i=1:5
 spsct_xtop4(i)=xtransl(4);
end

spsct_ytop4(1)=0;
spsct_ytop4(2)=colwidth(1);
for i=3:5
 spsct_ytop4(i)=spsct_ytop4(i-1)+colwidth(i-1);
end

spsct_ztop4(1)=polyval(xzroottop_crv,spsct_xtop4(1));
spsct_ztop4(2)=polyval(xz1top_crv,spsct_xtop4(2));
spsct_ztop4(3)=polyval(xz2top_crv,spsct_xtop4(3));
spsct_ztop4(4)=polyval(xz3top_crv,spsct_xtop4(4));
spsct_ztop4(5)=polyval(xz4top_crv,spsct_xtop4(5));

% ...FOR SECTION 5 (SIX POINTS)
% ~~~~~~~~~~~~~~~~~~~~~~~~~~~~~

for i=1:6
 spsct_xbot5(i)=xtransl(5);
end

spsct_ybot5(1)=0;
spsct_ybot5(2)=colwidth(1);
for i=3:6
 spsct_ybot5(i)=spsct_ybot5(i-1)+colwidth(i-1);
end

spsct_zbot5(1)=polyval(xzrootbot_crv,spsct_xbot5(1));
spsct_zbot5(2)=polyval(xz1bot_crv,spsct_xbot5(2));
spsct_zbot5(3)=polyval(xz2bot_crv,spsct_xbot5(3));
spsct_zbot5(4)=polyval(xz3bot_crv,spsct_xbot5(4));
spsct_zbot5(5)=polyval(xz4bot_crv,spsct_xbot5(5));
spsct_zbot5(6)=polyval(xz5bot_crv,spsct_xbot5(6));

%................................................

for i=1:6
```

```
 spsct_xtop5(i)=xtransl(5);
end

spsct_ytop5(1)=0;
spsct_ytop5(2)=colwidth(1);
for i=3:6
 spsct_ytop5(i)=spsct_ytop5(i-1)+colwidth(i-1);
end

spsct_ztop5(1)=polyval(xzroottop_crv,spsct_xtop5(1));
spsct_ztop5(2)=polyval(xz1top_crv,spsct_xtop5(2));
spsct_ztop5(3)=polyval(xz2top_crv,spsct_xtop5(3));
spsct_ztop5(4)=polyval(xz3top_crv,spsct_xtop5(4));
spsct_ztop5(5)=polyval(xz4top_crv,spsct_xtop5(5));
spsct_ztop5(6)=polyval(xz5top_crv,spsct_xtop5(6));

% ...FOR SECTION 6 (SEVEN POINTS)
% ~~~~~~~~~~~~~~~~~~~~~~~~~~~~~~~

for i=1:7
 spsct_xbot6(i)=xtransl(6);
end

spsct_ybot6(1)=0;
spsct_ybot6(2)=colwidth(1);
for i=3:7
 spsct_ybot6(i)=spsct_ybot6(i-1)+colwidth(i-1);
end

spsct_zbot6(1)=polyval(xzrootbot_crv,spsct_xbot6(1));
spsct_zbot6(2)=polyval(xz1bot_crv,spsct_xbot6(2));
spsct_zbot6(3)=polyval(xz2bot_crv,spsct_xbot6(3));
spsct_zbot6(4)=polyval(xz3bot_crv,spsct_xbot6(4));
spsct_zbot6(5)=polyval(xz4bot_crv,spsct_xbot6(5));
spsct_zbot6(6)=polyval(xz5bot_crv,spsct_xbot6(6));
spsct_zbot6(7)=polyval(xz6bot_crv,spsct_xbot6(7));

%.................................................

for i=1:7
 spsct_xtop6(i)=xtransl(6);
end

spsct_ytop6(1)=0;
spsct_ytop6(2)=colwidth(1);
for i=3:7
 spsct_ytop6(i)=spsct_ytop6(i-1)+colwidth(i-1);
end

spsct_ztop6(1)=polyval(xzroottop_crv,spsct_xtop6(1));
spsct_ztop6(2)=polyval(xz1top_crv,spsct_xtop6(2));
spsct_ztop6(3)=polyval(xz2top_crv,spsct_xtop6(3));
spsct_ztop6(4)=polyval(xz3top_crv,spsct_xtop6(4));
spsct_ztop6(5)=polyval(xz4top_crv,spsct_xtop6(5));
spsct_ztop6(6)=polyval(xz5top_crv,spsct_xtop6(6));
spsct_ztop6(7)=polyval(xz6top_crv,spsct_xtop6(7));

% ...FOR SECTION 7 (EIGHT POINTS)
% ~~~~~~~~~~~~~~~~~~~~~~~~~~~~~~~

for i=1:8
 spsct_xbot7(i)=xtransl(7);
end

spsct_ybot7(1)=0;
spsct_ybot7(2)=colwidth(1);
for i=3:8
 spsct_ybot7(i)=spsct_ybot7(i-1)+colwidth(i-1);
end

spsct_zbot7(1)=polyval(xzrootbot_crv,spsct_xbot7(1));
spsct_zbot7(2)=polyval(xz1bot_crv,spsct_xbot7(2));
spsct_zbot7(3)=polyval(xz2bot_crv,spsct_xbot7(3));
spsct_zbot7(4)=polyval(xz3bot_crv,spsct_xbot7(4));
spsct_zbot7(5)=polyval(xz4bot_crv,spsct_xbot7(5));
spsct_zbot7(6)=polyval(xz5bot_crv,spsct_xbot7(6));
```



```
spsct_zbot7(7)=polyval(xz6bot_crv,spsct_xbot7(7));
spsct_zbot7(8)=polyval(xz7bot_crv,spsct_xbot7(8));

%.................................................

for i=1:8
 spsct_xtop7(i)=xtransl(7);
end

spsct_ytop7(1)=0;
spsct_ytop7(2)=colwidth(1);
for i=3:8
 spsct_ytop7(i)=spsct_ytop7(i-1)+colwidth(i-1);
end

spsct_ztop7(1)=polyval(xzroottop_crv,spsct_xtop7(1));
spsct_ztop7(2)=polyval(xz1top_crv,spsct_xtop7(2));
spsct_ztop7(3)=polyval(xz2top_crv,spsct_xtop7(3));
spsct_ztop7(4)=polyval(xz3top_crv,spsct_xtop7(4));
spsct_ztop7(5)=polyval(xz4top_crv,spsct_xtop7(5));
spsct_ztop7(6)=polyval(xz5top_crv,spsct_xtop7(6));
spsct_ztop7(7)=polyval(xz6top_crv,spsct_xtop7(7));
spsct_ztop7(8)=polyval(xz7top_crv,spsct_xtop7(8));

% ...FOR SECTION 8 (NINE POINTS)
% ~~~~~~~~~~~~~~~~~~~~~~~~~~~~~~

for i=1:9
 spsct_xbot8(i)=xtransl(8);
end

spsct_ybot8(1)=0;
spsct_ybot8(2)=colwidth(1);
for i=3:9
 spsct_ybot8(i)=spsct_ybot8(i-1)+colwidth(i-1);
end

spsct_zbot8(1)=polyval(xzrootbot_crv,spsct_xbot8(1));
spsct_zbot8(2)=polyval(xz1bot_crv,spsct_xbot8(2));
spsct_zbot8(3)=polyval(xz2bot_crv,spsct_xbot8(3));
spsct_zbot8(4)=polyval(xz3bot_crv,spsct_xbot8(4));
spsct_zbot8(5)=polyval(xz4bot_crv,spsct_xbot8(5));
spsct_zbot8(6)=polyval(xz5bot_crv,spsct_xbot8(6));
spsct_zbot8(7)=polyval(xz6bot_crv,spsct_xbot8(7));
spsct_zbot8(8)=polyval(xz7bot_crv,spsct_xbot8(8));
spsct_zbot8(9)=polyval(xz8bot_crv,spsct_xbot8(9));

%.................................................

for i=1:9
 spsct_xtop8(i)=xtransl(8);
end

spsct_ytop8(1)=0;
spsct_ytop8(2)=colwidth(1);
for i=3:9
 spsct_ytop8(i)=spsct_ytop8(i-1)+colwidth(i-1);
end

spsct_ztop8(1)=polyval(xzroottop_crv,spsct_xtop8(1));
spsct_ztop8(2)=polyval(xz1top_crv,spsct_xtop8(2));
spsct_ztop8(3)=polyval(xz2top_crv,spsct_xtop8(3));
spsct_ztop8(4)=polyval(xz3top_crv,spsct_xtop8(4));
spsct_ztop8(5)=polyval(xz4top_crv,spsct_xtop8(5));
spsct_ztop8(6)=polyval(xz5top_crv,spsct_xtop8(6));
spsct_ztop8(7)=polyval(xz6top_crv,spsct_xtop8(7));
spsct_ztop8(8)=polyval(xz7top_crv,spsct_xtop8(8));
spsct_ztop8(9)=polyval(xz8top_crv,spsct_xtop8(9));

% ...FOR SECTION 9 (TEN POINTS)
% ~~~~~~~~~~~~~~~~~~~~~~~~~~~~~

for i=1:10
 spsct_xbot9(i)=xtransl(9);
end
```

```
spsct_ybot9(1)=0;
spsct_ybot9(2)=colwidth(1);
for i=3:10
 spsct_ybot9(i)=spsct_ybot9(i-1)+colwidth(i-1);
end

spsct_zbot9(1)=polyval(xzrootbot_crv,spsct_xbot9(1));
spsct_zbot9(2)=polyval(xz1bot_crv,spsct_xbot9(2));
spsct_zbot9(3)=polyval(xz2bot_crv,spsct_xbot9(3));
spsct_zbot9(4)=polyval(xz3bot_crv,spsct_xbot9(4));
spsct_zbot9(5)=polyval(xz4bot_crv,spsct_xbot9(5));
spsct_zbot9(6)=polyval(xz5bot_crv,spsct_xbot9(6));
spsct_zbot9(7)=polyval(xz6bot_crv,spsct_xbot9(7));
spsct_zbot9(8)=polyval(xz7bot_crv,spsct_xbot9(8));
spsct_zbot9(9)=polyval(xz8bot_crv,spsct_xbot9(9));
spsct_zbot9(10)=polyval(xz9bot_crv,spsct_xbot9(10));

%.................................................

for i=1:10
 spsct_xtop9(i)=xtransl(9);
end

spsct_ytop9(1)=0;
spsct_ytop9(2)=colwidth(1);
for i=3:10
 spsct_ytop9(i)=spsct_ytop9(i-1)+colwidth(i-1);
end

spsct_ztop9(1)=polyval(xzroottop_crv,spsct_xtop9(1));
spsct_ztop9(2)=polyval(xz1top_crv,spsct_xtop9(2));
spsct_ztop9(3)=polyval(xz2top_crv,spsct_xtop9(3));
spsct_ztop9(4)=polyval(xz3top_crv,spsct_xtop9(4));
spsct_ztop9(5)=polyval(xz4top_crv,spsct_xtop9(5));
spsct_ztop9(6)=polyval(xz5top_crv,spsct_xtop9(6));
spsct_ztop9(7)=polyval(xz6top_crv,spsct_xtop9(7));
spsct_ztop9(8)=polyval(xz7top_crv,spsct_xtop9(8));
spsct_ztop9(9)=polyval(xz8top_crv,spsct_xtop9(9));
spsct_ztop9(10)=polyval(xz9top_crv,spsct_xtop9(10));

% ...FOR SECTION 10 (ELEVEN POINTS)
% ~~~~~~~~~~~~~~~~~~~~~~~~~~~~~~~~

for i=1:11
 spsct_xbot10(i)=xtransl(10);
end

spsct_ybot10(1)=0;
spsct_ybot10(2)=colwidth(1);
for i=3:11
 spsct_ybot10(i)=spsct_ybot10(i-1)+colwidth(i-1);
end

spsct_zbot10(1)=polyval(xzrootbot_crv,spsct_xbot10(1));
spsct_zbot10(2)=polyval(xz1bot_crv,spsct_xbot10(2));
spsct_zbot10(3)=polyval(xz2bot_crv,spsct_xbot10(3));
spsct_zbot10(4)=polyval(xz3bot_crv,spsct_xbot10(4));
spsct_zbot10(5)=polyval(xz4bot_crv,spsct_xbot10(5));
spsct_zbot10(6)=polyval(xz5bot_crv,spsct_xbot10(6));
spsct_zbot10(7)=polyval(xz6bot_crv,spsct_xbot10(7));
spsct_zbot10(8)=polyval(xz7bot_crv,spsct_xbot10(8));
spsct_zbot10(9)=polyval(xz8bot_crv,spsct_xbot10(9));
spsct_zbot10(10)=polyval(xz9bot_crv,spsct_xbot10(10));
spsct_zbot10(11)=polyval(xz10bot_crv,spsct_xbot10(11));

%.................................................

for i=1:11
 spsct_xtop10(i)=xtransl(10);
end

spsct_ytop10(1)=0;
spsct_ytop10(2)=colwidth(1);
for i=3:11
 spsct_ytop10(i)=spsct_ytop10(i-1)+colwidth(i-1);
end
```



```
spsct_ztop10(1)=polyval(xzroottop_crv,spsct_xtop10(1));
spsct_ztop10(2)=polyval(xz1top_crv,spsct_xtop10(2));
spsct_ztop10(3)=polyval(xz2top_crv,spsct_xtop10(3));
spsct_ztop10(4)=polyval(xz3top_crv,spsct_xtop10(4));
spsct_ztop10(5)=polyval(xz4top_crv,spsct_xtop10(5));
spsct_ztop10(6)=polyval(xz5top_crv,spsct_xtop10(6));
spsct_ztop10(7)=polyval(xz6top_crv,spsct_xtop10(7));
spsct_ztop10(8)=polyval(xz7top_crv,spsct_xtop10(8));
spsct_ztop10(9)=polyval(xz8top_crv,spsct_xtop10(9));
spsct_ztop10(10)=polyval(xz9top_crv,spsct_xtop10(10));
spsct_ztop10(11)=polyval(xz10top_crv,spsct_xtop10(11));

% ...FOR SECTION 11 (TWELVE POINTS)
% ~~~~~~~~~~~~~~~~~~~~~~~~~~~~~~~~

for i=1:12
 spsct_xbot11(i)=xtransl(11);
end

spsct_ybot11(1)=0;
spsct_ybot11(2)=colwidth(1);
for i=3:12
 spsct_ybot11(i)=spsct_ybot11(i-1)+colwidth(i-1);
end

spsct_zbot11(1)=polyval(xzrootbot_crv,spsct_xbot11(1));
spsct_zbot11(2)=polyval(xz1bot_crv,spsct_xbot11(2));
spsct_zbot11(3)=polyval(xz2bot_crv,spsct_xbot11(3));
spsct_zbot11(4)=polyval(xz3bot_crv,spsct_xbot11(4));
spsct_zbot11(5)=polyval(xz4bot_crv,spsct_xbot11(5));
spsct_zbot11(6)=polyval(xz5bot_crv,spsct_xbot11(6));
spsct_zbot11(7)=polyval(xz6bot_crv,spsct_xbot11(7));
spsct_zbot11(8)=polyval(xz7bot_crv,spsct_xbot11(8));
spsct_zbot11(9)=polyval(xz8bot_crv,spsct_xbot11(9));
spsct_zbot11(10)=polyval(xz9bot_crv,spsct_xbot11(10));
spsct_zbot11(11)=polyval(xz10bot_crv,spsct_xbot11(11));
spsct_zbot11(12)=polyval(xz11bot_crv,spsct_xbot11(12));

%.................................................

for i=1:12
 spsct_xtop11(i)=xtransl(11);
end

spsct_ytop11(1)=0;
spsct_ytop11(2)=colwidth(1);
for i=3:12
 spsct_ytop11(i)=spsct_ytop11(i-1)+colwidth(i-1);
end

spsct_ztop11(1)=polyval(xzroottop_crv,spsct_xtop11(1));
spsct_ztop11(2)=polyval(xz1top_crv,spsct_xtop11(2));
spsct_ztop11(3)=polyval(xz2top_crv,spsct_xtop11(3));
spsct_ztop11(4)=polyval(xz3top_crv,spsct_xtop11(4));
spsct_ztop11(5)=polyval(xz4top_crv,spsct_xtop11(5));
spsct_ztop11(6)=polyval(xz5top_crv,spsct_xtop11(6));
spsct_ztop11(7)=polyval(xz6top_crv,spsct_xtop11(7));
spsct_ztop11(8)=polyval(xz7top_crv,spsct_xtop11(8));
spsct_ztop11(9)=polyval(xz8top_crv,spsct_xtop11(9));
spsct_ztop11(10)=polyval(xz9top_crv,spsct_xtop11(10));
spsct_ztop11(11)=polyval(xz10top_crv,spsct_xtop11(11));
spsct_ztop11(12)=polyval(xz11top_crv,spsct_xtop11(12));

% ...FOR SECTION 12 (THIRTEEN POINTS)
% ~~~~~~~~~~~~~~~~~~~~~~~~~~~~~~~~~~

for i=1:13
 spsct_xbot12(i)=xtransl(12);
end

spsct_ybot12(1)=0;
spsct_ybot12(2)=colwidth(1);
for i=3:13
 spsct_ybot12(i)=spsct_ybot12(i-1)+colwidth(i-1);
end
```

```
spsct_zbot12(1)=polyval(xzrootbot_crv,spsct_xbot12(1));
spsct_zbot12(2)=polyval(xz1bot_crv,spsct_xbot12(2));
spsct_zbot12(3)=polyval(xz2bot_crv,spsct_xbot12(3));
spsct_zbot12(4)=polyval(xz3bot_crv,spsct_xbot12(4));
spsct_zbot12(5)=polyval(xz4bot_crv,spsct_xbot12(5));
spsct_zbot12(6)=polyval(xz5bot_crv,spsct_xbot12(6));
spsct_zbot12(7)=polyval(xz6bot_crv,spsct_xbot12(7));
spsct_zbot12(8)=polyval(xz7bot_crv,spsct_xbot12(8));
spsct_zbot12(9)=polyval(xz8bot_crv,spsct_xbot12(9));
spsct_zbot12(10)=polyval(xz9bot_crv,spsct_xbot12(10));
spsct_zbot12(11)=polyval(xz10bot_crv,spsct_xbot12(11));
spsct_zbot12(12)=polyval(xz11bot_crv,spsct_xbot12(12));
spsct_zbot12(13)=polyval(xz12bot_crv,spsct_xbot12(13));

%.................................................

for i=1:13
 spsct_xtop12(i)=xtransl(12);
end

spsct_ytop12(1)=0;
spsct_ytop12(2)=colwidth(1);
for i=3:13
 spsct_ytop12(i)=spsct_ytop12(i-1)+colwidth(i-1);
end

spsct_ztop12(1)=polyval(xzroottop_crv,spsct_xtop12(1));
spsct_ztop12(2)=polyval(xz1top_crv,spsct_xtop12(2));
spsct_ztop12(3)=polyval(xz2top_crv,spsct_xtop12(3));
spsct_ztop12(4)=polyval(xz3top_crv,spsct_xtop12(4));
spsct_ztop12(5)=polyval(xz4top_crv,spsct_xtop12(5));
spsct_ztop12(6)=polyval(xz5top_crv,spsct_xtop12(6));
spsct_ztop12(7)=polyval(xz6top_crv,spsct_xtop12(7));
spsct_ztop12(8)=polyval(xz7top_crv,spsct_xtop12(8));
spsct_ztop12(9)=polyval(xz8top_crv,spsct_xtop12(9));
spsct_ztop12(10)=polyval(xz9top_crv,spsct_xtop12(10));
spsct_ztop12(11)=polyval(xz10top_crv,spsct_xtop12(11));
spsct_ztop12(12)=polyval(xz11top_crv,spsct_xtop12(12));
spsct_ztop12(13)=polyval(xz12top_crv,spsct_xtop12(13));

% ...FOR SECTION 13 (FOURTHEEN POINTS)
% ~~~~~~~~~~~~~~~~~~~~~~~~~~~~~~~~~~~

for i=1:14
 spsct_xbot13(i)=xtransl(13);
end

spsct_ybot13(1)=0;
spsct_ybot13(2)=colwidth(1);
for i=3:14
 spsct_ybot13(i)=spsct_ybot13(i-1)+colwidth(i-1);
end

spsct_zbot13(1)=polyval(xzrootbot_crv,spsct_xbot13(1));
spsct_zbot13(2)=polyval(xz1bot_crv,spsct_xbot13(2));
spsct_zbot13(3)=polyval(xz2bot_crv,spsct_xbot13(3));
spsct_zbot13(4)=polyval(xz3bot_crv,spsct_xbot13(4));
spsct_zbot13(5)=polyval(xz4bot_crv,spsct_xbot13(5));
spsct_zbot13(6)=polyval(xz5bot_crv,spsct_xbot13(6));
spsct_zbot13(7)=polyval(xz6bot_crv,spsct_xbot13(7));
spsct_zbot13(8)=polyval(xz7bot_crv,spsct_xbot13(8));
spsct_zbot13(9)=polyval(xz8bot_crv,spsct_xbot13(9));
spsct_zbot13(10)=polyval(xz9bot_crv,spsct_xbot13(10));
spsct_zbot13(11)=polyval(xz10bot_crv,spsct_xbot13(11));
spsct_zbot13(12)=polyval(xz11bot_crv,spsct_xbot13(12));
spsct_zbot13(13)=polyval(xz12bot_crv,spsct_xbot13(13));
spsct_zbot13(14)=polyval(xz13bot_crv,spsct_xbot13(14));

%.................................................

for i=1:14
 spsct_xtop13(i)=xtransl(13);
end

spsct_ytop13(1)=0;
```



```
spsct_ytop13(2)=colwidth(1);
for i=3:14
 spsct_ytop13(i)=spsct_ytop13(i-1)+colwidth(i-1);
end

spsct_ztop13(1)=polyval(xzroottop_crv,spsct_xtop13(1));
spsct_ztop13(2)=polyval(xz1top_crv,spsct_xtop13(2));
spsct_ztop13(3)=polyval(xz2top_crv,spsct_xtop13(3));
spsct_ztop13(4)=polyval(xz3top_crv,spsct_xtop13(4));
spsct_ztop13(5)=polyval(xz4top_crv,spsct_xtop13(5));
spsct_ztop13(6)=polyval(xz5top_crv,spsct_xtop13(6));
spsct_ztop13(7)=polyval(xz6top_crv,spsct_xtop13(7));
spsct_ztop13(8)=polyval(xz7top_crv,spsct_xtop13(8));
spsct_ztop13(9)=polyval(xz8top_crv,spsct_xtop13(9));
spsct_ztop13(10)=polyval(xz9top_crv,spsct_xtop13(10));
spsct_ztop13(11)=polyval(xz10top_crv,spsct_xtop13(11));
spsct_ztop13(12)=polyval(xz11top_crv,spsct_xtop13(12));
spsct_ztop13(13)=polyval(xz12top_crv,spsct_xtop13(13));
spsct_ztop13(14)=polyval(xz13top_crv,spsct_xtop13(14));

% ...FOR SECTION 14 (FIFTEEN POINTS)
% ~~~~~~~~~~~~~~~~~~~~~~~~~~~~~~~~~

for i=1:15
 spsct_xbot14(i)=xtransl(14);
end

spsct_ybot14(1)=0;
spsct_ybot14(2)=colwidth(1);
for i=3:15
 spsct_ybot14(i)=spsct_ybot14(i-1)+colwidth(i-1);
end

spsct_zbot14(1)=polyval(xzrootbot_crv,spsct_xbot14(1));
spsct_zbot14(2)=polyval(xz1bot_crv,spsct_xbot14(2));
spsct_zbot14(3)=polyval(xz2bot_crv,spsct_xbot14(3));
spsct_zbot14(4)=polyval(xz3bot_crv,spsct_xbot14(4));
spsct_zbot14(5)=polyval(xz4bot_crv,spsct_xbot14(5));
spsct_zbot14(6)=polyval(xz5bot_crv,spsct_xbot14(6));
spsct_zbot14(7)=polyval(xz6bot_crv,spsct_xbot14(7));
spsct_zbot14(8)=polyval(xz7bot_crv,spsct_xbot14(8));
spsct_zbot14(9)=polyval(xz8bot_crv,spsct_xbot14(9));
spsct_zbot14(10)=polyval(xz9bot_crv,spsct_xbot14(10));
spsct_zbot14(11)=polyval(xz10bot_crv,spsct_xbot14(11));
spsct_zbot14(12)=polyval(xz11bot_crv,spsct_xbot14(12));
spsct_zbot14(13)=polyval(xz12bot_crv,spsct_xbot14(13));
spsct_zbot14(14)=polyval(xz13bot_crv,spsct_xbot14(14));
spsct_zbot14(15)=polyval(xz14bot_crv,spsct_xbot14(15));

%.................................................

for i=1:15
 spsct_xtop14(i)=xtransl(14);
end

spsct_ytop14(1)=0;
spsct_ytop14(2)=colwidth(1);
for i=3:15
 spsct_ytop14(i)=spsct_ytop14(i-1)+colwidth(i-1);
end

spsct_ztop14(1)=polyval(xzroottop_crv,spsct_xtop14(1));
spsct_ztop14(2)=polyval(xz1top_crv,spsct_xtop14(2));
spsct_ztop14(3)=polyval(xz2top_crv,spsct_xtop14(3));
spsct_ztop14(4)=polyval(xz3top_crv,spsct_xtop14(4));
spsct_ztop14(5)=polyval(xz4top_crv,spsct_xtop14(5));
spsct_ztop14(6)=polyval(xz5top_crv,spsct_xtop14(6));
spsct_ztop14(7)=polyval(xz6top_crv,spsct_xtop14(7));
spsct_ztop14(8)=polyval(xz7top_crv,spsct_xtop14(8));
spsct_ztop14(9)=polyval(xz8top_crv,spsct_xtop14(9));
spsct_ztop14(10)=polyval(xz9top_crv,spsct_xtop14(10));
spsct_ztop14(11)=polyval(xz10top_crv,spsct_xtop14(11));
spsct_ztop14(12)=polyval(xz11top_crv,spsct_xtop14(12));
spsct_ztop14(13)=polyval(xz12top_crv,spsct_xtop14(13));
spsct_ztop14(14)=polyval(xz13top_crv,spsct_xtop14(14));
spsct_ztop14(15)=polyval(xz14top_crv,spsct_xtop14(15));
```

```
% ...FOR SECTION 15 (SIXTEEN POINTS)
% ~~~~~~~~~~~~~~~~~~~~~~~~~~~~~~~~~~
% (From tip LE to tip TE)

for i=1:16
 spsct_xbot15(i)=xtransl(15);            % =0.3982 ?
end

spsct_ybot15(1)=0;
spsct_ybot15(2)=colwidth(1);
for i=3:16
 spsct_ybot15(i)=spsct_ybot15(i-1)+colwidth(i-1); % spsct_ybot15(16)=0.6226 ?
end

spsct_zbot15(1)=polyval(xzrootbot_crv,spsct_xbot15(1));
spsct_zbot15(2)=polyval(xz1bot_crv,spsct_xbot15(2));
spsct_zbot15(3)=polyval(xz2bot_crv,spsct_xbot15(3));
spsct_zbot15(4)=polyval(xz3bot_crv,spsct_xbot15(4));
spsct_zbot15(5)=polyval(xz4bot_crv,spsct_xbot15(5));
spsct_zbot15(6)=polyval(xz5bot_crv,spsct_xbot15(6));
spsct_zbot15(7)=polyval(xz6bot_crv,spsct_xbot15(7));
spsct_zbot15(8)=polyval(xz7bot_crv,spsct_xbot15(8));
spsct_zbot15(9)=polyval(xz8bot_crv,spsct_xbot15(9));
spsct_zbot15(10)=polyval(xz9bot_crv,spsct_xbot15(10));
spsct_zbot15(11)=polyval(xz10bot_crv,spsct_xbot15(11));
spsct_zbot15(12)=polyval(xz11bot_crv,spsct_xbot15(12));
spsct_zbot15(13)=polyval(xz12bot_crv,spsct_xbot15(13));
spsct_zbot15(14)=polyval(xz13bot_crv,spsct_xbot15(14));
spsct_zbot15(15)=polyval(xz14bot_crv,spsct_xbot15(15));
spsct_zbot15(16)=polyval(xz15bot_crv,spsct_xbot15(16));

%.................................................

for i=1:16
 spsct_xtop15(i)=xtransl(15);
end

spsct_ytop15(1)=0;
spsct_ytop15(2)=colwidth(1);
for i=3:16
 spsct_ytop15(i)=spsct_ytop15(i-1)+colwidth(i-1);  % spsct_ytop15(16)=0.6226 ?
end

spsct_ztop15(1)=polyval(xzroottop_crv,spsct_xtop15(1));
spsct_ztop15(2)=polyval(xz1top_crv,spsct_xtop15(2));
spsct_ztop15(3)=polyval(xz2top_crv,spsct_xtop15(3));
spsct_ztop15(4)=polyval(xz3top_crv,spsct_xtop15(4));
spsct_ztop15(5)=polyval(xz4top_crv,spsct_xtop15(5));
spsct_ztop15(6)=polyval(xz5top_crv,spsct_xtop15(6));
spsct_ztop15(7)=polyval(xz6top_crv,spsct_xtop15(7));
spsct_ztop15(8)=polyval(xz7top_crv,spsct_xtop15(8));
spsct_ztop15(9)=polyval(xz8top_crv,spsct_xtop15(9));
spsct_ztop15(10)=polyval(xz9top_crv,spsct_xtop15(10));
spsct_ztop15(11)=polyval(xz10top_crv,spsct_xtop15(11));
spsct_ztop15(12)=polyval(xz11top_crv,spsct_xtop15(12));
spsct_ztop15(13)=polyval(xz12top_crv,spsct_xtop15(13));
spsct_ztop15(14)=polyval(xz13top_crv,spsct_xtop15(14));
spsct_ztop15(15)=polyval(xz14top_crv,spsct_xtop15(15));
spsct_ztop15(16)=polyval(xz15top_crv,spsct_xtop15(16));

% ...FOR SECTION 16 (SIXTEEN POINTS)
% ~~~~~~~~~~~~~~~~~~~~~~~~~~~~~~~~~~
% (From tip LE to tip TE)

for i=1:16
 spsct_xbot16(i)=xtransl(15)+(0.1983/12);
end

spsct_ybot16(1)=0;
spsct_ybot16(2)=colwidth(1);
for i=3:16
 spsct_ybot16(i)=spsct_ybot16(i-1)+colwidth(i-1); % spsct_ybot16(16)=0.6226  ?
end

spsct_zbot16(1)=polyval(xzrootbot_crv,spsct_xbot16(1));
```



```
spsct_zbot16(2)=polyval(xz1bot_crv,spsct_xbot16(2));
spsct_zbot16(3)=polyval(xz2bot_crv,spsct_xbot16(3));
spsct_zbot16(4)=polyval(xz3bot_crv,spsct_xbot16(4));
spsct_zbot16(5)=polyval(xz4bot_crv,spsct_xbot16(5));
spsct_zbot16(6)=polyval(xz5bot_crv,spsct_xbot16(6));
spsct_zbot16(7)=polyval(xz6bot_crv,spsct_xbot16(7));
spsct_zbot16(8)=polyval(xz7bot_crv,spsct_xbot16(8));
spsct_zbot16(9)=polyval(xz8bot_crv,spsct_xbot16(9));
spsct_zbot16(10)=polyval(xz9bot_crv,spsct_xbot16(10));
spsct_zbot16(11)=polyval(xz10bot_crv,spsct_xbot16(11));
spsct_zbot16(12)=polyval(xz11bot_crv,spsct_xbot16(12));
spsct_zbot16(13)=polyval(xz12bot_crv,spsct_xbot16(13));
spsct_zbot16(14)=polyval(xz13bot_crv,spsct_xbot16(14));
spsct_zbot16(15)=polyval(xz14bot_crv,spsct_xbot16(15));
spsct_zbot16(16)=polyval(xz15bot_crv,spsct_xbot16(16));

%.................................................

for i=1:16
 spsct_xtop16(i)=xtransl(15)+(0.1983/12);
end

spsct_ytop16(1)=0;
spsct_ytop16(2)=colwidth(1);
for i=3:16
 spsct_ytop16(i)=spsct_ytop16(i-1)+colwidth(i-1);  % spsct_ytop16(16)=0.6226 ?
end

spsct_ztop16(1)=polyval(xzroottop_crv,spsct_xtop16(1));
spsct_ztop16(2)=polyval(xz1top_crv,spsct_xtop16(2));
spsct_ztop16(3)=polyval(xz2top_crv,spsct_xtop16(3));
spsct_ztop16(4)=polyval(xz3top_crv,spsct_xtop16(4));
spsct_ztop16(5)=polyval(xz4top_crv,spsct_xtop16(5));
spsct_ztop16(6)=polyval(xz5top_crv,spsct_xtop16(6));
spsct_ztop16(7)=polyval(xz6top_crv,spsct_xtop16(7));
spsct_ztop16(8)=polyval(xz7top_crv,spsct_xtop16(8));
spsct_ztop16(9)=polyval(xz8top_crv,spsct_xtop16(9));
spsct_ztop16(10)=polyval(xz9top_crv,spsct_xtop16(10));
spsct_ztop16(11)=polyval(xz10top_crv,spsct_xtop16(11));
spsct_ztop16(12)=polyval(xz11top_crv,spsct_xtop16(12));
spsct_ztop16(13)=polyval(xz12top_crv,spsct_xtop16(13));
spsct_ztop16(14)=polyval(xz13top_crv,spsct_xtop16(14));
spsct_ztop16(15)=polyval(xz14top_crv,spsct_xtop16(15));
spsct_ztop16(16)=polyval(xz15top_crv,spsct_xtop16(16));

% ...FOR SECTION 17 (SIXTEEN POINTS)
% ~~~~~~~~~~~~~~~~~~~~~~~~~~~~~~~~~~
% (From tip LE to tip TE)

for i=1:16
 spsct_xbot17(i)=xtransl(15)+2*(0.1983/12);
end

spsct_ybot17(1)=0;
spsct_ybot17(2)=colwidth(1);
for i=3:16
 spsct_ybot17(i)=spsct_ybot17(i-1)+colwidth(i-1); % spsct_ybot17(16)=0.6226  ?
end

spsct_zbot17(1)=polyval(xzrootbot_crv,spsct_xbot17(1));
spsct_zbot17(2)=polyval(xz1bot_crv,spsct_xbot17(2));
spsct_zbot17(3)=polyval(xz2bot_crv,spsct_xbot17(3));
spsct_zbot17(4)=polyval(xz3bot_crv,spsct_xbot17(4));
spsct_zbot17(5)=polyval(xz4bot_crv,spsct_xbot17(5));
spsct_zbot17(6)=polyval(xz5bot_crv,spsct_xbot17(6));
spsct_zbot17(7)=polyval(xz6bot_crv,spsct_xbot17(7));
spsct_zbot17(8)=polyval(xz7bot_crv,spsct_xbot17(8));
spsct_zbot17(9)=polyval(xz8bot_crv,spsct_xbot17(9));
spsct_zbot17(10)=polyval(xz9bot_crv,spsct_xbot17(10));
spsct_zbot17(11)=polyval(xz10bot_crv,spsct_xbot17(11));
spsct_zbot17(12)=polyval(xz11bot_crv,spsct_xbot17(12));
spsct_zbot17(13)=polyval(xz12bot_crv,spsct_xbot17(13));
spsct_zbot17(14)=polyval(xz13bot_crv,spsct_xbot17(14));
spsct_zbot17(15)=polyval(xz14bot_crv,spsct_xbot17(15));
spsct_zbot17(16)=polyval(xz15bot_crv,spsct_xbot17(16));
```

```
%.....................................................

for i=1:16
 spsct_xtop17(i)=xtransl(15)+2*(0.1983/12);
end

spsct_ytop17(1)=0;
spsct_ytop17(2)=colwidth(1);
for i=3:16
 spsct_ytop17(i)=spsct_ytop17(i-1)+colwidth(i-1);  % spsct_ytop17(16)=0.6226 ?
end

spsct_ztop17(1)=polyval(xzroottop_crv,spsct_xtop17(1));
spsct_ztop17(2)=polyval(xz1top_crv,spsct_xtop17(2));
spsct_ztop17(3)=polyval(xz2top_crv,spsct_xtop17(3));
spsct_ztop17(4)=polyval(xz3top_crv,spsct_xtop17(4));
spsct_ztop17(5)=polyval(xz4top_crv,spsct_xtop17(5));
spsct_ztop17(6)=polyval(xz5top_crv,spsct_xtop17(6));
spsct_ztop17(7)=polyval(xz6top_crv,spsct_xtop17(7));
spsct_ztop17(8)=polyval(xz7top_crv,spsct_xtop17(8));
spsct_ztop17(9)=polyval(xz8top_crv,spsct_xtop17(9));
spsct_ztop17(10)=polyval(xz9top_crv,spsct_xtop17(10));
spsct_ztop17(11)=polyval(xz10top_crv,spsct_xtop17(11));
spsct_ztop17(12)=polyval(xz11top_crv,spsct_xtop17(12));
spsct_ztop17(13)=polyval(xz12top_crv,spsct_xtop17(13));
spsct_ztop17(14)=polyval(xz13top_crv,spsct_xtop17(14));
spsct_ztop17(15)=polyval(xz14top_crv,spsct_xtop17(15));
spsct_ztop17(16)=polyval(xz15top_crv,spsct_xtop17(16));

% ...FOR SECTION 18 (SIXTEEN POINTS)
% ~~~~~~~~~~~~~~~~~~~~~~~~~~~~~~~~~~
% (From tip LE to tip TE)

for i=1:16
 spsct_xbot18(i)=xtransl(15)+3*(0.1983/12);
end

spsct_ybot18(1)=0;
spsct_ybot18(2)=colwidth(1);
for i=3:16
 spsct_ybot18(i)=spsct_ybot18(i-1)+colwidth(i-1); % spsct_ybot18(16)=0.6226  ?
end

spsct_zbot18(1)=polyval(xzrootbot_crv,spsct_xbot18(1));
spsct_zbot18(2)=polyval(xz1bot_crv,spsct_xbot18(2));
spsct_zbot18(3)=polyval(xz2bot_crv,spsct_xbot18(3));
spsct_zbot18(4)=polyval(xz3bot_crv,spsct_xbot18(4));
spsct_zbot18(5)=polyval(xz4bot_crv,spsct_xbot18(5));
spsct_zbot18(6)=polyval(xz5bot_crv,spsct_xbot18(6));
spsct_zbot18(7)=polyval(xz6bot_crv,spsct_xbot18(7));
spsct_zbot18(8)=polyval(xz7bot_crv,spsct_xbot18(8));
spsct_zbot18(9)=polyval(xz8bot_crv,spsct_xbot18(9));
spsct_zbot18(10)=polyval(xz9bot_crv,spsct_xbot18(10));
spsct_zbot18(11)=polyval(xz10bot_crv,spsct_xbot18(11));
spsct_zbot18(12)=polyval(xz11bot_crv,spsct_xbot18(12));
spsct_zbot18(13)=polyval(xz12bot_crv,spsct_xbot18(13));
spsct_zbot18(14)=polyval(xz13bot_crv,spsct_xbot18(14));
spsct_zbot18(15)=polyval(xz14bot_crv,spsct_xbot18(15));
spsct_zbot18(16)=polyval(xz15bot_crv,spsct_xbot18(16));

%.....................................................

for i=1:16
 spsct_xtop18(i)=xtransl(15)+3*(0.1983/12);
end

spsct_ytop18(1)=0;
spsct_ytop18(2)=colwidth(1);
for i=3:16
 spsct_ytop18(i)=spsct_ytop18(i-1)+colwidth(i-1);  % spsct_ytop18(16)=0.6226 ?
end

spsct_ztop18(1)=polyval(xzroottop_crv,spsct_xtop18(1));
spsct_ztop18(2)=polyval(xz1top_crv,spsct_xtop18(2));
spsct_ztop18(3)=polyval(xz2top_crv,spsct_xtop18(3));
spsct_ztop18(4)=polyval(xz3top_crv,spsct_xtop18(4));
```



```
spsct_ztop18(5)=polyval(xz4top_crv,spsct_xtop18(5));
spsct_ztop18(6)=polyval(xz5top_crv,spsct_xtop18(6));
spsct_ztop18(7)=polyval(xz6top_crv,spsct_xtop18(7));
spsct_ztop18(8)=polyval(xz7top_crv,spsct_xtop18(8));
spsct_ztop18(9)=polyval(xz8top_crv,spsct_xtop18(9));
spsct_ztop18(10)=polyval(xz9top_crv,spsct_xtop18(10));
spsct_ztop18(11)=polyval(xz10top_crv,spsct_xtop18(11));
spsct_ztop18(12)=polyval(xz11top_crv,spsct_xtop18(12));
spsct_ztop18(13)=polyval(xz12top_crv,spsct_xtop18(13));
spsct_ztop18(14)=polyval(xz13top_crv,spsct_xtop18(14));
spsct_ztop18(15)=polyval(xz14top_crv,spsct_xtop18(15));
spsct_ztop18(16)=polyval(xz15top_crv,spsct_xtop18(16));

% ...FOR SECTION 19 (SIXTEEN POINTS)
% ~~~~~~~~~~~~~~~~~~~~~~~~~~~~~~~~~~
% (From tip LE to tip TE)

for i=1:16
 spsct_xbot19(i)=xtransl(15)+4*(0.1983/12);
end

spsct_ybot19(1)=0;
spsct_ybot19(2)=colwidth(1);
for i=3:16
 spsct_ybot19(i)=spsct_ybot19(i-1)+colwidth(i-1); % spsct_ybot19(16)=0.6226  ?
end

spsct_zbot19(1)=polyval(xzrootbot_crv,spsct_xbot19(1));
spsct_zbot19(2)=polyval(xz1bot_crv,spsct_xbot19(2));
spsct_zbot19(3)=polyval(xz2bot_crv,spsct_xbot19(3));
spsct_zbot19(4)=polyval(xz3bot_crv,spsct_xbot19(4));
spsct_zbot19(5)=polyval(xz4bot_crv,spsct_xbot19(5));
spsct_zbot19(6)=polyval(xz5bot_crv,spsct_xbot19(6));
spsct_zbot19(7)=polyval(xz6bot_crv,spsct_xbot19(7));
spsct_zbot19(8)=polyval(xz7bot_crv,spsct_xbot19(8));
spsct_zbot19(9)=polyval(xz8bot_crv,spsct_xbot19(9));
spsct_zbot19(10)=polyval(xz9bot_crv,spsct_xbot19(10));
spsct_zbot19(11)=polyval(xz10bot_crv,spsct_xbot19(11));
spsct_zbot19(12)=polyval(xz11bot_crv,spsct_xbot19(12));
spsct_zbot19(13)=polyval(xz12bot_crv,spsct_xbot19(13));
spsct_zbot19(14)=polyval(xz13bot_crv,spsct_xbot19(14));
spsct_zbot19(15)=polyval(xz14bot_crv,spsct_xbot19(15));
spsct_zbot19(16)=polyval(xz15bot_crv,spsct_xbot19(16));

%.....................................................

for i=1:16
 spsct_xtop19(i)=xtransl(15)+4*(0.1983/12);
end

spsct_ytop19(1)=0;
spsct_ytop19(2)=colwidth(1);
for i=3:16
 spsct_ytop19(i)=spsct_ytop19(i-1)+colwidth(i-1);  % spsct_ytop19(16)=0.6226 ?
end

spsct_ztop19(1)=polyval(xzroottop_crv,spsct_xtop19(1));
spsct_ztop19(2)=polyval(xz1top_crv,spsct_xtop19(2));
spsct_ztop19(3)=polyval(xz2top_crv,spsct_xtop19(3));
spsct_ztop19(4)=polyval(xz3top_crv,spsct_xtop19(4));
spsct_ztop19(5)=polyval(xz4top_crv,spsct_xtop19(5));
spsct_ztop19(6)=polyval(xz5top_crv,spsct_xtop19(6));
spsct_ztop19(7)=polyval(xz6top_crv,spsct_xtop19(7));
spsct_ztop19(8)=polyval(xz7top_crv,spsct_xtop19(8));
spsct_ztop19(9)=polyval(xz8top_crv,spsct_xtop19(9));
spsct_ztop19(10)=polyval(xz9top_crv,spsct_xtop19(10));
spsct_ztop19(11)=polyval(xz10top_crv,spsct_xtop19(11));
spsct_ztop19(12)=polyval(xz11top_crv,spsct_xtop19(12));
spsct_ztop19(13)=polyval(xz12top_crv,spsct_xtop19(13));
spsct_ztop19(14)=polyval(xz13top_crv,spsct_xtop19(14));
spsct_ztop19(15)=polyval(xz14top_crv,spsct_xtop19(15));
spsct_ztop19(16)=polyval(xz15top_crv,spsct_xtop19(16));

% ...FOR SECTION 20 (SIXTEEN POINTS)
% ~~~~~~~~~~~~~~~~~~~~~~~~~~~~~~~~~~
% (From tip LE to tip TE)
```

```
for i=1:16
 spsct_xbot20(i)=xtransl(15)+5*(0.1983/12);
end

spsct_ybot20(1)=0;
spsct_ybot20(2)=colwidth(1);
for i=3:16
 spsct_ybot20(i)=spsct_ybot20(i-1)+colwidth(i-1); % spsct_ybot20(16)=0.6226  ?
end

spsct_zbot20(1)=polyval(xzrootbot_crv,spsct_xbot20(1));
spsct_zbot20(2)=polyval(xz1bot_crv,spsct_xbot20(2));
spsct_zbot20(3)=polyval(xz2bot_crv,spsct_xbot20(3));
spsct_zbot20(4)=polyval(xz3bot_crv,spsct_xbot20(4));
spsct_zbot20(5)=polyval(xz4bot_crv,spsct_xbot20(5));
spsct_zbot20(6)=polyval(xz5bot_crv,spsct_xbot20(6));
spsct_zbot20(7)=polyval(xz6bot_crv,spsct_xbot20(7));
spsct_zbot20(8)=polyval(xz7bot_crv,spsct_xbot20(8));
spsct_zbot20(9)=polyval(xz8bot_crv,spsct_xbot20(9));
spsct_zbot20(10)=polyval(xz9bot_crv,spsct_xbot20(10));
spsct_zbot20(11)=polyval(xz10bot_crv,spsct_xbot20(11));
spsct_zbot20(12)=polyval(xz11bot_crv,spsct_xbot20(12));
spsct_zbot20(13)=polyval(xz12bot_crv,spsct_xbot20(13));
spsct_zbot20(14)=polyval(xz13bot_crv,spsct_xbot20(14));
spsct_zbot20(15)=polyval(xz14bot_crv,spsct_xbot20(15));
spsct_zbot20(16)=polyval(xz15bot_crv,spsct_xbot20(16));

%.................................................

for i=1:16
 spsct_xtop20(i)=xtransl(15)+5*(0.1983/12);
end

spsct_ytop20(1)=0;
spsct_ytop20(2)=colwidth(1);
for i=3:16
 spsct_ytop20(i)=spsct_ytop20(i-1)+colwidth(i-1);  % spsct_ytop20(16)=0.6226 ?
end

spsct_ztop20(1)=polyval(xzroottop_crv,spsct_xtop20(1));
spsct_ztop20(2)=polyval(xz1top_crv,spsct_xtop20(2));
spsct_ztop20(3)=polyval(xz2top_crv,spsct_xtop20(3));
spsct_ztop20(4)=polyval(xz3top_crv,spsct_xtop20(4));
spsct_ztop20(5)=polyval(xz4top_crv,spsct_xtop20(5));
spsct_ztop20(6)=polyval(xz5top_crv,spsct_xtop20(6));
spsct_ztop20(7)=polyval(xz6top_crv,spsct_xtop20(7));
spsct_ztop20(8)=polyval(xz7top_crv,spsct_xtop20(8));
spsct_ztop20(9)=polyval(xz8top_crv,spsct_xtop20(9));
spsct_ztop20(10)=polyval(xz9top_crv,spsct_xtop20(10));
spsct_ztop20(11)=polyval(xz10top_crv,spsct_xtop20(11));
spsct_ztop20(12)=polyval(xz11top_crv,spsct_xtop20(12));
spsct_ztop20(13)=polyval(xz12top_crv,spsct_xtop20(13));
spsct_ztop20(14)=polyval(xz13top_crv,spsct_xtop20(14));
spsct_ztop20(15)=polyval(xz14top_crv,spsct_xtop20(15));
spsct_ztop20(16)=polyval(xz15top_crv,spsct_xtop20(16));

% ...FOR SECTION 21 (SIXTEEN POINTS)
% ~~~~~~~~~~~~~~~~~~~~~~~~~~~~~~~~~~
% (From tip LE to tip TE)

for i=1:16
 spsct_xbot21(i)=xtransl(15)+6*(0.1983/12);
end

spsct_ybot21(1)=0;
spsct_ybot21(2)=colwidth(1);
for i=3:16
 spsct_ybot21(i)=spsct_ybot21(i-1)+colwidth(i-1); % spsct_ybot21(16)=0.6226  ?
end

spsct_zbot21(1)=polyval(xzrootbot_crv,spsct_xbot21(1));
spsct_zbot21(2)=polyval(xz1bot_crv,spsct_xbot21(2));
spsct_zbot21(3)=polyval(xz2bot_crv,spsct_xbot21(3));
spsct_zbot21(4)=polyval(xz3bot_crv,spsct_xbot21(4));
spsct_zbot21(5)=polyval(xz4bot_crv,spsct_xbot21(5));
```



```
spsct_zbot21(6)=polyval(xz5bot_crv,spsct_xbot21(6));
spsct_zbot21(7)=polyval(xz6bot_crv,spsct_xbot21(7));
spsct_zbot21(8)=polyval(xz7bot_crv,spsct_xbot21(8));
spsct_zbot21(9)=polyval(xz8bot_crv,spsct_xbot21(9));
spsct_zbot21(10)=polyval(xz9bot_crv,spsct_xbot21(10));
spsct_zbot21(11)=polyval(xz10bot_crv,spsct_xbot21(11));
spsct_zbot21(12)=polyval(xz11bot_crv,spsct_xbot21(12));
spsct_zbot21(13)=polyval(xz12bot_crv,spsct_xbot21(13));
spsct_zbot21(14)=polyval(xz13bot_crv,spsct_xbot21(14));
spsct_zbot21(15)=polyval(xz14bot_crv,spsct_xbot21(15));
spsct_zbot21(16)=polyval(xz15bot_crv,spsct_xbot21(16));

%.................................................

for i=1:16
 spsct_xtop21(i)=xtransl(15)+6*(0.1983/12);
end

spsct_ytop21(1)=0;
spsct_ytop21(2)=colwidth(1);
for i=3:16
 spsct_ytop21(i)=spsct_ytop21(i-1)+colwidth(i-1);  % spsct_ytop21(16)=0.6226 ?
end

spsct_ztop21(1)=polyval(xzroottop_crv,spsct_xtop21(1));
spsct_ztop21(2)=polyval(xz1top_crv,spsct_xtop21(2));
spsct_ztop21(3)=polyval(xz2top_crv,spsct_xtop21(3));
spsct_ztop21(4)=polyval(xz3top_crv,spsct_xtop21(4));
spsct_ztop21(5)=polyval(xz4top_crv,spsct_xtop21(5));
spsct_ztop21(6)=polyval(xz5top_crv,spsct_xtop21(6));
spsct_ztop21(7)=polyval(xz6top_crv,spsct_xtop21(7));
spsct_ztop21(8)=polyval(xz7top_crv,spsct_xtop21(8));
spsct_ztop21(9)=polyval(xz8top_crv,spsct_xtop21(9));
spsct_ztop21(10)=polyval(xz9top_crv,spsct_xtop21(10));
spsct_ztop21(11)=polyval(xz10top_crv,spsct_xtop21(11));
spsct_ztop21(12)=polyval(xz11top_crv,spsct_xtop21(12));
spsct_ztop21(13)=polyval(xz12top_crv,spsct_xtop21(13));
spsct_ztop21(14)=polyval(xz13top_crv,spsct_xtop21(14));
spsct_ztop21(15)=polyval(xz14top_crv,spsct_xtop21(15));
spsct_ztop21(16)=polyval(xz15top_crv,spsct_xtop21(16));

% ...FOR SECTION 22 (SIXTEEN POINTS)
% ~~~~~~~~~~~~~~~~~~~~~~~~~~~~~~~~~~
% (From tip LE to tip TE)

for i=1:16
 spsct_xbot22(i)=xtransl(15)+7*(0.1983/12);
end

spsct_ybot22(1)=0;
spsct_ybot22(2)=colwidth(1);
for i=3:16
 spsct_ybot22(i)=spsct_ybot22(i-1)+colwidth(i-1); % spsct_ybot22(16)=0.6226  ?
end

spsct_zbot22(1)=polyval(xzrootbot_crv,spsct_xbot22(1));
spsct_zbot22(2)=polyval(xz1bot_crv,spsct_xbot22(2));
spsct_zbot22(3)=polyval(xz2bot_crv,spsct_xbot22(3));
spsct_zbot22(4)=polyval(xz3bot_crv,spsct_xbot22(4));
spsct_zbot22(5)=polyval(xz4bot_crv,spsct_xbot22(5));
spsct_zbot22(6)=polyval(xz5bot_crv,spsct_xbot22(6));
spsct_zbot22(7)=polyval(xz6bot_crv,spsct_xbot22(7));
spsct_zbot22(8)=polyval(xz7bot_crv,spsct_xbot22(8));
spsct_zbot22(9)=polyval(xz8bot_crv,spsct_xbot22(9));
spsct_zbot22(10)=polyval(xz9bot_crv,spsct_xbot22(10));
spsct_zbot22(11)=polyval(xz10bot_crv,spsct_xbot22(11));
spsct_zbot22(12)=polyval(xz11bot_crv,spsct_xbot22(12));
spsct_zbot22(13)=polyval(xz12bot_crv,spsct_xbot22(13));
spsct_zbot22(14)=polyval(xz13bot_crv,spsct_xbot22(14));
spsct_zbot22(15)=polyval(xz14bot_crv,spsct_xbot22(15));
spsct_zbot22(16)=polyval(xz15bot_crv,spsct_xbot22(16));

%.................................................

for i=1:16
 spsct_xtop22(i)=xtransl(15)+7*(0.1983/12);
```

```
end

spsct_ytop22(1)=0;
spsct_ytop22(2)=colwidth(1);
for i=3:16
 spsct_ytop22(i)=spsct_ytop22(i-1)+colwidth(i-1);  % spsct_ytop22(16)=0.6226 ?
end

spsct_ztop22(1)=polyval(xzroottop_crv,spsct_xtop22(1));
spsct_ztop22(2)=polyval(xz1top_crv,spsct_xtop22(2));
spsct_ztop22(3)=polyval(xz2top_crv,spsct_xtop22(3));
spsct_ztop22(4)=polyval(xz3top_crv,spsct_xtop22(4));
spsct_ztop22(5)=polyval(xz4top_crv,spsct_xtop22(5));
spsct_ztop22(6)=polyval(xz5top_crv,spsct_xtop22(6));
spsct_ztop22(7)=polyval(xz6top_crv,spsct_xtop22(7));
spsct_ztop22(8)=polyval(xz7top_crv,spsct_xtop22(8));
spsct_ztop22(9)=polyval(xz8top_crv,spsct_xtop22(9));
spsct_ztop22(10)=polyval(xz9top_crv,spsct_xtop22(10));
spsct_ztop22(11)=polyval(xz10top_crv,spsct_xtop22(11));
spsct_ztop22(12)=polyval(xz11top_crv,spsct_xtop22(12));
spsct_ztop22(13)=polyval(xz12top_crv,spsct_xtop22(13));
spsct_ztop22(14)=polyval(xz13top_crv,spsct_xtop22(14));
spsct_ztop22(15)=polyval(xz14top_crv,spsct_xtop22(15));
spsct_ztop22(16)=polyval(xz15top_crv,spsct_xtop22(16));

% ...FOR SECTION 23 (SIXTEEN POINTS)
% ~~~~~~~~~~~~~~~~~~~~~~~~~~~~~~~~~~
% (From tip LE to tip TE)

for i=1:16
 spsct_xbot23(i)=xtransl(15)+8*(0.1983/12);
end

spsct_ybot23(1)=0;
spsct_ybot23(2)=colwidth(1);
for i=3:16
 spsct_ybot23(i)=spsct_ybot23(i-1)+colwidth(i-1); % spsct_ybot23(16)=0.6226  ?
end

spsct_zbot23(1)=polyval(xzrootbot_crv,spsct_xbot23(1));
spsct_zbot23(2)=polyval(xz1bot_crv,spsct_xbot23(2));
spsct_zbot23(3)=polyval(xz2bot_crv,spsct_xbot23(3));
spsct_zbot23(4)=polyval(xz3bot_crv,spsct_xbot23(4));
spsct_zbot23(5)=polyval(xz4bot_crv,spsct_xbot23(5));
spsct_zbot23(6)=polyval(xz5bot_crv,spsct_xbot23(6));
spsct_zbot23(7)=polyval(xz6bot_crv,spsct_xbot23(7));
spsct_zbot23(8)=polyval(xz7bot_crv,spsct_xbot23(8));
spsct_zbot23(9)=polyval(xz8bot_crv,spsct_xbot23(9));
spsct_zbot23(10)=polyval(xz9bot_crv,spsct_xbot23(10));
spsct_zbot23(11)=polyval(xz10bot_crv,spsct_xbot23(11));
spsct_zbot23(12)=polyval(xz11bot_crv,spsct_xbot23(12));
spsct_zbot23(13)=polyval(xz12bot_crv,spsct_xbot23(13));
spsct_zbot23(14)=polyval(xz13bot_crv,spsct_xbot23(14));
spsct_zbot23(15)=polyval(xz14bot_crv,spsct_xbot23(15));
spsct_zbot23(16)=polyval(xz15bot_crv,spsct_xbot23(16));

%.................................................

for i=1:16
 spsct_xtop23(i)=xtransl(15)+8*(0.1983/12);
end

spsct_ytop23(1)=0;
spsct_ytop23(2)=colwidth(1);
for i=3:16
 spsct_ytop23(i)=spsct_ytop23(i-1)+colwidth(i-1);  % spsct_ytop23(16)=0.6226 ?
end

spsct_ztop23(1)=polyval(xzroottop_crv,spsct_xtop23(1));
spsct_ztop23(2)=polyval(xz1top_crv,spsct_xtop23(2));
spsct_ztop23(3)=polyval(xz2top_crv,spsct_xtop23(3));
spsct_ztop23(4)=polyval(xz3top_crv,spsct_xtop23(4));
spsct_ztop23(5)=polyval(xz4top_crv,spsct_xtop23(5));
spsct_ztop23(6)=polyval(xz5top_crv,spsct_xtop23(6));
spsct_ztop23(7)=polyval(xz6top_crv,spsct_xtop23(7));
spsct_ztop23(8)=polyval(xz7top_crv,spsct_xtop23(8));
```



```
spsct_ztop23(9)=polyval(xz8top_crv,spsct_xtop23(9));
spsct_ztop23(10)=polyval(xz9top_crv,spsct_xtop23(10));
spsct_ztop23(11)=polyval(xz10top_crv,spsct_xtop23(11));
spsct_ztop23(12)=polyval(xz11top_crv,spsct_xtop23(12));
spsct_ztop23(13)=polyval(xz12top_crv,spsct_xtop23(13));
spsct_ztop23(14)=polyval(xz13top_crv,spsct_xtop23(14));
spsct_ztop23(15)=polyval(xz14top_crv,spsct_xtop23(15));
spsct_ztop23(16)=polyval(xz15top_crv,spsct_xtop23(16));

% ...FOR SECTION 24 (SIXTEEN POINTS)
% ~~~~~~~~~~~~~~~~~~~~~~~~~~~~~~~~~~
% (From tip LE to tip TE)

for i=1:16
 spsct_xbot24(i)=xtransl(15)+9*(0.1983/12);
end

spsct_ybot24(1)=0;
spsct_ybot24(2)=colwidth(1);
for i=3:16
 spsct_ybot24(i)=spsct_ybot24(i-1)+colwidth(i-1); % spsct_ybot24(16)=0.6226  ?
end

spsct_zbot24(1)=polyval(xzrootbot_crv,spsct_xbot24(1));
spsct_zbot24(2)=polyval(xz1bot_crv,spsct_xbot24(2));
spsct_zbot24(3)=polyval(xz2bot_crv,spsct_xbot24(3));
spsct_zbot24(4)=polyval(xz3bot_crv,spsct_xbot24(4));
spsct_zbot24(5)=polyval(xz4bot_crv,spsct_xbot24(5));
spsct_zbot24(6)=polyval(xz5bot_crv,spsct_xbot24(6));
spsct_zbot24(7)=polyval(xz6bot_crv,spsct_xbot24(7));
spsct_zbot24(8)=polyval(xz7bot_crv,spsct_xbot24(8));
spsct_zbot24(9)=polyval(xz8bot_crv,spsct_xbot24(9));
spsct_zbot24(10)=polyval(xz9bot_crv,spsct_xbot24(10));
spsct_zbot24(11)=polyval(xz10bot_crv,spsct_xbot24(11));
spsct_zbot24(12)=polyval(xz11bot_crv,spsct_xbot24(12));
spsct_zbot24(13)=polyval(xz12bot_crv,spsct_xbot24(13));
spsct_zbot24(14)=polyval(xz13bot_crv,spsct_xbot24(14));
spsct_zbot24(15)=polyval(xz14bot_crv,spsct_xbot24(15));
spsct_zbot24(16)=polyval(xz15bot_crv,spsct_xbot24(16));

%.................................................

for i=1:16
 spsct_xtop24(i)=xtransl(15)+9*(0.1983/12);
end

spsct_ytop24(1)=0;
spsct_ytop24(2)=colwidth(1);
for i=3:16
 spsct_ytop24(i)=spsct_ytop24(i-1)+colwidth(i-1);  % spsct_ytop24(16)=0.6226 ?
end

spsct_ztop24(1)=polyval(xzroottop_crv,spsct_xtop24(1));
spsct_ztop24(2)=polyval(xz1top_crv,spsct_xtop24(2));
spsct_ztop24(3)=polyval(xz2top_crv,spsct_xtop24(3));
spsct_ztop24(4)=polyval(xz3top_crv,spsct_xtop24(4));
spsct_ztop24(5)=polyval(xz4top_crv,spsct_xtop24(5));
spsct_ztop24(6)=polyval(xz5top_crv,spsct_xtop24(6));
spsct_ztop24(7)=polyval(xz6top_crv,spsct_xtop24(7));
spsct_ztop24(8)=polyval(xz7top_crv,spsct_xtop24(8));
spsct_ztop24(9)=polyval(xz8top_crv,spsct_xtop24(9));
spsct_ztop24(10)=polyval(xz9top_crv,spsct_xtop24(10));
spsct_ztop24(11)=polyval(xz10top_crv,spsct_xtop24(11));
spsct_ztop24(12)=polyval(xz11top_crv,spsct_xtop24(12));
spsct_ztop24(13)=polyval(xz12top_crv,spsct_xtop24(13));
spsct_ztop24(14)=polyval(xz13top_crv,spsct_xtop24(14));
spsct_ztop24(15)=polyval(xz14top_crv,spsct_xtop24(15));
spsct_ztop24(16)=polyval(xz15top_crv,spsct_xtop24(16));

% ...FOR SECTION 25 (SIXTEEN POINTS)
% ~~~~~~~~~~~~~~~~~~~~~~~~~~~~~~~~~~
% (From tip LE to tip TE)

for i=1:16
 spsct_xbot25(i)=xtransl(15)+10*(0.1983/12);
end
```

```
spsct_ybot25(1)=0;
spsct_ybot25(2)=colwidth(1);
for i=3:16
 spsct_ybot25(i)=spsct_ybot25(i-1)+colwidth(i-1); % spsct_ybot25(16)=0.6226  ?
end

spsct_zbot25(1)=polyval(xzrootbot_crv,spsct_xbot25(1));
spsct_zbot25(2)=polyval(xz1bot_crv,spsct_xbot25(2));
spsct_zbot25(3)=polyval(xz2bot_crv,spsct_xbot25(3));
spsct_zbot25(4)=polyval(xz3bot_crv,spsct_xbot25(4));
spsct_zbot25(5)=polyval(xz4bot_crv,spsct_xbot25(5));
spsct_zbot25(6)=polyval(xz5bot_crv,spsct_xbot25(6));
spsct_zbot25(7)=polyval(xz6bot_crv,spsct_xbot25(7));
spsct_zbot25(8)=polyval(xz7bot_crv,spsct_xbot25(8));
spsct_zbot25(9)=polyval(xz8bot_crv,spsct_xbot25(9));
spsct_zbot25(10)=polyval(xz9bot_crv,spsct_xbot25(10));
spsct_zbot25(11)=polyval(xz10bot_crv,spsct_xbot25(11));
spsct_zbot25(12)=polyval(xz11bot_crv,spsct_xbot25(12));
spsct_zbot25(13)=polyval(xz12bot_crv,spsct_xbot25(13));
spsct_zbot25(14)=polyval(xz13bot_crv,spsct_xbot25(14));
spsct_zbot25(15)=polyval(xz14bot_crv,spsct_xbot25(15));
spsct_zbot25(16)=polyval(xz15bot_crv,spsct_xbot25(16));

%.................................................

for i=1:16
 spsct_xtop25(i)=xtransl(15)+10*(0.1983/12);
end

spsct_ytop25(1)=0;
spsct_ytop25(2)=colwidth(1);
for i=3:16
 spsct_ytop25(i)=spsct_ytop25(i-1)+colwidth(i-1);  % spsct_ytop25(16)=0.6226 ?
end

spsct_ztop25(1)=polyval(xzroottop_crv,spsct_xtop25(1));
spsct_ztop25(2)=polyval(xz1top_crv,spsct_xtop25(2));
spsct_ztop25(3)=polyval(xz2top_crv,spsct_xtop25(3));
spsct_ztop25(4)=polyval(xz3top_crv,spsct_xtop25(4));
spsct_ztop25(5)=polyval(xz4top_crv,spsct_xtop25(5));
spsct_ztop25(6)=polyval(xz5top_crv,spsct_xtop25(6));
spsct_ztop25(7)=polyval(xz6top_crv,spsct_xtop25(7));
spsct_ztop25(8)=polyval(xz7top_crv,spsct_xtop25(8));
spsct_ztop25(9)=polyval(xz8top_crv,spsct_xtop25(9));
spsct_ztop25(10)=polyval(xz9top_crv,spsct_xtop25(10));
spsct_ztop25(11)=polyval(xz10top_crv,spsct_xtop25(11));
spsct_ztop25(12)=polyval(xz11top_crv,spsct_xtop25(12));
spsct_ztop25(13)=polyval(xz12top_crv,spsct_xtop25(13));
spsct_ztop25(14)=polyval(xz13top_crv,spsct_xtop25(14));
spsct_ztop25(15)=polyval(xz14top_crv,spsct_xtop25(15));
spsct_ztop25(16)=polyval(xz15top_crv,spsct_xtop25(16));

% ...FOR SECTION 26 (SIXTEEN POINTS)
% ~~~~~~~~~~~~~~~~~~~~~~~~~~~~~~~~~~
% (From tip LE to tip TE)

for i=1:16
 spsct_xbot26(i)=xtransl(15)+11*(0.1983/12);
end

spsct_ybot26(1)=0;
spsct_ybot26(2)=colwidth(1);
for i=3:16
 spsct_ybot26(i)=spsct_ybot26(i-1)+colwidth(i-1); % spsct_ybot26(16)=0.6226  ?
end

spsct_zbot26(1)=polyval(xzrootbot_crv,spsct_xbot26(1));
spsct_zbot26(2)=polyval(xz1bot_crv,spsct_xbot26(2));
spsct_zbot26(3)=polyval(xz2bot_crv,spsct_xbot26(3));
spsct_zbot26(4)=polyval(xz3bot_crv,spsct_xbot26(4));
spsct_zbot26(5)=polyval(xz4bot_crv,spsct_xbot26(5));
spsct_zbot26(6)=polyval(xz5bot_crv,spsct_xbot26(6));
spsct_zbot26(7)=polyval(xz6bot_crv,spsct_xbot26(7));
spsct_zbot26(8)=polyval(xz7bot_crv,spsct_xbot26(8));
spsct_zbot26(9)=polyval(xz8bot_crv,spsct_xbot26(9));
```



```
spsct_zbot26(10)=polyval(xz9bot_crv,spsct_xbot26(10));
spsct_zbot26(11)=polyval(xz10bot_crv,spsct_xbot26(11));
spsct_zbot26(12)=polyval(xz11bot_crv,spsct_xbot26(12));
spsct_zbot26(13)=polyval(xz12bot_crv,spsct_xbot26(13));
spsct_zbot26(14)=polyval(xz13bot_crv,spsct_xbot26(14));
spsct_zbot26(15)=polyval(xz14bot_crv,spsct_xbot26(15));
spsct_zbot26(16)=polyval(xz15bot_crv,spsct_xbot26(16));

%.................................................

for i=1:16
 spsct_xtop26(i)=xtransl(15)+11*(0.1983/12);
end

spsct_ytop26(1)=0;
spsct_ytop26(2)=colwidth(1);
for i=3:16
 spsct_ytop26(i)=spsct_ytop26(i-1)+colwidth(i-1);  % spsct_ytop26(16)=0.6226 ?
end

spsct_ztop26(1)=polyval(xzroottop_crv,spsct_xtop26(1));
spsct_ztop26(2)=polyval(xz1top_crv,spsct_xtop26(2));
spsct_ztop26(3)=polyval(xz2top_crv,spsct_xtop26(3));
spsct_ztop26(4)=polyval(xz3top_crv,spsct_xtop26(4));
spsct_ztop26(5)=polyval(xz4top_crv,spsct_xtop26(5));
spsct_ztop26(6)=polyval(xz5top_crv,spsct_xtop26(6));
spsct_ztop26(7)=polyval(xz6top_crv,spsct_xtop26(7));
spsct_ztop26(8)=polyval(xz7top_crv,spsct_xtop26(8));
spsct_ztop26(9)=polyval(xz8top_crv,spsct_xtop26(9));
spsct_ztop26(10)=polyval(xz9top_crv,spsct_xtop26(10));
spsct_ztop26(11)=polyval(xz10top_crv,spsct_xtop26(11));
spsct_ztop26(12)=polyval(xz11top_crv,spsct_xtop26(12));
spsct_ztop26(13)=polyval(xz12top_crv,spsct_xtop26(13));
spsct_ztop26(14)=polyval(xz13top_crv,spsct_xtop26(14));
spsct_ztop26(15)=polyval(xz14top_crv,spsct_xtop26(15));
spsct_ztop26(16)=polyval(xz15top_crv,spsct_xtop26(16));

% ...FOR SECTION 27 (SIXTEEN POINTS)
% ~~~~~~~~~~~~~~~~~~~~~~~~~~~~~~~~~~
% (From tip LE to tip TE)

for i=1:16
 spsct_xbot27(i)=xtransl(15)+0.1983;  % 0.1983=scale(15)
end

spsct_ybot27(1)=0;
spsct_ybot27(2)=colwidth(1);
for i=3:16
 spsct_ybot27(i)=spsct_ybot27(i-1)+colwidth(i-1); % spsct_ybot27(16)=0.6226  ?
end

spsct_zbot27(1)=polyval(xzrootbot_crv,spsct_xbot27(1));
spsct_zbot27(2)=polyval(xz1bot_crv,spsct_xbot27(2));
spsct_zbot27(3)=polyval(xz2bot_crv,spsct_xbot27(3));
spsct_zbot27(4)=polyval(xz3bot_crv,spsct_xbot27(4));
spsct_zbot27(5)=polyval(xz4bot_crv,spsct_xbot27(5));
spsct_zbot27(6)=polyval(xz5bot_crv,spsct_xbot27(6));
spsct_zbot27(7)=polyval(xz6bot_crv,spsct_xbot27(7));
spsct_zbot27(8)=polyval(xz7bot_crv,spsct_xbot27(8));
spsct_zbot27(9)=polyval(xz8bot_crv,spsct_xbot27(9));
spsct_zbot27(10)=polyval(xz9bot_crv,spsct_xbot27(10));
spsct_zbot27(11)=polyval(xz10bot_crv,spsct_xbot27(11));
spsct_zbot27(12)=polyval(xz11bot_crv,spsct_xbot27(12));
spsct_zbot27(13)=polyval(xz12bot_crv,spsct_xbot27(13));
spsct_zbot27(14)=polyval(xz13bot_crv,spsct_xbot27(14));
spsct_zbot27(15)=polyval(xz14bot_crv,spsct_xbot27(15));
spsct_zbot27(16)=polyval(xz15bot_crv,spsct_xbot27(16));

%.................................................

for i=1:16
 spsct_xtop27(i)=xtransl(15)+0.1983;   %0.1983=scale(15)
end

spsct_ytop27(1)=0;
spsct_ytop27(2)=colwidth(1);
```

```
for i=3:16
 spsct_ytop27(i)=spsct_ytop27(i-1)+colwidth(i-1);  % spsct_ytop27(16)=0.6226 ?
end

spsct_ztop27(1)=polyval(xzroottop_crv,spsct_xtop27(1));
spsct_ztop27(2)=polyval(xz1top_crv,spsct_xtop27(2));
spsct_ztop27(3)=polyval(xz2top_crv,spsct_xtop27(3));
spsct_ztop27(4)=polyval(xz3top_crv,spsct_xtop27(4));
spsct_ztop27(5)=polyval(xz4top_crv,spsct_xtop27(5));
spsct_ztop27(6)=polyval(xz5top_crv,spsct_xtop27(6));
spsct_ztop27(7)=polyval(xz6top_crv,spsct_xtop27(7));
spsct_ztop27(8)=polyval(xz7top_crv,spsct_xtop27(8));
spsct_ztop27(9)=polyval(xz8top_crv,spsct_xtop27(9));
spsct_ztop27(10)=polyval(xz9top_crv,spsct_xtop27(10));
spsct_ztop27(11)=polyval(xz10top_crv,spsct_xtop27(11));
spsct_ztop27(12)=polyval(xz11top_crv,spsct_xtop27(12));
spsct_ztop27(13)=polyval(xz12top_crv,spsct_xtop27(13));
spsct_ztop27(14)=polyval(xz13top_crv,spsct_xtop27(14));
spsct_ztop27(15)=polyval(xz14top_crv,spsct_xtop27(15));
spsct_ztop27(16)=polyval(xz15top_crv,spsct_xtop27(16));

% ...FOR SECTION 28 (FIFTEEN POINTS)
% ~~~~~~~~~~~~~~~~~~~~~~~~~~~~~~~~~~

for i=1:15
 spsct_xbot28(i)=xtransl(14)+scale(14);
end

spsct_ybot28(1)=0;
spsct_ybot28(2)=colwidth(1);
for i=3:15
 spsct_ybot28(i)=spsct_ybot28(i-1)+colwidth(i-1);
end

spsct_zbot28(1)=polyval(xzrootbot_crv,spsct_xbot28(1));
spsct_zbot28(2)=polyval(xz1bot_crv,spsct_xbot28(2));
spsct_zbot28(3)=polyval(xz2bot_crv,spsct_xbot28(3));
spsct_zbot28(4)=polyval(xz3bot_crv,spsct_xbot28(4));
spsct_zbot28(5)=polyval(xz4bot_crv,spsct_xbot28(5));
spsct_zbot28(6)=polyval(xz5bot_crv,spsct_xbot28(6));
spsct_zbot28(7)=polyval(xz6bot_crv,spsct_xbot28(7));
spsct_zbot28(8)=polyval(xz7bot_crv,spsct_xbot28(8));
spsct_zbot28(9)=polyval(xz8bot_crv,spsct_xbot28(9));
spsct_zbot28(10)=polyval(xz9bot_crv,spsct_xbot28(10));
spsct_zbot28(11)=polyval(xz10bot_crv,spsct_xbot28(11));
spsct_zbot28(12)=polyval(xz11bot_crv,spsct_xbot28(12));
spsct_zbot28(13)=polyval(xz12bot_crv,spsct_xbot28(13));
spsct_zbot28(14)=polyval(xz13bot_crv,spsct_xbot28(14));
spsct_zbot28(15)=polyval(xz14bot_crv,spsct_xbot28(15));

%.................................................

for i=1:15
 spsct_xtop28(i)=xtransl(14)+scale(14);
end

spsct_ytop28(1)=0;
spsct_ytop28(2)=colwidth(1);
for i=3:15
 spsct_ytop28(i)=spsct_ytop28(i-1)+colwidth(i-1);
end

spsct_ztop28(1)=polyval(xzroottop_crv,spsct_xtop28(1));
spsct_ztop28(2)=polyval(xz1top_crv,spsct_xtop28(2));
spsct_ztop28(3)=polyval(xz2top_crv,spsct_xtop28(3));
spsct_ztop28(4)=polyval(xz3top_crv,spsct_xtop28(4));
spsct_ztop28(5)=polyval(xz4top_crv,spsct_xtop28(5));
spsct_ztop28(6)=polyval(xz5top_crv,spsct_xtop28(6));
spsct_ztop28(7)=polyval(xz6top_crv,spsct_xtop28(7));
spsct_ztop28(8)=polyval(xz7top_crv,spsct_xtop28(8));
spsct_ztop28(9)=polyval(xz8top_crv,spsct_xtop28(9));
spsct_ztop28(10)=polyval(xz9top_crv,spsct_xtop28(10));
spsct_ztop28(11)=polyval(xz10top_crv,spsct_xtop28(11));
spsct_ztop28(12)=polyval(xz11top_crv,spsct_xtop28(12));
spsct_ztop28(13)=polyval(xz12top_crv,spsct_xtop28(13));
spsct_ztop28(14)=polyval(xz13top_crv,spsct_xtop28(14));
```



```
spsct_ztop28(15)=polyval(xz14top_crv,spsct_xtop28(15));

% ...FOR SECTION 29 (FOURTEEN POINTS)
% ~~~~~~~~~~~~~~~~~~~~~~~~~~~~~~~~~~~

for i=1:14
 spsct_xbot29(i)=xtransl(13)+scale(13);
end

spsct_ybot29(1)=0;
spsct_ybot29(2)=colwidth(1);
for i=3:14
 spsct_ybot29(i)=spsct_ybot29(i-1)+colwidth(i-1);
end

spsct_zbot29(1)=polyval(xzrootbot_crv,spsct_xbot29(1));
spsct_zbot29(2)=polyval(xz1bot_crv,spsct_xbot29(2));
spsct_zbot29(3)=polyval(xz2bot_crv,spsct_xbot29(3));
spsct_zbot29(4)=polyval(xz3bot_crv,spsct_xbot29(4));
spsct_zbot29(5)=polyval(xz4bot_crv,spsct_xbot29(5));
spsct_zbot29(6)=polyval(xz5bot_crv,spsct_xbot29(6));
spsct_zbot29(7)=polyval(xz6bot_crv,spsct_xbot29(7));
spsct_zbot29(8)=polyval(xz7bot_crv,spsct_xbot29(8));
spsct_zbot29(9)=polyval(xz8bot_crv,spsct_xbot29(9));
spsct_zbot29(10)=polyval(xz9bot_crv,spsct_xbot29(10));
spsct_zbot29(11)=polyval(xz10bot_crv,spsct_xbot29(11));
spsct_zbot29(12)=polyval(xz11bot_crv,spsct_xbot29(12));
spsct_zbot29(13)=polyval(xz12bot_crv,spsct_xbot29(13));
spsct_zbot29(14)=polyval(xz13bot_crv,spsct_xbot29(14));

%.................................................

for i=1:14
 spsct_xtop29(i)=xtransl(13)+scale(13);
end

spsct_ytop29(1)=0;
spsct_ytop29(2)=colwidth(1);
for i=3:14
 spsct_ytop29(i)=spsct_ytop29(i-1)+colwidth(i-1);
end

spsct_ztop29(1)=polyval(xzroottop_crv,spsct_xtop29(1));
spsct_ztop29(2)=polyval(xz1top_crv,spsct_xtop29(2));
spsct_ztop29(3)=polyval(xz2top_crv,spsct_xtop29(3));
spsct_ztop29(4)=polyval(xz3top_crv,spsct_xtop29(4));
spsct_ztop29(5)=polyval(xz4top_crv,spsct_xtop29(5));
spsct_ztop29(6)=polyval(xz5top_crv,spsct_xtop29(6));
spsct_ztop29(7)=polyval(xz6top_crv,spsct_xtop29(7));
spsct_ztop29(8)=polyval(xz7top_crv,spsct_xtop29(8));
spsct_ztop29(9)=polyval(xz8top_crv,spsct_xtop29(9));
spsct_ztop29(10)=polyval(xz9top_crv,spsct_xtop29(10));
spsct_ztop29(11)=polyval(xz10top_crv,spsct_xtop29(11));
spsct_ztop29(12)=polyval(xz11top_crv,spsct_xtop29(12));
spsct_ztop29(13)=polyval(xz12top_crv,spsct_xtop29(13));
spsct_ztop29(14)=polyval(xz13top_crv,spsct_xtop29(14));

% ...FOR SECTION 30 (THIRTEEN POINTS)
% ~~~~~~~~~~~~~~~~~~~~~~~~~~~~~~~~~~~

for i=1:13
 spsct_xbot30(i)=xtransl(12)+scale(12);
end

spsct_ybot30(1)=0;
spsct_ybot30(2)=colwidth(1);
for i=3:13
 spsct_ybot30(i)=spsct_ybot30(i-1)+colwidth(i-1);
end

spsct_zbot30(1)=polyval(xzrootbot_crv,spsct_xbot30(1));
spsct_zbot30(2)=polyval(xz1bot_crv,spsct_xbot30(2));
spsct_zbot30(3)=polyval(xz2bot_crv,spsct_xbot30(3));
spsct_zbot30(4)=polyval(xz3bot_crv,spsct_xbot30(4));
spsct_zbot30(5)=polyval(xz4bot_crv,spsct_xbot30(5));
spsct_zbot30(6)=polyval(xz5bot_crv,spsct_xbot30(6));
```

```
spsct_zbot30(7)=polyval(xz6bot_crv,spsct_xbot30(7));
spsct_zbot30(8)=polyval(xz7bot_crv,spsct_xbot30(8));
spsct_zbot30(9)=polyval(xz8bot_crv,spsct_xbot30(9));
spsct_zbot30(10)=polyval(xz9bot_crv,spsct_xbot30(10));
spsct_zbot30(11)=polyval(xz10bot_crv,spsct_xbot30(11));
spsct_zbot30(12)=polyval(xz11bot_crv,spsct_xbot30(12));
spsct_zbot30(13)=polyval(xz12bot_crv,spsct_xbot30(13));

%.................................................

for i=1:13
 spsct_xtop30(i)=xtransl(12)+scale(12);
end

spsct_ytop30(1)=0;
spsct_ytop30(2)=colwidth(1);
for i=3:13
 spsct_ytop30(i)=spsct_ytop30(i-1)+colwidth(i-1);
end

spsct_ztop30(1)=polyval(xzroottop_crv,spsct_xtop30(1));
spsct_ztop30(2)=polyval(xz1top_crv,spsct_xtop30(2));
spsct_ztop30(3)=polyval(xz2top_crv,spsct_xtop30(3));
spsct_ztop30(4)=polyval(xz3top_crv,spsct_xtop30(4));
spsct_ztop30(5)=polyval(xz4top_crv,spsct_xtop30(5));
spsct_ztop30(6)=polyval(xz5top_crv,spsct_xtop30(6));
spsct_ztop30(7)=polyval(xz6top_crv,spsct_xtop30(7));
spsct_ztop30(8)=polyval(xz7top_crv,spsct_xtop30(8));
spsct_ztop30(9)=polyval(xz8top_crv,spsct_xtop30(9));
spsct_ztop30(10)=polyval(xz9top_crv,spsct_xtop30(10));
spsct_ztop30(11)=polyval(xz10top_crv,spsct_xtop30(11));
spsct_ztop30(12)=polyval(xz11top_crv,spsct_xtop30(12));
spsct_ztop30(13)=polyval(xz12top_crv,spsct_xtop30(13));

% ...FOR SECTION 31 (TWELVE POINTS)
% ~~~~~~~~~~~~~~~~~~~~~~~~~~~~~~~~

for i=1:12
 spsct_xbot31(i)=xtransl(11)+scale(11);
end

spsct_ybot31(1)=0;
spsct_ybot31(2)=colwidth(1);
for i=3:12
 spsct_ybot31(i)=spsct_ybot31(i-1)+colwidth(i-1);
end

spsct_zbot31(1)=polyval(xzrootbot_crv,spsct_xbot31(1));
spsct_zbot31(2)=polyval(xz1bot_crv,spsct_xbot31(2));
spsct_zbot31(3)=polyval(xz2bot_crv,spsct_xbot31(3));
spsct_zbot31(4)=polyval(xz3bot_crv,spsct_xbot31(4));
spsct_zbot31(5)=polyval(xz4bot_crv,spsct_xbot31(5));
spsct_zbot31(6)=polyval(xz5bot_crv,spsct_xbot31(6));
spsct_zbot31(7)=polyval(xz6bot_crv,spsct_xbot31(7));
spsct_zbot31(8)=polyval(xz7bot_crv,spsct_xbot31(8));
spsct_zbot31(9)=polyval(xz8bot_crv,spsct_xbot31(9));
spsct_zbot31(10)=polyval(xz9bot_crv,spsct_xbot31(10));
spsct_zbot31(11)=polyval(xz10bot_crv,spsct_xbot31(11));
spsct_zbot31(12)=polyval(xz11bot_crv,spsct_xbot31(12));

%.................................................

for i=1:12
 spsct_xtop31(i)=xtransl(11)+scale(11);
end

spsct_ytop31(1)=0;
spsct_ytop31(2)=colwidth(1);
for i=3:12
 spsct_ytop31(i)=spsct_ytop31(i-1)+colwidth(i-1);
end

spsct_ztop31(1)=polyval(xzroottop_crv,spsct_xtop31(1));
spsct_ztop31(2)=polyval(xz1top_crv,spsct_xtop31(2));
spsct_ztop31(3)=polyval(xz2top_crv,spsct_xtop31(3));
spsct_ztop31(4)=polyval(xz3top_crv,spsct_xtop31(4));
```



```
spsct_ztop31(5)=polyval(xz4top_crv,spsct_xtop31(5));
spsct_ztop31(6)=polyval(xz5top_crv,spsct_xtop31(6));
spsct_ztop31(7)=polyval(xz6top_crv,spsct_xtop31(7));
spsct_ztop31(8)=polyval(xz7top_crv,spsct_xtop31(8));
spsct_ztop31(9)=polyval(xz8top_crv,spsct_xtop31(9));
spsct_ztop31(10)=polyval(xz9top_crv,spsct_xtop31(10));
spsct_ztop31(11)=polyval(xz10top_crv,spsct_xtop31(11));
spsct_ztop31(12)=polyval(xz11top_crv,spsct_xtop31(12));

% ...FOR SECTION 32 (ELEVEN POINTS)
% ~~~~~~~~~~~~~~~~~~~~~~~~~~~~~~~~

for i=1:11
 spsct_xbot32(i)=xtransl(10)+scale(10);
end

spsct_ybot32(1)=0;
spsct_ybot32(2)=colwidth(1);
for i=3:11
 spsct_ybot32(i)=spsct_ybot32(i-1)+colwidth(i-1);
end

spsct_zbot32(1)=polyval(xzrootbot_crv,spsct_xbot32(1));
spsct_zbot32(2)=polyval(xz1bot_crv,spsct_xbot32(2));
spsct_zbot32(3)=polyval(xz2bot_crv,spsct_xbot32(3));
spsct_zbot32(4)=polyval(xz3bot_crv,spsct_xbot32(4));
spsct_zbot32(5)=polyval(xz4bot_crv,spsct_xbot32(5));
spsct_zbot32(6)=polyval(xz5bot_crv,spsct_xbot32(6));
spsct_zbot32(7)=polyval(xz6bot_crv,spsct_xbot32(7));
spsct_zbot32(8)=polyval(xz7bot_crv,spsct_xbot32(8));
spsct_zbot32(9)=polyval(xz8bot_crv,spsct_xbot32(9));
spsct_zbot32(10)=polyval(xz9bot_crv,spsct_xbot32(10));
spsct_zbot32(11)=polyval(xz10bot_crv,spsct_xbot32(11));

%.................................................

for i=1:11
 spsct_xtop32(i)=xtransl(10)+scale(10);
end

spsct_ytop32(1)=0;
spsct_ytop32(2)=colwidth(1);
for i=3:11
 spsct_ytop32(i)=spsct_ytop32(i-1)+colwidth(i-1);
end

spsct_ztop32(1)=polyval(xzroottop_crv,spsct_xtop32(1));
spsct_ztop32(2)=polyval(xz1top_crv,spsct_xtop32(2));
spsct_ztop32(3)=polyval(xz2top_crv,spsct_xtop32(3));
spsct_ztop32(4)=polyval(xz3top_crv,spsct_xtop32(4));
spsct_ztop32(5)=polyval(xz4top_crv,spsct_xtop32(5));
spsct_ztop32(6)=polyval(xz5top_crv,spsct_xtop32(6));
spsct_ztop32(7)=polyval(xz6top_crv,spsct_xtop32(7));
spsct_ztop32(8)=polyval(xz7top_crv,spsct_xtop32(8));
spsct_ztop32(9)=polyval(xz8top_crv,spsct_xtop32(9));
spsct_ztop32(10)=polyval(xz9top_crv,spsct_xtop32(10));
spsct_ztop32(11)=polyval(xz10top_crv,spsct_xtop32(11));

% ...FOR SECTION 33 (TEN POINTS)
% ~~~~~~~~~~~~~~~~~~~~~~~~~~~~~

for i=1:10
 spsct_xbot33(i)=xtransl(9)+scale(9);
end

spsct_ybot33(1)=0;
spsct_ybot33(2)=colwidth(1);
for i=3:10
 spsct_ybot33(i)=spsct_ybot33(i-1)+colwidth(i-1);
end

spsct_zbot33(1)=polyval(xzrootbot_crv,spsct_xbot33(1));
spsct_zbot33(2)=polyval(xz1bot_crv,spsct_xbot33(2));
spsct_zbot33(3)=polyval(xz2bot_crv,spsct_xbot33(3));
spsct_zbot33(4)=polyval(xz3bot_crv,spsct_xbot33(4));
spsct_zbot33(5)=polyval(xz4bot_crv,spsct_xbot33(5));
```

```
spsct_zbot33(6)=polyval(xz5bot_crv,spsct_xbot33(6));
spsct_zbot33(7)=polyval(xz6bot_crv,spsct_xbot33(7));
spsct_zbot33(8)=polyval(xz7bot_crv,spsct_xbot33(8));
spsct_zbot33(9)=polyval(xz8bot_crv,spsct_xbot33(9));
spsct_zbot33(10)=polyval(xz9bot_crv,spsct_xbot33(10));

%.................................................

for i=1:10
 spsct_xtop33(i)=xtransl(9)+scale(9);
end

spsct_ytop33(1)=0;
spsct_ytop33(2)=colwidth(1);
for i=3:10
 spsct_ytop33(i)=spsct_ytop33(i-1)+colwidth(i-1);
end

spsct_ztop33(1)=polyval(xzroottop_crv,spsct_xtop33(1));
spsct_ztop33(2)=polyval(xz1top_crv,spsct_xtop33(2));
spsct_ztop33(3)=polyval(xz2top_crv,spsct_xtop33(3));
spsct_ztop33(4)=polyval(xz3top_crv,spsct_xtop33(4));
spsct_ztop33(5)=polyval(xz4top_crv,spsct_xtop33(5));
spsct_ztop33(6)=polyval(xz5top_crv,spsct_xtop33(6));
spsct_ztop33(7)=polyval(xz6top_crv,spsct_xtop33(7));
spsct_ztop33(8)=polyval(xz7top_crv,spsct_xtop33(8));
spsct_ztop33(9)=polyval(xz8top_crv,spsct_xtop33(9));
spsct_ztop33(10)=polyval(xz9top_crv,spsct_xtop33(10));

% ...FOR SECTION 34 (NINE POINTS)
% ~~~~~~~~~~~~~~~~~~~~~~~~~~~~~~~

for i=1:9
 spsct_xbot34(i)=xtransl(8)+scale(8);
end

spsct_ybot34(1)=0;
spsct_ybot34(2)=colwidth(1);
for i=3:9
 spsct_ybot34(i)=spsct_ybot34(i-1)+colwidth(i-1);
end

spsct_zbot34(1)=polyval(xzrootbot_crv,spsct_xbot34(1));
spsct_zbot34(2)=polyval(xz1bot_crv,spsct_xbot34(2));
spsct_zbot34(3)=polyval(xz2bot_crv,spsct_xbot34(3));
spsct_zbot34(4)=polyval(xz3bot_crv,spsct_xbot34(4));
spsct_zbot34(5)=polyval(xz4bot_crv,spsct_xbot34(5));
spsct_zbot34(6)=polyval(xz5bot_crv,spsct_xbot34(6));
spsct_zbot34(7)=polyval(xz6bot_crv,spsct_xbot34(7));
spsct_zbot34(8)=polyval(xz7bot_crv,spsct_xbot34(8));
spsct_zbot34(9)=polyval(xz8bot_crv,spsct_xbot34(9));

%.................................................

for i=1:9
 spsct_xtop34(i)=xtransl(8)+scale(8);
end

spsct_ytop34(1)=0;
spsct_ytop34(2)=colwidth(1);
for i=3:9
 spsct_ytop34(i)=spsct_ytop34(i-1)+colwidth(i-1);
end

spsct_ztop34(1)=polyval(xzroottop_crv,spsct_xtop34(1));
spsct_ztop34(2)=polyval(xz1top_crv,spsct_xtop34(2));
spsct_ztop34(3)=polyval(xz2top_crv,spsct_xtop34(3));
spsct_ztop34(4)=polyval(xz3top_crv,spsct_xtop34(4));
spsct_ztop34(5)=polyval(xz4top_crv,spsct_xtop34(5));
spsct_ztop34(6)=polyval(xz5top_crv,spsct_xtop34(6));
spsct_ztop34(7)=polyval(xz6top_crv,spsct_xtop34(7));
spsct_ztop34(8)=polyval(xz7top_crv,spsct_xtop34(8));
spsct_ztop34(9)=polyval(xz8top_crv,spsct_xtop34(9));

% ...FOR SECTION 35 (EIGHT POINTS)
% ~~~~~~~~~~~~~~~~~~~~~~~~~~~~~~~~
```



```
for i=1:8
 spsct_xbot35(i)=xtransl(7)+scale(7);
end

spsct_ybot35(1)=0;
spsct_ybot35(2)=colwidth(1);
for i=3:8
 spsct_ybot35(i)=spsct_ybot35(i-1)+colwidth(i-1);
end

spsct_zbot35(1)=polyval(xzrootbot_crv,spsct_xbot35(1));
spsct_zbot35(2)=polyval(xz1bot_crv,spsct_xbot35(2));
spsct_zbot35(3)=polyval(xz2bot_crv,spsct_xbot35(3));
spsct_zbot35(4)=polyval(xz3bot_crv,spsct_xbot35(4));
spsct_zbot35(5)=polyval(xz4bot_crv,spsct_xbot35(5));
spsct_zbot35(6)=polyval(xz5bot_crv,spsct_xbot35(6));
spsct_zbot35(7)=polyval(xz6bot_crv,spsct_xbot35(7));
spsct_zbot35(8)=polyval(xz7bot_crv,spsct_xbot35(8));

%.................................................

for i=1:8
 spsct_xtop35(i)=xtransl(7)+scale(7);
end

spsct_ytop35(1)=0;
spsct_ytop35(2)=colwidth(1);
for i=3:8
 spsct_ytop35(i)=spsct_ytop35(i-1)+colwidth(i-1);
end

spsct_ztop35(1)=polyval(xzroottop_crv,spsct_xtop35(1));
spsct_ztop35(2)=polyval(xz1top_crv,spsct_xtop35(2));
spsct_ztop35(3)=polyval(xz2top_crv,spsct_xtop35(3));
spsct_ztop35(4)=polyval(xz3top_crv,spsct_xtop35(4));
spsct_ztop35(5)=polyval(xz4top_crv,spsct_xtop35(5));
spsct_ztop35(6)=polyval(xz5top_crv,spsct_xtop35(6));
spsct_ztop35(7)=polyval(xz6top_crv,spsct_xtop35(7));
spsct_ztop35(8)=polyval(xz7top_crv,spsct_xtop35(8));

% ...FOR SECTION 36 (SEVEN POINTS)
% ~~~~~~~~~~~~~~~~~~~~~~~~~~~~~~~~

for i=1:7
 spsct_xbot36(i)=xtransl(6)+scale(6);
end

spsct_ybot36(1)=0;
spsct_ybot36(2)=colwidth(1);
for i=3:7
 spsct_ybot36(i)=spsct_ybot36(i-1)+colwidth(i-1);
end

spsct_zbot36(1)=polyval(xzrootbot_crv,spsct_xbot36(1));
spsct_zbot36(2)=polyval(xz1bot_crv,spsct_xbot36(2));
spsct_zbot36(3)=polyval(xz2bot_crv,spsct_xbot36(3));
spsct_zbot36(4)=polyval(xz3bot_crv,spsct_xbot36(4));
spsct_zbot36(5)=polyval(xz4bot_crv,spsct_xbot36(5));
spsct_zbot36(6)=polyval(xz5bot_crv,spsct_xbot36(6));
spsct_zbot36(7)=polyval(xz6bot_crv,spsct_xbot36(7));

%.................................................

for i=1:7
 spsct_xtop36(i)=xtransl(6)+scale(6);
end

spsct_ytop36(1)=0;
spsct_ytop36(2)=colwidth(1);
for i=3:7
 spsct_ytop36(i)=spsct_ytop36(i-1)+colwidth(i-1);
end

spsct_ztop36(1)=polyval(xzroottop_crv,spsct_xtop36(1));
spsct_ztop36(2)=polyval(xz1top_crv,spsct_xtop36(2));
```

```
spsct_ztop36(3)=polyval(xz2top_crv,spsct_xtop36(3));
spsct_ztop36(4)=polyval(xz3top_crv,spsct_xtop36(4));
spsct_ztop36(5)=polyval(xz4top_crv,spsct_xtop36(5));
spsct_ztop36(6)=polyval(xz5top_crv,spsct_xtop36(6));
spsct_ztop36(7)=polyval(xz6top_crv,spsct_xtop36(7));

% ...FOR SECTION 37 (SIX POINTS)
% ~~~~~~~~~~~~~~~~~~~~~~~~~~~~~~

for i=1:6
 spsct_xbot37(i)=xtransl(5)+scale(5);
end

spsct_ybot37(1)=0;
spsct_ybot37(2)=colwidth(1);
for i=3:6
 spsct_ybot37(i)=spsct_ybot37(i-1)+colwidth(i-1);
end

spsct_zbot37(1)=polyval(xzrootbot_crv,spsct_xbot37(1));
spsct_zbot37(2)=polyval(xz1bot_crv,spsct_xbot37(2));
spsct_zbot37(3)=polyval(xz2bot_crv,spsct_xbot37(3));
spsct_zbot37(4)=polyval(xz3bot_crv,spsct_xbot37(4));
spsct_zbot37(5)=polyval(xz4bot_crv,spsct_xbot37(5));
spsct_zbot37(6)=polyval(xz5bot_crv,spsct_xbot37(6));

%.................................................

for i=1:6
 spsct_xtop37(i)=xtransl(5)+scale(5);
end

spsct_ytop37(1)=0;
spsct_ytop37(2)=colwidth(1);
for i=3:6
 spsct_ytop37(i)=spsct_ytop37(i-1)+colwidth(i-1);
end

spsct_ztop37(1)=polyval(xzroottop_crv,spsct_xtop37(1));
spsct_ztop37(2)=polyval(xz1top_crv,spsct_xtop37(2));
spsct_ztop37(3)=polyval(xz2top_crv,spsct_xtop37(3));
spsct_ztop37(4)=polyval(xz3top_crv,spsct_xtop37(4));
spsct_ztop37(5)=polyval(xz4top_crv,spsct_xtop37(5));
spsct_ztop37(6)=polyval(xz5top_crv,spsct_xtop37(6));

% ...FOR SECTION 38 (FIVE POINTS)
% ~~~~~~~~~~~~~~~~~~~~~~~~~~~~~~

for i=1:5
 spsct_xbot38(i)=xtransl(4)+scale(4);
end

spsct_ybot38(1)=0;
spsct_ybot38(2)=colwidth(1);
for i=3:5
 spsct_ybot38(i)=spsct_ybot38(i-1)+colwidth(i-1);
end

spsct_zbot38(1)=polyval(xzrootbot_crv,spsct_xbot38(1));
spsct_zbot38(2)=polyval(xz1bot_crv,spsct_xbot38(2));
spsct_zbot38(3)=polyval(xz2bot_crv,spsct_xbot38(3));
spsct_zbot38(4)=polyval(xz3bot_crv,spsct_xbot38(4));
spsct_zbot38(5)=polyval(xz4bot_crv,spsct_xbot38(5));

%.................................................

for i=1:5
 spsct_xtop38(i)=xtransl(4)+scale(4);
end

spsct_ytop38(1)=0;
spsct_ytop38(2)=colwidth(1);
for i=3:5
 spsct_ytop38(i)=spsct_ytop38(i-1)+colwidth(i-1);
end
```



```
spsct_ztop38(1)=polyval(xzroottop_crv,spsct_xtop38(1));
spsct_ztop38(2)=polyval(xz1top_crv,spsct_xtop38(2));
spsct_ztop38(3)=polyval(xz2top_crv,spsct_xtop38(3));
spsct_ztop38(4)=polyval(xz3top_crv,spsct_xtop38(4));
spsct_ztop38(5)=polyval(xz4top_crv,spsct_xtop38(5));

% ...FOR SECTION 39 (FOUR POINTS)
% ~~~~~~~~~~~~~~~~~~~~~~~~~~~~~~

for i=1:4
 spsct_xbot39(i)=xtransl(3)+scale(3);
end

spsct_ybot39(1)=0;
spsct_ybot39(2)=colwidth(1);
for i=3:4
 spsct_ybot39(i)=spsct_ybot39(i-1)+colwidth(i-1);
end

spsct_zbot39(1)=polyval(xzrootbot_crv,spsct_xbot39(1));
spsct_zbot39(2)=polyval(xz1bot_crv,spsct_xbot39(2));
spsct_zbot39(3)=polyval(xz2bot_crv,spsct_xbot39(3));
spsct_zbot39(4)=polyval(xz3bot_crv,spsct_xbot39(4));

%.................................................

for i=1:4
 spsct_xtop39(i)=xtransl(3)+scale(3);
end

spsct_ytop39(1)=0;
spsct_ytop39(2)=colwidth(1);
for i=3:4
 spsct_ytop39(i)=spsct_ytop39(i-1)+colwidth(i-1);
end

spsct_ztop39(1)=polyval(xzroottop_crv,spsct_xtop39(1));
spsct_ztop39(2)=polyval(xz1top_crv,spsct_xtop39(2));
spsct_ztop39(3)=polyval(xz2top_crv,spsct_xtop39(3));
spsct_ztop39(4)=polyval(xz3top_crv,spsct_xtop39(4));

% ...FOR SECTION 40 (THREE POINTS)
% ~~~~~~~~~~~~~~~~~~~~~~~~~~~~~~

for i=1:3
 spsct_xbot40(i)=xtransl(2)+scale(2);
end

spsct_ybot40(1)=0;
spsct_ybot40(2)=colwidth(1);
spsct_ybot40(3)=spsct_ybot40(2)+colwidth(2);

spsct_zbot40(1)=polyval(xzrootbot_crv,spsct_xbot40(1));
spsct_zbot40(2)=polyval(xz1bot_crv,spsct_xbot40(2));
spsct_zbot40(3)=polyval(xz2bot_crv,spsct_xbot40(3));

%.................................................

for i=1:3
 spsct_xtop40(i)=xtransl(2)+scale(2);
end

spsct_ytop40(1)=0;
spsct_ytop40(2)=colwidth(1);
spsct_ytop40(3)=spsct_ytop40(2)+colwidth(2);

spsct_ztop40(1)=polyval(xzroottop_crv,spsct_xtop40(1));
spsct_ztop40(2)=polyval(xz1top_crv,spsct_xtop40(2));
spsct_ztop40(3)=polyval(xz2top_crv,spsct_xtop40(3));

% ...FOR SECTION 41 (TWO POINTS)
% ~~~~~~~~~~~~~~~~~~~~~~~~~~~~~~

for i=1:2
 spsct_xbot41(i)=xtransl(1)+scale(1);
end
```

```
spsct_ybot41(1)=0;
spsct_ybot41(2)=colwidth(1);

spsct_zbot41(1)=polyval(xzrootbot_crv,spsct_xbot41(1));
spsct_zbot41(2)=polyval(xz1bot_crv,spsct_xbot41(2));

%................................................

for i=1:2
 spsct_xtop41(i)=xtransl(1)+scale(1);
end

spsct_ytop41(1)=0;
spsct_ytop41(2)=colwidth(1);

spsct_ztop41(1)=polyval(xzroottop_crv,spsct_xtop41(1));
spsct_ztop41(2)=polyval(xz1top_crv,spsct_xtop41(2));

% ...AT THE ROOT TRAILING EDGE (ONE POINT)
% ~~~~~~~~~~~~~~~~~~~~~~~~~~~~~~~~~~~~~~~

spsct_xbotTE=0.6439;
spsct_ybotTE=0;
spsct_zbotTE=polyval(xzrootbot_crv,0.6439);

spsct_xtopTE=0.6439;
spsct_ytopTE=0;
spsct_ztopTE=polyval(xzroottop_crv,0.6439);


% PLOTTING THE RESULTS - YZ NON-SMOOTHED
% --------------------------------------
plot(spsct_ybotLE,spsct_zbotLE,'o',spsct_ytopLE,spsct_ztopLE,'o')
axis([0 0.7 -0.016 0.016]);pause
plot(spsct_ybot1,spsct_zbot1,spsct_ytop1,spsct_ztop1)
axis([0 0.7 -0.016 0.016]);pause
plot(spsct_ybot2,spsct_zbot2,spsct_ytop2,spsct_ztop2)
axis([0 0.7 -0.016 0.016]);pause
plot(spsct_ybot3,spsct_zbot3,spsct_ytop3,spsct_ztop3)
axis([0 0.7 -0.016 0.016]);pause
plot(spsct_ybot4,spsct_zbot4,spsct_ytop4,spsct_ztop4)
axis([0 0.7 -0.016 0.016]);pause
plot(spsct_ybot5,spsct_zbot5,spsct_ytop5,spsct_ztop5)
axis([0 0.7 -0.016 0.016]);pause
plot(spsct_ybot6,spsct_zbot6,spsct_ytop6,spsct_ztop6)
axis([0 0.7 -0.016 0.016]);pause
plot(spsct_ybot7,spsct_zbot7,spsct_ytop7,spsct_ztop7)
axis([0 0.7 -0.016 0.016]);pause
plot(spsct_ybot8,spsct_zbot8,spsct_ytop8,spsct_ztop8)
axis([0 0.7 -0.016 0.016]);pause
plot(spsct_ybot9,spsct_zbot9,spsct_ytop9,spsct_ztop9)
axis([0 0.7 -0.016 0.016]);pause
plot(spsct_ybot10,spsct_zbot10,spsct_ytop10,spsct_ztop10)
axis([0 0.7 -0.016 0.016]);pause
plot(spsct_ybot11,spsct_zbot11,spsct_ytop11,spsct_ztop11)
axis([0 0.7 -0.016 0.016]);pause
plot(spsct_ybot12,spsct_zbot12,spsct_ytop12,spsct_ztop12)
axis([0 0.7 -0.016 0.016]);pause
plot(spsct_ybot13,spsct_zbot13,spsct_ytop13,spsct_ztop13)
axis([0 0.7 -0.016 0.016]);pause
plot(spsct_ybot14,spsct_zbot14,spsct_ytop14,spsct_ztop14)
axis([0 0.7 -0.016 0.016]);pause
plot(spsct_ybot15,spsct_zbot15,spsct_ytop15,spsct_ztop15)
axis([0 0.7 -0.016 0.016]);pause
plot(spsct_ybot16,spsct_zbot16,spsct_ytop16,spsct_ztop16)
axis([0 0.7 -0.016 0.016]);pause
plot(spsct_ybot17,spsct_zbot17,spsct_ytop17,spsct_ztop17)
axis([0 0.7 -0.016 0.016]);pause
plot(spsct_ybot18,spsct_zbot18,spsct_ytop18,spsct_ztop18)
axis([0 0.7 -0.016 0.016]);pause
plot(spsct_ybot19,spsct_zbot19,spsct_ytop19,spsct_ztop19)
axis([0 0.7 -0.016 0.016]);pause
plot(spsct_ybot20,spsct_zbot20,spsct_ytop20,spsct_ztop20)
axis([0 0.7 -0.016 0.016]);pause
plot(spsct_ybot21,spsct_zbot21,spsct_ytop21,spsct_ztop21)
```



```
axis([0 0.7 -0.016 0.016]);pause
plot(spsct_ybot22,spsct_zbot22,spsct_ytop22,spsct_ztop22)
axis([0 0.7 -0.016 0.016]);pause
plot(spsct_ybot23,spsct_zbot23,spsct_ytop23,spsct_ztop23)
axis([0 0.7 -0.016 0.016]);pause
plot(spsct_ybot24,spsct_zbot24,spsct_ytop24,spsct_ztop24)
axis([0 0.7 -0.016 0.016]);pause
plot(spsct_ybot25,spsct_zbot25,spsct_ytop25,spsct_ztop25)
axis([0 0.7 -0.016 0.016]);pause
plot(spsct_ybot26,spsct_zbot26,spsct_ytop26,spsct_ztop26)
axis([0 0.7 -0.016 0.016]);pause
plot(spsct_ybot27,spsct_zbot27,spsct_ytop27,spsct_ztop27)
axis([0 0.7 -0.016 0.016]);pause
plot(spsct_ybot28,spsct_zbot28,spsct_ytop28,spsct_ztop28)
axis([0 0.7 -0.016 0.016]);pause
plot(spsct_ybot29,spsct_zbot29,spsct_ytop29,spsct_ztop29)
axis([0 0.7 -0.016 0.016]);pause
plot(spsct_ybot30,spsct_zbot30,spsct_ytop30,spsct_ztop30)
axis([0 0.7 -0.016 0.016]);pause
plot(spsct_ybot31,spsct_zbot31,spsct_ytop31,spsct_ztop31)
axis([0 0.7 -0.016 0.016]);pause
plot(spsct_ybot32,spsct_zbot32,spsct_ytop32,spsct_ztop32)
axis([0 0.7 -0.016 0.016]);pause
plot(spsct_ybot33,spsct_zbot33,spsct_ytop33,spsct_ztop33)
axis([0 0.7 -0.016 0.016]);pause
plot(spsct_ybot34,spsct_zbot34,spsct_ytop34,spsct_ztop34)
axis([0 0.7 -0.016 0.016]);pause
plot(spsct_ybot35,spsct_zbot35,spsct_ytop35,spsct_ztop35)
axis([0 0.7 -0.016 0.016]);pause
plot(spsct_ybot36,spsct_zbot36,spsct_ytop36,spsct_ztop36)
axis([0 0.7 -0.016 0.016]);pause
plot(spsct_ybot37,spsct_zbot37,spsct_ytop37,spsct_ztop37)
axis([0 0.7 -0.016 0.016]);pause
plot(spsct_ybot38,spsct_zbot38,spsct_ytop38,spsct_ztop38)
axis([0 0.7 -0.016 0.016]);pause
plot(spsct_ybot39,spsct_zbot39,spsct_ytop39,spsct_ztop39)
axis([0 0.7 -0.016 0.016]);pause
plot(spsct_ybot40,spsct_zbot40,spsct_ytop40,spsct_ztop40)
axis([0 0.7 -0.016 0.016]);pause
plot(spsct_ybot41,spsct_zbot41,spsct_ytop41,spsct_ztop41)
axis([0 0.7 -0.016 0.016]);pause
plot(spsct_ybotTE,spsct_zbotTE,'o',spsct_ytopTE,spsct_ztopTE,'o')
axis([0 0.7 -0.016 0.016]);pause


plot(spsct_ybotLE,spsct_zbotLE,'o',spsct_ytopLE,spsct_ztopLE,'o', ...
  spsct_ybot1,spsct_zbot1,'y',spsct_ytop1,spsct_ztop1,'y', ...
  spsct_ybot2,spsct_zbot2,'m',spsct_ytop2,spsct_ztop2,'m', ...
  spsct_ybot5,spsct_zbot5,'c',spsct_ytop5,spsct_ztop5,'c', ...
  spsct_ybot6,spsct_zbot6,'r',spsct_ytop6,spsct_ztop6,'r', ...
  spsct_ybot9,spsct_zbot9,'g',spsct_ytop9,spsct_ztop9,'g', ...
  spsct_ybot11,spsct_zbot11,'b',spsct_ytop11,spsct_ztop11,'b', ...
  spsct_ybot15,spsct_zbot15,'w',spsct_ytop15,spsct_ztop15,'w')
xlabel('Unit Spanwise Location (-y direction)')
ylabel('Unit Vertical Location (z dierction)')
title('F5 Wing - Spanwise Sections From FWD Apex to Tip L.E.')
grid
pause

plot(spsct_ybot16,spsct_zbot16,'y',spsct_ytop16,spsct_ztop16,'y', ...
  spsct_ybot18,spsct_zbot18,'m',spsct_ytop18,spsct_ztop18,'m', ...
  spsct_ybot19,spsct_zbot19,'c',spsct_ytop19,spsct_ztop19,'c', ...
  spsct_ybot21,spsct_zbot21,'r',spsct_ytop21,spsct_ztop21,'r', ...
  spsct_ybot22,spsct_zbot22,'g',spsct_ytop22,spsct_ztop22,'g', ...
  spsct_ybot24,spsct_zbot24,'b',spsct_ytop24,spsct_ztop24,'b', ...
  spsct_ybot25,spsct_zbot25,'w',spsct_ytop25,spsct_ztop25,'w', ...
  spsct_ybot27,spsct_zbot27,'y',spsct_ytop27,spsct_ztop27,'y')
xlabel('Unit Spanwise Location (-y direction)')
ylabel('Unit Vertical Location (z dierction)')
title('F5 Wing - Spanwise Sections From Tip L.E. to Tip T.E.')
grid
pause

plot(spsct_ybot28,spsct_zbot28,'y',spsct_ytop28,spsct_ztop28,'y', ...
  spsct_ybot30,spsct_zbot30,'m',spsct_ytop30,spsct_ztop30,'m', ...
  spsct_ybot32,spsct_zbot32,'c',spsct_ytop32,spsct_ztop32,'c', ...
```

```
   spsct_ybot34,spsct_zbot34,'r',spsct_ytop34,spsct_ztop34,'r', ...
   spsct_ybot36,spsct_zbot36,'g',spsct_ytop36,spsct_ztop36,'g', ...
   spsct_ybot38,spsct_zbot38,'b',spsct_ytop38,spsct_ztop38,'b', ...
   spsct_ybot41,spsct_zbot41,'w',spsct_ytop41,spsct_ztop41,'w', ...
   spsct_ybotTE,spsct_zbotTE,'o',spsct_ytopTE,spsct_ztopTE,'o')
grid
xlabel('Unit Spanwise Location (-y direction)')
ylabel('Unit Vertical Location (z dierction)')
title('F5 Wing - Spanwise Sections From Tip T.E. to AFT Apex')
pause


plot3(spsct_xbot20,spsct_ybot20,spsct_zbot20,'b', ...
      spsct_xtop20,spsct_ytop20,spsct_ztop20,'b', ...
      spsct_xbot10,spsct_ybot10,spsct_zbot10,'g', ...
      spsct_xtop10,spsct_ytop10,spsct_ztop10,'g', ...
      spsct_xbot5,spsct_ybot5,spsct_zbot5,'y', ...
      spsct_xtop5,spsct_ytop5,spsct_ztop5,'y')
xlabel('Chordwise Direction (x)')
ylabel('Spanwise Direction (-y)')
zlabel('Height (z)')
title('F5 Wing RH side Spanwise Sections')
pause

plot3(spsct_xbot1,spsct_ybot1,spsct_zbot1,'y', ...
      spsct_xtop1,spsct_ytop1,spsct_ztop1,'y', ...
      spsct_xbot8,spsct_ybot8,spsct_zbot8,'m', ...
      spsct_xtop8,spsct_ytop8,spsct_ztop8,'m', ...
      spsct_xbot15,spsct_ybot15,spsct_zbot15,'c', ...
      spsct_xtop15,spsct_ytop15,spsct_ztop15,'c', ...
      spsct_xbot27,spsct_ybot27,spsct_zbot27,'b', ...
      spsct_xtop27,spsct_ytop27,spsct_ztop27,'b', ...
      spsct_xbot34,spsct_ybot34,spsct_zbot34,'w', ...
      spsct_xtop34,spsct_ytop34,spsct_ztop34,'w', ...
      spsct_xbot41,spsct_ybot41,spsct_zbot41,'y', ...
      spsct_xtop41,spsct_ytop41,spsct_ztop41,'y')
pause

% FITTING EACH YZ CURVE WITH A POLYNOMIAL
% ---------------------------------------

xsection=zeros(1,41);
%diary on
yibot1=0:0.001:spsct_ybot1(2);
zibot1=spline(spsct_ybot1,spsct_zbot1,yibot1);
yz1bot_crv=polyval(yibot1,zibot1,3);
%plot(spsct_ybot1,spsct_zbot1,'o',yibot1,zibot1)
coef1_bot=polyfit(yibot1,zibot1,3)
xsection(1)=spsct_xbot1(1);
xsection(1)
%
yitop1=0:0.001:spsct_ytop1(2);
zitop1=spline(spsct_ytop1,spsct_ztop1,yitop1);
yz1top_crv=polyval(yitop1,zitop1,3);
%plot(spsct_ytop1,spsct_ztop1,'o',yitop1,zitop1)
coef1_top=polyfit(yitop1,zitop1,3)
xsection(1)=spsct_xtop1(1);
xsection(1)
%
%
yibot2=0:0.001:spsct_ybot2(3);
zibot2=spline(spsct_ybot2,spsct_zbot2,yibot2);
yz2bot_crv=polyval(yibot2,zibot2,3);
%plot(spsct_ybot2,spsct_zbot2,'o',yibot2,zibot2)
coef2_bot=polyfit(yibot2,zibot2,3)
xsection(2)=spsct_xbot2(1);
xsection(2)
%
yitop2=0:0.001:spsct_ytop2(3);
zitop2=spline(spsct_ytop2,spsct_ztop2,yitop2);
yz2top_crv=polyval(yitop2,zitop2,3);
%plot(spsct_ytop2,spsct_ztop2,'o',yitop2,zitop2)
coef2_top=polyfit(yitop2,zitop2,3)
xsection(2)=spsct_xtop2(1);
xsection(2)
%
```



```
%
yibot3=0:0.001:spsct_ybot3(4);
zibot3=spline(spsct_ybot3,spsct_zbot3,yibot3);
yz3bot_crv=polyval(yibot3,zibot3,3);
%plot(spsct_ybot3,spsct_zbot3,'o',yibot3,zibot3)
coef3_bot=polyfit(yibot3,zibot3,3)
xsection(3)=spsct_xbot3(1);
xsection(3)
%
yitop3=0:0.001:spsct_ytop3(4);
zitop3=spline(spsct_ytop3,spsct_ztop3,yitop3);
yz3top_crv=polyval(yitop3,zitop3,3);
%plot(spsct_ytop3,spsct_ztop3,'o',yitop3,zitop3)
coef3_top=polyfit(yitop3,zitop3,3)
xsection(3)=spsct_xtop3(1);
xsection(3)
%
%
yibot4=0:0.001:spsct_ybot4(5);
zibot4=spline(spsct_ybot4,spsct_zbot4,yibot4);
yz4bot_crv=polyval(yibot4,zibot4,3);
%plot(spsct_ybot4,spsct_zbot4,'o',yibot4,zibot4)
coef4_bot=polyfit(yibot4,zibot4,3)
xsection(4)=spsct_xbot4(1);
xsection(4)
%
yitop4=0:0.001:spsct_ytop4(5);
zitop4=spline(spsct_ytop4,spsct_ztop4,yitop4);
yz4top_crv=polyval(yitop4,zitop4,3);
%plot(spsct_ytop4,spsct_ztop4,'o',yitop4,zitop4)
coef4_top=polyfit(yitop4,zitop4,3)
xsection(4)=spsct_xtop4(1);
xsection(4)
%
%
yibot5=0:0.001:spsct_ybot5(6);
zibot5=spline(spsct_ybot5,spsct_zbot5,yibot5);
yz5bot_crv=polyval(yibot5,zibot5,3);
%plot(spsct_ybot5,spsct_zbot5,'o',yibot5,zibot5)
coef5_bot=polyfit(yibot5,zibot5,3)
xsection(5)=spsct_xbot5(1);
xsection(5)
%
yitop5=0:0.001:spsct_ytop5(6);
zitop5=spline(spsct_ytop5,spsct_ztop5,yitop5);
yz5top_crv=polyval(yitop5,zitop5,3);
%plot(spsct_ytop5,spsct_ztop5,'o',yitop5,zitop5)
coef5_top=polyfit(yitop5,zitop5,3)
xsection(5)=spsct_xtop5(1);
xsection(5)
%
%
yibot6=0:0.001:spsct_ybot6(7);
zibot6=spline(spsct_ybot6,spsct_zbot6,yibot6);
yz6bot_crv=polyval(yibot6,zibot6,3);
%plot(spsct_ybot6,spsct_zbot6,'o',yibot6,zibot6)
coef6_bot=polyfit(yibot6,zibot6,3)
xsection(6)=spsct_xbot6(1);
xsection(6)
%
yitop6=0:0.001:spsct_ytop6(7);
zitop6=spline(spsct_ytop6,spsct_ztop6,yitop6);
yz6top_crv=polyval(yitop6,zitop6,3);
%plot(spsct_ytop6,spsct_ztop6,'o',yitop6,zitop6)
coef6_top=polyfit(yitop6,zitop6,3)
xsection(6)=spsct_xtop6(1);
xsection(6)
%
%
yibot7=0:0.001:spsct_ybot7(8);
zibot7=spline(spsct_ybot7,spsct_zbot7,yibot7);
yz7bot_crv=polyval(yibot7,zibot7,3);
%plot(spsct_ybot7,spsct_zbot7,'o',yibot7,zibot7)
coef7_bot=polyfit(yibot7,zibot7,3)
xsection(7)=spsct_xbot7(1);
xsection(7)
```

```
%
yitop7=0:0.001:spsct_ytop7(8);
zitop7=spline(spsct_ytop7,spsct_ztop7,yitop7);
yz7top_crv=polyval(yitop7,zitop7,3);
%plot(spsct_ytop7,spsct_ztop7,'o',yitop7,zitop7)
coef7_top=polyfit(yitop7,zitop7,3)
xsection(7)=spsct_xtop7(1);
xsection(7)
%
%
yibot8=0:0.001:spsct_ybot8(9);
zibot8=spline(spsct_ybot8,spsct_zbot8,yibot8);
yz8bot_crv=polyval(yibot8,zibot8,3);
%plot(spsct_ybot8,spsct_zbot8,'o',yibot8,zibot8)
coef8_bot=polyfit(yibot8,zibot8,3)
xsection(8)=spsct_xbot8(1);
xsection(8)
%
yitop8=0:0.001:spsct_ytop8(9);
zitop8=spline(spsct_ytop8,spsct_ztop8,yitop8);
yz8top_crv=polyval(yitop8,zitop8,3);
%plot(spsct_ytop8,spsct_ztop8,'o',yitop8,zitop8)
coef8_top=polyfit(yitop8,zitop8,3)
xsection(8)=spsct_xtop8(1);
xsection(8)
%
%
yibot9=0:0.001:spsct_ybot9(10);
zibot9=spline(spsct_ybot9,spsct_zbot9,yibot9);
yz9bot_crv=polyval(yibot9,zibot9,3);
%plot(spsct_ybot9,spsct_zbot9,'o',yibot9,zibot9)
coef9_bot=polyfit(yibot9,zibot9,3)
xsection(9)=spsct_xbot9(1);
xsection(9)
%
yitop9=0:0.001:spsct_ytop9(10);
zitop9=spline(spsct_ytop9,spsct_ztop9,yitop9);
yz9top_crv=polyval(yitop9,zitop9,3);
%plot(spsct_ytop9,spsct_ztop9,'o',yitop9,zitop9)
coef9_top=polyfit(yitop9,zitop9,3)
xsection(9)=spsct_xtop9(1);
xsection(9)
%
%
yibot10=0:0.001:spsct_ybot10(11);
zibot10=spline(spsct_ybot10,spsct_zbot10,yibot10);
yz10bot_crv=polyval(yibot10,zibot10,3);
%plot(spsct_ybot10,spsct_zbot10,'o',yibot10,zibot10)
coef10_bot=polyfit(yibot10,zibot10,3)
xsection(10)=spsct_xbot10(1);
xsection(10)
%
yitop10=0:0.001:spsct_ytop10(11);
zitop10=spline(spsct_ytop10,spsct_ztop10,yitop10);
yz10top_crv=polyval(yitop10,zitop10,3);
%plot(spsct_ytop10,spsct_ztop10,'o',yitop10,zitop10)
coef10_top=polyfit(yitop10,zitop10,3)
xsection(10)=spsct_xtop10(1);
xsection(10)
%
%
yibot11=0:0.001:spsct_ybot11(12);
zibot11=spline(spsct_ybot11,spsct_zbot11,yibot11);
yz11bot_crv=polyval(yibot11,zibot11,3);
%plot(spsct_ybot11,spsct_zbot11,'o',yibot11,zibot11)
coef11_bot=polyfit(yibot11,zibot11,3)
xsection(11)=spsct_xbot11(1);
xsection(11)
%
yitop11=0:0.001:spsct_ytop11(12);
zitop11=spline(spsct_ytop11,spsct_ztop11,yitop11);
yz11top_crv=polyval(yitop11,zitop11,3);
%plot(spsct_ytop11,spsct_ztop11,'o',yitop11,zitop11)
coef11_top=polyfit(yitop11,zitop11,3)
xsection(11)=spsct_xtop11(1);
xsection(11)
```



```
%
%
yibot12=0:0.001:spsct_ybot12(13);
zibot12=spline(spsct_ybot12,spsct_zbot12,yibot12);
yz12bot_crv=polyval(yibot12,zibot12,3);
%plot(spsct_ybot12,spsct_zbot12,'o',yibot12,zibot12)
coef12_bot=polyfit(yibot12,zibot12,3)
xsection(12)=spsct_xbot12(1);
xsection(12)
%
yitop12=0:0.001:spsct_ytop12(13);
zitop12=spline(spsct_ytop12,spsct_ztop12,yitop12);
yz12top_crv=polyval(yitop12,zitop12,3);
%plot(spsct_ytop12,spsct_ztop12,'o',yitop12,zitop12)
coef12_top=polyfit(yitop12,zitop12,3)
xsection(12)=spsct_xtop12(1);
xsection(12)
%
%
yibot13=0:0.001:spsct_ybot13(14);
zibot13=spline(spsct_ybot13,spsct_zbot13,yibot13);
yz13bot_crv=polyval(yibot13,zibot13,3);
%plot(spsct_ybot13,spsct_zbot13,'o',yibot13,zibot13)
coef13_bot=polyfit(yibot13,zibot13,3)
xsection(13)=spsct_xbot13(1);
xsection(13)
%
yitop13=0:0.001:spsct_ytop13(14);
zitop13=spline(spsct_ytop13,spsct_ztop13,yitop13);
yz13top_crv=polyval(yitop13,zitop13,3);
%plot(spsct_ytop13,spsct_ztop13,'o',yitop13,zitop13)
coef13_top=polyfit(yitop13,zitop13,3)
xsection(13)=spsct_xtop13(1);
xsection(13)
%
%
yibot14=0:0.001:spsct_ybot14(15);
zibot14=spline(spsct_ybot14,spsct_zbot14,yibot14);
yz14bot_crv=polyval(yibot14,zibot14,3);
%plot(spsct_ybot14,spsct_zbot14,'o',yibot14,zibot14)
coef14_bot=polyfit(yibot14,zibot14,3)
xsection(14)=spsct_xbot14(1);
xsection(14)
%
yitop14=0:0.001:spsct_ytop14(15);
zitop14=spline(spsct_ytop14,spsct_ztop14,yitop14);
yz14top_crv=polyval(yitop14,zitop14,3);
%plot(spsct_ytop14,spsct_ztop14,'o',yitop14,zitop14)
coef14_top=polyfit(yitop14,zitop14,3)
xsection(14)=spsct_xtop14(1);
xsection(14)
%
%
yibot15=0:0.001:spsct_ybot15(16);
zibot15=spline(spsct_ybot15,spsct_zbot15,yibot15);
yz15bot_crv=polyval(yibot15,zibot15,3);
%plot(spsct_ybot15,spsct_zbot15,'o',yibot15,zibot15)
coef15_bot=polyfit(yibot15,zibot15,3)
xsection(15)=spsct_xbot15(1);
xsection(15)
%
yitop15=0:0.001:spsct_ytop15(16);
zitop15=spline(spsct_ytop15,spsct_ztop15,yitop15);
yz15top_crv=polyval(yitop15,zitop15,3);
%plot(spsct_ytop15,spsct_ztop15,'o',yitop15,zitop15)
coef15_top=polyfit(yitop15,zitop15,3)
xsection(15)=spsct_xtop15(1);
xsection(15)
%
%
yibot16=0:0.001:spsct_ybot16(16);
zibot16=spline(spsct_ybot16,spsct_zbot16,yibot16);
yz16bot_crv=polyval(yibot16,zibot16,3);
%plot(spsct_ybot16,spsct_zbot16,'o',yibot16,zibot16)
coef16_bot=polyfit(yibot16,zibot16,3)
xsection(16)=spsct_xbot16(1);
```

```
xsection(16)
%
yitop16=0:0.001:spsct_ytop16(16);
zitop16=spline(spsct_ytop16,spsct_ztop16,yitop16);
yz16top_crv=polyval(yitop16,zitop16,3);
%plot(spsct_ytop16,spsct_ztop16,'o',yitop16,zitop16)
coef16_top=polyfit(yitop16,zitop16,3)
xsection(16)=spsct_xtop16(1);
xsection(16)
%
%
yibot17=0:0.001:spsct_ybot17(16);
zibot17=spline(spsct_ybot17,spsct_zbot17,yibot17);
yz17bot_crv=polyval(yibot17,zibot17,3);
%plot(spsct_ybot17,spsct_zbot17,'o',yibot17,zibot17)
coef17_bot=polyfit(yibot17,zibot17,3)
xsection(17)=spsct_xbot17(1);
xsection(17)
%
yitop17=0:0.001:spsct_ytop17(16);
zitop17=spline(spsct_ytop17,spsct_ztop17,yitop17);
yz17top_crv=polyval(yitop17,zitop17,3);
%plot(spsct_ytop17,spsct_ztop17,'o',yitop17,zitop17)
coef17_top=polyfit(yitop17,zitop17,3)
xsection(17)=spsct_xtop17(1);
xsection(17)
%
%
yibot18=0:0.001:spsct_ybot18(16);
zibot18=spline(spsct_ybot18,spsct_zbot18,yibot18);
yz18bot_crv=polyval(yibot18,zibot18,3);
%plot(spsct_ybot18,spsct_zbot18,'o',yibot18,zibot18)
coef18_bot=polyfit(yibot18,zibot18,3)
xsection(18)=spsct_xbot18(1);
xsection(18)
%
yitop18=0:0.001:spsct_ytop18(16);
zitop18=spline(spsct_ytop18,spsct_ztop18,yitop18);
yz18top_crv=polyval(yitop18,zitop18,3);
%plot(spsct_ytop18,spsct_ztop18,'o',yitop18,zitop18)
coef18_top=polyfit(yitop18,zitop18,3)
xsection(18)=spsct_xtop18(1);
xsection(18)
%
%
yibot19=0:0.001:spsct_ybot19(16);
zibot19=spline(spsct_ybot19,spsct_zbot19,yibot19);
yz19bot_crv=polyval(yibot19,zibot19,3);
%plot(spsct_ybot19,spsct_zbot19,'o',yibot19,zibot19)
coef19_bot=polyfit(yibot19,zibot19,3)
xsection(19)=spsct_xbot19(1);
xsection(19)
%
yitop19=0:0.001:spsct_ytop19(16);
zitop19=spline(spsct_ytop19,spsct_ztop19,yitop19);
yz19top_crv=polyval(yitop19,zitop19,3);
%plot(spsct_ytop19,spsct_ztop19,'o',yitop19,zitop19)
coef19_top=polyfit(yitop19,zitop19,3)
xsection(19)=spsct_xtop19(1);
xsection(19)
%
%
yibot20=0:0.001:spsct_ybot20(16);
zibot20=spline(spsct_ybot20,spsct_zbot20,yibot20);
yz20bot_crv=polyval(yibot20,zibot20,3);
%plot(spsct_ybot20,spsct_zbot20,'o',yibot20,zibot20)
coef20_bot=polyfit(yibot20,zibot20,3)
xsection(20)=spsct_xbot20(1);
xsection(20)
%
yitop20=0:0.001:spsct_ytop20(16);
zitop20=spline(spsct_ytop20,spsct_ztop20,yitop20);
yz20top_crv=polyval(yitop20,zitop20,3);
%plot(spsct_ytop20,spsct_ztop20,'o',yitop20,zitop20)
coef20_top=polyfit(yitop20,zitop20,3)
xsection(20)=spsct_xtop20(1);
```



```
xsection(20)
%
%
yibot21=0:0.001:spsct_ybot21(16);
zibot21=spline(spsct_ybot21,spsct_zbot21,yibot21);
yz21bot_crv=polyval(yibot21,zibot21,3);
%plot(spsct_ybot21,spsct_zbot21,'o',yibot21,zibot21)
coef21_bot=polyfit(yibot21,zibot21,3)
xsection(21)=spsct_xbot21(1);
xsection(21)
%
yitop21=0:0.001:spsct_ytop21(16);
zitop21=spline(spsct_ytop21,spsct_ztop21,yitop21);
yz21top_crv=polyval(yitop21,zitop21,3);
%plot(spsct_ytop21,spsct_ztop21,'o',yitop21,zitop21)
coef21_top=polyfit(yitop21,zitop21,3)
xsection(21)=spsct_xtop21(1);
xsection(21)
%
%
yibot22=0:0.001:spsct_ybot22(16);
zibot22=spline(spsct_ybot22,spsct_zbot22,yibot22);
yz22bot_crv=polyval(yibot22,zibot22,3);
%plot(spsct_ybot22,spsct_zbot22,'o',yibot22,zibot22)
coef22_bot=polyfit(yibot22,zibot22,3)
xsection(22)=spsct_xbot22(1);
xsection(22)
%
yitop22=0:0.001:spsct_ytop22(16);
zitop22=spline(spsct_ytop22,spsct_ztop22,yitop22);
yz22top_crv=polyval(yitop22,zitop22,3);
%plot(spsct_ytop22,spsct_ztop22,'o',yitop22,zitop22)
coef22_top=polyfit(yitop22,zitop22,3)
xsection(22)=spsct_xtop22(1);
xsection(22)
%
%
yibot23=0:0.001:spsct_ybot23(16);
zibot23=spline(spsct_ybot23,spsct_zbot23,yibot23);
yz23bot_crv=polyval(yibot23,zibot23,3);
plot(spsct_ybot23,spsct_zbot23,'o',yibot23,zibot23)
coef23_bot=polyfit(yibot23,zibot23,3)
xsection(23)=spsct_xbot23(1);
xsection(23)
%
yitop23=0:0.001:spsct_ytop23(16);
zitop23=spline(spsct_ytop23,spsct_ztop23,yitop23);
yz23top_crv=polyval(yitop23,zitop23,3);
%plot(spsct_ytop23,spsct_ztop23,'o',yitop23,zitop23)
coef23_top=polyfit(yitop23,zitop23,3)
xsection(23)=spsct_xtop23(1);
xsection(23)
%
%
yibot24=0:0.001:spsct_ybot24(16);
zibot24=spline(spsct_ybot24,spsct_zbot24,yibot24);
yz24bot_crv=polyval(yibot24,zibot24,3);
%plot(spsct_ybot24,spsct_zbot24,'o',yibot24,zibot24)
coef24_bot=polyfit(yibot24,zibot24,3)
xsection(24)=spsct_xbot24(1);
xsection(24)
%
yitop24=0:0.001:spsct_ytop24(16);
zitop24=spline(spsct_ytop24,spsct_ztop24,yitop24);
yz24top_crv=polyval(yitop24,zitop24,3);
%plot(spsct_ytop24,spsct_ztop24,'o',yitop24,zitop24)
coef24_top=polyfit(yitop24,zitop24,3)
xsection(24)=spsct_xtop24(1);
xsection(24)
%
%
yibot25=0:0.001:spsct_ybot25(16);
zibot25=spline(spsct_ybot25,spsct_zbot25,yibot25);
yz25bot_crv=polyval(yibot25,zibot25,3);
%plot(spsct_ybot25,spsct_zbot25,'o',yibot25,zibot25)
coef25_bot=polyfit(yibot25,zibot25,3)
```

```
xsection(25)=spsct_xbot25(1);
xsection(25)
%
yitop25=0:0.001:spsct_ytop25(16);
zitop25=spline(spsct_ytop25,spsct_ztop25,yitop25);
yz25top_crv=polyval(yitop25,zitop25,3);
%plot(spsct_ytop25,spsct_ztop25,'o',yitop25,zitop25)
coef25_top=polyfit(yitop25,zitop25,3)
xsection(25)=spsct_xtop25(1);
xsection(25)
%
%
yibot26=0:0.001:spsct_ybot26(16);
zibot26=spline(spsct_ybot26,spsct_zbot26,yibot26);
yz26bot_crv=polyval(yibot26,zibot26,3);
%plot(spsct_ybot26,spsct_zbot26,'o',yibot26,zibot26)
coef26_bot=polyfit(yibot26,zibot26,3)
xsection(26)=spsct_xbot26(1);
xsection(26)
%
yitop26=0:0.001:spsct_ytop26(16);
zitop26=spline(spsct_ytop26,spsct_ztop26,yitop26);
yz26top_crv=polyval(yitop26,zitop26,3);
%plot(spsct_ytop26,spsct_ztop26,'o',yitop26,zitop26)
coef26_top=polyfit(yitop26,zitop26,3)
xsection(26)=spsct_xtop26(1);
xsection(26)
%
%
yibot27=0:0.001:spsct_ybot27(16);
zibot27=spline(spsct_ybot27,spsct_zbot27,yibot27);
yz27bot_crv=polyval(yibot27,zibot27,3);
%plot(spsct_ybot27,spsct_zbot27,'o',yibot27,zibot27)
coef27_bot=polyfit(yibot27,zibot27,3)
xsection(27)=spsct_xbot27(1);
xsection(27)
%
yitop27=0:0.001:spsct_ytop27(16);
zitop27=spline(spsct_ytop27,spsct_ztop27,yitop27);
yz27top_crv=polyval(yitop27,zitop27,3);
%plot(spsct_ytop27,spsct_ztop27,'o',yitop27,zitop27)
coef27_top=polyfit(yitop27,zitop27,3)
xsection(27)=spsct_xtop27(1);
xsection(27)
%
%
yibot28=0:0.001:spsct_ybot28(15);
zibot28=spline(spsct_ybot28,spsct_zbot28,yibot28);
yz28bot_crv=polyval(yibot28,zibot28,3);
%plot(spsct_ybot28,spsct_zbot28,'o',yibot28,zibot28)
coef28_bot=polyfit(yibot28,zibot28,3)
xsection(28)=spsct_xbot28(1);
xsection(28)
%
yitop28=0:0.001:spsct_ytop28(15);
zitop28=spline(spsct_ytop28,spsct_ztop28,yitop28);
yz28top_crv=polyval(yitop28,zitop28,3);
%plot(spsct_ytop28,spsct_ztop28,'o',yitop28,zitop28)
coef28_top=polyfit(yitop28,zitop28,3)
xsection(28)=spsct_xtop28(1);
xsection(28)
%
%
yibot29=0:0.001:spsct_ybot29(14);
zibot29=spline(spsct_ybot29,spsct_zbot29,yibot29);
yz29bot_crv=polyval(yibot29,zibot29,3);
%plot(spsct_ybot29,spsct_zbot29,'o',yibot29,zibot29)
coef29_bot=polyfit(yibot29,zibot29,3)
xsection(29)=spsct_xbot29(1);
xsection(29)
%
yitop29=0:0.001:spsct_ytop29(14);
zitop29=spline(spsct_ytop29,spsct_ztop29,yitop29);
yz29top_crv=polyval(yitop29,zitop29,3);
%plot(spsct_ytop29,spsct_ztop29,'o',yitop29,zitop29)
coef29_top=polyfit(yitop29,zitop29,3)
```



```
xsection(29)=spsct_xtop29(1);
xsection(29)
%
%
yibot30=0:0.001:spsct_ybot30(13);
zibot30=spline(spsct_ybot30,spsct_zbot30,yibot30);
yz30bot_crv=polyval(yibot30,zibot30,3);
%plot(spsct_ybot30,spsct_zbot30,'o',yibot30,zibot30)
coef30_bot=polyfit(yibot30,zibot30,3)
xsection(30)=spsct_xbot30(1);
xsection(30)
%
yitop30=0:0.001:spsct_ytop30(13);
zitop30=spline(spsct_ytop30,spsct_ztop30,yitop30);
yz30top_crv=polyval(yitop30,zitop30,3);
%plot(spsct_ytop30,spsct_ztop30,'o',yitop30,zitop30)
coef30_top=polyfit(yitop30,zitop30,3)
xsection(30)=spsct_xtop30(1);
xsection(30)
%
%
yibot31=0:0.001:spsct_ybot31(12);
zibot31=spline(spsct_ybot31,spsct_zbot31,yibot31);
yz31bot_crv=polyval(yibot31,zibot31,3);
%plot(spsct_ybot31,spsct_zbot31,'o',yibot31,zibot31)
coef31_bot=polyfit(yibot31,zibot31,3)
xsection(31)=spsct_xbot31(1);
xsection(31)
%
yitop31=0:0.001:spsct_ytop31(12);
zitop31=spline(spsct_ytop31,spsct_ztop31,yitop31);
yz31top_crv=polyval(yitop31,zitop31,3);
%plot(spsct_ytop31,spsct_ztop31,'o',yitop31,zitop31)
coef31_top=polyfit(yitop31,zitop31,3)
xsection(31)=spsct_xtop31(1);
xsection(31)
%
%
yibot32=0:0.001:spsct_ybot32(11);
zibot32=spline(spsct_ybot32,spsct_zbot32,yibot32);
yz32bot_crv=polyval(yibot32,zibot32,3);
%plot(spsct_ybot32,spsct_zbot32,'o',yibot32,zibot32)
coef32_bot=polyfit(yibot32,zibot32,3)
xsection(32)=spsct_xbot32(1);
xsection(32)
%
yitop32=0:0.001:spsct_ytop32(11);
zitop32=spline(spsct_ytop32,spsct_ztop32,yitop32);
yz32top_crv=polyval(yitop32,zitop32,3);
%plot(spsct_ytop32,spsct_ztop32,'o',yitop32,zitop32)
coef32_top=polyfit(yitop32,zitop32,3)
xsection(32)=spsct_xtop32(1);
xsection(32)
%
%
yibot33=0:0.001:spsct_ybot33(10);
zibot33=spline(spsct_ybot33,spsct_zbot33,yibot33);
yz33bot_crv=polyval(yibot33,zibot33,3);
%plot(spsct_ybot33,spsct_zbot33,'o',yibot33,zibot33)
coef33_bot=polyfit(yibot33,zibot33,3)
xsection(33)=spsct_xbot33(1);
xsection(33)
%
yitop33=0:0.001:spsct_ytop33(10);
zitop33=spline(spsct_ytop33,spsct_ztop33,yitop33);
yz33top_crv=polyval(yitop33,zitop33,3);
%plot(spsct_ytop33,spsct_ztop33,'o',yitop33,zitop33)
coef33_top=polyfit(yitop33,zitop33,3)
xsection(33)=spsct_xtop33(1);
xsection(33)
%
%
yibot34=0:0.001:spsct_ybot34(9);
zibot34=spline(spsct_ybot34,spsct_zbot34,yibot34);
yz34bot_crv=polyval(yibot34,zibot34,3);
%plot(spsct_ybot34,spsct_zbot34,'o',yibot34,zibot34)
```

```
coef34_bot=polyfit(yibot34,zibot34,3)
xsection(34)=spsct_xbot34(1);
xsection(34)
%
yitop34=0:0.001:spsct_ytop34(9);
zitop34=spline(spsct_ytop34,spsct_ztop34,yitop34);
yz34top_crv=polyval(yitop34,zitop34,3);
%plot(spsct_ytop34,spsct_ztop34,'o',yitop34,zitop34)
coef34_top=polyfit(yitop34,zitop34,3)
xsection(34)=spsct_xtop34(1);
xsection(34)
%
%
yibot35=0:0.001:spsct_ybot35(8);
zibot35=spline(spsct_ybot35,spsct_zbot35,yibot35);
yz35bot_crv=polyval(yibot35,zibot35,3);
%plot(spsct_ybot35,spsct_zbot35,'o',yibot35,zibot35)
coef35_bot=polyfit(yibot35,zibot35,3)
xsection(35)=spsct_xbot35(1);
xsection(35)
%
yitop35=0:0.001:spsct_ytop35(8);
zitop35=spline(spsct_ytop35,spsct_ztop35,yitop35);
yz35top_crv=polyval(yitop35,zitop35,3);
%plot(spsct_ytop35,spsct_ztop35,'o',yitop35,zitop35)
coef35_top=polyfit(yitop35,zitop35,3)
xsection(35)=spsct_xtop35(1);
xsection(35)
%
%
yibot36=0:0.001:spsct_ybot36(7);
zibot36=spline(spsct_ybot36,spsct_zbot36,yibot36);
yz36bot_crv=polyval(yibot36,zibot36,3);
%plot(spsct_ybot36,spsct_zbot36,'o',yibot36,zibot36)
coef36_bot=polyfit(yibot36,zibot36,3)
xsection(36)=spsct_xbot36(1);
xsection(36)
%
yitop36=0:0.001:spsct_ytop36(7);
zitop36=spline(spsct_ytop36,spsct_ztop36,yitop36);
yz36top_crv=polyval(yitop36,zitop36,3);
%plot(spsct_ytop36,spsct_ztop36,'o',yitop36,zitop36)
coef36_top=polyfit(yitop36,zitop36,3)
xsection(36)=spsct_xtop36(1);
xsection(36)
%
%
yibot37=0:0.001:spsct_ybot37(6);
zibot37=spline(spsct_ybot37,spsct_zbot37,yibot37);
yz37bot_crv=polyval(yibot37,zibot37,3);
%plot(spsct_ybot37,spsct_zbot37,'o',yibot37,zibot37)
coef37_bot=polyfit(yibot37,zibot37,3)
xsection(37)=spsct_xbot37(1);
xsection(37)
%
yitop37=0:0.001:spsct_ytop37(6);
zitop37=spline(spsct_ytop37,spsct_ztop37,yitop37);
yz37top_crv=polyval(yitop37,zitop37,3);
%plot(spsct_ytop37,spsct_ztop37,'o',yitop37,zitop37)
coef37_top=polyfit(yitop37,zitop37,3)
xsection(37)=spsct_xtop37(1);
xsection(37)
%
%
yibot38=0:0.001:spsct_ybot38(5);
zibot38=spline(spsct_ybot38,spsct_zbot38,yibot38);
yz38bot_crv=polyval(yibot38,zibot38,3);
%plot(spsct_ybot38,spsct_zbot38,'o',yibot38,zibot38)
coef38_bot=polyfit(yibot38,zibot38,3)
xsection(38)=spsct_xbot38(1);
xsection(38)
%
yitop38=0:0.001:spsct_ytop38(5);
zitop38=spline(spsct_ytop38,spsct_ztop38,yitop38);
yz38top_crv=polyval(yitop38,zitop38,3);
%plot(spsct_ytop38,spsct_ztop38,'o',yitop38,zitop38)
```



```
coef38_top=polyfit(yitop38,zitop38,3)
xsection(38)=spsct_xtop38(1);
xsection(38)
%
%
yibot39=0:0.001:spsct_ybot39(4);
zibot39=spline(spsct_ybot39,spsct_zbot39,yibot39);
yz39bot_crv=polyval(yibot39,zibot39,3);
%plot(spsct_ybot39,spsct_zbot39,'o',yibot39,zibot39)
coef39_bot=polyfit(yibot39,zibot39,3)
xsection(39)=spsct_xbot39(1);
xsection(39)
%
yitop39=0:0.001:spsct_ytop39(4);
zitop39=spline(spsct_ytop39,spsct_ztop39,yitop39);
yz39top_crv=polyval(yitop39,zitop39,3);
%plot(spsct_ytop39,spsct_ztop39,'o',yitop39,zitop39)
coef39_top=polyfit(yitop39,zitop39,3)
xsection(39)=spsct_xtop39(1);
xsection(39)
%
%
yibot40=0:0.001:spsct_ybot40(3);
zibot40=spline(spsct_ybot40,spsct_zbot40,yibot40);
yz40bot_crv=polyval(yibot40,zibot40,3);
%plot(spsct_ybot40,spsct_zbot40,'o',yibot40,zibot40)
coef40_bot=polyfit(yibot40,zibot40,3)
xsection(40)=spsct_xbot40(1);
xsection(40)
%
yitop40=0:0.001:spsct_ytop40(3);
zitop40=spline(spsct_ytop40,spsct_ztop40,yitop40);
yz40top_crv=polyval(yitop40,zitop40,3);
%plot(spsct_ytop40,spsct_ztop40,'o',yitop40,zitop40)
coef40_top=polyfit(yitop40,zitop40,3)
xsection(40)=spsct_xtop40(1);
xsection(40)
%
%
yibot41=0:0.001:spsct_ybot41(2);
zibot41=spline(spsct_ybot41,spsct_zbot41,yibot41);
yz41bot_crv=polyval(yibot41,zibot41,3);
%plot(spsct_ybot41,spsct_zbot41,'o',yibot41,zibot41)
coef41_bot=polyfit(yibot41,zibot41,3)
xsection(41)=spsct_xbot41(1);
xsection(41)
%
yitop41=0:0.001:spsct_ytop41(2);
zitop41=spline(spsct_ytop41,spsct_ztop41,yitop41);
yz41top_crv=polyval(yitop41,zitop41,3);
%plot(spsct_ytop41,spsct_ztop41,'o',yitop41,zitop41)
coef41_top=polyfit(yitop41,zitop41,3)
xsection(41)=spsct_xtop41(1);
xsection(41)
%diary off

% PLOTTING THE RESULTS - YZ SMOOTHED BY CURVEFIT
% ----------------------------------------------

plot(spsct_ybotLE,spsct_zbotLE,'o',spsct_ytopLE,spsct_ztopLE,'o')
axis([0 0.7 -0.016 0.016]);pause
plot( yibot1, zibot1, yitop1, zitop1)
axis([0 0.7 -0.016 0.016]);pause
plot( yibot2, zibot2, yitop2, zitop2)
axis([0 0.7 -0.016 0.016]);pause
plot( yibot3, zibot3, yitop3, zitop3)
axis([0 0.7 -0.016 0.016]);pause
plot( yibot4, zibot4, yitop4, zitop4)
axis([0 0.7 -0.016 0.016]);pause
plot( yibot5, zibot5, yitop5, zitop5)
axis([0 0.7 -0.016 0.016]);pause
plot( yibot6, zibot6, yitop6, zitop6)
axis([0 0.7 -0.016 0.016]);pause
plot( yibot7, zibot7, yitop7, zitop7)
axis([0 0.7 -0.016 0.016]);pause
plot( yibot8, zibot8, yitop8, zitop8)
```

```
axis([0 0.7 -0.016 0.016]);pause
plot( yibot9, zibot9, yitop9, zitop9)
axis([0 0.7 -0.016 0.016]);pause
plot( yibot10, zibot10, yitop10, zitop10)
axis([0 0.7 -0.016 0.016]);pause
plot( yibot11, zibot11, yitop11, zitop11)
axis([0 0.7 -0.016 0.016]);pause
plot( yibot12, zibot12, yitop12, zitop12)
axis([0 0.7 -0.016 0.016]);pause
plot( yibot13, zibot13, yitop13, zitop13)
axis([0 0.7 -0.016 0.016]);pause
plot( yibot14, zibot14, yitop14, zitop14)
axis([0 0.7 -0.016 0.016]);pause
plot( yibot15, zibot15, yitop15, zitop15)
axis([0 0.7 -0.016 0.016]);pause
plot( yibot16, zibot16, yitop16, zitop16)
axis([0 0.7 -0.016 0.016]);pause
plot( yibot17, zibot17, yitop17, zitop17)
axis([0 0.7 -0.016 0.016]);pause
plot( yibot18, zibot18, yitop18, zitop18)
axis([0 0.7 -0.016 0.016]);pause
plot( yibot19, zibot19, yitop19, zitop19)
axis([0 0.7 -0.016 0.016]);pause
plot( yibot20, zibot20, yitop20, zitop20)
axis([0 0.7 -0.016 0.016]);pause
plot( yibot21, zibot21, yitop21, zitop21)
axis([0 0.7 -0.016 0.016]);pause
plot( yibot22, zibot22, yitop22, zitop22)
axis([0 0.7 -0.016 0.016]);pause
plot( yibot23, zibot23, yitop23, zitop23)
axis([0 0.7 -0.016 0.016]);pause
plot( yibot24, zibot24, yitop24, zitop24)
axis([0 0.7 -0.016 0.016]);pause
plot( yibot25, zibot25, yitop25, zitop25)
axis([0 0.7 -0.016 0.016]);pause
plot( yibot26, zibot26, yitop26, zitop26)
axis([0 0.7 -0.016 0.016]);pause
plot( yibot27, zibot27, yitop27, zitop27)
axis([0 0.7 -0.016 0.016]);pause
plot( yibot28, zibot28, yitop28, zitop28)
axis([0 0.7 -0.016 0.016]);pause
plot( yibot29, zibot29, yitop29, zitop29)
axis([0 0.7 -0.016 0.016]);pause
plot( yibot30, zibot30, yitop30, zitop30)
axis([0 0.7 -0.016 0.016]);pause
plot( yibot31, zibot31, yitop31, zitop31)
axis([0 0.7 -0.016 0.016]);pause
plot( yibot32, zibot32, yitop32, zitop32)
axis([0 0.7 -0.016 0.016]);pause
plot( yibot33, zibot33, yitop33, zitop33)
axis([0 0.7 -0.016 0.016]);pause
plot( yibot34, zibot34, yitop34, zitop34)
axis([0 0.7 -0.016 0.016]);pause
plot( yibot35, zibot35, yitop35, zitop35)
axis([0 0.7 -0.016 0.016]);pause
plot( yibot36, zibot36, yitop36, zitop36)
axis([0 0.7 -0.016 0.016]);pause
plot( yibot37, zibot37, yitop37, zitop37)
axis([0 0.7 -0.016 0.016]);pause
plot( yibot38, zibot38, yitop38, zitop38)
axis([0 0.7 -0.016 0.016]);pause
plot( yibot39, zibot39, yitop39, zitop39)
axis([0 0.7 -0.016 0.016]);pause
plot( yibot40, zibot40, yitop40, zitop40)
axis([0 0.7 -0.016 0.016]);pause
plot( yibot41, zibot41, yitop41, zitop41)
axis([0 0.7 -0.016 0.016]);pause
plot(spsct_ybotTE,spsct_zbotTE,'o',spsct_ytopTE,spsct_ztopTE,'o')
axis([0 0.7 -0.016 0.016]);pause

plot(spsct_ybotLE,spsct_zbotLE,'o',spsct_ytopLE,spsct_ztopLE,'o', ...
   yibot1, zibot1,'y', yitop1, zitop1,'y', ...
   yibot2, zibot2,'m', yitop2, zitop2,'m', ...
   yibot5, zibot5,'c', yitop5, zitop5,'c', ...
   yibot6, zibot6,'r', yitop6, zitop6,'r', ...
   yibot9, zibot9,'g', yitop9, zitop9,'g', ...
```



```
   yibot11, zibot11,'b', yitop11, zitop11,'b', ...
   yibot15, zibot15,'w', yitop15, zitop15,'w')
xlabel('Unit Spanwise Location (-y direction)')
ylabel('Unit Vertical Location (z direction)')
title('F5 Wing - Spanwise Sections From FWD Apex to Tip L.E. - Smoothed')
grid
pause

plot( yibot16, zibot16,'y', yitop16, zitop16,'y', ...
   yibot18, zibot18,'m', yitop18, zitop18,'m', ...
   yibot19, zibot19,'c', yitop19, zitop19,'c', ...
   yibot21, zibot21,'r', yitop21, zitop21,'r', ...
   yibot22, zibot22,'g', yitop22, zitop22,'g', ...
   yibot24, zibot24,'b', yitop24, zitop24,'b', ...
   yibot25, zibot25,'w', yitop25, zitop25,'w', ...
   yibot27, zibot27,'y', yitop27, zitop27,'y')
xlabel('Unit Spanwise Location (-y direction)')
ylabel('Unit Vertical Location (z dierction)')
title('F5 Wing - Spanwise Sections From Tip L.E. to Tip T.E. - Smoothed')
grid
pause

plot( yibot28, zibot28,'y', yitop28, zitop28,'y', ...
   yibot30, zibot30,'m', yitop30, zitop30,'m', ...
   yibot32, zibot32,'c', yitop32, zitop32,'c', ...
   yibot34, zibot34,'r', yitop34, zitop34,'r', ...
   yibot36, zibot36,'g', yitop36, zitop36,'g', ...
   yibot38, zibot38,'b', yitop38, zitop38,'b', ...
   yibot41, zibot41,'w', yitop41, zitop41,'w', ...
   spsct_ybotTE,spsct_zbotTE,'o',spsct_ytopTE,spsct_ztopTE,'o')
grid
xlabel('Unit Spanwise Location (-y direction)')
ylabel('Unit Vertical Location (z direction)')
title('F5 Wing - Spanwise Sections From Tip T.E. to AFT Apex - Smoothed')
pause

% 3D PLOT 'NOT EXECUTED'.  X STRING IS SHORTER (LESS DENSE)
% ---------------------------------------------------------
%plot3(spsct_xbot20, yibot20, zibot20,'b', ...
%      spsct_xtop20, yitop20, zitop20,'b', ...
%      spsct_xbot10, yibot10, zibot10,'g', ...
%      spsct_xtop10, yitop10, zitop10,'g', ...
%      spsct_xbot5, yibot5, zibot5,'y', ...
%      spsct_xtop5, yitop5, zitop5,'y')
%xlabel('Chordwise Direction (x)')
%ylabel('Spanwise Direction (-y)')
%zlabel('Height (z)')
%title('F5 Wing RH side Spanwise Sections - Smoothed')
%pause
%
%plot3(spsct_xbot1, yibot1, zibot1,'y', ...
%      spsct_xtop1, yitop1, zitop1,'y', ...
%      spsct_xbot8, yibot8, zibot8,'m', ...
%      spsct_xtop8, yitop8, zitop8,'m', ...
%      spsct_xbot15, yibot15, zibot15,'c', ...
%      spsct_xtop15, yitop15, zitop15,'c', ...
%      spsct_xbot27, yibot27, zibot27,'b', ...
%      spsct_xtop27, yitop27, zitop27,'b', ...
%      spsct_xbot34, yibot34, zibot34,'w', ...
%      spsct_xtop34, yitop34, zitop34,'w', ...
%      spsct_xbot41, yibot41, zibot41,'y', ...
%      spsct_xtop41, yitop41, zitop41,'y')
%pause

% ************************************************************************
% ************************************************************************
%  THE FOLLOWING SECTION USES RESULTS OF OTHER ROUTINES TO CALCULATE THE AREAS
% ************************************************************************
% ************************************************************************

% LONGITUDINAL CIRCLES EQUIVALENT AREA
% ------------------------------------
% (41 element string of areas calculated seperately using 'int.m')
%  ONE SIDE OF THE SECTION

Abot=[ 0.0002 0.0006    0.0010    0.0014    0.0019    0.0024    0.0028 ...
```

```
    0.0033    0.0036    0.0039    0.0040    0.0042    0.0043    0.0043 ...
    0.0043    0.0034    0.0031    0.0027    0.0023    0.0019    0.0015 ...
    0.0013    0.0011    0.0010    0.0009    0.0009    0.0009    0.0009 ...
    0.0009    0.0009    0.0008    0.0007    0.0005    0.0005    0.0004 ...
    0.0003    0.0003    0.0002    0.0001    0.0001    0.0000];

Atop=[ 0.0003 0.0011    0.0020    0.0028    0.0037    0.0046    0.0052 ...
    0.0057    0.0060    0.0063    0.0064    0.0066    0.0066    0.0066 ...
    0.0066    0.0046    0.0035    0.0028    0.0023    0.0018    0.0015 ...
    0.0013    0.0011    0.0010    0.0009    0.0010    0.0009    0.0010 ...
    0.0009    0.0008    0.0008    0.0007    0.0006    0.0005    0.0004 ...
    0.0003    0.0002    0.0001    0.0001    0.0000    0.0000];

Agap=[    0    0.0001    0.0002    0.0003    0.0004    0.0004    0.0005 ...
    0.0005    0.0006    0.0006    0.0007    0.0005    0.0005    0.0006 ...
    0.0006    0.0034    0.0046    0.0054    0.0057    0.0059    0.0058 ...
    0.0054    0.0046    0.0037    0.0026    0.0012         0         0 ...
         0         0    0.0001         0    0.0001         0         0 ...
         0    0.0001         0         0         0    0.0000];


midarea=Abot+Atop+Agap;
area=2*midarea;
xsectionper=xsection/0.6439;

for i=1:41
 r(i)=sqrt(area(i)/pi);
end

diary on
% SPANWISE CROSS-SECTION LOCATION, AREA, AND EQUIVALENT CIRCLE RADIUS AND DIAMETER
% ------------------------------------------------------------------------------

% NOTE: The L.E. and T.E. Apex are not included. Their values are as follows:
%
%                L.E. Apex:  xsection=0       area=0
%                T.E. Apex:  xsection=0.6439  area=0

xsection
area
r
D=2*r;
D

diary off
! mv diary area.out
! hp3si -text area.out

% PLOTTING THE RESULTS - LONGITUDINAL AREA CHANGE
% -----------------------------------------------

plot(xsectionper,Abot)
xlabel('Longitudinal Location - Percent Root Chord')
ylabel('Spanwise Lower Section Area')
title('F5 WING - SPANWISE LOWER CROSS-SECTION AREA')
grid
pause
%print

plot(xsectionper,Atop)
xlabel('Longitudinal Location - Percent Root Chord')
ylabel('Spanwise Upper Section Area')
title('F5 WING - SPANWISE UPPER CROSS-SECTION AREA')
grid
pause
%print

plot(xsectionper,Agap)
xlabel('Longitudinal Location - Percent Root Chord')
ylabel('Spanwise Gap Section Area')
title('F5 WING - SPANWISE GAP CROSS-SECTION AREA')
grid
pause
%print

plot(xsectionper,area)
```



```
xlabel('Longitudinal Location - Percent Root Chord')
ylabel('Spanwise Total Section Area')
title('F5 WING - SPANWISE TOTAL CROSS-SECTION AREA')
grid
pause
%print

% NON-DIMENSIONALIZING THE LONGITUDINAL LOCATION FOR ABOVE PLOT
% -------------------------------------------------------------

xsectionpernd=xsectionper/xsectionper(41);
plot(xsectionpernd,area)
xlabel('Longitudinal Location - Percent Root Chord')
ylabel('Spanwise Total Section Area')
title('F5 WING - SPANWISE TOTAL CROSS-SECTION AREA')
grid
pause
%print

% FITTING A POLYNOMIAL TO THE AUGMENTED AREA CURVE ABOVE
% ------------------------------------------------------
% (Arrays will be augmented with point 0 of 0 area)

xsectionpernd_aug= [0.0000  0.0661  0.1281  0.1942  0.2523  0.3123 ...
    0.3664  0.4164  0.4645  0.5025  0.5406  0.5686  0.5926  0.6106 ...
    0.6186  0.6246  0.6505  0.6764  0.7022  0.7281  0.7540  0.7798 ...
    0.8057  0.8316  0.8574  0.8833  0.9092  0.9350  0.9342  0.9351 ...
    0.9373  0.9401  0.9435  0.9480  0.9525  0.9583  0.9642  0.9707 ...
    0.9778  0.9847  0.9926  1.0000];

area_aug= [ 0.0000  0.0010  0.0036  0.0064  0.0090  0.0120  0.0148 ...
    0.0170  0.0190  0.0204  0.0216  0.0222  0.0226  0.0228  0.0230 ...
    0.0230  0.0228  0.0224  0.0218  0.0206  0.0192  0.0176  0.0160 ...
    0.0136  0.0114  0.0088  0.0062  0.0036  0.0038  0.0036  0.0034 ...
    0.0034  0.0028  0.0024  0.0020  0.0016  0.0012  0.0012  0.0006 ...
    0.0004  0.0002  0.0000];

plot(xsectionpernd_aug,area_aug)
xlabel('Longitudinal Location - Percent Root Chord')
ylabel('Spanwise Total Section Area')
title('F5 WING - SPANWISE TOTAL CROSS-SECTION AREA - APEX TO APEX')
grid
pause
%print

xi=0:0.035:1;
yi=spline(xsectionpernd_aug,area_aug,xi);
plot(xsectionpernd_aug,area_aug,'o',xi,yi)
QofX=polyfit(xi,yi,10)
%Q = polyval(coef,X)

% CHECKING THE INTEGRATION RESULTS USING TRAPEZOID METHOD
% -------------------------------------------------------
% (Using routine 'areacheck.m') (Augmented with Apex 0 area)

area_check=[ 0.000 0.0011 0.0033  0.0062  0.0090  0.0120    0.0146    0.0169 ...
   0.0190    0.0204    0.0215    0.0222    0.0227    0.0229    0.0230 ...
   0.0230    0.0229    0.0225    0.0217    0.0206    0.0192    0.0176 ...
   0.0157    0.0136    0.0113    0.0089    0.0063    0.0036    0.0037 ...
   0.0036    0.0034    0.0031    0.0028    0.0025    0.0021    0.0017 ...
   0.0013    0.0009    0.0006    0.0004    0.0002    0.0001];


plot(xsectionpernd_aug,area_aug,xsectionpernd_aug,area_check,'*')
xlabel('Longitudinal Location - Percent Root Chord')
ylabel('Spanwise Total Section Area')
title('F5 WING - SPANWISE TOTAL CROSS-SECTION AREA - AUGMENTED')
grid
gtext('**** Trapezoid Method')
gtext('____ Integration Method')

save
! mv matlab.mat matlab_area.mat
```

APPENDIX F. F5 WING SPANWISE CROSS-SECTIONAL AREAS

This appendix provides the results of the computer code described in section **A-6** of chapter **IV**. It shows the area, radius and diameter of each of the 41 spanwise cross-sections defined along the chord of the F5 wing. Also, a plot is included that shows the distribution of the spanwise cross-sectional areas along the chord.

```
xsection =
  Columns 1 through 7
    0.0422    0.0819    0.1241    0.1612    0.1995    0.2341    0.2660
  Columns 8 through 14
    0.2967    0.3210    0.3453    0.3633    0.3786    0.3901    0.3952
  Columns 15 through 21
    0.3991    0.4156    0.4321    0.4486    0.4652    0.4817    0.4982
  Columns 22 through 28
    0.5147    0.5313    0.5478    0.5643    0.5808    0.5974    0.5968
  Columns 29 through 35
    0.5974    0.5988    0.6006    0.6028    0.6057    0.6086    0.6122
  Columns 36 through 41
    0.6160    0.6201    0.6247    0.6291    0.6341    0.6389

area =
  Columns 1 through 7
    0.0010    0.0036    0.0064    0.0090    0.0120    0.0148    0.0170
  Columns 8 through 14
    0.0190    0.0204    0.0216    0.0222    0.0226    0.0228    0.0230
  Columns 15 through 21
    0.0230    0.0228    0.0224    0.0218    0.0206    0.0192    0.0176
  Columns 22 through 28
    0.0160    0.0136    0.0114    0.0088    0.0062    0.0036    0.0038
  Columns 29 through 35
    0.0036    0.0034    0.0034    0.0028    0.0024    0.0020    0.0016
  Columns 36 through 41
    0.0012    0.0012    0.0006    0.0004    0.0002         0

r =
  Columns 1 through 7
    0.0178    0.0339    0.0451    0.0535    0.0618    0.0686    0.0736
  Columns 8 through 14
    0.0778    0.0806    0.0829    0.0841    0.0848    0.0852    0.0856
  Columns 15 through 21
    0.0856    0.0852    0.0844    0.0833    0.0810    0.0782    0.0748
  Columns 22 through 28
    0.0714    0.0658    0.0602    0.0529    0.0444    0.0339    0.0348
  Columns 29 through 35
    0.0339    0.0329    0.0329    0.0299    0.0276    0.0252    0.0226
```



```
  Columns 36 through 41
    0.0195    0.0195    0.0138    0.0113    0.0080         0

D =
  Columns 1 through 7
    0.0357    0.0677    0.0903    0.1070    0.1236    0.1373    0.1471
  Columns 8 through 14
    0.1555    0.1612    0.1658    0.1681    0.1696    0.1704    0.1711
  Columns 15 through 21
    0.1711    0.1704    0.1689    0.1666    0.1620    0.1564    0.1497
  Columns 22 through 28
    0.1427    0.1316    0.1205    0.1059    0.0888    0.0677    0.0696
  Columns 29 through 35
    0.0677    0.0658    0.0658    0.0597    0.0553    0.0505    0.0451
  Columns 36 through 41
    0.0391    0.0391    0.0276    0.0226    0.0160         0
```

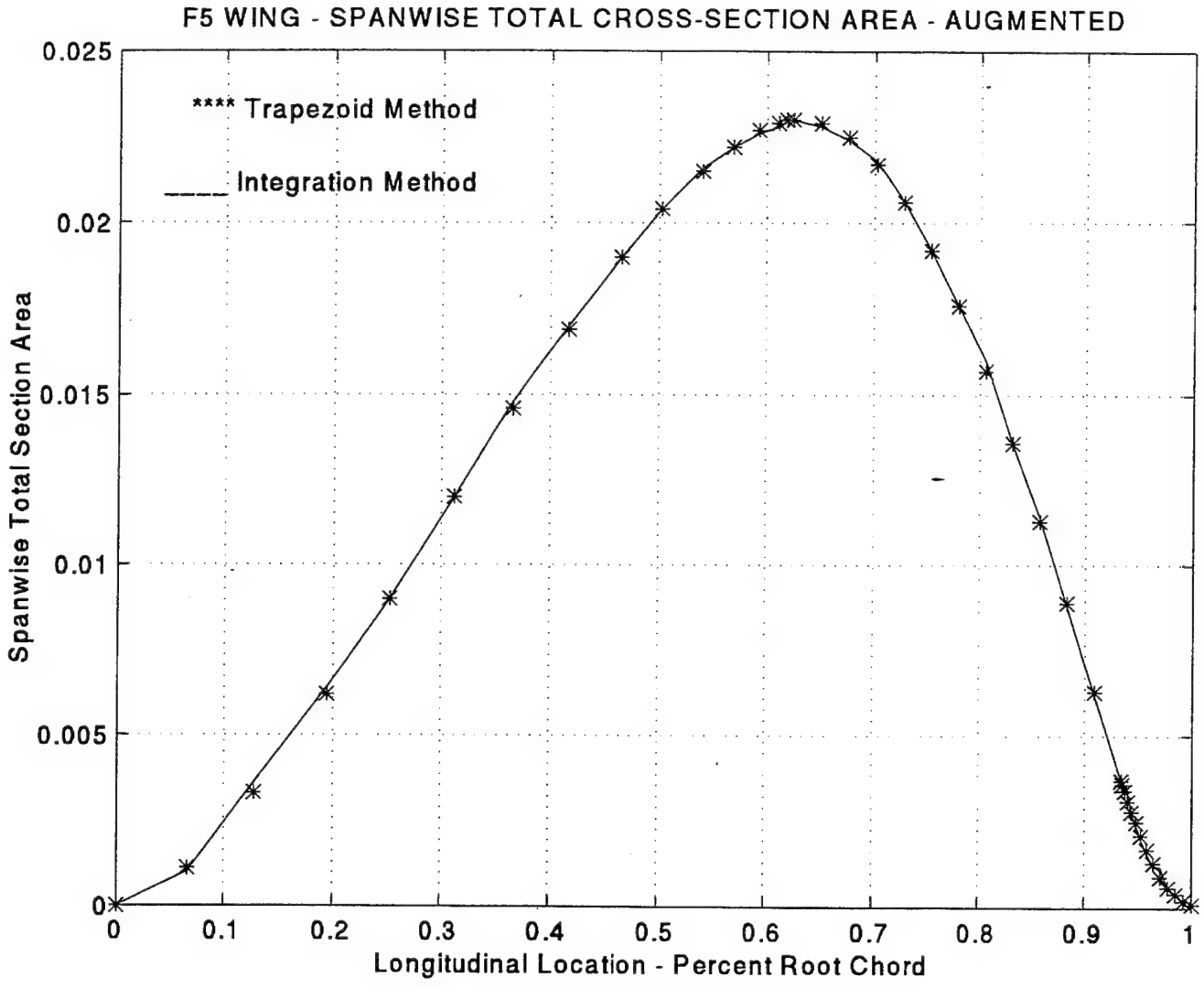
F5 WING - SPANWISE TOTAL CROSS-SECTION AREA - AUGMENTED
**** Trapezoid Method
____ Integration Method
Spanwise Total Section Area
Longitudinal Location - Percent Root Chord
0.025
0.02
0.015
0.01
0.005
0
0
0.1
0.2
0.3
0.4
0.5
0.6
0.7
0.8
0.9
1

APPENDIX G. TRIANGULAR WING SPANWISE CROSS-SECTIONAL AREAS

This appendix provides the radii of 46 spanwise cross-sectional areas with the x coordinate of their centroid along the chord of the triangular wing. This information is provided for the two cases of maximum thickness ratio treated: 0.098, and 0.196. A plot showing the distribution of the spanwise cross-sectional areas along the chord is also included for each case.

```
r =
  Columns 1 through 7
         0    0.0036    0.0070    0.0104    0.0137    0.0169    0.0199
  Columns 8 through 14
    0.0229    0.0258    0.0286    0.0312    0.0338    0.0362    0.0385
  Columns 15 through 21
    0.0407    0.0428    0.0447    0.0465    0.0481    0.0496    0.0510
  Columns 22 through 28
    0.0522    0.0532    0.0541    0.0547    0.0552    0.0555    0.0555
  Columns 29 through 35
    0.0553    0.0548    0.0541    0.0530    0.0516    0.0498    0.0475
  Columns 36 through 42
    0.0446    0.0410    0.0365    0.0306    0.0269    0.0222    0.0194
  Columns 43 through 46
    0.0159    0.0113    0.0080         0

x =
  Columns 1 through 7
         0    0.0250    0.0500    0.0750    0.1000    0.1250    0.1500
  Columns 8 through 14
    0.1750    0.2000    0.2250    0.2500    0.2750    0.3000    0.3250
  Columns 15 through 21
    0.3500    0.3750    0.4000    0.4250    0.4500    0.4750    0.5000
  Columns 22 through 28
    0.5250    0.5500    0.5750    0.6000    0.6250    0.6500    0.6750
  Columns 29 through 35
    0.7000    0.7250    0.7500    0.7750    0.8000    0.8250    0.8500
  Columns 36 through 42
    0.8750    0.9000    0.9250    0.9500    0.9625    0.9750    0.9813
  Columns 43 through 46
    0.9876    0.9938    0.9969    1.0000
```

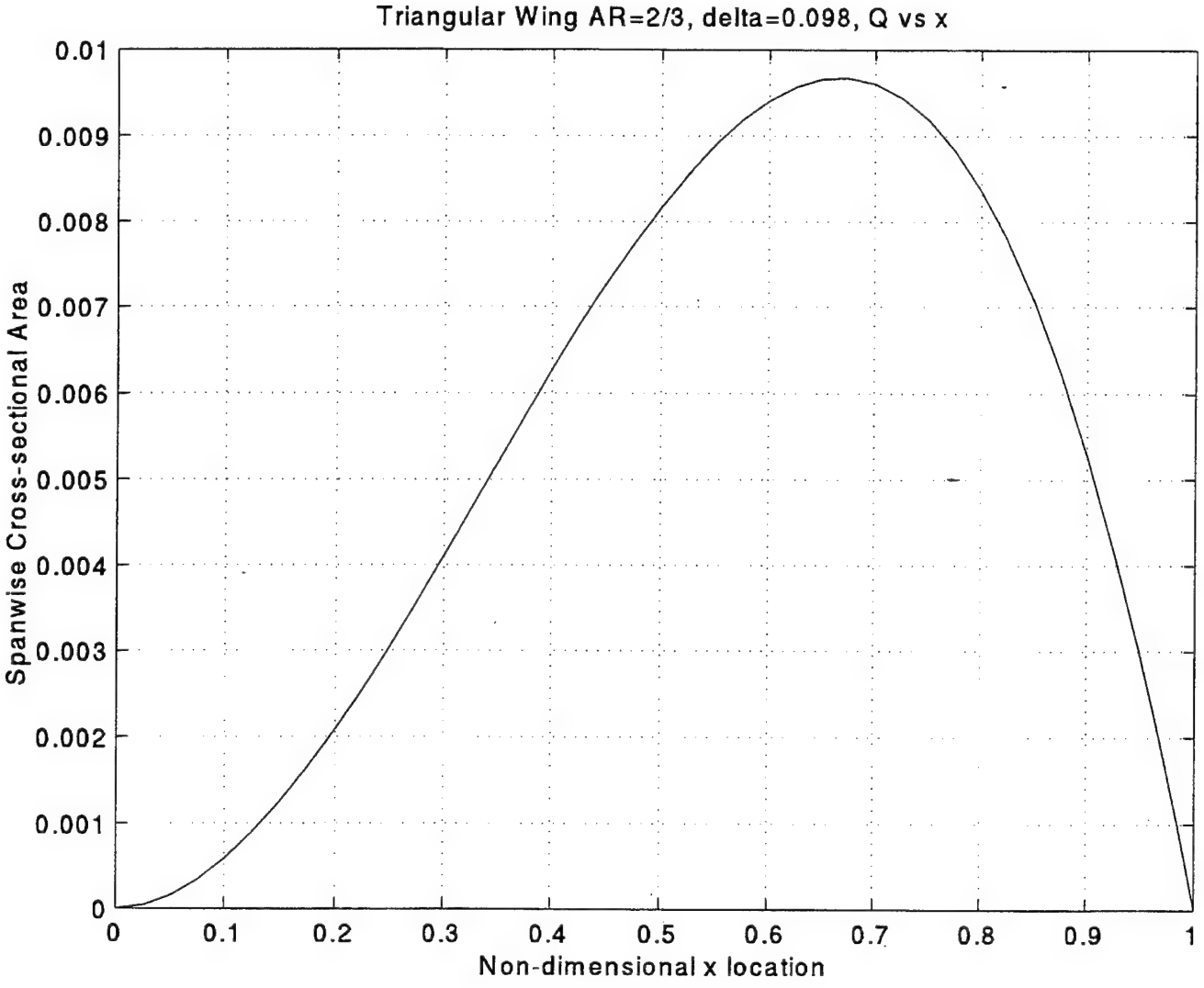
Triangular Wing AR=2/3, delta=0.098, Q vs x
Spanwise Cross-sectional Area
Non-dimensional x location
0.01
0.009
0.008
0.007
0.006
0.005
0.004
0.003
0.002
0.001
0
0
0.1
0.2
0.3
0.4
0.5
0.6
0.7
0.8
0.9
1

```
r =

  Columns 1 through 7

         0    0.0050    0.0099    0.0147    0.0193    0.0238    0.0282

  Columns 8 through 14

    0.0324    0.0365    0.0404    0.0442    0.0478    0.0512    0.0545

  Columns 15 through 21

    0.0575    0.0605    0.0632    0.0657    0.0681    0.0702    0.0721

  Columns 22 through 28

    0.0738    0.0752    0.0764    0.0774    0.0781    0.0784    0.0785

  Columns 29 through 35

    0.0782    0.0775    0.0765    0.0750    0.0730    0.0704    0.0671

  Columns 36 through 42

    0.0631    0.0580    0.0517    0.0433    0.0380    0.0314    0.0274

  Columns 43 through 46

    0.0224    0.0160    0.0113         0

x =

  Columns 1 through 7

         0    0.0250    0.0500    0.0750    0.1000    0.1250    0.1500

  Columns 8 through 14

    0.1750    0.2000    0.2250    0.2500    0.2750    0.3000    0.3250

  Columns 15 through 21

    0.3500    0.3750    0.4000    0.4250    0.4500    0.4750    0.5000

  Columns 22 through 28

    0.5250    0.5500    0.5750    0.6000    0.6250    0.6500    0.6750

  Columns 29 through 35

    0.7000    0.7250    0.7500    0.7750    0.8000    0.8250    0.8500

  Columns 36 through 42

    0.8750    0.9000    0.9250    0.9500    0.9625    0.9750    0.9813

  Columns 43 through 46

    0.9876    0.9938    0.9969    1.0000
```

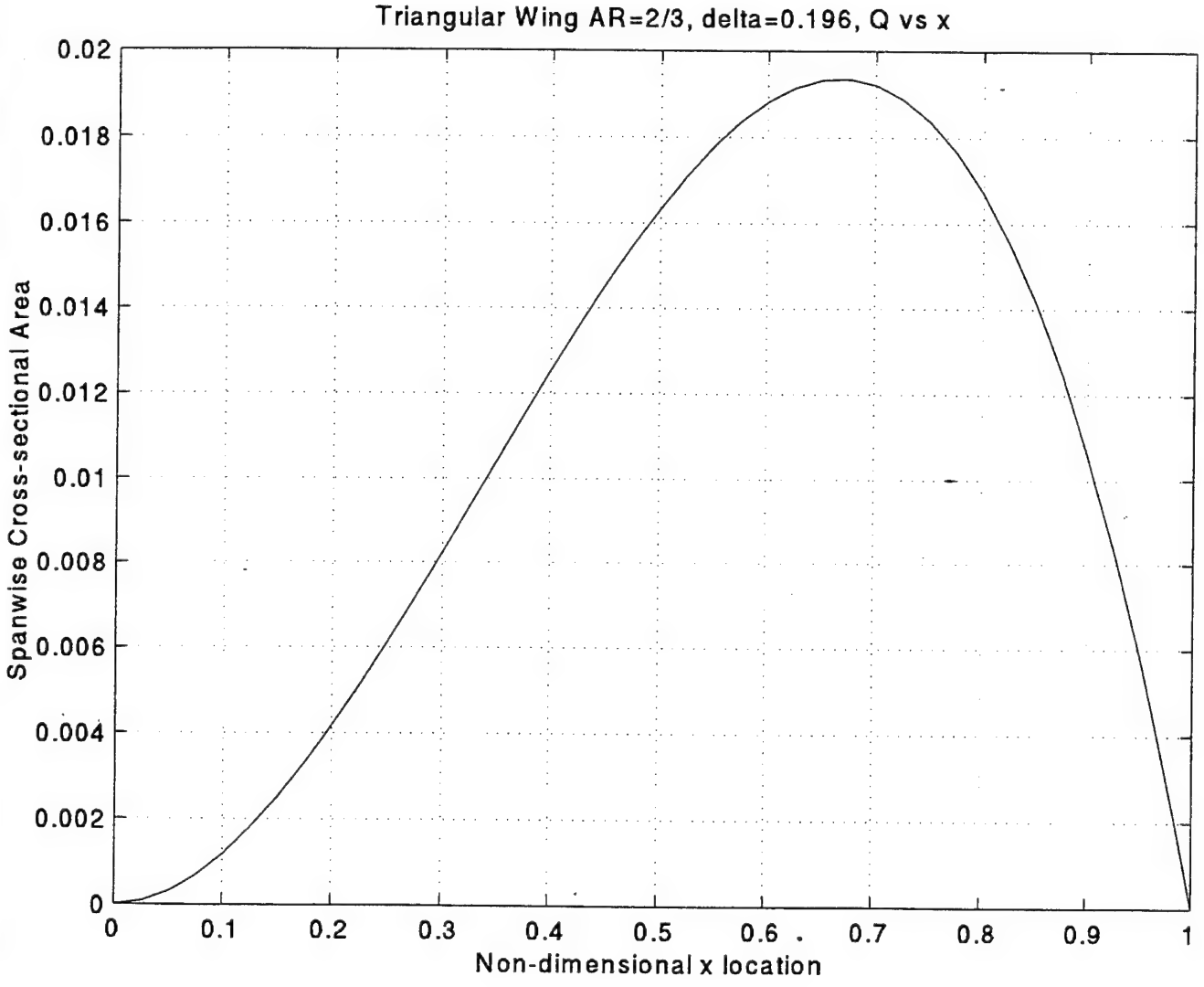
Triangular Wing AR=2/3, delta=0.196, Q vs x
Spanwise Cross-sectional Area
Non-dimensional x location
0.02
0.018
0.016
0.014
0.012
0.01
0.008
0.006
0.004
0.002
0
0
0.1
0.2
0.3
0.4
0.5
0.6
0.7
0.8
0.9
1

APPENDIX H. AUTOMATED EXTRACTION OF CL AND CM

This appendix presents two short programs written in the UNIX AWK language used to extract CL and CM at each time-step of the PMARC output file 'DATA6'. These programs introduced in section **B-4** of chapter **V** are specific to the case of the F5 wing treated in this study. The location of CL and CM in the output file can vary depending on the configuration modelled.

```
CM EXTRACTION
*************

#!/bin/sh
# AWK Script to extract the total cm value from
# the PMARC output DATA6 file.
# Finds "WIND AXES" and skips 32 lines then picks the fourth field ($4
# which is the total cm value
#
echo
echo Reads in DATA6 file for a simple wing with symmetry
echo and its wingtips for a total of four patches
echo
echo cm total data is put in file \"outcm\*
awk '
       /WIND AXES/  {
                      NL = 32
                      for(i=0;i<NL;++i)
                      getline      # Gets 32 line after WIND AXES term
                      print $4     # Gets fourth field (cm value)
                    }
   '  DATA6 > outcm


CL EXTRACTION
*************

#!/bin/sh
# AWK Script to extract the total CL value from
# the PMARC output DATA6 file.
# Finds "WIND AXES" and skips 32 lines then picks first field ($1)
# which is the total CL value
#
echo
echo Reads in DATA6 file for a simple wing with symmetry
echo and its wingtips for a total of four patches
echo
echo CL total data is put in file \"outCL\*
awk '
       /WIND AXES/  {
                      NL = 32
                      for(i=0;i<NL;++i)
                      getline      # Gets 32 line after WIND AXES term
                      print $1     # Gets first field (CL value)
                    }
   '  DATA6 > outCL
```

LIST OF REFERENCES

1. Ashby, D.L., Dudley, M.R. Iguchi, S.K., Browne, L., and Katz, J., *Potential Flow Theory and Operation Guide for The Panel Code PMARC_12*, NASA TM-102851, Ames Research Center, Moffett Field, CA, December 1992.

2. Burris, S., *Subsonic Load Analysis Manual*, Developed for Use by Naval Postgraduate School Aerospace Engineering Department, Monterey, CA, 1994.

3. Lambert, M.A., *Evaluation of The NASA-Ames Panel Method (PMARC) for Aerodynamic Missile Design*, Master's Thesis, Naval Postgraduate School, Monterey, CA, June 1987.

4. Bertin, J.J., and Smith, M.L., *Aerodynamics for Engineers*, 2nd edition, Prentice-Hall, 1989.

5. Weber, J. and Brebner, G.G., *Low-Speed Tests on 45-Degree Swept-Back Wings, Part I Pressure Measurements on Wings of Aspects Ratio 5*, Reports and Memoranda 2882, Aeronautical Research Council, 1958.

6. Margason, R.J. et al, *Subsonic Panel Methods - A Comparison of Several Production Codes*, AIAA Paper 85-0280, presented at the 23rd AIAA Aerospace Sciences Meeting, Reno, Nev., January 1985.

7. Abbott, I.H., and Von Doenhoff, A.E., *Theory and Wing Sections Including a Summary of Airfoil Data*, Dover, New York, 1959.

8. Schlichting, H., and Truckenbrodt, E., *Aerodynamik des Flugzeuges*, Vol. 2, Chap. 7, Springer-Verlag, Berlin, 1969.

9. Ashley, H., and Landahl, M., *Aerodynamics of Wings and Bodies*, Dover, New York, 1965.

10. Margason, R.J., and Lamar, J.E., *Vortex-Lattice Fortran Program for Estimating Subsonic Aerodynamic Characteristics of Complex Planforms*, NASA Technical Notes TN D-6142, National Aeronautics and Space Administration, Washington, D.C., February 1971.

11. Teng, N. H., *The Development of a Computer Code for The Numerical Solution of Unsteady, Inviscid and Incompressible Flow over an Airfoil*, Master's Thesis, Naval Postgraduate School, Monterey, CA, June 1987.

12. Borland, C.J., *Transonic Steady and Unsteady Aerodynamics for Aeroelastic Applications*, Volume I, XTRAN35, Technical Development Summary, AFWAL-TR-85-3124, January 1986.

13. F5 Wing Cross-Section Coordinates, Obtained from Prof. Platzer, M.F., Naval Postgraduate School, Monterey, CA, June 1995.

14. Platzer, M.F., *The Equivalence or Area Rule*, Lecture Notes for AE3501, Naval Postgraduate School, Monterey, CA, 1995.

15. Keune, F., *Low Aspect Ratio Wings with Small Thickness at Zero Lift in Subsonic and Supersonic Flow*, Technical Notes KTH-AERO TN21, Royal Institute of Technology, Stockholm 1952.

16. MAPLE, Analytical Solver, University of Waterloo, 1992.

17. Rom, J., *High Angle of Attack Aerodynamics, Subsonic, Transonic, and Supersonic Flows*, Springer-Verlag, New York, 1992.

18. Keith, S.R., *General Visualization System*, Sterling Software, Palo Alto, CA, 1993.

19. Platzer, M.F., *On Quasi-Slender Body Theory for Oscillating Low Aspect Ratio Wings and Bodies of Revolution in Supersonic Flow*, NASA Technical Memorandum, NASA TM X-53295, April 1965.

INITIAL DISTRIBUTION LIST

1. Defense Technical Information Center 2
   8725 John J. Kingman Rd., STE 0944
   Ft. Belvoir, VA 22060-6218

2. Library Code 13 2
   Naval Postgraduate School
   Monterey, CA 93943-5101

3. Chairman 1
   Department of Aeronautics and Astronautics, Code AA
   Naval Postgraduate School
   699 Dyer Road, Room 137
   Monterey, CA 93943-5106

4. Dr. Max F. Platzer 5
   Department of Aeronautics and Astronautics, Code AA/PL
   Naval Postgraduate School
   699 Dyer Road, Room 137
   Monterey, CA 93943-5106

5. Dr. Ismail Tuncer 1
   Department of Aeronautics and Astronautics, Code AA/Tu
   Naval Postgraduate School
   699 Dyer Road, Room 137
   Monterey, CA 93943-5106

6. Mark A. Lambert 1
   Naval Air Warfare Center - Weapons Division
   Code 472110D
   China Lake, CA 93555

7. DSIS 3 1
   Director Scientific Information Services
   National Defence Headquarters - Canada
   Ottawa, (ONTARIO)
   Canada K1A 0K2

8. Alain Carrier 2
   28 Beaussier
   Gatineau, (QUEBEC)
   Canada J8T 7Z5

9. DAEPM (FT-428) 1
National Defence Headquarters - Canada
Attn. Mr. Zatwchec
Maj. Gen. J.R. Pearkes Bldg
101 Col By Dr.
Ottawa, (ONTARIO)
Canada K1A 0K2